PhD

Cardosin A Molecular Determinants and Biosynthetic Pathways

Cláudia Sofia Pereira

2012

Cardosin A Molecular Determinants and Biosynthetic Pathways

Cláudia Sofia Pereira

Defended October 29th, 2012 before the jury:

Vitor Vasconcelos – ***President of the jury***

Nadine Paris – ***Examiner/Rewiever***
Isaura Simões - ***Examiner/Rewiever***
Jean-Marc Neuhaus - ***Examiner***
Rui Malhó – ***Examiner***

Béatrice Satiat-Jeunemaitre - ***Supervisor***
José Pissarra - ***Supervisor***

Joint supervision between Universidade do Porto and Université Paris Sud

2012

Cardosin A Molecular Determinants and Biosynthetic Pathways

Cláudia Sofia Pereira

PhD in Biology

Biology Department

Supervisor (*Universidade do Porto***)**
José Pissarra, Professor Associado, Faculdade de Ciências da Universidade do Porto

Supervisor (*Université Paris Sud***)**
Béatrice Satiat-Jeunemaitre, Directeur de Recherche 2, Institut des Sciences du Végétal - Centre National de la Recherce Scientifique

Joint supervision between Universidade do Porto

and Université Paris Sud

2012

ACKNOWLEDGEMENTS

Em primeiro lugar gostaria de agradecer ao meu orientador, José Pissarra, pela oportunidade em participar neste projeto que desde início senti como o “meu projeto”. Pela confiança que depositou em mim e no meu trabalho e que acabou por se refletir na liberdade que sempre tive no delineamento das experiências e na gestão do projeto. Muito obrigada pelo acompanhamento científico e pessoal, pelo encorajamento e pela amizade, que me ajudaram a crescer como cientista.

To Béatrice, my co-supervisor, I have to thank for having received me (the Portuguese girl) in her lab and for trusting in my project for the beginning even when things didn’t worked as planned. Once she told me I didn’t need a supervisor, but a friend who talk to. Thank you for being that friend.

À professora Susana um agradecimento especial por todo o apoio, dedicação e sobretudo pela amizade e preocupação sempre demonstrados. Muito obrigada por toda a ajuda e discussão de ideias, que mesmo quando eram diferentes nos obrigava a trabalhar e a querer saber mais!

À Diana, minha colega de bancada de sempre, com a qual partilhei muitos minipreps e Westerns, para além de muitas outras coisas, entre elas uma grande amizade! Um muito obrigado pela ajuda e pela partilha de conhecimento ao longo de todos estes anos. Talvez um dia voltaremos a partilhar uma bancada, quem sabe?

À Anocas piquenita, uma grande amiga e cientista! O “monstrinho” que fui criando e que agora está ao melhor nível! Muito obrigada querida amiga pela amizade, pela ajuda, pela partilha, pelos sorrisos e por me aturares nos melhores e nos piores momentos.

Ao Alberto, meu colega de freima doutoral e de muitas (saudáveis) discussões em torno da ciência, e não só! Obrigada pela boa disposição, pela disponibilidade e por toda a ajuda ao longo deste tempo.

À Susana e à Sara, obrigada pela constante boa disposição e pela ajuda em algumas tarefas que não teria conseguido superar sem vocês! Go girls!! A ciência espera-vos para um futuro brilhante!

À Patrícia Duarte um grande obrigada por me aturar sempre com um sorriso mesmo quando eu me metia entre ela e os protoplastos. Obrigada por toda a ajuda científica e pela amizade que fomos descobrindo ao longo do tempo.

Ao Mário, Sofia e Ana Marta, os melhores vizinhos do Mundo, um grande obrigado pela amizade, pela ajuda, pelas brincadeiras, pelos almoços, pelos folhadinhos, por organizarem o chá da Margarida… Enfim! Vocês são espetaculares! Ajudam a tornar o laboratório um lugar agradável para trabalhar e onde dá vontade de estar!

A toda a malta que foi passando pelo lab 2.61, desde mestrandos, estagiários a voluntários, que contribuem para que este seja o laboratório mais bem-disposto e produtivo do corredor e arredores!

A todos os colegas e professores do Departamento de Biologia, que de uma maneira ou de outra me foram ajudando ao longo destes longos anos, um agradecimento especial.

To all my colleagues at the ISV a big thank you for all the help and all the coaching in electron microscopy! You are all very nice and I am grateful for knowing you all.

À Paula Veríssimo por me ter aceite no laboratório dela em cima da hora e por toda a ajuda que disponibilizou ao tentar desesperadamente que a cardosina mostrasse alguma atividade. Ainda não desisti, vamos tentar novamente!

À minha família, particularmente aos meus pais, ao meu irmão, aos meus avós e à minha sogra, obrigada pelo apoio e pela compreensão nas ausências e nas más-disposições que vêm com este trabalho, especialmente nesta reta final. Valeu a pena!

Ao Pedro e ao Tiago, os afilhados mais lindos do mundo. Um sorriso e uma brincadeira fazem milagres quando uma eletroforese corre mal!

À Margarida, pelo sorriso, pelo mimo, pelo amor incondicional. Tornas a vida mais alegre e colorida!

Ao Vítor, por tudo… e pelas pequenas coisas! Não teria chegado aqui sem ti.

SUMMARY

The aspartic proteinase cardosin A is a vacuolar enzyme found to accumulate in protein storage vacuoles and lytic vacuoles in the flowers and in protein bodies in seeds of the native plant cardoon. Cardosin A has been first isolated almost two decades ago and has been extensively characterized since, both in terms of distribution within the tissues and of enzyme biochemistry. In the native system, several roles have been addressed to cardosin A in reproduction, mobilization of reserves and membrane remodeling. To participate in such diverse events, cardosin A must accumulate and travel to different compartments inside the cell: protein storage vacuoles, lytic vacuoles, cytoplasmic membrane (and eventually outside the cell). However, not much information is available regarding cardosin A biogenesis, sorting or trafficking to the different compartments, mainly because the protocols available are difficult to apply in cardoon plants. Recent studies have approached the expression of cardosin A in *Arabidopsis thaliana* and *Nicotiana tabacum* with promising results for the use of this systems in the study of cardosin A. In this work, these preliminary observations were the starting point of a detailed study of cardosin A expression, localisation, sorting and trafficking routes, resourcing to several and very different methods. It has been showed that transient expression of cardosin A in *Nicotiana tabacum* leaf is a good system to explore cardosin A trafficking inside the cell, as the protein is processed in a similar manner as the control and accumulates in the vacuole. Furthermore, an *Arabidopsis thaliana* line expressing cardosin A under an inducible promoter was explored to understand cardosin A dynamics in terms of vacuolar accumulation during seed germination events. Similarly to the *Nicotiana tabacum* one, this system was also validated for cardosin A expression and it allowed to conclude that the protein's expression did not retrieved any phenotype to the cells or individuals. However, experiments conducted in BY-2 cells revealed to be inconclusive since cardosin A expression in this system is not predictable. The data obtained along this work using several cardosin A mutated forms, lacking specific domains or point-mutated, allowed to determine that cardosin A has two Vacuolar Sorting Determinants in its protein sequence: the PSI, an unconventional sorting determinant, and the C-terminal peptide, a C-terminus sorting determinant by definition. Furthermore, it was also demonstrated that each domain represents a different route to the vacuole: the PSI bypasses the Golgi Apparatus and the C-terminal peptide follows a classic Endoplasmic Reticulum-Golgi Apparatus-Prevacuole route to the vacuole. This difference in the trafficking routes is not observed for cardosin B sorting determinants as both the PSI and C-terminal peptide from cardosin B needs to pass the Golgi Apparatus to reach the vacuole. A putative role for glycosylation in the trafficking routes is further discussed as cardosin A PSI, contrary to cardosin B, is not glycosylated. The production of mutants affecting cardosin A glycosylation sites supported this idea. Moreover,

cardosin A expression in germinating *Arabidopsis thaliana* seeds revealed a differential accumulation in non-germinated and germinated seedlings. Cardosin A was detected along the secretory pathway to the Protein Storage Vacuole in association with the Endoplasmic Reticulum, Golgi Apparatus, Prevacuole and newly formed Lytic Vacuoles. The drug Brefeldin A caused the protein to be retained in the Golgi Apparatus, despite some amount being still detected in the vacuole, not being clear if the Golgi Apparatus bypass observed in *Nicotiana tabacum* leaves occurs in this system. As a whole, cardosin A confirmed to be a good model to study vacuolar sorting in these two systems that complement each other in terms of approaches available. This study provided good results in order to understand in more detail cardosin A biology in particular and vacuolar trafficking of plant Aspartic Proteinases as a group. Also, this study, particularly in what concerns expression in *Arabidopsis thaliana*, is a good starting point to further studies involving the use of fluorescent fusions and to explore in more detail the relation of cardosin A and development.

RÉSUMÉ

La cardosine A est une protease aspartique identifiée dans les cellules du chardon *Cynara cardunculus*. La cardosine A a été isolée il y a plus de 20 ans, il a été montré qu'elle s'accumule dans les vacuoles de reserve et les vacuoles lytiques des tissus floraux, et dans les corps protéiques des graines. Depuis, sa distribution dans tous les tissus de la plante et ses caractéristiques enzymatiques ont été caractérisées, essentiellement par approches biochimiques. La cardosine A aurait des fonctions essentielles dans la reproduction, la mobilisation de réserves protéiques, et le remaniement de membranes. Pour assumer ces différentes fonctions, la cardosine A doit pouvoir transiter et s'accumuler dans différents compartiments intracellulaires : vacuole de stockage, vacuoles lytiques, ou autres compartiments membranaires dans le cytoplasme, ou éventuellement dans la paroi. Il n'y a cependant que très peu de données disponibles sur les mécanismes de biosynthèse, de tri, de transport et d'adressage aux différents compartiments cellulaires. Ce manque d'informations est en partie dû à la difficulté de transposer aux chardons des protocoles conventionnels de biologie cellulaire. De récents travaux ont permis de tester l'expression de la cardosine A dans des systèmes hétérologues tels que *Arabidopsis thaliana* et *Nicotiana tabacum*, suggérant que ces modèles expérimentaux pourraient être utilisés pour une meilleure compréhension de la biologie intracellulaire de la cardosine A. Ces données sont le point de départ d'une étude détaillée sur l'expression de la cardosine A, sa localisation, les mécanismes mis en œuvre pour son transport, tri et adressage dans la cellule. Les résultats de cette étude montrent que l'expression transitoire de la cardosine A dans les feuilles de *Nicotiana tabacum* est un bon modèle expérimental pour explorer le transport de la cardosine A dans la cellule. En effet dans ce système les mécanismes de maturation et de transport de la protéine à la vacuole sont conservés. De plus, une lignée stable d'*Arabidopsis thaliana* exprimant la cardosine A sous promoteur inductible s'est également avérée un bon modèle d'étude du transport intracellulaire de la cardosine A, où l'accumulation vacuolaire de la cardosine A peut être étudiée au cours de la germination de la graine. L'expression de la cardosine A n'altère ni le phénotype, ni le développement, ni aucune structure subcellulaire de la plante hôte. Par contre, des essais d'expression en système cellulaire basés sur des cultures en suspension BY2 se sont révélés peu concluants, les observations n'étant pas similaires à ce qui est observé dans la plante native. L'utilisation de ces systèmes hétérologues a permis de combiner l'expression de formes mutées de la cardosine A (dans lesquelles des séquences spécifiques ou des acides aminés avaient été tronqués ou modifiés) avec des approches de biochimie et d'imagerie cellulaire pour identifier des signatures moléculaires responsables de l'adressage vacuolaire de la protéine. Nos résultats montrent que la cardosine A a deux déterminants vacuolaires dans sa séquence protéique : le domaine

“PSI”, qui définit un déterminant d’adressage vacuolaire original et propre à certaines protéases aspartiques, et un peptide C-terminal appartenant à la classe bien définie des ctVSD. De plus, les résultats montrent que la présence de ces deux déterminants illustre la capacité d’emprunter deux routes distinctes pour atteindre la vacuole : le domaine PSI peut permettre d’attendre la vacuole sans passer par le Golgi, tandis que le domaine C-ter négocie un transport classique Reticulum, Golgi, Prévacuole, Vacuole. Cette capacité à choisir deux routes différentes n’est pas observée pour la cardosine B, autre protéase aspartique du chardon présentant une haute homologie de séquence avec la cardosine A. Pour la cardosine B, le domaine PSI et le domaine C-ter négocient tous les deux un transport par le Golgi. Pour expliquer cette capacité de la cardosine A à emprunter deux routes vacuolaires différentes, l’hypothèse d’un rôle possible de la glycosylation dans le tri des protéines entre les deux routes vacuolaires est alors étudiée. En effet le domaine PSI de la cardosine A n’est pas glycosylé, alors que celui de la cardosine B est glycosylé. La production de mutants de cardosine A affectés dans leur site de glycosylation confirme cette hypothèse de travail. L’expression de la cardosine A dans les graines en germination d’*Arabidopsis thaliana* révèle que la protéine peut s’accumuler d’une manière différentielle dans les graines en absence de germination ou pendant la germination. La cardosine A a été détectée dans des graines tout au long du système endomembranaire (Reticulum, Golgi, Compartiment Prévacuolaire) jusqu’à la vacuole de réserve ou dans les vacuoles lytiques en formation au cours du développement. Les expériences de blocage de transport du Reticulum au Golgi n’ont pas permis de conclure d’une manière certaine si les accumulations vacuolaires dérivaient d’un transport pouvant court-circuiter le Golgi comme dans les feuilles de Nicotiana. Au total, la cardosine A constitue une protéine modèle pour étudier les transports vacuolaires chez *Nicotiana tabacum* and A*rabidopsis thaliana*, deux systèmes hétérologues qui permettent de développer des méthodes complémentaires pour une exploration fonctionnelle des mécanismes impliqués. Cette étude permet de contribuer à une meilleure connaissance de la biologie des cardosines en particulier, et des protéases aspartiques en général. L’établissement de la lignée stable d’Arabidopsis exprimant la cardosin A taguée à une protéine fluorescente permettra une étude plus détaillée de la régulation des mécanismes de transport de la cardosine A au cours du développement de la plante.

RESUMO

A cardosina A é uma proteinase aspártica vacuolar normalmente identificada em vacúolos de armazenamento proteico e vacúolos líticos nas flores e em corpos proteicos em sementes de cardo, a planta nativa. A cardosina A foi isolada pela primeira vez há quase duas décadas e tem sido extensivamente caracterizada, quer em termos de distribuição tecidular e quer em termos bioquímicos. Na planta nativa vários papéis fisiológicos têm sido atribuídos à cardosina A, nomeadamente na reprodução, mobilização de reservas e remodelação de membranas. Para participar em eventos tão distintos, a localização e trânsito intracelular da cardosina A deve também variar ao longo dos vários compartimentos celulares: vacúolos de armazenamento proteico, vacúolos líticos, membrana citoplasmática (e, eventualmente, fora da célula). No entanto, a informação disponível relacionada com a biogénese, direccionamento ou trânsito para os diferentes compartimentos é ainda escassa, principalmente porque os protocolos disponíveis são de difícil aplicação na planta do cardo. Estudos recentes têm abordado a expressão da cardosina A em *Arabidopsis thaliana* e *Nicotiana tabacum* com resultados promissores para o uso destes sistemas no estudo desta proteína. Neste trabalho, estas observações preliminares foram o ponto de partida de um estudo detalhado da expressão, localização, direcionamento e vias de trânsito da cardosina A, recorrendo a vários e diferentes métodos. Ao longo deste estudo mostrou-se que a expressão transiente de cardosina A em folhas de *Nicotiana tabacum* é um bom sistema para explorar o trajeto da cardosina A no interior da célula, já que a proteína é processada de uma maneira semelhante à proteína nativa e se acumula no vacúolo. Além disso, uma linha de *Arabidopsis thaliana* com expressão da cardosina A sob ação de um promotor indutível foi utilizada para estudar a dinâmica da cardosina A em termos de acumulação vacuolar durante a germinação das sementes. Da mesma forma que o sistema de *Nicotiana tabacum*, este foi também validado para a expressão da cardosina A e permitiu concluir que a expressão da proteína não confere qualquer fenótipo às células ou indivíduos. No entanto, experiências realizadas em células BY-2 revelaram-se inconclusivas, já que a expressão da cardosina A expressão neste sistema não é previsível. Os dados obtidos ao longo deste trabalho envolvendo formas mutadas da cardosina, com deleção de domínios específicos ou mutações pontuais, permitiram determinar que a cardosina A possui dois sinais de endereçamento vacuolares, na sua sequência proteica: o PSI, um sinal não convencional, e o péptido C-terminal, um sinal de endereçamento C-terminal por definição. Foi também demonstrado que cada domínio representa uma via diferente para o vacúolo: o PSI escapa ao complexo de Aparelho de Golgi enquanto o péptido C-terminal segue um percurso clássico Retículo Endoplasmático-Aparelho de Golgi-Compartimento Prevacuolar para o Vacúolo. Esta diferença nas vias de trânsito não é observada para os sinais de endereçamento

vacuolar da cardosina B já que tanto como o PSI e como o péptido C-terminal precisam de passar pelo Aparelho de Golgi para alcançar o vacúolo. Um possível papel para a glicosilação nas vias de trânsito é abordado já que o PSI da cardosina A, ao contrário do da cardosina B, não é glicosilado. O estudo de mutações induzidas nos locais de glicosilação da cardosina A suportou esta hipótese. Para além disso, a expressão da cardosina A em sementes de *Arabidopsis thaliana* revelou uma acumulação diferencial em sementes não germinadas e em plântulas muito jovens. A cardosina A foi detetada ao longo da via secretora para o vacúolo de armazenamento proteico, em associação com o Retículo Endoplasmático, Aparelho de Golgi, Compartimento Prevacuolar e vacúolos líticos recém-formados. O tratamento com a droga Brefeldina A causou a retenção da proteína no Aparelho de Golgi, apesar de ter sido ainda detetada cardosina A no vacúolo, não sendo claro se o escape ao Aparelho de Golgi, observado nas folhas de *Nicotiana tabacum*, ocorre neste sistema. Em conclusão, este estudo permitiu confirmar que a cardosina A é um bom modelo para o estudo do direcionamento vacuolar nestes dois sistemas, que se complementam em termos de abordagens disponíveis. Este estudo proporcionou bons resultados a fim de compreender mais detalhadamente a biologia da cardosina em particular e o trânsito vacuolar das proteinases aspárticas de plantas, como um todo. Além disso, este estudo, e particularmente no que diz respeito à expressão em *Arabidopsis thaliana*, é um bom ponto de partida para outros ensaios envolvendo a utilização de fusões com proteínas fluorescentes e para explorar em mais detalhe a relação entre a cardosina A e o desenvolvimento.

TABLE OF CONTENTS

LIST OF TABLES

LIST OF FIGURES

ABBREVIATIONS

µg - microgram

µL - microliter

Aleu-GFP – Aleurain fused to Green Fluorescent Protein

APs – Aspartic Proteinases

APS – Ammonium persulfate

ARF1 - ADP-Ribosylation Factor 1

Arg – Arginine (aminoacid)

Asn – Asparagine (aminoacid)

ATP – Adenosine-triphosphate

B5 – Gamborg's B5 medium

BFA – Brefeldin A

BiP - Binding protein

Bl – Barley lectin

BSA – Bovine serum albumine

BY2 – Bright Yellow 2 cells

CaMV – Cauliflower Mosaic Virus

CCV – Clathrin Coated Vesicle

cDNA – Complementary DNA

CHC – clathrin heavy chains

CLC - clathrin light chains

CLSM – Confocal Laser Scanning Microscopy

C-ter – C-terminal peptide

ctVSD – C-terminal vacuolar sorting determinant

cv. - cultivar

Cys – Cysteine (aminoacid)

d - day

Dex - Dexamethasone

DIC – Differential Interference Contrast

DIP - dark intrinsic protein

DMF - N,N-Dimethylformamide

DMSO - Dimethyl sulfoxide

DNA – Deoxyribonucleic acid

dNTPs – Deoxyribonucleotides tri-phosphate

DSG - Aspartate-Serine-Glycine motif

DTG - Aspartate-Threonine-Glycine

DTT - Dithiothreitol

DV – Dense vesicle

EDTA - Ethylenediaminetetraacetic acid

EE – Early Endosome

En6 – 6 times enhancer

ER – Endoplasmic reticulum

ERAD - ER-associated protein degradation

ERES – ER export sites

ESCRT - endosomal sorting complex

FP – Fluorescent protein

GA – Golgi apparatus

GAP - GTPase-activating protein

GDP - guanine diphosphate

GEF - guanidine-nucleotide exchange factor

GFP – Green Fluorescent Protein

Glc – Glutamine (aminoacid)

Gly – Glycine (aminoacid)

GNL1-YFP – GNOM like1- Yellow Fluorescent protein

GTP - Guanosine-5'-triphosphate

GUS - β-glucuronidase

H - hour

HEPES - 4-(2-hydroxyethyl)-1-piperazineethanesulfonic acid

Hsp70 - 70 kilodalton heat shock proteins

Hsp90 - 90 kilodalton heat shock proteins

Hygr - Hygromycin

Ile - Isoleucine

IPTG - Isopropyl β-D-1-thiogalactopyranoside

Kb - Kilobase

kDa - Kilodalton

kV - Kilovolts

KV - KDEL vesicles

LB – Luria Bertani medium

LE – late endosome

LRW – London resin White

LV – Lytic vacuole

M-6-P - mannose 6-phosphate

mF - microfarads

Min - minute

mL – milliliter

mM - millimolar

mm - millimeter

MOPS - 3-Morpholinopropanesulfonic acid

mRFP – Red Fluorescent Protein

MS – Murashige and Skoog medium

MVB – Multivesicular Body

NBT-BCIP - Nitro Blue Tetrazolium- 5-bromo-4-chloro-3-indolyl phosphate, p-toluidine salt

Nm - nanometer

OD – Optical Density

ON - Overnight

p - protoplasts

PAC – Precursor accumulating vesicles

PBS – phosphate buffer saline

PCD – programmed cell death

PCR – Polymerase Chain Reaction

PCR - partially coated reticulum

PDI - protein disulfide isomerase

PEG - Polyethylene Glycol

PM – Plasma membrane

Pre – Signal peptide present in aspartic proteinases precursor

Pro – Prosegment present in aspartic proteinases precursor

PSI – Plant Specific Insert

PSV – Protein Storage Vacuole

psVSD – physical structure vacuolar sorting determinant

PV72 - type I membrane protein

PVC – Prevacuolar Compartment

RB – Right Border

RGD - Arginine-Glycine-Asparagine motif

RME - receptor-mediated endocytosis

RMR - Receptor Homology-transmembrane-RING H2 domain

Rpm – rotation per minute

RT – Room Temperature

SAPLIP – saposin-like protein

SDS – Sodium dodecyl sulphate

SDS-PAGE – SDS-Polyacrylamide gel electrophoresis

Sec-GFP – Secreted Green Fluorescent Protein

Ser – Serine (aminoacid)

SNARE - soluble N-ethylmaleimide sensitive factor adaptor protein receptor

SP – Signal Peptide

ssVSD – sequence specific vacuolar sorting domain

STET – sucrose-triton-EDTA-Tris buffer

ST-GFP – Syaliltransferase-green fluorescent protein

TAE – Tris-acetate-EDTA buffer

TBS – Tris buffer saline

TBS-T - Tris buffer saline with tween 20

TCA – Trichloroacetic acid

TEM – Transmission Electron Microscopy

TEMED - N, N, N', N'-Tetramethylethylenediamine

TGN – Trans-Golgi network

Thr – Threonine (aminoacid)

TIP – Tonoplast Intrinsic Protein

Tnos – Nopaline synthase terminator

UDP – Uranyl diphosphate

UPR - Unfolded Protein Response

UV - UltraViolet

V - volt

V - vacuoles

VAMP - Vesicle associated membrane protein

VSD – vacuolar sorting determinant

VSR – vacuolar sorting receptor

VSS – vacuolar sorting signal

WT – Wild type

1.INTRODUCTION

1.1. SCIENTIFIC CONTEXT OF THE THESIS

Plants play an important role in worlds' economy as they represent the major source of food, but also of textiles, building materials, bio-fuels and medicinal products. In the past decades, plants have also been exploited for the production of recombinant pharmaceutical products, such as edible vaccines, antibiotics and vitamins. Plant biologists are currently joining efforts for plant science to progress in the direction of a definition of integrated circuits of metabolic pathways and sub-cellular structures to accompanying the challenges imposed by animal and yeast sciences.

Besides understanding plants as a whole organism it is fundamental to track the subcellular mechanisms beneath. Identifying the molecules (proteins and enzymes), their biogenesis and their functions is fundamental to understand their role in plant cell homeostasis and ultimately to develop rational crop improvement strategies. The plant cell is effectively an integrated community of membrane-delimited compartments, each of which has evolved to optimize and separate specific biochemical functions. Functional organization of the endomembranes is a key cell infrastructure to permit to the cell the continuous adaptation needed for the metabolic and structural changes occurring in vegetative and reproductive tissues. The major production line of the cell biosynthetic factory is made by distinct organelles constitutive of the cell secretory pathway: Endoplasmic Reticulum, Golgi Apparatus, Endosomes, Pre-vacuolar and Vacuolar compartments. The specificities of plant endomembrane biology, notably the Endoplasmic Reticulum-Golgi complex (Hawes & Satiat-Jeunemaitre 2005; Moreau et al. 2007) or the endosomal and vacuolar organization, outline the amazing ability of plant cells to re-organize its membrane system according to the cell need.

The today studies on plant endomembrane focus on several lines of research: the functional characterization of compartments designing the endomembrane system, the identification of pathways and vesicle carriers to transport cargo molecules from one compartment to the other and the identification of molecular machineries associated with these transport specificities. Any protein trafficking within the endomembrane system is orchestrated by all the events, permitting to reach the right compartment, by the right route, at the right time.

Cardosin A, the model protein in this project, is an aspartic proteinase extracted from cardoon which is of great economical interest in Portugal. Cardosin A has been previously identified as a protein trafficking through the endomembrane system, and ending in the vacuolar compartments. The main question guiding our project was to

know how Cardosin A reaches the vacuole. In order to develop a proper experimental strategy to answer this question (see chapter 2 of this manuscript), a literature survey of the endomembrane system was first needed to (1) frame this complex field of protein trafficking through the endomembrane system (paragraph 1.2 of this section) and to (2) better understand the biology of Cardosin A protein (paragraph 1.3. of this section).

1.2. PLANT ENDOMEMBRANE AND SECRETORY PATHWAY: A BIBLIOGRAPHY SURVEY

The today studies on plant endomembrane system focus on two main lines of research: the functional characterisation of compartments designing this endomembrane system, and the identification of the molecular machinery involved in the dialogue/transport of cargo molecules between these compartments. Many reviews and books treat the subject of membrane trafficking within eukaryotic cells, under different lights, focused on distinct aspects, based on several biological models, headed by sometimes controversial hypotheses. In this literature survey, we have chosen to concentrate on the events known to be involved in vacuolar trafficking, and its surroundings, which should provide the keys to establish our experimental strategy.

1.2.1. The endomembrane system

The endomembrane system of eukaryotic cells includes organelles belonging to the secretory and endocytic pathways: the endoplasmic reticulum, the Golgi apparatus, the trans-Golgi network, the prevacuolar compartment, endosomes, lytic and storage compartments (vacuoles) and the plasma membrane (Figure 1.1) (Nebenführ 2002). The structural integrity and functional complexity of each of these compartments is essential for processing, targeting and transport of macromolecules (Satiat-Jeunemaitre et al. 1999; Vitale & Galili, 2001; Foresti & Denecke, 2008).

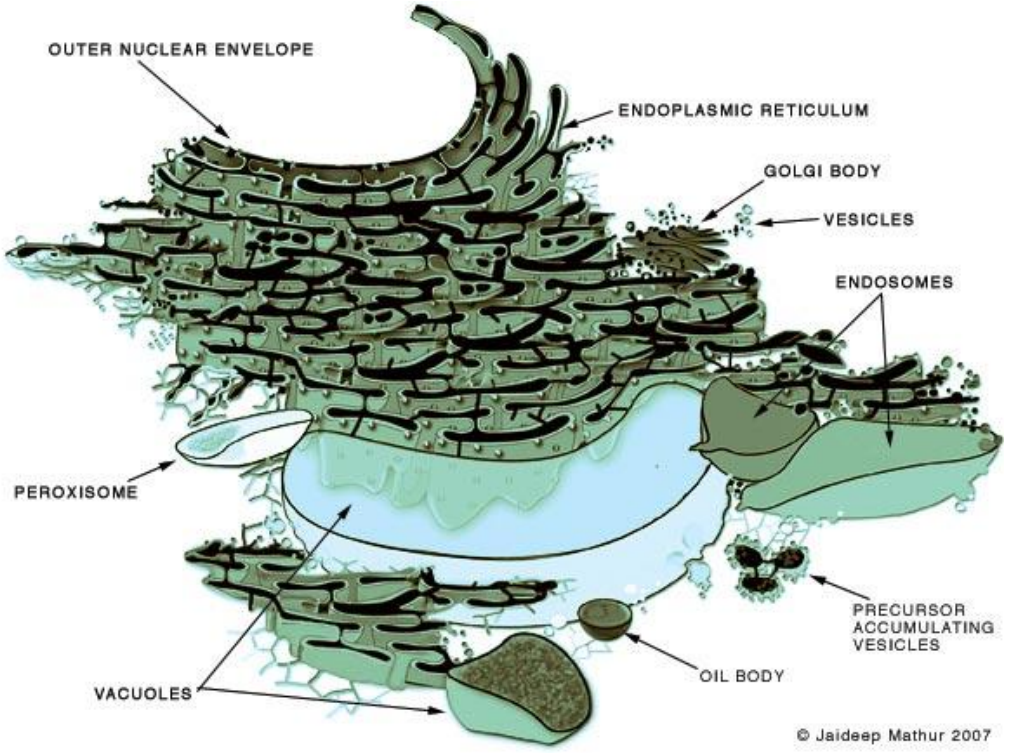

Figure 1.1 Schematic representation of the endomembrane system of a plant cell. Adapted from http://www.illuminatedcell.com.

The plant endomembrane system shares its basic characteristics with yeast and mammalian equivalents but, at the same time, a variety of specific adaptations mark its distinction. This exclusivity is for instance flagrant in its functional relations with the cytoskeleton, in the variety of cargo molecules transport routes, and in some specificities in molecular machinery associated with these transport events (Nebenführ, 2002; Frigerio & Hawes, 2008).

The isolation and cloning of the fluorescent reporter Green Fluorescent Protein (GFP) for expression in plant cells has allowed a revolution in the study of cell endomembranes. In a short time-span the fluorescent proteins have become unreplaceable tools for *in vivo* investigation of the regulation and dynamics of intracellular compartments (Sheen et al. 1995; Satiat-Jeunemaitre et al. 1999; Brandizzi et al. 2004). GFPs' characteristics are enormous. It is a non-invasive reporter that retains its fluorescence even when fused to other proteins and is expressed in a wide range of biological systems. GFP is extremely photostable and presents no toxicity to cells, can be expressed both in the N- or C-terminal ends of other proteins and does not affect the partner protein's activity. Furthermore, GFP and GFP-tagged proteins can be directly observed in living cells (Sheen et al. 1995; Satiat-Jeunemaitre et al. 1999). The enormous success of GFP motivated the search and production of novel fluorescent proteins ranging other colors of the visible spectra (Shaner et al. 2004). Nowadays,

having organelle-targeted probes using different color variants we can shed light into the plant cell and observe the different organelles and the interactions occurring between them. The availability of probes and protocols for its expression in several systems associated to the development of optical instrumentation for its observation have been revolutionizing the imaging of plant endomembranes (Mathur, 2007; Shaner et al. 2007; Held et al. 2008). More recently a novel fluorescent protein category has become available: photoconvertible and photoactivatable fluorescent proteins, commonly termed “optical highlighters”. These proteins have the characteristic of switching their fluorescent emission spectra as a result of structural changes induced by a specific wavelength pulse. They allow specific tracking of organelles or protein movements and pulse-chase analysis within a differentially labeled population (Shaner et al. 2007; Brown et al. 2010; Mathur & Radhamony, 2010).

Endoplasmic Reticulum

The Endoplasmic Reticulum (ER) is the starting point of the endomembrane system chain and has several important roles such as synthesis, quality control and export of proteins, calcium storage, phospholipid synthesis and fold and oligomeric proteins assembly. The traditional view of the ER network describes the existence of the smooth ER, composed of tubular structures without ribosomes, and the rough ER, mostly composed of ribosome-associated cisternae. However, recent findings have changed this view into a more dynamic one, where the distinct ER shape is correlated with specific cellular conditions and in response to specific stimuli (for review, Sparkes et al. 2011). Unlike in mammals, the remodelling and movement of the ER network in dependent on actin cytoskeleton and is independent of the Golgi apparatus, despite the physical connectivity existent between them. Recent observations allowed proposing that besides movement of the entire ER network, the membrane surface of the ER is also mobile. Despite being clear that ER architecture is influenced by the cytoskeleton, it is also clear that other factors are responsible for maintaining its structure. Structural proteins, such as Reticulons, DP1/Yop1 and dynamin-like GTPases, and membrane lipid composition seems to play a key role in ER cisternae and tubules shaping (for review, Sparkes et al. 2011).

Proteins destined to the secretory pathway enter the ER cotranslationally in a process dependent on a N-terminal signal peptide, which is removed while the nascent polypeptide is emerging into the ER lumen. The removal of the signal peptide is essential for correct folding of the nascent protein, and non-removal of this segment causes the

protein to remain anchored to the membrane. The current model for protein translocation into the ER considers the existence of a multiprotein pore (translocon pore) where the nascent polypeptide emerges on the ER lumen and begins to fold. Protein folding in the ER is assisted by folding enzymes such as protein disulfide isomerase (PDI), which catalyses the formation of disulfide bridges (for review, Vitale & Denecke, 1999). N-linked glycosylation of secretory proteins is also acquired in the luminal side of the translocon pore, where the enzyme oligosaccharyl transferase transfers the oligosaccharide from a lipid burier in the ER membrane to the Asn residues of the newly formed polypeptide.

Most of the ER resident proteins are folding and assembly helpers that keeps the newly synthesised proteins in this organelle until they acquire the correct folding to be then transported to the following destination. These proteins also participate in the retention of mal-folded proteins in the ER in a process commonly denominated quality control that is part of the Unfolded Protein Response (UPR) pathway (for review, Vitale & Boston, 2008). Interestingly, an increase of misfolded protein in the ER induces the increase of these quality control helper proteins, resulting in the removal of defective proteins from their normal pathway and their targeting for degradation. The impairment of progressing in the secretory pathway is caused by permanent association of the mis-folded proteins with ER chaperones, namely from the BiP (Binding protein) family (Pimpl et al. 2006). This prolonged interaction results in ER-associated protein degradation (ERAD), a protein degradation pathway where misfolded proteins are dislocated to the cytosol, ubiquitinated and eventually degraded by the proteasome (Pimpl et al. 2006; Vitale & Boston 2008).

Golgi Apparatus

In plants, the Golgi apparatus (GA) is a central key in relation to the synthesis of cell wall polysaccharides, for glycolipids and glycoproteins for the cellular membranes. It has thus an important role in the modification and targeting of the protein and is involved in folding, processing and storage of proteins. In contrast to mammalian cells where the GA is several times limited to a perinuclear region, in plant cells the GA are distributed within the cytoplasm and in tight relation with the ER (Vitale & Galili, 2001; Hawes & Satiat-Jeunemaitre, 2005).

Early electron microscopy studies describe the plant GA as a complex tubulo-saccular structure, with some contacts with endoplasmic reticulum. Indeed, the GA is functionally divided into individual cisternae, generally regarded as functionally

independent. It is described as a polarized structure, since the morphology and the enzymatic activity gradually change from the cis-face to the trans-face (Satiat-Jeunemaitre et al. 1999; Neumann et al. 2003; Masclaux et al. 2005). This polar organisation is then correlated with a functional division of the GA into cis-, medial- and trans-cisternae, where the cis-face corresponds to the entry site, closer to the ER, and the trans-face would correspond to the exit/maturing site (Hawes & Satiat-Jeunemaitre 2005). Associated with the Golgi stacks at the trans-face is described, for the animal models, a Trans-Golgi Network (TGN). However, the exact nature and functionality of a distinct TGN in plant cells is still controversial and the term has been attributed to the structural profiles the trans-most cisternae of the GA can display. This last cisternae presents in all cases various degrees of tubulation and may appear fully distinct from the Golgi stack, only partially detached or cohesive with the rest of the stack (for review, Hawes & Satiat-Jeunemaitre, 2005). In any case, the TGN was accepted as analogous to the partially coated reticulum (PCR), a tubulo-vesicular compartment, with clathrin buds, which may function as an early endosome. Currently, it is accepted that the plant TGN is not just the trans-most GA compartment but is a completely separate organelle (Foresti & Denecke, 2008). Recent observations suggested that the TGN is a semipermanent independent organelle that cycles on and off of the GA stacks (Kang et al. 2011).

The distribution of GA enzymatic machinery is quite stable across the GA stacks which contrast with the continuous flow of secretory products, in a process that requires a large number of regulatory proteins (Nebenführ & Staehelin, 2001). The majority of GA-resident enzymes are integral membrane proteins and the mechanism associated to the retention in the GA seems to be related to the presence of a signal anchor sequence in the transmembrane domain (Hawes & Satiat-Jeunemaitre 2005). This mechanism of retention in the GA is thought to be conserved across kingdoms as the signal anchor from both rat and human transferases is sufficient to target an engineered GFP to the plant GA.

Contrastingly with the mammals and saccharomyces Golgi elements that are static structures or present slower movements, plant GA displays translational movements and is viewed as “mobile factories” involved not only in the production but also in the distribution of secretory products. In a similar fashion as the ER, the GA in plant cells move along actin filaments using myosin motors. Interestingly, the GA movements are not uniform but follow a stop-and-go pattern (Nebenführ & Staehelin, 2001). Despite the motility of the Golgi bodies, the stacks are very stable during movement and does not seem to lose their shape or even stop intra-GA transport. This stability is due to a ribosome-free “Golgi matrix” around the GA that is

thought to have a role in protecting the stacks (Nebenführ & Staehelin, 2001; Hawes & Satiat-Jeunemaitre, 2005). Furthermore, the intercisternal elements and oligomerisation of transferases also seems to be involved in binding the cisternae together (Hawes & Satiat-Jeunemaitre 2005).

Several authors propose the existence of a membrane continuum between the ER and GA, based in co-visualization of both compartments under electron or fluorescence microscopy. These observations suggest that GA stacks are associated to the cortical ER network and appear to be attached and move over the surface of the ER tubules. Furthermore, and supporting this idea, the biochemical separation between ER and GA membranes has proved to be difficult in plant cells (Boevink et al. 1998; Saint-Jore et al. 2002; Hawes & Satiat-Jeunemaitre 2005). This close association led to the proposal that the GA would be a differentiated domain of the ER and thus the regulation of its biogenesis would be totally dependent on membrane flow from the ER (Hawes & Satiat-Jeunemaitre 2005). GA biogenesis from the ER membranes has also been suggested for other eukaryotic models, but the distinct molecular signature of ER and GA is yet to be explained by this model.

Vacuoles

In most of the plant cells, the vacuole is the largest structure present and plays several roles in maintaining organization and cellular function and is involved in intracellular digestion of various materials, maintaining of turgor and accumulation of nutrients, ions and secondary metabolites. In seeds, the most abundant are protein storage vacuoles (PSVs) whereas in vegetative tissues the vacuolar functions are accomplished by large central vacuoles denominated lytic vacuoles (LV) (Matsuoka & Nakamura, 1991; Martinoia et al. 2007). The plant vacuolar system can become quite complex as in the same cell can co-exist two types of functionality distinct vacuoles (Paris et al. 1996). Each type of vacuole is commonly characterized by the type of aquaporin present in the tonoplast - tonoplast intrinsic proteins (TIPs): TIP-γ, lytic vacuole and α-TIP, protein storage vacuole (Vitale & Raikhel, 1999; Paris & Neuhaus, 2002). However, the real situation can be much more complicated since overlap of both markers has been observed in vacuolar remodeling during transition between distinct types of vacuoles (Olbrich et al. 2007; Bolte et al. 2011). Furthermore, specialized vacuoles can be found in specific cells

as the ones responsible for rapid water loss during movement of pulvini in *Mimosa pudica* motor cells (Martinoia et al. 2007).

Lytic vacuoles correspond to the large central vacuole observed in vegetative tissues. It contains hydrolytic enzymes, including aspartate proteinases, cysteine proteinases and nucleases, that degrade cellular materials that are no longer required (Hara-Nishimura & Hatsugai 2011). The lytic vacuoles are also involved in defense-related mechanisms related to programmed cell death (PCD), in a process denominated by vacuole-mediated cell death. Two different ways for vacuole-mediated cell death are described: destructive type, involving collapse of the tonoplast, and a non-destructive type, occurring trough membrane fusion of the vacuolar membrane and the plasma membrane. This response is not only used against pathogens or toxins, but is also a developmental mechanism for cell death to generate integuments and tracheary elements (Hara-Nishimura & Hatsugai 2011).

PSVs is mostly abundant in seeds and was first describe to be composed of three morphological distinct regions, being the matrix and the crystalloid responsible for protein storage and the globoid, composed of phytic acid crystals (Jiang et al. 2000; Jiang et al. 2001). This description has later been composed with results that demonstrated that the crystalloid also contains integral membrane proteins and lipids. This internal structure was described as a result from uptake of cytoplasmic prevacuolar organelles (dark intrinsic protein organelles - DIP) (Jiang et al. 2000). Furthermore, Jiang et al. (2001) demonstrated that the globoid was also defined by a membrane marked with vacuolar H^+-pyrophosphatase and γ-TIP, indicating that proteins destined for the globoid are sorted in a different manner from the proteins destined to the PSV and proposed a model by in which a globoid compartment could be assembled within the developing PSV.

Vacuolar development and remodeling during seed germination has gained a notorious importance given the immense changes occurring in a short time. During seed germination, storage protein, which provide a source of reduced nitrogen, and inorganic minerals need to be mobilized to support seedling growth. In addition, a lytic aqueous vacuolar compartment has to be formed to provide turgor pressure driving cell expansion and to promote radicle protrusion and embryo elongation. It has been proposed that vacuolar membranes of PSV are transformed into those of central vacuoles upon germination (Maeshima et al. 1994). Findings in soybean and pumpkin have shown that during germination the PSV undergoes an important dedifferentiation with gradual degradation of α-TIP, internalisation of the tonoplast and formation of a new tonoplast carrying vacuolar H+-ATPase, V-PPase and γ-TIP (Maeshima et al., 1994; Inoue et al. 1995). However, this rearrangement

of the vacuole seems to be related to the type of cell, and eventually its specialization, since Olbrich et al. (2007) observed that in meristematic cells a single vacuole type is formed initially presenting characteristics of both PSV and LV, that is gradually transformed into a central vacuole as the differentiation proceed. Recently, Bolte and colaborators (2011) described the remodeling of *Arabidopsis thaliana* vacuome upon germination, illustrating the complexity of this system. Their results demonstrate a rapid and extreme reorganization of PSVs and LVs during early stages of seed germination, with the coexistence of two distinct compartments with very distinguishable roles.

The vacuolar metabolome has gained interest recently as the preliminary results obtained provide the basis for future studies to compare the storage and lytic metabolomes that would allow a more comprehensive understanding of the vacuolar systems of transport and metabolism (Tohge et al. 2011).

1.2.2. The vesicular carriers and main trafficking routes

Most of the secretory compounds begin their synthesis in the cytosol and their target is dependent on the information in their amino acid sequence. In the case of proteins destined for the secretory pathway, the sequence contains a signal peptide (SP) for the ER. Soluble proteins destined to enter the secretory pathway are synthesized on ribosomes bound to the ER membrane and, depending on the information contained in the peptide chain, a newly synthesized protein can be retained in the ER, be directed to the GA for further sorting to specific compartments, such as the plasma membrane or the vacuoles or bypass the Golgi to go over towards other membranous structures (Figure 1.2) (Neuhaus & Rogers, 1998; Nebenführ, 2002; Hanton et al. 2007; Held et al. 2008).

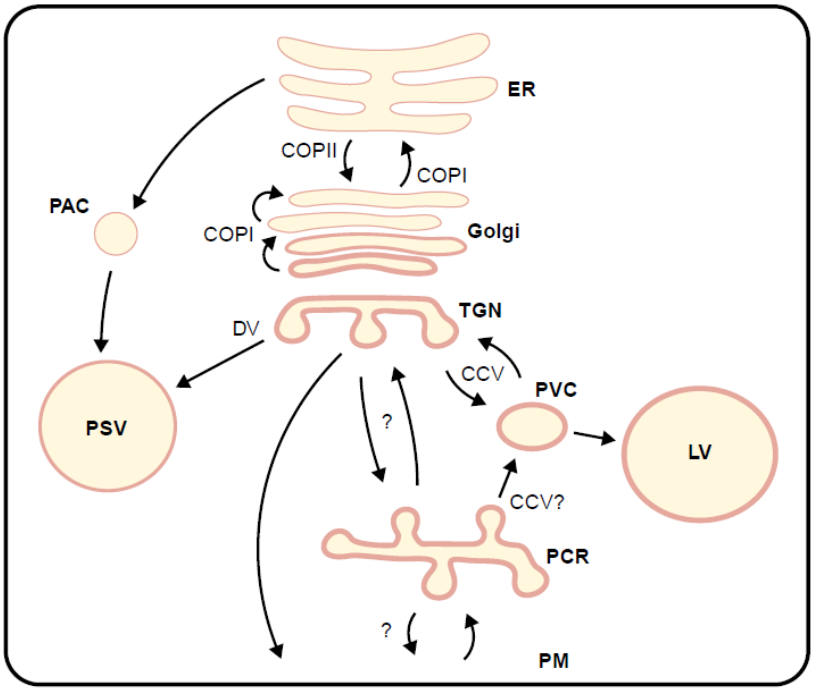

Figure 1.2 Drawing of the secretory membrane system and membrane exchange routes. Forward and retrograde transport routes between compartments are represented along with the transport vesicles. ER – Endoplasmic Reticulum; PAC – Precursor accumulating vesicle; DV – Dense vesicle; PSV – Protein storage vacuole; CCV – Clathrin coated vesicle; PVC – Prevacuolar compartment; LV – Lytic vacuole; PCR – Partially-coated reticulum – PM – Plasma membrane. Adapted from Nebenführ (2002).

The forward transport of molecules to the distal compartments of the cell must be balanced by a retrograde transport to allow membranes and carriers turnover between compartments (Held et al. 2008).

The transport of proteins and membranes between the different compartments of the secretory pathway is mediated by small carriers comprising the transport vesicles. This mechanism is, in its essence, similar along the different transition points of the secretory pathway, despite the molecular effectors in the processes may differ between compartments (Figure 1.2). In plant cells two types of vesicles can be distinguished based on their surface morphology: non-coated and coated. The non-coated vesicles may be involved in cargo molecule transport to the plasma membrane (exocytic vesicles) or protein storage vacuole (Precursor accumulating vesicles and dense vesicles). They display a smooth surfaced. Most of them originate from ER-Golgi budding membranes, or in some cases from plasma membrane. The coated vesicles on the contrary are formed with a protein coat on their cytoplasmic surface, which is later removed to allow vesicle fusion, as is the case of COPI, COPII and clathrin-coated vesicles, that work in the ER-GA and TGN-vacuole/plasma membrane, respectively (Hanton et al. 2005).

Relating to coated vesicles, the assembly mechanism is similar between then, involving the formation of a proteinaceous membrane coat that will deform the membrane to form a bud and eventually a vesicle (Nebenführ, 2002). GTPases from the Ras superfamily are activated by a specific guanidine-nucleotide exchange factor (GEF) and control the assembly of the coat vesicle. A dynamin-like GTPase will also participate in the process by controlling the release of the transport vesicle from the membrane. Finally, the transport vesicle needs to release its cargo in the target compartment. This process is mediated by SNARE molecules (soluble N-ethylmaleimide sensitive factor adaptor protein receptor): v-SNARE in the transport vesicle and t-SNARE in the target. The interaction between these two SNARES is regulated by small GTPases from the Rab/Ypt family and will allow vesicle fusion and cargo release (Nebenführ, 2002; Hanton et al. 2005).

Precursor accumulating vesicles

Precursor accumulating vesicles (PACs) were identified in seeds and are related to a GA-independent pathway for storage protein in maturating cotyledons (Hara-Nishimura et al. 1998). These vesicles contain mainly unglycosylated storage proteins and precursor molecules that are further activated in the vacuole. The formation of the vesicle results from protein agglomerates in the ER that eventually buds from the membrane in direction to the PSV. This mechanism was first thought to be independent of signal receptors, but the isolation of a type I membrane protein - PV72 (a member of the family of vacuolar sorting receptors) - from PAC vesicles anticipated the existence of sorting receptors for storage proteins (Jurgens, 2004). The final step of incorporation in the PSV can occur by one of two modes: autophagy of the vesicle by the vacuoles or membrane fusion between PAC vesicles and the vacuoles. None of this processes has been completely illustrated with the existence of evidences for both mechanisms (Hara-Nishimura et al. 1998). Despite existing a GA-bypass of proteins transported in PAC vesicles, storage proteins carrying complex glycan chains has been observed in the periphery of such vesicles. This may indicate that these glycoproteins have been sequestered into the PAC vesicle en route to the PSV or they may be transported to the GA and recycled back to the ER for transport (Hanton et al. 2005).

Dense vesicles

Similarly to PAC, dense vesicles (DV) have been described in endosperm and cotyledons of several plant seeds and participate in protein transport between the GA and the PSV. DV begin to form at the cis-most GA cisternae and seems to undergo maturation as it progresses through the stack. This type of uncoated vesicle carries diverse cargo molecules: storage proteins (unprocessed and mature), precursor molecules and inactive endoproteases. No vacuolar receptor has been identified in DV, but they are known to carry the PSV aquaporin αTIP (Robinson et al. 1998).

The aggregation of proteins in the GA cisternae is accepted as the mechanism for vesicle induction, whether is not known if this event is chaperone-mediated or if it occurs spontaneously after a critical concentration of protein is exceeded. This aggregated protein mass interacts with a hydrophobic subpopulation of the same proteins which are already attached to the membrane at the TGN and induces the budding of the secretory granule. Membrane association and aggregation resulting from hydrophobic protein-protein interaction will be the basis for vesicle release (Robinson et al. 1998). A mechanism similar to the one regulating secretion in mammalian gland cells has been suggested in which proteins can aggregate around membrane-bound nucleation factors interacting with the GA membrane triggering DV budding. The plant-specific RMR protein has been pointed as a potential candidate for the nucleation factor (Jolliffe et al. 2005). The incorporation of the vesicle in the PSV may occur by autophagy or membrane fusion, as described for the PAC vesicles.

COP vesicles

Despite originating in different compartments (ER and GA, respectively) COPII and COP I transport are very similar. The formation of both coat vesicles requires the activation of a specific small GTPase followed by the recruitment of structural elements to the membrane, resulting in the formation of the vesicle.

COPII is basically composed of three cytosolic components: the small GTPase Sar1p (secretion associated, ras-related protein1) and two structural heterodimers, Sec23/24 and Sec13/31 (Matheson et al. 2006). The formation of COPII vesicles begins with the recruitment of coating components from the cytoplasm to the ER surface by the action of Sar1p (Barlowe 2003). Sar1, which is inactive when bound to cytosolic guanine diphosphate (GDP), undergoes activation by the action of a guanine-nucleotide-exchange factor (GEF), more specifically the

Sec12p located in the ER membrane (Figure 1.3). Sar1p activation will be responsible for the recruitment of the heterodimeric complex of Sec23-Sec24p to generate a pre-budding complex. This action finally induces membrane curvature and deformation and eventually budding of COPII vesicles (Hanton et al. 2005). The protein coat must then be released to allow vesicle fusion with the target membrane in the GA. Sar1p mediates this process trough hydrolysis of GTP, causing a conformational change and release of Sar1 from the membrane, which, in turn, causes the dissociation of the coat proteins. The membranous vesicle can then fuse with the GA membrane and released the cargo (Figure 1.3) (Futai et al. 2004; Hanton et al. 2005).

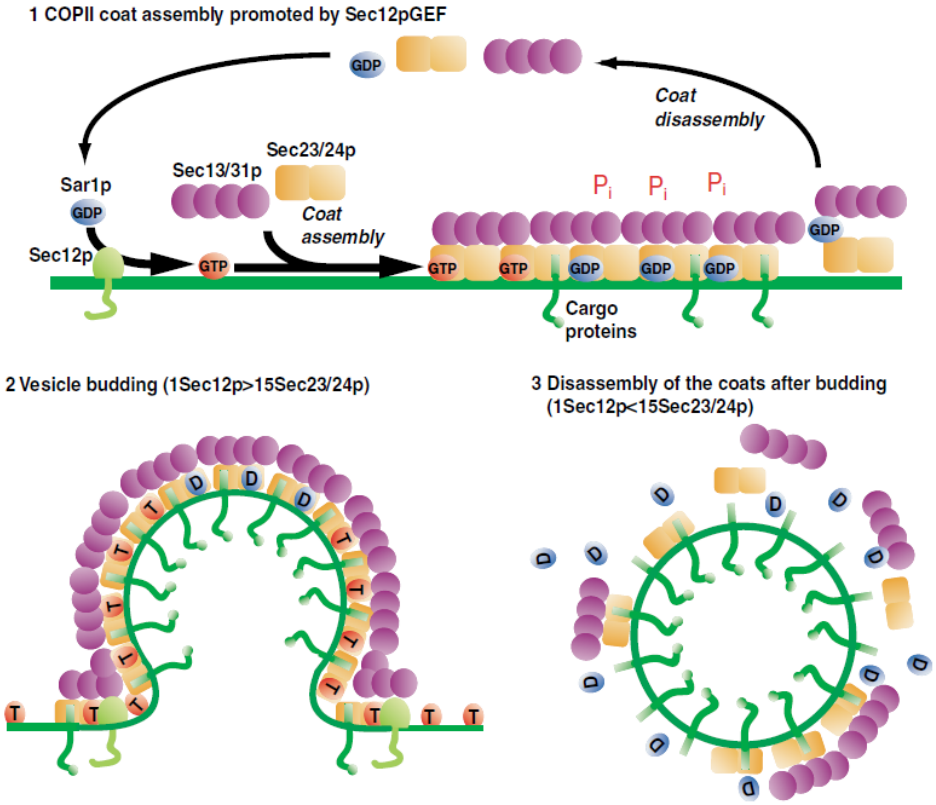

Figure 1.3 Schematic representation of the formation and disassembly of a COP II vesicle. Adapted from Futai et al. (2004).

The retrograde route is mediated by COPI-coated vesicles, which consists of the small GTPase ADP-RIBOSYLATION FACTOR1 (ARF1) plus a heptameric complex of structural coat components (Matheson et al. 2006). COPI vesicles consists of a coatomer, a stable cytosolic complex comprising seven subunits and z-COP, as well as the small GTPase ARF1p. In a similar process to the one described for COP II assembly, COPI coat assembly (Figure 1.4) is initiated by the exchange of GDP for GTP by ARF1p. This form will then interact with p23, a GA membrane

protein, through the myristoylated N-terminus of the GTPase. Interaction of ARF1p with the membrane occurs by the exchange of GDP for GTP (mediated by a GEF). The activated membrane-associated ARF1p recruits the preassembled coatomer from the cytosol inducing membrane curvature of the membrane and, finally, a vesicle that can then bud from the membrane (Hanton et al. 2005; Beck et al. 2009).

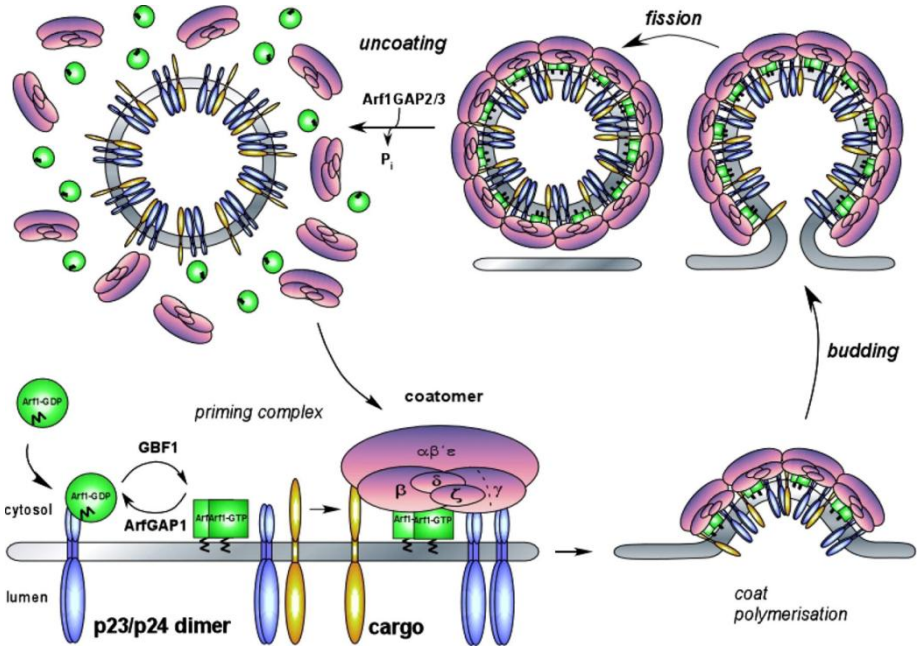

Figure 1.4 Sequential steps in the formation of a COPI-vesicle. Adapted from Beck et al. (2009)

The importance of the secretory pathway, and particularly ER-to-GA routes mediated by COP vesicles, is clearly demonstrated by the disruption of COP-mediated transport which has a dramatic effect on protein transport within the cell. Interferences in the GTPase activity of Sar1p, for instance, lead to blockage of anterograde vesicular transport between ER and the GA, both in plants and animals. The fungal macrocyclic lactone Brefeldin A (BFA) is known to inhibit the function of ARF GTPases by interacting with their associated GEFs, blocking the transport between the ER and the GA. Furthermore, inhibition of COPI function results in impaired ER export and disruption of the ERES. The inhibition of vesicle budding or fusion also affect the both anterograde and retrograde transport, resulting in an inhibition of both pathways (Hanton et al. 2005).

Clathrin-coated vesicles

Clathrin-coated vesicles (CCVs) are known to form at the plasma membrane (participating in receptor-mediated endocytosis - RME) and at the TGN (being involved in vacuolar trafficking). Clathrin is one of the major coat proteins of CCV along with adaptors or assembly proteins (APs). Dynamins belong to the GTPase class of proteins and also participates in CCV assembling by scission of the vesicle from the membrane (Brodsky et al. 2001). The basic unit of clathrin is termed triskelion (three-legged pinwheel shape). Triskelions are hexameric units possessing three heavy chains (CHC) and three light chains (CLC) polypeptides with the ability to form a polyhedral lattice. This self-assembly property of clathrin coat is fundamental for selectively sequester protein cargo (Robinson et al. 1998).

CCVs formation requires the interaction not only of CCVs coat proteins but also cargo molecules (Figure 1.5). The cargo molecules are associated to the cargo receptor (a transmembrane protein) and the complex thus formed is recognized by adaptin and further combined with the coat protein in the cytosolic side. Each coat protein unit has binding sites for several adaptor molecules, cargo receptors and cargo, resulting in a concentration of cargo proteins in the budding area. After budding, dynamin constricts the neck of the forming vesicle allowing its release from the membrane, in an ATP-dependent manner. Uncoat of CCVs is achieved by dissociation of coat proteins from lipids and from each other. Clathrin and adaptors dissociate from CCVs in separate steps and is promoted by adaptor phosphorylation in the clathrin-binding domain. Following hydrolysis and coat dissociation, a pool of cytosolic clathrin associated with hsp70 forms a cytosolic complex ternary complex that will stimulates guanine nucleotide exchange (ARF1 and Rab proteins) contributing to clathrin recruitment at the TGN (Brodsky et al. 2001).

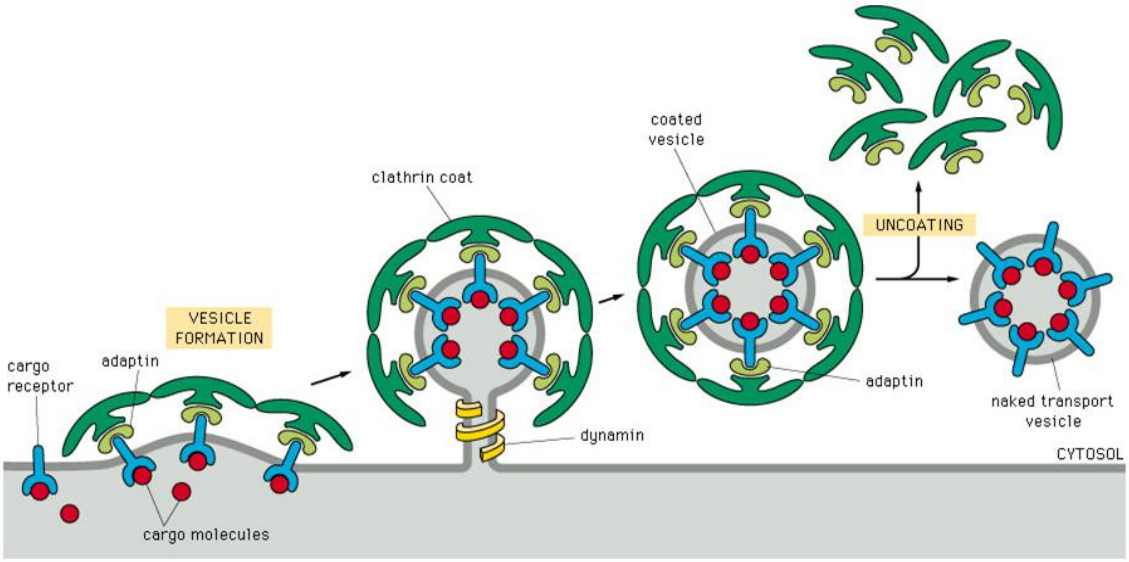

Figure 1.5 Schematic representation of clathrin-coated vesicles. Adapted from Alberts et al. 2004.

1.2.3.Vesicle exchange machinery

The proteins responsible for determining the specificity and subsequent fusion between a transport vesicle and their corresponding target membrane are, among others, Rab GTPases and SNAREs. Both Rab and SNAREs have a characteristic endomembrane distribution in eukaryotic cells which determines the specificity of the recognition between transport vesicles and target membranes. In a simplistic manner, anchoring of a transport vesicle to the membrane compartment is regulated by a specific Rab GTPase and the specificity of membrane fusion is dependent on the pairing of the transport vesicle SNARE (v-SNARE) with the SNARE located in the acceptor membrane (t-SNAREs). The pairing between the v- and t-SNAREs will allow a physical proximity between the two membranes necessary for fusion to occur and the subsequent release of the contents of the vesicle in the lumen of the target organelle (Sanderfoot & Raikhel 1999).

After docking to the target organelle, the transport vesicle, already deprived from the coat, needs to fuse to the target membrane in a process that is executed by SNARE proteins (Figure 1.6). The SNARE family is conserved among all eukaryotes and is characterized by a common heptad-repeat motif. SNAREs are classified according to the conserved arginine or glutamine present at the “0-layer” in Q- and R-SNAREs, alongside of the operational t- and v-SNARE classification (Pratelli et al. 2004). Both operational (t- and v- forms) and structural (R- and Q- forms)

designations are commonly used, despite the last ones are more frequently found. The SNARE complex is a stable complex composed of four SNARE molecules that will be responsible to pull in close proximity the membrane bilayer of the transport vesicle and the target membrane, to allow membrane fusion. This fusion is a highly specific process that requires a specific combination of SNARE proteins regulated by specific Rab GTPases (Ebine & Ueda 2009).

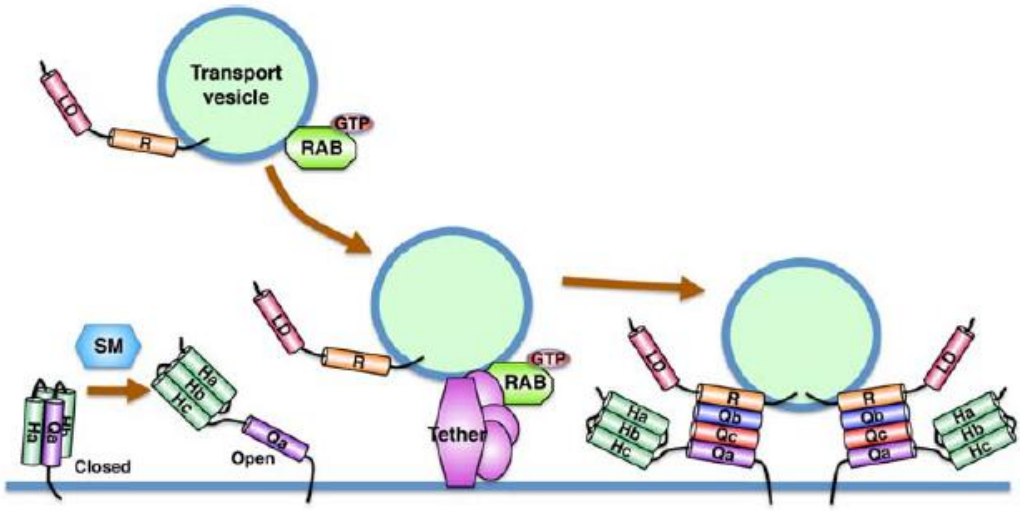

Figure 1.6 Model for a general mechanism of vesicle tethering and fusion mediated by SNARE proteins. Adapted from Ebine & Ueda (2009).

The full sequencing of Arabidopsis genome has provided a considerable amount of information related to vesicle trafficking elements. Through comparison with animal sequences, a diversity of SNARE proteins (68 in Arabidopsis compared with 35 in humans, 21 in yeast and 20 in Drosophila) has been identified and addressed to specific compartments of the endomembrane system. The most characterized SNARE family in Arabidopsis is syntaxin-like Q-SNARE that is grouped according to their sequence homology and subcellular localisation and function (Figure 1.7).

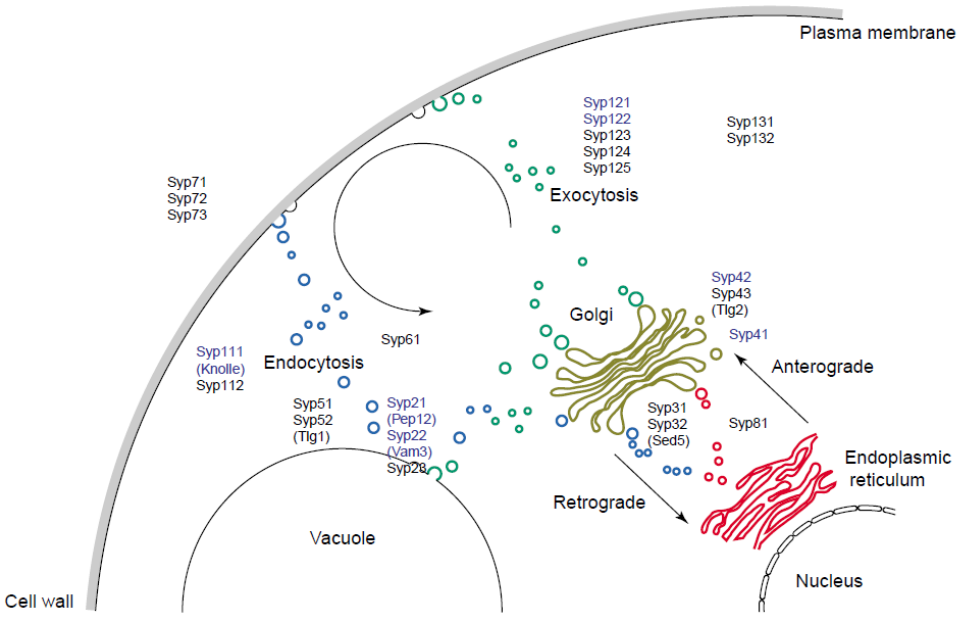

Figure 1.7 Localization of Arabidopsis syntaxin-like Q-SNAREs, known (blue text) or presumed (black), based on homologies with mammal and yeast SNAREs. Adapted from Pratelli et al. (2004).

Arabidopsis R-SNAREs – vesicle associated ones – are much less characterized. However, Arabidopsis VAMP isoforms show high homology with the mammalian VAMP7 proteins, which participate in endosomal and lysosomal trafficking (for review, Pratelli et al. 2004).

Indeed, plant cells seem to have assigned unique roles for SNAREs in fulfilling unique functions. In a similar fashion, expansion of Rab GTPases is closely associated with divergence and specialization of membrane trafficking pathways. Rab GTPases represent a subfamily of small regulatory GTPases from the ras superfamily that regulates several steps of vesicular trafficking. Rab proteins cycle between an inactive GDP- and active GTP-bound states, acting like molecular switches (Ebine & Ueda 2009). Together with SNARE proteins, they promote the initial docking and subsequent fusion of specific transport vesicle ns organellar membranes. Rab GTPases has also been involved in other cell regulatory processes as interactions between the transport vesicles and the cytoskeleton. The regulatory nature of Rab GTPases is based in interactions with a large number of regulatory and effector molecules, such as GTPase-activating protein (GAP – catalyzing the GTP to GDP hydrolysis) and GDP/GTP exchange factor (GEF – catalyzing the GTP to GDP hydrolysis) (Rutherford & Moore 2002; Ebine & Ueda 2009). In Arabidopsis, Rab GTPases are subdivided into eight groups and each group is involved in the vesicle trafficking between different compartments (Figure 1.8), as already described for SNARE proteins.

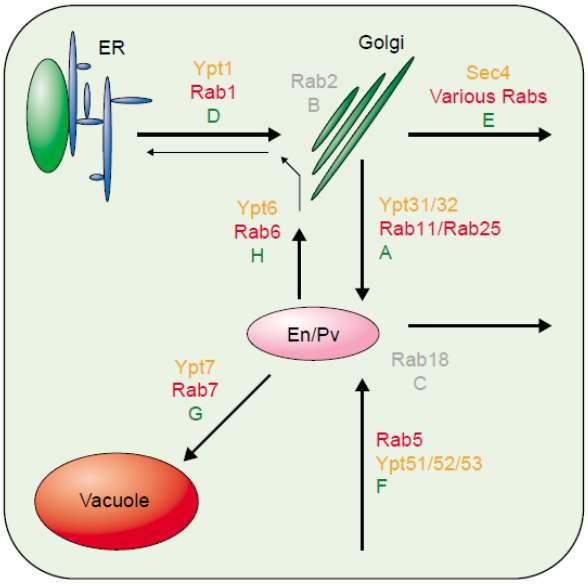

Figure 1.8 The trafficking pathways of a generic eukaryotic cell. The letters A to H represent probable sites of action of proteins in the eight major clades of the Arabidopsis Rab phylogeny. ER – Endoplasmic reticulum; En/Pv – Endosome/Prevacuole. Adapted from Rutherford & Moore (2002).

1.2.4. How to reach the vacuole

Proteins inserted in the ER have different ways to reach the vacuole, and may use different halt-stations to do so. For instance they may go through the GA, or bypass the GA, they may reach the plasma membrane and come back to the vacuole or they may be stored in intermediate compartments before to be delivered. In the following section, we examine proposed models to finally achieve vacuolar transport.

ER-to-GA transport

Protein export from the ER in direction to the GA is restricted to specific domains designated ER export sites (ERES) that, in contrast to the relative immobility observed in mammals, are highly mobile in plants. This motility, associated to the close spatial relationship existing between ER and GA led to the presentation of three explanatory models of ER-to-Golgi protein transport (Figure 1.9) (for review, Neumann et al. 2003; Hanton et al. 2005). The first model, termed “vacuum cleaner” model, argues that the GA cisternae moves over the surface of the ER collecting proteins, which implies that the entire surface of the ER has the

ability to export proteins (Boevink et al. 1998). The second model – “stop-and-go” - assumes that the GA cisternae receive cargo molecules from the ER at specific export sites (Nebenführ et al. 1999). If on one hand this theory shows a highest specificity for the transport of molecules between the ER and GA, on the other it presents the ER as a static surface. However, none of these models included data supporting a correlation between cargo transport and GA movement. The use of in vivo technologies allowed to shed some light into this matter and demonstrated that ERES can move over the ER and are closely linked to GA (da Silva et al. 2004). Thus, a third model was proposed - the “motile ERES” model – postulating that the ERES movement is in close relation to GA and allows continual transfer of cargo molecules between the two compartments (for review, Hanton et al. 2005).

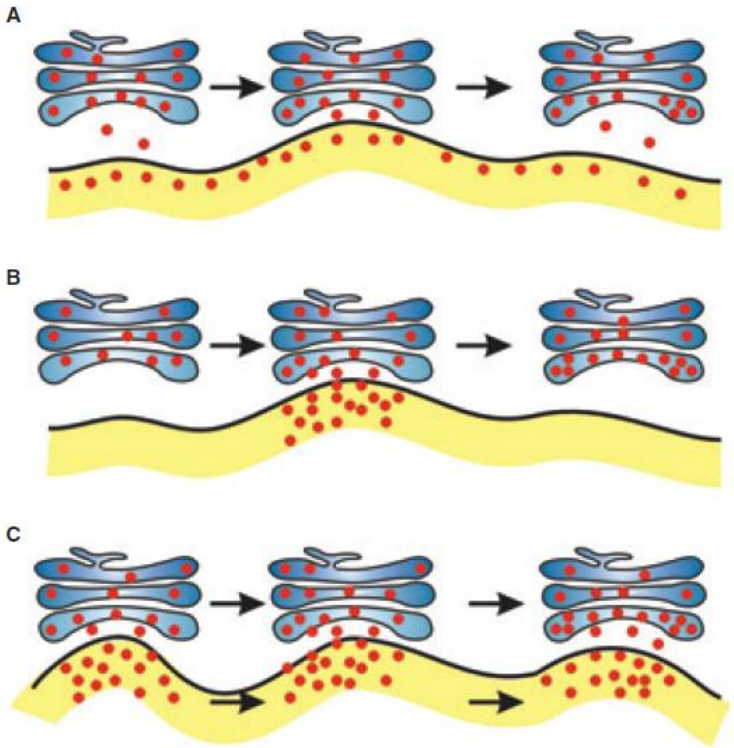

Figure 1.9 Schematic models for ER-to-GA protein transport. A) The vacuum cleaner model; B) The stop-and-go model. C) The mobile ERES model. Adapted from Hanton et al. (2005).

As already mentioned, the transport of proteins and membranes between subcellular compartments of the secretory pathway is mediated by transport vesicles. In the ER-GA interface the vesicle budding and function are highly conserved mechanisms between species. Export from the ER to the GA occurs via a COPII-mediated mechanism, localized at the ERES that contain essential proteins for export (Figure 1.10) (Hawes & Satiat-Jeunemaitre, 2005; Hanton et al. 2006;

Hanton et al. 2009). However, these forward transport needs to be balanced and one retrograde pathway mediated by COPI vesicles exists, to carry cargo molecules back from the Golgi to the ER (Figure 1.10) (Hanton et al. 2005). Retrieval of proteins from the GA back to the ER is needed for several reasons. Firstly, some proteins that are intended to stay in the ER may escape unintentionally in the lumen of transport vesicles, and need to be rescue back. Furthermore, proteins involved in the export machinery itself may also be retrieved to be used again in a subsequent round of vesicle assembly (Hanton et al. 2005).

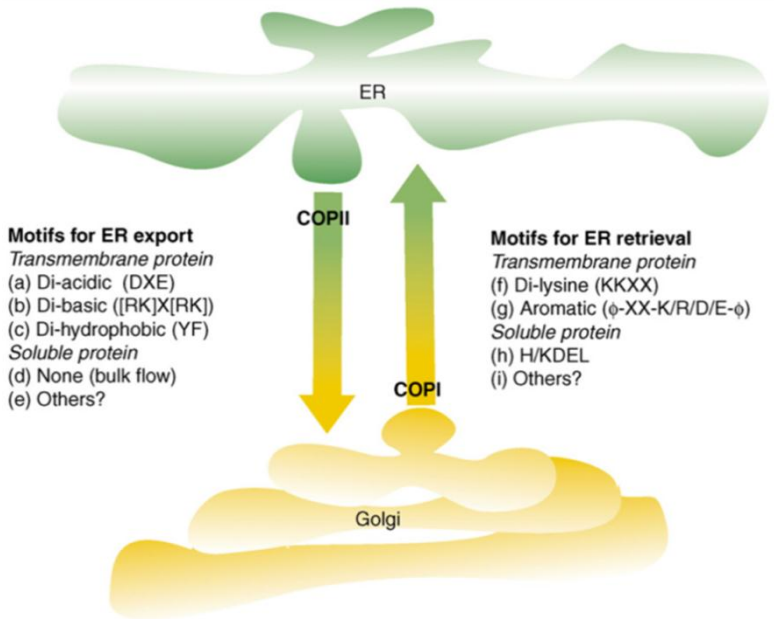

Figure 1.10 Anterograde and retrograde trafficking between ER and GA. Protein motifs important for cargo recognition and ER-to-GA transport in plant cells. ER – Endoplasmic reticulum. Adapted from Matheson et al. (2006).

The mechanism by which proteins are recruited into the transport vesicles is a subject not yet clearly understood and seems to vary depending on the nature of the cargo protein. It has been shown that soluble secretory proteins exit the ER via a bulk flow mechanism although the existence of receptors in the vesicle membrane cannot be ruled and various motifs that mediate the export of transmembrane proteins from the ER have been identified (Figure 1.10) (Matheson et al. 2006; Moreau et al. 2007). Studies reporting the influence in ER export of certain amino acid motifs in the cytosolic domains of transmembrane proteins are available: a di-hydrophobic motif interacting with COPII coat subunits *in vitro*; the involvement of a di-basic motif in the transport of a prolyl hydroxylase-green fluorescent protein fusion and a role for di-acidic motifs for different types of Golgi-localized proteins (Moreau et al. 2007). In contrast to the anterograde route, it has been demonstrated

that the retrograde transport depends on signals that mediate the transport of transmembrane and soluble proteins (Matheson et al. 2006). The tetrapeptide H/KDEL motif is located at the extreme C-terminus of many soluble ER-resident proteins and interacts with a receptor molecule in the cis-Golgi, where it triggers the formation of COPI vesicles. Similarly, a di-lysine motif is thought to interact with the COPI coat at the cis-Golgi and drives the protein back to the ER (Matheson et al. 2006; Moreau et al. 2007).

Cargo molecules entering the secretory pathway are processed along their transport to their final destination. The maturation of the N-linked Oligosaccharides is one of the processing which actually may help to identify the routes taken by the cargo molecules, as glycosylation signature reveals the potential contact of the cargo molecule with enzymes specific for one compartment. In eukaryotic cells, the N-glycans play several roles as the prevention of proteolytic degradation of glycoproteins or helping in the correct folding and activity (Lerouge et al. 1998; Rayon et al. 1998). Oligosaccharide side chains added to secretory proteins in the ER are modified by GA enzymes from their high-mannose type to the complex type, resulting in the addition of a variety of different sugars in different linkages (Nebenführ & Staehelin, 2001). N-glycosylation is the most important modification experienced by proteins in the ER and the GA. Asparagine-linked glycosylation is a common co-translational modification, with the addition of carbohydrates to the nascent polypeptides, but may also occur after the translation process (Pattison & Amtmann 2009; Schoberer & Strasser 2011). N-glycosylation starts in the RE with the transfer of an oligosaccharide precursor (Glc3Man9GlcNAc2) from a lipid carrier termed dolichol, to Asn residues of the nascent polypeptide (Rayon et al. 1998; Pattison & Amtmann, 2009). It is accepted that the mechanisms and enzymes involved in the process are conserved among humans, yeast and plants (Farid et al. 2011; Schoberer & Strasser 2011). The N-glycan formation at the ER level is linked to protein folding and protein quality control and has been shown to be important in plant development and defense mechanisms (Pattison & Amtmann 2009). Further processing of the N-linked glycans occurs in the GA and is performed by different Golgi-α-mannosidases and N-acetylglucosaminyltransferases, β1,2-xylosyl-transferase and α1,3-fucosyltransferase. This enzymes are distribute differently within the GA cisternae with the enzymes that act early tending to reside in the cis- and medial-cisternae, while the ones acting in the final part localizing in the trans-cisternae and the TGN (Schoberer & Strasser 2011). Based on the type and extend of N-glycans trimming they can be grouped in different categories: simple (acquired

in the ER), complex, hybrid and paucimannosidic type (transformed in the GA) (Lerouge et al. 1998).

Post-GA transport

The secretory pathway proteins enter the Golgi apparatus by the cis-face and will be moving along the cisternae in the direction trans-face, where most of the proteins leave the Golgi apparatus towards the cell membrane or vacuolar system. From the trans-Golgi network, transit routes to the cytoplasmic membrane and transport to the vacuole diverge. Proteins lacking a signal enter the so-called default pathway, being transported in vesicles that eventually fuse with the plasma membrane, releasing their contents to the outside (Neuhaus & Rogers 1998). In terms of vesicle trafficking the situation on the far end of the GA is more complex and with more intervenients than on its cis-face as there is a protein sorting triangle between TGN, vacuole and endosome/plasma membrane (Figure 1.11). The elevated number of SNARE proteins existing in the trans-GA illustrated the high differentiation degree and the large number of specific membrane-recognition events possible (Nebenführ et al. 2002). Secretory and endocytic trafficking pathways intersect in post-Golgi compartments of the endomembrane system. The post-Golgi compartments are considered morphologically distinct: trans-Golgi network/ early endosome, multivesicular body/prevacuolar compartment/late endosome and two types of vacuole. The cell plate is also considered a post-GA compartment, despite being a transient organelle. The recycling endosome has already been described for animal cells, but so far, in plants, no clear evidence of its existence has been provided. Conversely to the observed in animals and yeast, the TGN in plants, besides being involved in secretory protein trafficking, corresponds to the early endosome (EE). (Richter et al. 2009; Park & Jürgens, 2011).

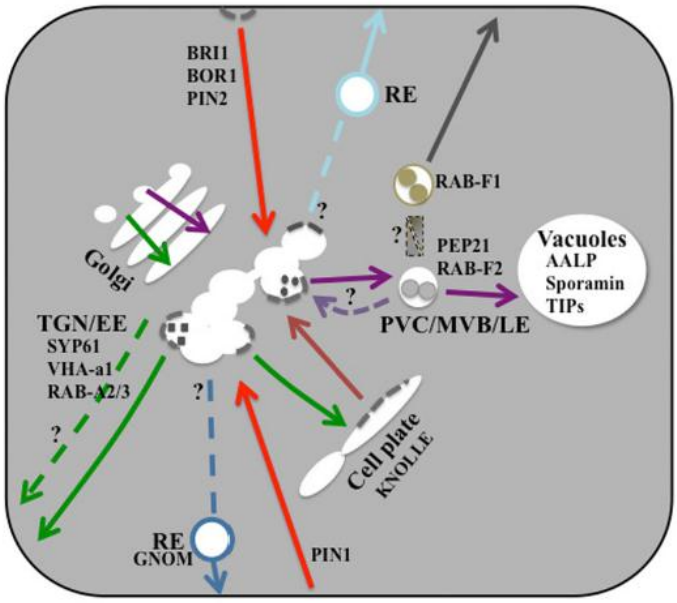

Figure 1.11 Schematic representation of post-Golgi trafficking. Purple line: vacuolar trafficking pathway; pale purple-colored dashed line: VSR (Vacuolar sorting receptor) recycling; green-colored dashed line: putative secretory pathways to the PM (Plasma membrane); green-colored line: Cell-plate formation; salmon-colored line: Molecular machineries involved in protein retrieval from the cell plate; red-colored line: endocytosis; gray-colored dashed line: clathrin; blue and pale blue dashed lines: multiple types of REs. Small-sized letters indicate representative molecular markers for post-Golgi trafficking pathways. TGN/EE – Trans-Golgi network/Early endosome; PVC/MVB/LE – Prevacuolar compartment/Mutivesicular body/Late endosome. Adapted from Park & Jürgens (2011).

Multivesicular bodies (MVBs) possess distinct intralumenal vesicles formed by local endosomal sorting complex (ESCRT). MVBs act as a prevacuolar compartment (PVC) in route to the lytic vacuoles (LV), thus functionally corresponding to the late endosome (LE) of animal cells. It is generally accepted that MVBs fuse with the tonoplast, releasing their membrane-bound cargo into the vacuole. The origin of the MVBs in plant cells is still controversial: GA/TGN-derived vesicles appear to fuse with one another to form pre-MVBs from which MVBs mature or MVBs mature from TGNs by being pinched off and forming ESCRT-mediated intralumenal vesicles (Park & Jürgens, 2011). Recently, it was proposed the existence of an intermediate compartment between the PVC and the LV in tobacco leaf epidermis (Foresti & Gershlick, 2010), but more studies are needed to confirm its localisation and function.

Secretion of proteins destined to the plasma membrane (PM) and out of the cell occurs via a default pathway, since no signals or receptors seems to be involved. However, this pathway is not well characterized yet and actors in the traffic must be clarified. The length of the hydrophobic region of the transmembrane

domain of secreted proteins appears to be related with their retention in the GA (protein with a short membrane span) or trafficking to the plasma membrane, if they present a longer membrane span (Brandizzi et al. 2002; Park & Jürgens, 2011). Interestingly, the default pathway in dividing cells changes from the PM to the cell-plate with the GA/TGN-derived vesicles delivering the necessary material. Data available till now suggest that both secretory and endocytic pathways contribute to cell plate formation (Park & Jürgens, 2011).

Other major trafficking activity in the post-GA is endocytosis of PM proteins, that are recycled back to the PM or targeted to the vacuole for degradation (Richter et al. 2009). It is not completely understood where these two routes diverge or even what mechanisms define the sorting, but it seems probable that the sorting occurs at the TGN and is involving MVB/PVC. Furthermore, it was recently described that ubiquitination of PM endocytic proteins would be a signal for vacuolar targeting and degradation. After ubiquitination, proteins seem to be recognized by ESCRT (endosomal sorting complex required for transport) complexes, which in turn promote MVB formation (Otegui & Spitzer 2008).

Finally, and conversely to the other routes described, vacuolar sorting of secretory proteins requires positive sorting at the TGN. The cargo proteins destined to the vacuole are recognized at the GA level by vacuolar sorting receptors (VSRs) and is released into PVC/MVB after fusion of the transport carriers with their membrane. The VSR is then recycled back to the TGN and the cargo molecules are transported to the vacuole, where occurs the fusion of the PVC/MVB with the tonoplast (Foresti & Gershlick, 2010). As the trafficking to the vacuole can occur by different routes and may involve different intermediates it will be approached in more detail in the next section.

Vacuolar routes

Vacuolar sorting is nowadays and since the last decade one of the most advanced and attractive research field in what concerns secretory protein trafficking. In a simplified version of protein transport to the vacuolar system two post-Golgi routes can be considered, ending in different vacuolar compartments - lytic or storage protein - which are closely related to the type of signal present (N- or C - terminal) (Bassham & Raikhel, 2000; Paris & Neuhaus, 2002). However, the

existence of direct routes from the ER to the vacuoles has been demonstrated and may represent a general mechanism of vacuolar ontogeny in plant seeds (Vitale & Galili, 2001). In the GA-mediated pathway the proteins leave the ER in COPII vesicles to the GA and from here are transported to the vacuole *via* the prevacuolar compartment (PVC) (Figure 1.12). Studying storage proteins, additional pathways bypassing the GA were discovered in seeds: the proteins can be directly delivered to the vacuole in large vesicles that bud from the ER (Figure 1.12) or leave the ER in KDEL vesicles (KV) that eventually fuse to the PSV (Vitale & Raikhel, 1999;Vitale & Galili, 2001). Contrary to the initial observations, direct ER-to-Vacuole transport is not limited to storage proteins being already described for tonoplast aquaporins and processing enzymes (Gomez & Chrispeels 1993; Pereira, 2008).

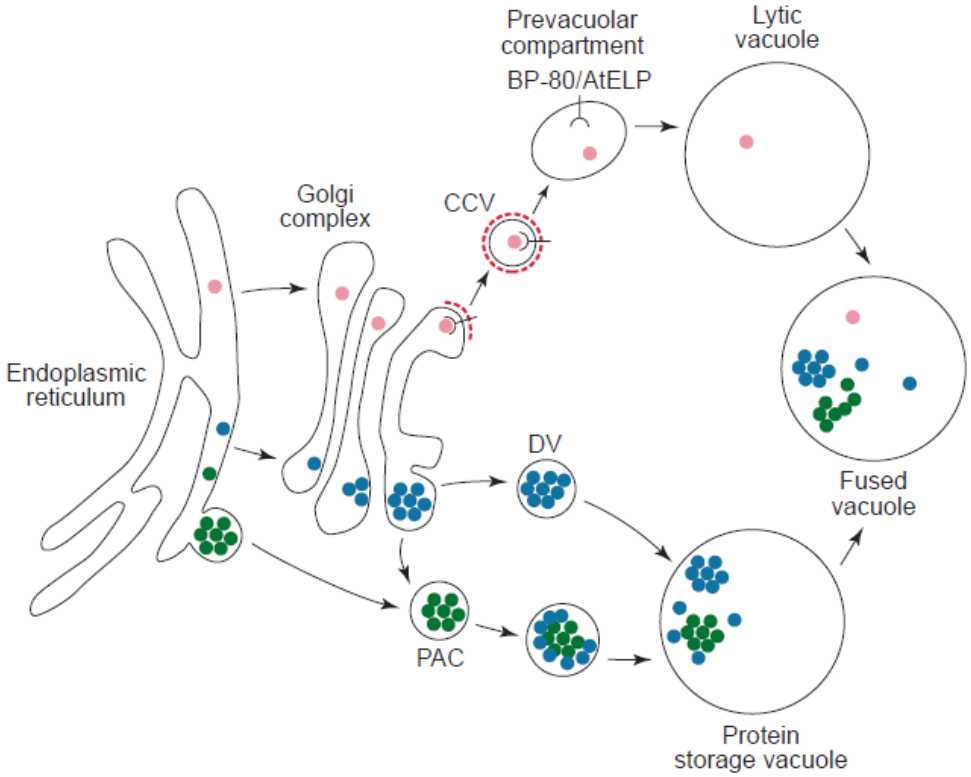

Figure 1.12 Schematic representation of protein routes to the vacuoles. CCV – Clathrin coated vesicles; DV – dense vesicles; PAC – Precursor accumulating vesicles. Adapted from Vitale & Raikhel (1999).

Transport to the lytic vacuole occurs after recognition of the sorting signal by the receptor BP-80, a membrane protein responsible for packaging the cargo-protein in clathrin-coated vesicles for transport to the pre-vacuolar compartment and, finally, to the lytic vacuole. Other proteins, which have a C-terminal signal or a signal in the middle of the protein sequence, are transported to the vacuole in dense vesicles derived from the Golgi complex. There is also a third route, less studied and observed in storage organs, in which proteins do not pass through the Golgi

apparatus and are transported to the vacuole in vesicles derived from the endoplasmic reticulum (precursor-accumulating vesicles) (Bassham & Raikhel 2000).

Identification of Vacuolar Sorting Receptors and Vacuolar Sorting Determinants are therefore a key signature to understand protein trafficking to the vacuole. A more detailed analysis on these vacuolar signatures will be presented below.

Vacuolar Sorting Receptors

Soluble proteins destined for the lysosome/ vacuole are known to traffic through the GA where they are recruited into clathrin-coated vesicles by specific receptors with the ability to bind a specific feature on the ligand protein at neutral pH, and then release the ligand protein at an acidic pH when the transport vesicle fuse with the target organelle or prevacuolar compartment. Vacuolar sorting receptors (VSR) then recycle back to the Golgi apparatus in a mechanism that makes the sorting process efficient as one receptor can participate in sorting of multiple ligand molecules (Zouhar & Rojo, 2009; Wang et al. 2011). Soluble cargo proteins carrying N- or C-terminal sorting sequences generally bind to a corresponding VSR for target delivery at the trans-GA or TGN. However, a recent experiment suggested that this recognition occurs at an earlier step, while the proteins are still in the ER (Niemes et al. 2010). Two families of putative vacuolar sorting receptors have been identified in plants. The Vacuolar Sorting Receptor (VSR) family, containing seven members in Arabidopsis, and the Receptor Homology-transmembrane-RING H2 domain (RMR) family, that comprises six members (Zouhar & Rojo, 2009).

In plant cells, the VSR proteins belong to the BP-80 family and they recognize a protein sequence on ligand molecules that contain a NIPR (Asn- Pro-Ile-Arg) or similar motif. BP-80 possesses a low affinity for storage proteins and available data is indicative of the participation of this receptor in targeting to LV, via CCVs, rather than PSV (Robinson et al. 2005). Studies in Arabidopsis involving mutants allowed the identification of VSR1, VSR3 and VSR4 as major sorting

receptors with a redundant function in targeting soluble cargo both for PSV and LV (Zouhar 2010). This suggests the involvement of vacuolar sorting receptors not only in protein sorting but also in vacuolar biogenesis, particularly in early embryogenesis, where a great remodeling of the vacuome is observed.

RMRs were identified as PSV sorting receptors in Arabidopsis, tobacco, and rice and are known to interact with the C-terminal vacuolar sorting sequences of storage proteins *in vitro* (for review, Park & Jürgens, 2011). Structurally, RMR are similar to VSR and is predicted to be a type I integral membrane protein that contains a typical N-terminal signal peptide, followed by a protease-associated domain, responsible for protein–protein interaction, and a single transmembrane domain (Wang et al. 2011). The most characterized RMR are AtRMR1 and AtRMR2 and they were localised at the GA, a PVC-like organelle, in the PSV and associated to large intravacuolar structures termed “crystalloids”. Further observations confirmed that RMR proteins trafficked through the GA in a pathway distinct from that of BP-80. Unlike the VSRs, this type of vacuolar receptors is not recycled but travels in aggregates with the soluble cargo proteins (Park et al. 2005; Wang et al. 2011). Recent studies from Park et al. (2007) revealed that AtRMR2 bound specifically to C-terminal vacuolar sorting determinant sequences, but only if they were presented with a free C-terminus. Interestingly, this interaction was not pH dependent conversely to the interaction of BP-80 with its sequence-specific ligands. These results allowed confirming the existence of two different sorting pathways to the different types of vacuole: RMR proteins specifically bind to peptides corresponding to sorting determinants for the PSV and BP-80⁄AtVSR1 participate in the sorting pathway to the lytic vacuole in a pH-dependent manner.

Vacuolar Sorting Determinants

For all eukaryotic cells, the transport from the Golgi apparatus to the vacuole or lysosomes requires a positive information from the protein. In mammals, the signal to transport proteins to the lysosome is the addition of a mannose 6-phosphate residue during the passage through the Golgi complex. In plant cells, the vacuolar sorting is part of the peptide sequence (Paris & Neuhaus, 2002; Zouhar & Rojo, 2009). Several vacuolar sorting determinants (VSS/VSD) have been described in plants and they can be grouped into three major groups. The sequence specific

sorting signals (ssVSD) require a conserved sequence, NPIR or similar, which do not tolerate significant changes. Usually this type of signal is located at the N-terminal of the protein directed to the lytic vacuole. The second main group comprises the signals present at the C-terminal region of the protein (ctVSD) and normally designate proteins destined to the protein storage vacuole. These signals do not have any homologous sequence or size set, sharing only that they are rich in hydrophobic amino acids and need to be exposed at the C-terminal to operate. Finally, the third group corresponds to signals dependent on the tertiary (physical) structure of proteins (psVSD) and is most common in storage proteins. These sorting signals are present in the protein sequence, which may correspond to more than one polypeptide, which arise when the protein acquires the native conformation (Neuhaus & Rogers, 1998; Jolliffe et al. 2003; Zouhar & Rojo, 2009).

For a peptide to be considered a true vacuolar sorting signal it must be both necessary and sufficient for this function. A signal is required if its removal redirect a vacuolar protein for the secretion pathway and is considered sufficient if it can redirect a protein to the vacuole that would normally be secreted (Paris & Neuhaus, 2002; Pompa et al. 2010). There are some described examples of vacuolar sorting determinants that satisfy these two assumptions (Table 1-1). In the group of sequence specific determinants the barley aleurain peptide - SSSSFADSNPIRPVTDRAAST - is described and also the sequence of sweet potato sporamin - RFNPIRLPTTHEPA. Although these two signals have a N-terminal position, it does not appear to be as important for targeting as the specificity of the sequence, since the sporamin A signal continues to be functional if transferred to a C-terminal position. Ricin, a toxin from *Ricinus communis*, has an internal vacuolar signal SLLIRPVVPNFN, linking A and B chains of the precursor form and is cleaved to yield the mature protein.

Table 1-1 Properties of sequences involved in protein vacuolar sorting. Adapted from Vitale & Raikhel (1999)

Sequence	Position in the protein	Location of the protein in its natural tissue	Sufficient[a]	Refs
HSRFNPIRLPTTHEPA (Sweet potato sporamin)	N	Vacuoles	Yes	5
SSSSFADSNPIR (Barley aleurain[b])	N	LV	Yes	5
VFAEAIAANSTLVAE (Barley lectin)	C	PSV	Yes	5
GLLVDTM (Tobacco chitinase)	C	Vacuoles	Yes	5
IAGF (Brazil nut 2S albumin)	C	PSV	No	18
AFVY (Common bean phaseolin)	C	PSV	ND	6
SLLIRPVVPNFN (Castor bean ricin)	Internal	PSV	ND	7

[a]The propeptides listed are necessary for the vacuolar targeting of the respective proteins; the fourth column indicates whether they are also sufficient to direct a reporter, secreted protein, to vacuoles.
[b]Partial sequence, which constitutes the N-terminus of the propeptide. The complete propeptide is longer.
Abbreviations: N, N-terminal; C, C-terminal; LV, lytic vacuoles; PSV, protein storage vacuoles; Vacuoles, not assigned to a specific type of vacuole; ND, not determined.

The position of the determinant does not appear to be relevant, as if added to the C-terminal region it is still capable of redirecting a protein to the vacuole (Paris & Neuhaus, 2002). Finally, the peptide of barley lectin VFAEAIA which engages in the group of C-terminal signals type is also necessary and sufficient for targeting proteins to the vacuole (Dombrowski et al. 1993).

However, protein sorting to the vacuole and the question on the efficiency of a single VSD is questioned by data showing the existence of two types of VSD in the same protein. It was shown that the C-terminal region of alpha-subunit of soybean beta-conglycinin has two sorting signals, one of the ctVSD type and other of the sequence-specific type (Nishizawa et al. 2006). This study shows that both of which function for trafficking to the PSVs, but it is not clear if both use the same VSR. Additionally, other study carried out with the storage protein phaseolin showed that a tetrapeptide at the C-terminus is required for proper vacuolar sorting. Based on this data, the importance of multiple copies of vacuolar determinant in assembled homo-oligomeric storage proteins is discussed and is far from being clear. The authors consider the possibility that the ratio between number of vacuolar sorting determinants and size of the passenger protein also plays a role in the efficiency of sorting (Nishizawa et al. 2006). Recently, Pompa et al. (2010) provided evidence

that the C-terminal segment of a phaseolin polypeptide undergoes homotypic interactions that allow the formation of a disulfide bond when a Cys residue is introduced proximal to the AFVY C-terminal vacuolar sorting signal. Furthermore, the authors claim that the vacuolar sorting signal of phaseolin is not necessary for those homotypic interactions, and its sorting function can be partially replaced by a C-terminal Cys residue.

In light of the recent advances in protein sorting to the vacuole, it is clear that the initial picture proposing three types of VSD directing proteins to a specific type of vacuole is not completely accurate and more studies are needed to clarify this aspect.

1.3. CARDOSINS AND VACUOLAR ROUTES

1.3.1. Cardosins, proteins of both economical and biological interest

Cardoon (*Cynara cardunculus* L. - Figure 1.13) belongs to the Asteraceae family and is distributed in central and southern Portugal, Madeira and the Canary Islands. For a long time that is used in the manufacture of various soft cheeses in Portugal and Spain, due to its milk clotting activity. This coagulant activity is due to the existence of aspartic proteinases present in the flowers (Cordeiro et al. 1994).

Figure 1.13 Cynara cardunculus. (a) Plant in its natural environment; (b) detail of an inflorescence; (c) in vitro cultures. Adapted from Pissarra et al. (2007).

Cardosins are APs that were first isolated and characterized from cardoon flowers. The APs content in cardoon flowers correspond to about 60% of total proteins in mature stigmas, which illustrates the high importance of these enzymes

in the system. Initially, two cardosins were isolated - A and B - which, although having high degree of similarity, are products of different genes and show significant differences with respect to enzymatic and kinetic properties (Veríssimo et al. 1996). In general, cardosin B has a broader specificity than cardosin A, although it has higher activity. Based on this observation it was proposed that while cardosin B may intervene in protein digestion in general, cardosin A would participate in more specific process and with a high degree of regulation. Later on, the genes encoding for cardosin A and B were isolated and characterized from the flowers of *Cynara cardunculus* along with two new aspartic proteinases, designated cardosins C and D, that have high similarity with cardosin A and are therefore designated cardosins-like (Pimentel et al. 2007). The pattern of accumulation of these specific cardosins A-like in plant tissues revealed some overlap with that of cardosin A suggesting that they may have additional or specific functions. More recently, novel cardosins-related genes were identified and characterized – termed cardosin E and G. These resemble cardosin A in terms of nucleotide and protein sequence, but are more active than cardosin A (Sarmento et al. 2009).

1.3.2. The cell biology of Cardosin

Cardosin A belongs to the aspartic proteinases' family of enzymes. It has been extensively studied and characterized, revealing a high degree of regulation. Cardosin A is a vacuolar protein with steady-state levels of expression along the plant, but is highly expressed in highly metabolically active tissues, such as developing flowers and seeds. It accumulates in different types of vacuoles and evidences from the native system point to the existence of different routes depending on the cell needs. Furthermore, the protein has two putative vacuolar sorting domains whose properties need to be explored. It is therefore an excellent tool to study vacuolar trafficking and sorting to the lytic and protein storage vacuoles. Moreover, another feature making relevant its study concerns the intracellular location of another aspartic proteinase from the same plant – cardosin B. Cardosins A and B, although sharing a high similarity in terms of nucleotide and amino acid sequences are located in different cellular compartments in flowers:

cardosin A is in the vacuole and cardosin B is secreted into the extracellular matrix. The similarity between the two brings up the question “why is cardosin B secreted?”.

It has been proposed a scheme for its processing based on cardosin cleavage sites using specific antibodies for different regions of the protein (Ramalho-Santos et al. 1998). The precursor molecule of cardosin A - procardosin A - undergoes proteolytic processing similar to that described for other plant APs (Figure 1.14). The first cleavage occurs between the 31 kDa chain and the PSI, giving rise to two intermediate forms of the protein (heavy chain with the prosegment and light chain plus the PSI). The following cleavage on the protein sequence occurs between the PSI and the light chain and processing is completed by removing the prosegment (Ramalho-Santos et al. 1998). Although similar, the processing of prophytepsin has some particular aspects: the prophytepsin in barley roots is sequentially processed by cleavage of the prosegment and partial removal of the PSI, unlike what happens with procardosin A, in which the PSI is completely removed (Ramalho-Santos et al. 1998; Simões & Faro 2004).

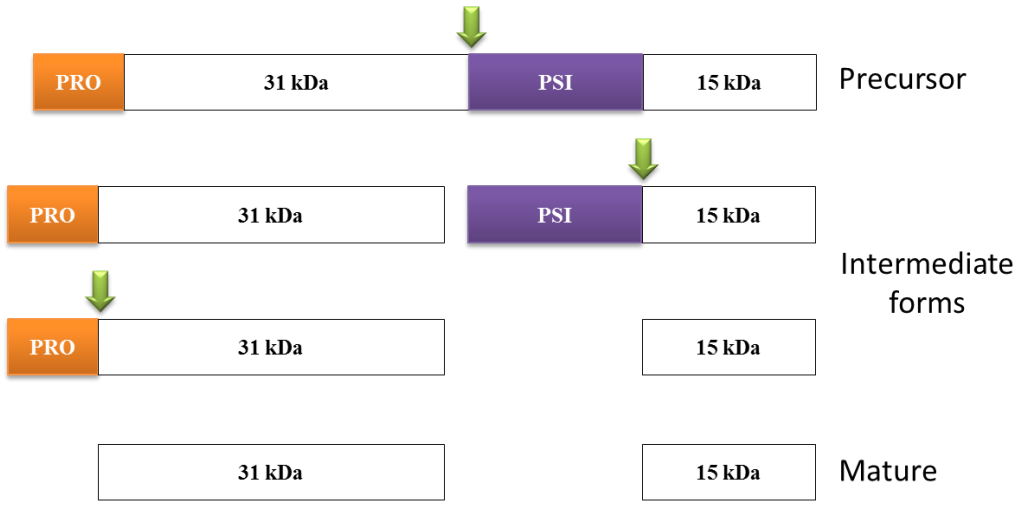

Figure 1.14 Cardosin A processing steps. The first cleavage occurs between the heavy chain and the PSI. Subsequent cleavages occurs to remove the PSI and the Prosegment (PRO), originating the mature enzyme composed of a heavy and a light chains.

A particular feature of cardosin A is the existence of a sequence Arg-Gly-Asp (RGD), a characteristic motif of integrin binding proteins. In mammalian tissues, such proteins facilitate various recognition functions such as cell adhesion, migration, signal, growth and differentiation (Faro et al. 1999). This sequence appears to be involved in interactions between cardosin A and a pollen protein, which leads to the hypothesis that cardosin may participate in the proteolytic mechanisms associated with the pollen tube growth (Faro et al. 1999; Frazão et al.

1999). Initially, three main possibilities for cardosin A the functions were proposed: involvement in floral senescence and participation in programmed cell death; involvement in defense against pathogens and involvement in pollen-pistil interaction (Ramalho-Santos et al. 1997). Recently, cardosin B has also been implicated in phenomena of programmed cell death in nucellar layers of the egg (Figueiredo et al. 2006) and cardosin A in the remodeling and permeabilization of membranes during germination (Pereira et al. 2008). In general, the expression of cardosin A seems related to organs and tissues which are under substantial morphological changes and its expression is most likely regulated along plant development (Faro et al. 1999; Pereira et al. 2008).

How specific of cardosin A are these features compared to the biology of other aspartic proteinases has to be evaluated.

1.3.3. Aspartic proteinases

The proteinases classification of is based on the amino acids present in their active site, the three-dimensional structure and mechanism of action. The major classes of proteinases include serine, cysteine, aspartic and metalloproteinases (Mutlu & Gal, 1999).

The aspartic proteinases (APs) (EC:3.4.23) are grouped into 14 different families according to the amino acid sequence, which are grouped into six lineages, based on their phylogenetic relationships and tertiary structure (Simões & Faro 2004). They represent a widely distributed class of proteinases, having already been identified and characterized in vertebrates, fungi, parasites, plants, nematodes, viruses and yeasts (Davies, 1990; Mutlu & Gal, 1999). APs from the A1 family are characterized by having high activity at acidic pH, being inhibited by pepstatin and having two aspartate residues responsible for catalytic activity (Davies 1990). In mammalian cells, the APs are usually found in acidic lysosomes, such as cathepsin D, or can be secreted (such as pepsin and renin) (Mutlu & Gal, 1999), while in plants they are normally located in the lytic/protein storage vacuoles or in the extracellular space. Among the various functions assigned to them, stand out the protein degradation and processing of poly-proteins (Mutlu & Gal, 1999). The proteinases found in mammals are involved in specific protein processing (retroviral proteases), and in protein degradation (cathepsin D and pepsin) and the regulation of blood

pressure (renin). The roles of the plant APs are not yet as defined as the ones attributed to mammalian ones and the functions proposed are derived from expression and localisation analysis in certain tissues and from co-localisation with putative substrates. Plant APs are then believe to participate in processing of other proteins and in storage protein degradation or in the activation of zymogens (inactive precursors) during the germination of seeds (Bethke et al. 1996; Frazão et al. 1999; Mutlu & Gal, 1999; Pereira et al. 2008). APs have also been associated with other protein degradation processes in plant tissues: in carnivorous plants the organs specialized in digesting the insects secrete APs; in protein degradation during senescence and programmed cell death (Mutlu & Gal, 1999; Figueiredo et al. 2006). Recently an additional role in the response to environmental stress has also been addressed, including dark, drought, UV-B light, wounding and salicylic acid abiotic induced-stresses (Timotijević et al. 2010).

Plant aspartic proteinases

A large number of APs have been identified and/or purified from monocotyledons (barley, corn, rice and wheat) and dicotyledons (Arabidopsis, Nicotiana and Cynara, among others). These proteinases were mostly characterized from seeds (dormant or not), but were also isolated APs from tobacco leaves and cardoon flowers (Veríssimo et al., 1996; Mutlu & Gal, 1999).

Despite the high similarity between plants and animals APs, there are some specific characteristics of the plant APs, which make them unique. Most of the plant APs described to date are synthesized as single-stranded preproenzimes (or zymogens) and are subsequently converted into the mature form. The primary structure of the precursor molecules is similar between the plant APs, characterized by the presence of a N-terminal sequence, responsible for addressing the protein to the endoplasmic reticulum, followed by a prosegment of about 40 amino acids and a N-terminal domain and a C-terminal domain separated by a region of about 100 amino acids called PSI (plant specific insert) (Figure 1.15) (for review, Simões & Faro, 2004; Pissarra et al. 2007).

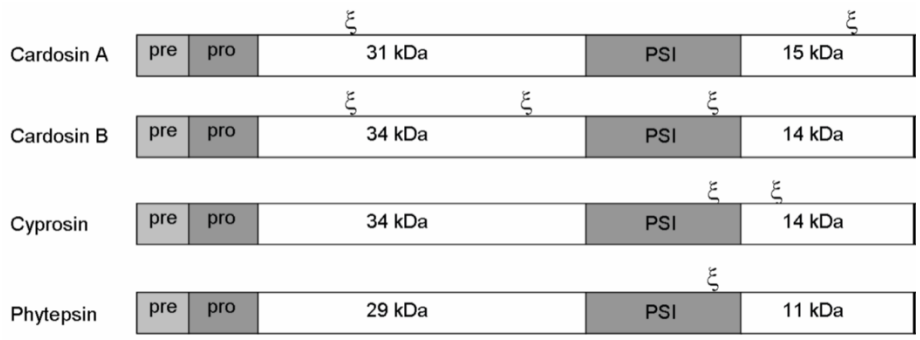

Figure 1.15 Schematic representation of the primary structure of several plant APs. Pre: signal peptide; Pro: prosegment; PSI: plant specific insert. Adapted from Pissarra et al. (2007).

While the prosegment is present in all APs and is associated with inactivation, folding, stability, and targeting of the zymogen, the PSI is characteristic of several (but nor the majority) plant APs and, to date, the only exceptions to this primary structure are nucelin expressed in barley nucellus, an AP-like protein, expressed in tobacco chloroplasts, and a CDR encoded AP-1, from *Arabidopsis thaliana*, which is involved in disease resistance (Simões & Faro 2004). The PSI has high homology with proteins similar to saposins (SAPLIPs) and any member of this family has 6 conserved cysteine residues, a number of hydrophobic residues and a conserved glycosylation site. The PSI has a particular characteristic when compared with saposins: there is a reversal of the N- and C-terminal domains of the saposins, where the C-terminal portion of saposin is linked to the N-terminal portion of another (Simões & Faro 2004). The function of the PSI is not completely understood. It is accepted that the PSI is not important for the enzyme activity, but participate in the proper folding and stability of APs structure, as observed for AtAP A1 protein (Mazorra-Manzano et al. 2010). In addition to this function and considering also the ability to interact with the lipid bi-layer of cell membranes, it has been suggested that this domain may be responsible for transporting the APs precursor form through membrane compartments, thereby mediating the transit to the vacuole (Simões & Faro 2004). Additionally, it was proved (Egas et al. 2000) that the PSI interacts with lipid membranes by promoting the release of its contents. This suggests that the action of the PSI can interfere with the permeability of cell membranes and can function as part of a defense mechanism against pathogens and as effector cell death (Egas et al. 2000). These features support the idea that the APs are bi-functional molecules, having a function on membrane destabilization beyond the proteolytic domain.

The plant APs share about 60% identity in the N- and C-terminal regions and approximately 44% identity with cathepsin-D, the nearest animal AP. Two catalytic motifs - Asp-Thr-Gly (DTG) and Asp-Ser-Gly (DSG) – are present in all plant APs belonging to A1 family, with the exception of chlapsin, an AP recently isolated and characterized from green algae *Chlamydomonas reinhardtii* that possesses the motifs DTG/DTG (Simões & Faro 2004; Almeida et al. 2012). With respect to the crystallographic structure, it has only been determined for two plant APs: cardosin A mature form (Figure 1.16 a - PDB code: 1B5F) and prophytepsin precursor form (Figure 1.16 b - PDB code: 1QDM) (Frazão et al. 1999 and Kervinen et al. 1999, respectively). The two APs are very similar to other APs of non-plant origin. Recently, it was reported the crystal structure of the PSI from an AP of *Solanum tuberosum* (Bryksa et al. 2011). This structure revealed an open V-shape configuration (Figure 1.16 c) similar to the one of human saposin C.

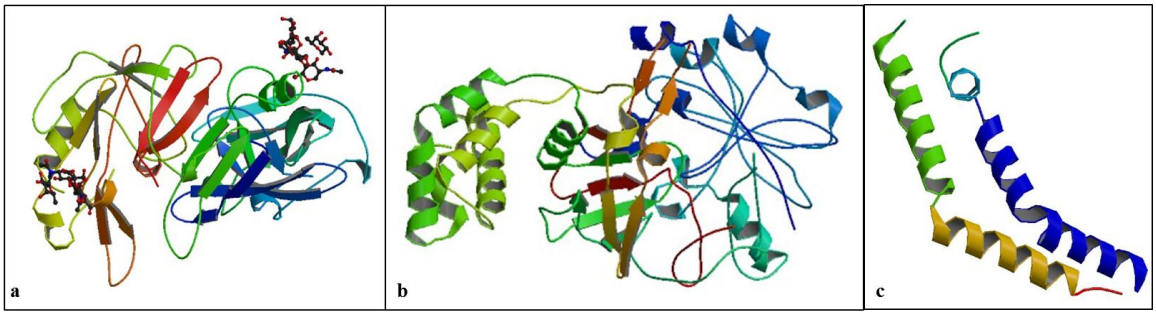

Figure 1.16 Crystallographic structure of mature cardosin A (a), prophytepsin (b) and Solanum tuberosum AP PSI (c). Drawings were obtained from PDB database.

A process for inactivation of precursor molecules of plant APs proposed by Kervinen et al. (1999), based on the three dimensional structure of prophytepsin, postulates that the catalytic site is blocked by the prosegment and some amino acids of the N-terminal region of a similar manner as described for animal APs. However, cardosins A and B, and two APs from rice have no mechanism for inactivation and *in vitro* tests using procardosin A confirmed that unlike other zymogens, these molecules are active (Simões & Faro 2004).

The precursor molecules of plant APs undergo various proteolytic cleavages to acquire its mature form, and the conversion of the zymogen in an active molecule is a proteolytic process which may involve auxiliary molecules or may be an autocatalytic process (Simões & Faro 2004). Three types of processing are described for the activation of an AP: complete self-processing, self-processing partially assisted by other proteinase and processing entirely assisted by a different

protease. The most common is partially autoprocessing, as in the case of cardosin A and cathepsin D, where the processing is supported by cysteine proteinases (Ramalho-Santos et al. 1998). The proteolytic processing of plant Aps starts by removing the signal peptide, after targeting to the endoplasmic reticulum. The processing steps include the removal of all or part of the PSI and the prosegment. It has been found that removal of prosegment is essential to the formation of an active protease, however, the removal mechanisms and the order in which they are removed may vary. In either case, the processing of precursor molecules of the plant APs leads to the formation of an enzyme with two chains without the prosegment and without the PSI and an organization similar to that found for microorganisms or mammalian APs (Simões & Faro 2004).

1.3.4. Cardosin A Localisation and sorting: the missing pieces in the puzzle

Although the mechanisms for cardosin A processing are already extensively characterized, little is known about their maturation process or the route the protein follows from the endoplasmic reticulum to the vacuole. Cardosin A has signal peptide for the endoplasmic reticulum and it is assumed that it follows to the Golgi apparatus. Although cardosin A may possess glycans of the complex type (changes acquired at the Golgi apparatus), the hypothesis that cardosin A follows a path independent of the Golgi apparatus is not discarded (Costa et al. 1996; Duarte et al. 2006). An alternative route for the transport of cardosin A to protein bodies, regardless of the Golgi complex, was observed in cardoon seeds, wherein the protein would be transported in ER-derived vesicles (Pereira et al. 2008). Therefore various routes can be proposed for cardosin A, depending on the cell/tissue/organ in which it is to be expressed, as the available data suggest a possible specialization of its trafficking pathways according to the type of cell and specific needs.

The routes followed by cardosin A from the Golgi apparatus to the vacuole and the sorting signals responsible for the targeting are still to be explained. The role of PSI in the targeting of APs to the vacuole has been extensively discussed, without little or any specific data on its effectiveness. It was proposed that the PSI can function as vacuolar sorting signal in a manner similar to what occurs for cathepsin D, which is jointly transported to the lysosome with saposins. Moreover, the role of PSI in vacuolar targeting may be more indirect and be related to the association of the precursor molecules to the membranes at the endoplasmic

reticulum level (Faro et al. 1999). An example of the latter is phytepsin. Based on sequence analysis and of crystal structure, Kervinen et al. (1999) proposed that the phytepsin's PSI enable region of contact with a receptor associated with the membranes in the Golgi apparatus. The complex thus formed was transported to the vacuole through vesicles from the secretory pathway. More recently, Terauchi et al. (2006) have shown that the role of vacuolar determinant that has been attributed to the PSI can be dependent on the type of vacuoles to which the AP is stored. These authors removed the PSI the region from two soybean APs - one that accumulates in the lytic vacuoles and other in protein storage vacuoles - and they concluded that it only changes the path of the one accumulating in the lytic vacuole. The importance of this region in the processing and/or vacuolar targeting of APs is still unclear, as several factors seem to constrain its operation.

Moreover, the C-terminal peptide of barley lectin (VFAEAIA) is very similar to C-terminal sequence of cardosin A and other plant APs. This region is responsible for targeting the lectin to the lytic vacuole, suggesting that the C-terminal sequence may also be the sorting signal for the plant vacuolar APs (Bednarek and Raikhel, 1991; Ramalho-Santos et al. 1998). The same applies to phaseolin, a protein whose accumulation in protein storage vacuoles of cotyledon cells is linked to a peptide at the C-terminal (Frigerio et al. 1998).

It is still not possible to rule a vacuolar sorting determinant dependent on the three-dimensional structure of cardosin A and therefore be related with small peptides spread over the protein sequence, that are brought together during the protein processing. For its part, the autoprocessing may also have great influence on the intracellular targeting and trafficking of cardosin A. By interfering with the correct processing of the enzyme, other problems can be triggered such as defects in the protein folding that cause the protein to be retaining in the quality control points existing in the secretory pathway, including the endoplasmic reticulum and the Golgi complex (Pedrazzini et al. 1997).

1.4. THESIS OBJECTIVES AND STRATEGIES

Cardosin A, a model protein to study vacuolar routes?

1.4.1. Objectives:

Cardosin A is a vacuolar aspartic proteinase extensively characterized, and despite the main processing steps have been approached, the route along the endomembrane system to the vacuole has not yet been elucidated. This is in part due to lack of characterized heterologous systems suitable for cardosin A expression. Therefore, **the first goal of this work** is the validation of heterologous systems for cardosin A expression and biogenesis.

Our second objective will be to identify the vacuolar sorting signals and the vacuolar route(s) of cardosin A. The identification of the vacuolar sorting determinant is most relevant for further studies employing cardosin A. There are several domains in the precursor protein that may act as possible targeting signals. We intend to evaluate the significance of each, using cardosin A constructs with mutations in some key regions, and subsequently define the polypeptide responsible for the targeting and evaluate its potential as vacuolar sorting determinant.

On the other hand, Cardosin A is known to accumulate both in PSVs and LV, depending on the type of tissue/cell were it is observed. We believe that this differential accumulation may be related to different vacuolar pathways so we intend to track cardosin A within the cell to define its vacuolar pathway in different physiological situations. Cardosin A glycosylation and activity are other issues that are not yet completely understood as it seems to interfere somehow with the proteinase processing, and consequently with its trafficking.

A third objective will be to have an integrated view on how/if developmental/physiological stage of plants may affect the protein trafficking. The “flexibility” of cardosin A trafficking pathways and its adaptation according the plant cell needs will be studied during seed germination. The exact mapping of cardosin A vacuolar pathway in germinating seeds, where it has been shown to exist multiple type of

vacuoles will retrieve interesting information about cardosin A involvement in membrane remodeling and mobilization of protein reserves, as proposed in the past.

1.4.2. Strategy

To reach these objectives, we have developed studies along 3 main axis:

1. Definition of the toolbox for Cardosin A biogenesis and trafficking studies (Chapter 1 of the Results section)

To work out proper heterologous models for cardosin A expression, 3 different systems presenting different characteristics, and consequently different advantages allowing the use of different strategies, were chosen: transient expression in *Nicotiana tabacum* leaves, Stable expression in BY-2 suspension-cultured cells and stable expression in *Arabidopsis thaliana* under the action of an inducible promoter. In this chapter we will obtain fusions of cardosin A with a fluorescent reporter to allow *in vivo* tracking of the protein. Furthermore we will evaluate if cardosin A (tagged and non-tagged versions) is correctly expressed and directed to the vacuole in those systems. Considering the stable expression systems, the possible effect of cardosin A overexpression in cell/plant phenotype will also be evaluated. In these chapter a vast plethora of methods will be used: biochemical approaches to assess cardosin A correct processing and expression; molecular biology techniques to obtain the chimeric fusions; confocal laser scanning microscopy to evaluate the fusion protein localisation in vivo; electron microscopy techniques to localize cardosin A within the cells and evaluate the cell ultrastructure.

2. Deciphering Cardosin A trafficking pathways in *Nicotiana tabacum (Chapter 2 of the Results section)*

In order to identify cardosin A vacuolar sorting determinant, mutated forms of the protein lacking one or both domains will be obtained and tested independently alone and tagged to a fluorescent reporter. Furthermore, the potential(s) vacuolar sorting domain(s) will be isolated and tested independently by means of a fusions with a normally secreted fluorescent reporter to demonstrate its ability in directing a protein to the vacuole. Using co-localisation techniques with specific markers of the endomembrane system, and blocking the transit between key cell compartments (both by the use of drugs and dominant-negative mutants affecting vesicle transport) we expect to obtain a picture of cardosin A and its mutated versions trafficking pathways. Finally, the using specific inhibitors and N-glycosylation/catalytic sites point mutations, we will be able to define the

importance of glycosylation and catalytic activity in cardosin A processing and sorting. In this section, advanced molecular biology techniques such as PCR and site-directed mutagenesis, will be used, coupled to biochemical and light imaging techniques, to evaluate the effects of the mutations induced in the DNA sequences.

3. Cardosin A biogenesis and trafficking in *Arabidopsis thaliana* seed germination (Chapter 3 of the Results section)

Cardosin A biogenesis and sorting in germinating seeds will be achieved by localisation and co-localisation of the protein with markers of the endomembrane system. Pharmacological approaches using drugs affecting the trafficking will also be used in this part of the work. The methodology here employed will be different from the above, as the *Arabidopsis thaliana* lines expressing cardosin A were already available for use and were transformed with a non-tagged version of the protein, imposing the use of specific antibodies. In a first approach cardosin A will be localised in the tissues by fluorescence microscopy allowing a general view of its distribution in the tissue. Additionally, electron microscopy techniques will be used to have a better resolution of cardosin A subcellular localisation. High-pressure cryofixation and cryosubstitution will be used as it has proven to give better results than the conventional chemical fixation.

1.4.3. Expected results

The data taken together should permit to have an integrated view of cardosin A biogenesis and sorting towards different types of vacuole, and to finally discuss the potential regulation of vacuolar pathways in plant cells, presented in a final Discussion section.

2.MATERIAL AND METHODS

2.1. CARDOSIN A STUDIES IN *NICOTIANA TABACUM* LEAVES

The study of cardosin A biogenesis and sorting in *Nicotiana tabacum* involved the production of molecular tools, such as a fusion between cardosin A and the fluorescent protein mCherry and novel cardosin A constructs with sequence alterations. The constructs produced were used to infiltrate *Nicotiana tabacum* leaves in a processed mediated by *Agrobacterium tumefaciens* and the results were evaluated by biochemical and optical microscopy approaches. The methods employed in this section are described in the following sections.

2.1.1. Production of molecular biology tools

In the course of this work several constructions with deletions, insertions or point mutations in the original Cardosin A sequence were prepared in order to study several aspects of its processing and trafficking. The methodology for obtaining and screening the constructions is summarized in Figure 2.1 and will be described in detail in the next topics.

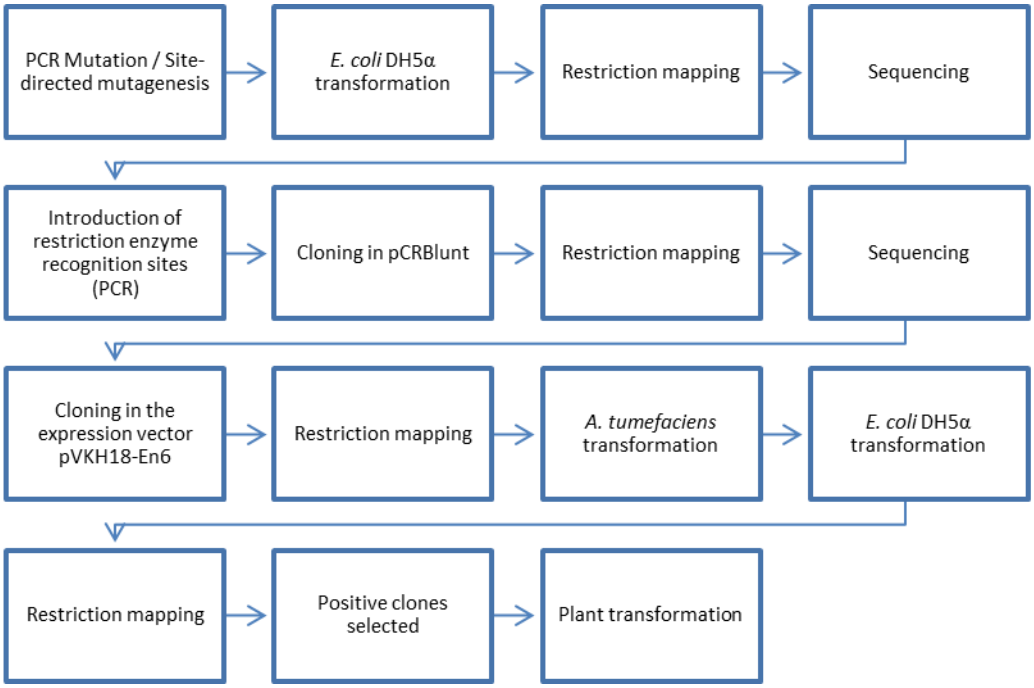

Figure 2.1: Flowchart representing the steps performed for obtaining, cloning and screening the constructs produced.

Design and Construction of Cardosin A Truncated Versions

To start studying cardosin A targeting to the vacuole several constructs were produced: cardosin A, cardosin AΔPSI (a deletion of the PSI region), cardosin AΔC-ter (a deletion of the C-terminal peptide VGFAEAA), and cardosin AΔ[PSI+C-ter] (deletion of both the PSI region and C-terminal peptide) (Figure 2.2).

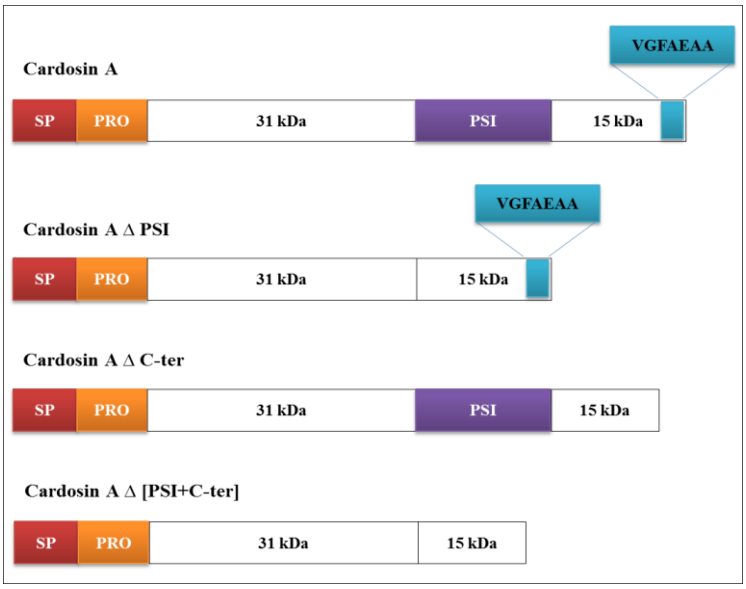

Figure 2.2: Schematic representation cardosin A processing and of cardosin A mutated versions. Three Cardosin A mutated versions were obtained in order to test its putative VSDs - cardosin AΔPSI: cardosin A after removal of the PSI domain; cardosin AΔC-ter: cardosin A without the C-terminal peptide VGFAEA; Cardosin AΔ[PSI+C-ter]: cardosin A lacking both regions.

All constructs used in this study were generated by Polymerase Chain Reaction (PCR) using specific primers containing a *Xba*I recognition site at 5' end and a *Sac*I recognition site at the 3' end (Table 2-1). Unmodified cardosin A (Duarte et al. 2008) was used as template for all PCR reactions, except to generate the double mutant, where the cardosin AΔPSI cDNA was used. To obtain the construction without the PSI, a linker composed of glycine and alanine residues was introduced between the heavy and the light chain to allow the proper folding of the protein. The introduction of these aminoacids was made with the PSI primers PSI3'_adapt and PSI5'_adapt.

Table 2-1: Primers used in the amplification of Cardosin A and its truncated versions.

Primer	Sequence	Description
A5'prime_Xba	TCTAGAGCCGCCACCATGGGTACCT	Introduction of a *kozak* consensus sequence and a X*ba* I recognition site (red).
A3'prime_Sac	CTGAGCTCTCAAGCTGCTTCTGCAAATC	Introduction a *Sac* I recognition site (red) after the STOP codon.
PSI3'_adapt	ACCTGCAGCACCACCCCCGTTAGCGCC AATTG	Primer designed for the 3' end of Cardosin A heavy chain. Introduction at the 3' end of an adaptor sequence compose of glycine and alanine residues and a *Pst* I recognition site (red).
PSI5'_adapt	GGTGCTGCAGGTGGTACTTCATCTGAA GAATTAC	Primer designed for the 5' end of Cardosin A light chain. Introduction at the 5' end of an adaptor sequence compose of glycine and alanine residues and a *Pst* I recognition site (red).
COOH3'_Sac	GAGCTCTAGTAAATTGCCATAATC	Introduction a *Sac* I recognition site (red) after the STOP codon.

PCR fragments were cloned using the Zero Blunt® cloning kit (Invitrogen) and analysed by restriction mapping. Positive clones were selected for sequencing with M13 primers [M13uni(-21) and M13rev(-29)] (Eurofins MWG Operon, http://www.eurofinsdna.com/home.html). Fragments were inserted into the *Xba*I and *Sac*I sites of the binary vector pVKH18-En6 (Sparkes et al. 2006) for expression in plant cells.

Fusion of Cardosin A versions with mCherry

To obtain fusions with the red fluorescent protein mCherry (Shaner et al. 2004) (Figure 2.3), mCherry (mCh) was PCR-amplified using specific primers (Table 2-2), introducing a *Sal*I recognition site into the 5` end and a *Sac*I and *BamH*I sites into the 3` end. To obtain a mCherry with the C-terminal sequence of cardosin A, a specific primer was designed allowing the removal of mCh STOP codon and the introduction of the C-terminal sequence (Table 2-2). The PCR fragments were sequenced and cloned into the *Sal*I and *Sac*I sites of pVKH18-En6-SP-mRFP, resulting in the replacement of mRFP by mCherry.

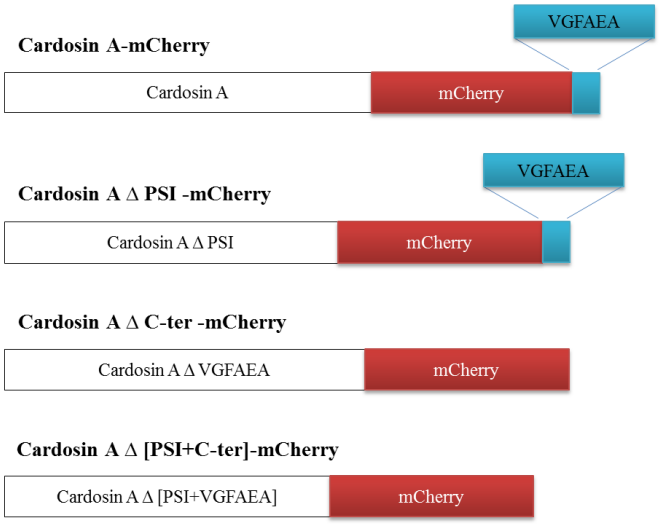

Figure 2.3: Schematic representation of cardosin A fluorescent chimaeras. cardosin A and the cardosin A mutated versions were fused to the N-terminus of mCherry.

Cardosin A constructs were also inserted into the vector containing mCherry to obtain in frame fusions, using the primers A5'prime_Xba and A3'prime_Sal (Table 2-2) to amplify Cardosin A and its truncated versions, allowing the removal of the STOP codon, again containing *Xba*I and *Sal*I sites. To amplify the cardosin A constructs without the C-terminal sequence, A3'prime_C-ter_Sal was used as reverse primer (Table 2-2). Selected clones were inserted into binary vector pVKH18-En6.

Table 2-2: Primers used in the amplification of mCherry, Cardosin A and its truncated versions for the production of the fluorescent fusions.

Primer	Sequence	Description
mCh_Fwd	CAGTCGACAATGGTGAGCAAGGGCG AG	Introduction of a *Sal* I recognition site into the 5` end (red)
mCh_Rev	CTGAGCTCGGATCCTTACTTGTACAG CTCGTCCATGC	Introduction a *Sac* I (red) and *BamH* I (green) recognition sites after the STOP codon.
mCh_C-ter_Rev	ACGAGCTCTCAAGCTGCTTCTGCAAA TCCAACCTTGTACAGCTCGTCCAT	Removal of mCherry STOP codon and introduction of Cardosin A C-terminal sequence (underlined). Introduction a *Sac* I (red) recognition site after the STOP codon.
A3'prime_Sal	GTCGACGCTGCTTCTGCAAATCCAAC	Removal of the STOP codon and introduction of a *Sal* I recognition site (red).
A3'prime_C-ter_Sal	GTCGACGCTAGTAAATTGCCATAATC AAACACTGTG	Removal of the STOP codon and the C-terminal sequence of Cardosin A. Introduction of a *Sal* I recognition site (red).

Isolation and cloning of Cardosin A and B domains with mCherry

To test the ability of the PSI (from cardosin A and from cardosin B) and C-ter sequence (integral sequence and shortened) to direct a protein to the vacuole, this motifs were isolated and placed with mCherry and a signal peptide for ER sorting. Barley lectin C-ter sequence (Dombrowski et al. 1993) and mCherry with only the signal peptide were used as positive and negative controls, respectively.

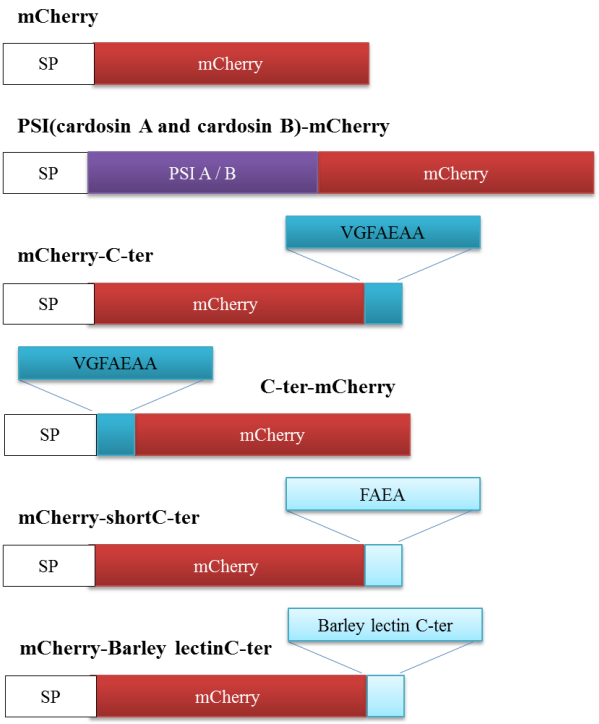

Figure 2.4 Schematic representation of mCherry variants containing the putative sorting motifs. The PSI domain was cloned between the signal peptide and mCherry, while Cardosin A peptide VGFAEA was tested at the C-terminal and N-terminal ends of mCherry. A short C-ter peptide (FAEA) fused to mCherry was also produced. SP-mCherry and Barley lectin C-ter were used as controls. SP – signal peptide

The PSI was amplified from the Cardosin A cDNA by PCR using specific primers (Table 2-3) allowing the introduction of *Sal*I recognition sites and cloned into the pVKH18-En6-SP-mCherry at the 5` end of mCherry. Cardosin B PSI was amplified using the same approach. To introduce the Cardosin A C-terminal peptide sequence into the 3` end of mCherry, the fluorescent protein was amplified by PCR using the reverse primer mCh_C-ter_Rev, introducing the peptide sequence and a *Sac*I recognition site. To introduce the short sequence the approach was the same, but using the primer mCh_FAEA_Rev, and to introduce the barley lectin C-ter the primer used was mCh_Bl_Rev (Table 2-3). mCh_Fwd was used as forward primer in all three cases. The introduction of the C-ter sequence in the N-terminal end of mCherry the approach was

similar, but the forward primer was modified to introduce the C-ter sequence and a *Sal* I recognition site. In this case, mCh_Rev was used as reverse primer. The modified mCherry sequences were cloned into pVKH18-En6-SP-mRFP, as described before.

Table 2-3: Primers used in the amplification of Cardosin A and B domains and cloning with mCherry.

Primer	Sequence	Description
PSIA_Fwd	ACGTCGACTGTCATGAACCAGCAATGCAA	Introduction of a *Sal* I recognition site into the 5` end (red)
PSIA_Rev	ACGTCGACGCACCACCTGCAGCACCACCGGATAAGTGTTCACACAACTCG	Introduction of a *Sal* I recognition site into the 3` end (red)
PSIB_Fwd	ACGTCGACTTTAAACCAACAATGCAAAACATTGG	Introduction of a *Sal* I recognition site into the 5` end (red)
PSIB_Fwd	ACGTCGACGCACCACCTGCAGCACCACCTTCTGCACTTGAAGTGGGTA	Introduction of a *Sal* I recognition site into the 3` end (red)
mCh_FAEA_Rev	AAGAGCTCTCATGCTTCTGCAAACTTGTACAGCTCGTCCA	Introduction of a *Sac* I recognition site into the 3` end (red)
mCh_BI_Rev	AAGAGCTCTCAGGCGATGGCCTCGGCGAAGACCTTGTACAGCTCGTTCCAT	Introduction of a *Sac* I recognition site into the 3` end (red)

Obtaining of Cardosin A inactive mutants

To evaluate the importance of Cardosin A activity in the enzyme processing and trafficking, three constructs were generated: Cardosin A inactivation in the first catalytic triade, cardosin A inactivation in the second catalytic triade and inactivation of both sites simultaneously (Figure 2.5).

The constructs were obtained by creating a mutation in the catalytic triade, modifying an aspartate to an alanine residue. The oligonucleotides used are described in the Table 2-4 and the DNA was amplified using the technique of site-directed mutagenesis and using unmodified cardosin A cDNA as template. Positive clones were confirmed by sequencing with M13 primers [M13uni(-21) and M13rev(-29)] (Eurofins MWG Operon, http://www.eurofinsdna.com/home.htmL) and were amplified again with the primers A5'prime_Xba and A3'prime_Sac, to allow cloning in the binary vector pVKH18-En6 for expression in plant cells.

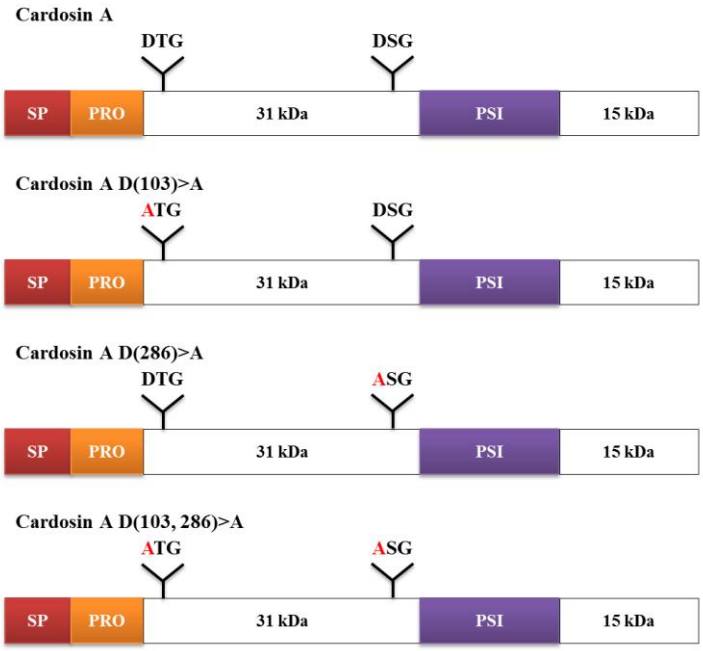

Figure 2.5 Schematic representation of cardosin A catalytic triades (DTG/DSG) and the point mutations introduced in the sequence, marked in red.

Table 2-4: Primers used in the site-directed mutagenesis to obtain inactivation of the catalytic triades.

Primer	Sequence	Description
D103A5'	GTTCACAGTGATTTTCGCTACCGGAAGT TCTGTTCTATGGGTGCCTT	Introduction of a point mutation in the 30th nucleotide of the primer [GAT (aspartic acid) changes to GCT (alanine) - green]
D103A3'	AAGGCACCCATAGAACAGAACTTCCGG TAGCGAAAATCACTGTGAAC	
D286A5'	TGGTTGTCAAGCATTTGCCGCCTCGGA ACCTCTTTGTTGTCAGGT	Introduction of a point mutation in the 30th nucleotide of the primer [GAC (aspartic acid) changes to GCC (alanine) - green]
D286A3'	ACCTGACAACAAAGAGGTTCCAGAGGC GGCAAATGCTTGACAACCA	

Obtaining of Cardosin A glycosylation mutants

Glycosylation is an important feature in terms of protein trafficking and processing. Cardosin A has two glycosylation sites, one in the heavy chain and other in the light chain. Three mutated versions were produced where the glycosylation sites were removed: mutation in the first site, in the second site and mutation in both sites. Moreover, a third glycosylation site was introduced in the PSI region, to simulate the conserved glycosylation site existing in several APs, but which is absent from cardosin A (Figure 2.6).

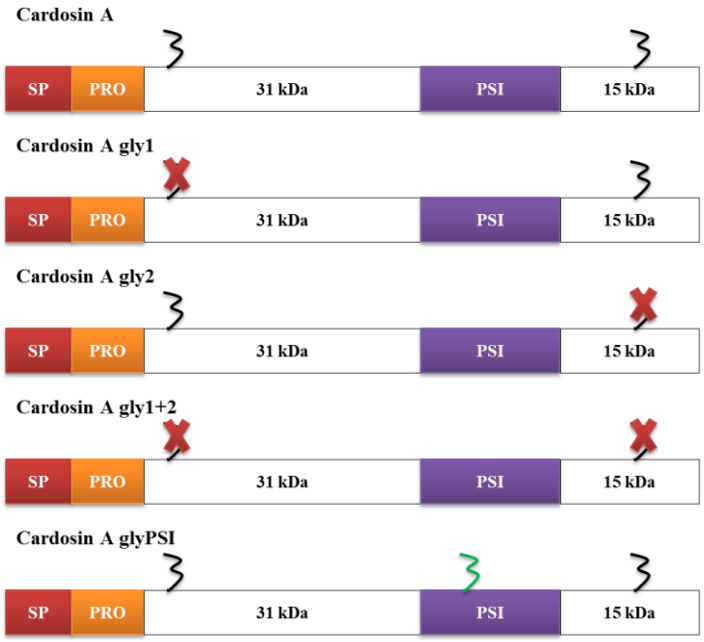

Figure 2.6 Schematic representation of cardosin A glycosylation sites and the mutated versions produced.

The mutations were inserted in the sequence by site-directed-mutagenesis and using the modified primers described in Table 2-5. Unmodified Cardosin A cDNA was used as template in the reactions. Positive clones were confirmed by sequencing with M13 primers [M13uni(-21) and M13rev(-29)] (Eurofins MWG Operon, http://www.eurofinsdna.com/home.htmL) and were amplified again with the primers A5'prime_Xba and A3'prime_Sac, to allow cloning in the binary vector pVKH18-En6 for expression in plant cells.

Table 2-5: Primers used in the site-directed mutagenesis to obtain cardosin A glycosylation mutants.

Primer	Sequence	Description
Amutgly1F	TCAAGTACCTACAAGGAAGCTGGGACA TCTGGCGCTATTA	Introduction of two point mutations in the 19th and 20th nucleotides [AAT (asparagine) changes to GCT (alanine) - green]
Amutgly1R	TAATAGCGCCAGATGTCCCAGCTTCCTT GTAGGTACTTGA	
Amutgly2F	CTCTTTCCTCCATGCCCGCTGTTTCCTT TACAATTGGTGG	Introduction of two point mutations in the 18th and 19th nucleotides [AAT (asparagine) changes to GCT (alanine) - green]
Amutgly2R	CCACCAATTGTAAAGGAAACAGCGGGC ATGGAGGAAAGAG	
AmutglyPSIF	GGATGCAAAACGAAATCAAACAAAACG AGACTGAAGATAAC	Introduction of a point mutation in the 25th nucleotide [AGC (serine) changes to AAC (asparagine) - green]
AmutglyPSIR	GTTATCTTCAGTCTCGTTTTTTTGATTTC GTTTTGCATCC	

2.1.2.Biological material – maintenance and transformation

***Nicotiana tabacum* system**

The analysis of the constructs produced during this work was performed using a transient expression method consisting in *Agrobacterium tumefaciens* mediated infiltration of *Nicotiana tabacum* leaf epidermis.

Germination and Maintenance of *N. tabacum*

Seeds of *N. tabacum* cv. SRI Petit Havana were germinated in petri dishes on filter paper, moistened with water. After germination, seedlings were transferred to individual pots with fertilized substrate (SiroPlant) and maintained in a growth chamber with a photoperiod of 16h light, 60% humidity and 22º C.

Agrobacterium-mediated Infiltration of *N. tabacum* Leaves

One mL of a fresh culture of *A. tumefaciens* transformed with the construct of interest was transferred to a 1.5 mL tube and centrifuged at 16000 xg for 1 minute. The pellet obtained was resuspended in 1 mL of infiltration buffer (10 mM $MgCl_2$ and 10 mM MES) and again centrifuged at 16000 xg for 1 minute. Then, the pellet was resuspended in 1 mL of infiltration buffer, this time supplemented with 100 mM of acetosyringone (3 ', 5'-dimethoxy-4'-hidroxiacetofona to 97%, Sigma-Aldrich), which contributes to increase the virulence *A. tumefaciens*. The samples were centrifuged at 16000 xg for 1 minute and the supernatant resuspended in 1 mL of infiltration buffer with 100 mM acetosyringone. A 1/5 dilution of the cell suspension was made and the absorbance read at 600 nm. Then the infiltration mixture was prepared according to the following equation: (desired OD600 / dilution OD600) x 1000 = required volume (µL) of the dilution to prepare 1 mL of infiltration mixture. Finally, using a 1 mL capacity syringe, without needle, a tobacco leaf was infiltrated, controlling the pressure applied with the syringe on the lower epidermis until the liquid enters through the stomata and infiltrates in the intercellular spaces. The plants were placed in the same growth conditions during the time of the assay.

2.1.3.Organelle isolation and Biochemical assays

Isolation of Protoplasts from *N. tabacum* Leaves

For protoplasts isolation, a *N. tabacum* infiltrated leaf with the construction of interest was used. Three and five days following infiltration, the spaces between two veins were cut and the lower epidermis sheet was removed mechanically, for more efficient digestion of the cell walls. The leaf pieces were then placed floating in enzymes solution [1% (w/v) cellulase and 0.25% (w/v) macerozyme, prepared in TEX medium [3 mM NH_4NO_3, 5 mM $CaCl_2.2H_2O$, 2.4 mM MES and 0.4 M sucrose in Gamborg B5 medium (Duchefa)] and incubated in the dark for approximately 16 hours at room temperature. The enzymes solution was always prepared fresh before each test. After the digestion period, protoplasts were recovered and filtered through a 100 nm nylon mesh. The original plate was washed with an extra 4 mL of TEX medium to release the remaining protoplasts, which were recovered as described. The filtered protoplasts suspension was carefully transferred to 15 mL centrifuge tubes and 1 mL of mannitol/W5 [Mannitol (400 mM) and W5 medium (154 mM NaCl, 125 mM $CaCl_2$, 5 mM KCl, 5 mM glucose and 1.4 mM MES, pH 5.6) at a ratio of 4:1] was added on top of it without mixing the two phases. The suspension was centrifuged at 100 xg for 10 minutes with Acc / Bcc = 1. After centrifugation, the intact protoplasts floats below the manitol/W5 layer and the damage ones formed a pellet. The protoplasts layer was recovered to a new tube with an excess of mannitol/W5 (which should be at least 3 times the volume of protoplasts) and the two phases were mixed. The suspension was centrifuged again at 100 xg for 5 minutes to pellet the protoplasts. Finally, the supernatant was removed and the protoplasts pellet stored on ice. A sample of 50 µL was stored for total protein extraction and the remaining volume was kept on ice and to be used for vacuoles preparation.

Preparation of Vacuoles from *N. tabacum* Protoplasts

The preparation of vacuoles from *N. tabacum* infiltrated leaves was performed following the protoplasts isolation. To the chilled protoplasts pellet 3 mL of lysis solution [0.2 M Mannitol 10% (w/v) Ficoll 400, 20 mM EDTA, 5 mM Hepes, pH 8.0, 2 mM DTT and 150 mg/mL BSA] preheated to 42 °C were added, resuspending the cells with a pipette. Cells were incubated at room temperature for 5 minutes with gentle shaking to allow lysis. After the lysis, a Ficoll gradient was

prepared to separate the vacuoles fraction: 1.5 mL of 5% (v/v) Ficoll buffer (lysis buffer and vacuoles buffer at 1:1 ratio) was carefully added on top of the lysate and then 0.75 mL of vacuoles buffer (0.6 M Mannitol, 10 mM Hepes, pH 7.5 and 150 mg/mL BSA) was also added so as to be visible an interface between all three solutions. The obtained gradient was centrifuged at 1500 xg for 20 minutes and the upper phase (enriched in vacuoles) was collected using a pipette with the tip cut off. The fraction of vacuoles was frozen in liquid nitrogen. The process of rapid freezing in liquid nitrogen vacuoles is sufficient to burst the tonoplast and release the vacuoles content.

Total protein extraction

Proteins were extracted from the leaf tissues or protoplasts fractions using the same approach. For protein extraction 70-100 mg of leaf tissue or 50-100 µL of protoplasts were used. For each sample, two volumes of extraction buffer [50 mM sodium citrate, pH 5.5; 5% (w/v) SDS, 0.01%(w/v) BSA, 150 mM NaCl, 2% (v/v) ß-mercaptoethanol and 10µL of protease inhibitor cocktail per 300 mg of leaf tissue] were added and the samples were vortexed briefly. The samples were then boiled for 10 minutes and centrifuged at 16000xg for 30 min. The supernatant was collected and stored at -80 °C. Quantification of protein samples was performed according to Bradford (1976).

Precipitation of Proteins - Trichloroacetic Acid Method

Vacuole protein fractions were precipitated by Trichloroacetic acid (TCA) using 1 volume of 20% (w/v) TCA and vortexing for 15 seconds. After incubation on ice for 15 minutes, the mixture was centrifuged at 15000 x*g* for 15 minutes at 4 ºC. After removal of the supernatant, 1 mL of ice cold acetone was added and samples were centrifuged again in the same conditions. This acetone-washing step was repeated and the pellet, air-dried, was resuspended in the appropriate volume of protein extraction buffer and boiled for 5 minutes. After a brief spin, supernatants were collected and stored at -80 ºC. Quantification of protein samples was performed according to Bradford (1976).

Denaturing Gel Electrophoresis

The analysis of protein expression was made by vertical electrophoresis on polyacrylamide gel under denaturing conditions. The electrophoresis apparatus -

mini Omnipage (Cleaver Scientific) – was mounted and a 12.5 % running gel prepared [1.57 mL distilled deionized water, 2.08 mL of polyacrylamide (30% acrylamide/bisacrilamide solution - BioRad), 1.25 mL 1.5 M Tris pH 8.8, 50 µL 10% (w/v) SDS, 50µL 10% (w/v) APS and 10 mL of TEMED (N, N, N', N'-Tetramethylethylenediamine - Sigma)]. The gel was added into the compartment between the glass and the plate, avoiding bubble formation. Ethanol was added on top of the running gel to allow polymerisation and the levelling of the gel surface. After polymerization the ethanol was removed, the surface of the gel washed with distilled and deionized water and the 4 % stacking gel prepared [1.4 mL distilled deionized water, 330 mL of polyacrylamide (30% acrylamide/Bis Solution - BioRad), 250 µL 0.5 M Tris pH 8.8, 0.5 µL phenol red, 20 µL 10% (w / v) SDS, 20µL 10% (w/v) APS and 10 mL of TEMED (N, N, N', N'-Tetramethylethylenediamine - Sigma). The gel was added over the running gel and the comb placed. Finally, the comb was removed and the wells washed with water. To the protein samples (15 µg of total protein) sample buffer for SDS-PAGE [0.225 M Tris-HCl pH 8, 50% (v/v) glycerol, 5% (w/v) SDS, 0.05% (w/v) Bromophenol Blue and 0.25 M DTT] was added at a ratio of 1:5 and the samples were incubated at 65 °C for 5 minutes immediately before application to gel. Electrophoresis was conducted at 100-150 V in running buffer for SDS-PAGE [165 mM Trizma base, 128 mM glycine and 1% (w/v) SDS].

Western Blotting

For detection of cardosin A and its truncated versions by Western blotting, an antibody specific for cardosin A recognizing different epitopes along the protein chain was used (Faro et al. 1999), while for mCherry fusions a commercially available antibody anti-mCherry was used (BioVision). After the end of the electrophoresis, the gel was removed from the support and incubated in transfer buffer [25 mM Tris, 192 mM Glycine, 20% (v/v) methanol]. A nitrocellulose membrane (Protran nitrocellulose Hybridization Transfer Membrane, 0.2 mM - Schleicher and Schuell) and two portions of 3MM paper with the dimensions of the gel were prepared and soaked in transfer buffer. The blotting was prepared in a transfer unit (Omnipage mini, Cleaver Scientific) according to the manufacturer's instructions. Transfer buffer was added to the unit until completely cover the membrane-gel cassette and 100 V were applied for 1 hour, with constant stirring. After the transfer process, the buffer was discarded and the membrane incubated for 2 minutes in TBS-T [50 mM Tris, 200 mM NaCl, 0.1% (v/v) Tween 20], to eliminate

possible traces of methanol. The solution was replaced with blocking solution [5% (w/v) skim milk, 1% (w/v) BSA and 0.5% (v/v) Tween-20 in TBS-T], and the membrane was incubated for 30 minutes in this solution at room temperature. The primary antibody was diluted in blocking solution and incubation took place for 1 hour at room temperature or alternatively at 4 °C for 16 hours with constant shaking. Then, three washings were performed in TBS-T, the first with the duration of 10 minutes and the followings for 5 minutes. The incubation with the secondary antibody - Alkaline phosphatase anti-rabbit IgG (H + L) (Vector), diluted in TBS-T – was performed for 1 hour at room temperature with constant shaking. After the incubation step, three washes were carried out similarly to the ones already described. Finally, the membrane was washed in water and incubated in a solution of NBT-BCIP (Western blue stabilized substrate for alkaline phosphatase, Promega) till the development of blue bands. The membrane was washed with water, incubated in STOP solution (20 mM EDTA) and dried between two sheets of 3MM paper.

2.1.4. Cell Imaging at the light level

CLSM Analysis

Cells expressing mCherry and/or GFP fusions were imaged using Confocal Laser Scanning Microscopy (CLSM, Leica SP2). mCherry emission was detected between 580-630 nm, using 561nm excitation. Single-colour imaging of GFP was done using 488nm excitation and fluorescence emission was detected between 500-528 nm. Transmission images were taken simultaneously in Nomarski mode DIC. Routinely, dual-colour imaging was run with fast simultaneous scanning.

Drug treatment assays

Tobacco leaves were co-infiltrated with the construction under analysis and a positive control construct (ST-GFP, Aleu-GFP or Sec-GFP). GNL1-YFP was used as a negative control for the effect of BFA. At 30-40 h after infiltration, infected areas of the leaves were infiltrated with 50 µM BFA, with 10 µM Wortmannin or with 10 µg/mL Tunicamycin. The infiltrated areas were removed and left to float on the same solution, at 21 °C in the dark. After 0, 1 and 2 h treatment, for BFA, and after 2 h, for Wortmannin and Tunicamycin, the cells were imaged using CLSM.

Dominant Negative Mutants Assay

Two dominant negative mutants affecting the ER-to-Golgi pathway were used in this work: RabD2a N121I (Batoko et al. 2000) and SarI H74L (Andreeva et al. 2000). These assays were carried out in *N. tabacum* leaf epidermis in a transient expression manner (see section 2.1.1.2). The constructs to test (cardosin A, mutated versions, or controls) were co-infiltrated with the wild-type version of the mutant (as control) or with the dominant negative mutant. Three days after infiltration a sample was taken from the infiltrated leaf and cells were imaged using CLSM.

2.2. CARDOSIN A STUDIES IN BRIGHT YELLOW-2 SUSPENSION CULTURED CELLS

The main goal in the study of cardosin A expression in Bright Yellow-2 (BY-2) cells was to obtain a cellular system were the protein could be tracked *in vivo*, from its synthesis to its final destination. The detailed procedures undertook in this study are described below.

2.2.1. Production of molecular biology tools

Cardosin A fusion with mCherry was already available for transformation BY-2 cells (see section 2.1.2 of this chapter). Additionally, a fusion of cardosin A with the photoconvertible protein Kaede was also produced.

Fusion of Cardosin A versions with fluorescent reporters

To obtain cardosin A-Kaede, sialyl-transferase in pVKH18En6 ST-Kaede (Brown et al. 2010) was replaced by a PCR-fragment of the cardosin sequence coding for the whole protein amplified by PCR. Cardosin A was amplified using the specific primers already described (A5'prime_Xba and A3'prime_Sal – see Table 2-1 and Table 2-2) introducing a Xba I recognition site in the N-terminal end and a Sal I recognition site in the C-terminal end and using native cardosin A miniprep as template. The amplified product was cloned into a T-overhang vector (pGEM-Teasy, Promega) and analyzed by restriction mapping and sequencing, with the universal primers M13uni(-21) and

M13rev(-29). Cardosin A was then cloned in pVKH18En6 in Xba I-Sal I sites, promoting the removal of the ST-Kaede and its replacement by Cardosin A. the methods used in DNA manipulation and analysis were already described in section 1.6.1.

2.2.2.Biological material – maintenance and transformation

BY-2 system

Bright Yellow-2 suspension cultured cells were transformed with two constructs produced during this work – cardosin A-Kaede and cardosin A-mCherry – resourcing to a method of co-cultivation with *Agrobaterium tumefaciens*.

Maintenance of BY-2 Cell Culture

Nicotiana tabacum Bright Yellow-2 suspension-cultured cells were grown in the dark at 27 °C with 130 rpm orbital shaking, in 250 mL Erlenmeyer flasks. The cells were subcultured every 7 days at 5/80 mL in BY2 medium [4,3 g/L Murashige and Skoog powder with vitamins (MS – Duchefa), 200 mg/L KH_2PO_4, 100 mg/L Mio-inositol, 30 g/L Sucrose, 2 g/L MES, pH 5,6] supplemented with 0,5 mg/mL Thiamine and 0,5 mg/mL 2,4-D. Callus tissue was obtained spreading 1mL of cultured cells onto BY2 medium with 1.5% (w/v) microagar.

BY-2 Transformation by Co-Cultivation

The transformation of BY-2 cells was made by co-cultivation with transformed *A. tumefaciens*. Three days before transformation, a new subculture was set-up and the day before the transformation an *A. tumefaciens* culture, containing the binary vector and the construction to be expressed, was prepared. To prepare the co-cultivation the absorbance at 600nm of the *A. tumefaciens* culture was measured and diluted to OD600 = 1.0 in LB medium. For each transformation, 2 mL of BY-2 cells were pipetted into a 40 mm Petri dish and 1 µL of 100 mM acetosyringone was added to each one. Next, *A. tumefaciens* culture carrying the construction in a binary vector was added to the cells. For each vector, two transformations using two different amounts of *A. tumefaciens* were used, i.e., 50 µL and 100 µL. The plates

were gently swirled to mix components. The plates were placed inside 90 mm Petri dishes, wrapped with Parafilm® and incubated at 27 °C. Two days after setting up the co-cultivation, the washing steps were conducted. The BY-2 cells from each plate were transferred into 15 mL centrifuge tubes, the plate rinsed with additional 5 mL of BY2 medium and added to the centrifuge tube. The cells were allowed to settle in the centrifuge tube and the supernatant was carefully removed. BY2 medium was again added into the tube with the cells to make a 14-15 mL final volume and mixed by gentle inversion. Cells were pelleted as before and this washing step was repeated two more times. A final wash using BY2 medium supplemented with 500 µg/mL cefotaxime was done and the cells were finally resuspended in 12 mL of BY2 medium with 500 µg/mL cefotaxime. Cells were then plated on selective and non-selective medium: 1 mL of washed cells was plated onto a 90 mm Petri dish containing BY2 medium plus 500 µg/mL cefotaxime (non selective) and 1 mL onto BY2/cefotaxime/50 µg/mL kanamycin plates (selective). Cells were spread over the agar surface by rocking and swirling the plate. Plates were wrapped with parafilm and incubated at 27 °C, in the dark, till the formation of calli (visible after 15 days – 1 month). To screen for transformants nine distinct calli were picked using a sterile forceps and transferred to a fresh plate containing BY2/ cefotaxime/kanamycin medium. The calli were allowed to grow for 7 days and then scored for growth and GFP production under a fluorescence microscope.

2.2.3. Cell Imaging at the light level

CLSM Analysis

Cells expressing mCherry or Kaede fusions were imaged using CLSM (Leica SP2). mCherry and the red Kaede emission were detected between 580-630 nm, using 561nm excitation. Single-colour imaging of green Kaede was done using 488nm excitation and fluorescence emission was detected between 500-528 nm. Transmission images were taken simultaneously in Nomarski mode DIC. UV-violet light exposure was used for photoconversion of Kaede protein. Dual-colour imaging was run with fast simultaneous scanning.

Drug treatment assays

BY-2 cells were treated with 50 µg/mL of BFA for 30 minutes and imaged using CLSM or fixed for TEM. As control, cells without BFA were used.

Immunolocalisation in BY-2 cells

Three and 5 days old BY2 cultures (WT and transformed lines) were selected and 10 mL of each culture were used. The cells were allowed to settle in a 15 mL tube and the media was replaced by fixative solution (3% (w/v) paraformaldehyde) and incubated for 1h. 5 washes of 5 minutes each were performed using MSB buffer (10% (v/v) PBS 10x, 10% (v/v) $MgSO_4$ 100 mM, 10% (v/v) EGTA 100mM, pH 6.8) and the cells were treated with a 1% (w/v) cellulase and 1% (v/v) pectinase solution for 15 minutes to promote a partial digestion of the cell wall. Following 2 more washes in MSB buffer, the cells were placed in a 10 well glass slide to obtain a thin layer of cells. Cells were allowed to dry and incubated in 0.5% (v/v) Triton x-100, prepared in MSB buffer, for 10 minutes in a wet chamber. Before blocking with 100 mg/10 mL BSA for 15 minutes, two washes of 10 minutes each were made. The incubation with primary antibodies was performed ON (overnight), in a wet chamber. Two different primary antibodies were used: anti-mRab and JIM84. Incubation with secondary antibody (Alexa Fluor 488, Invitrogen) was done at room temperature in the dark, for 1h. Three final washes were made in MSB buffer supplemented with fish gelatin and the preparation was sealed with a cover slip.

2.2.4. Transmission Electron Microscopy

Chemical Fixation for Epoxi Resin Inclusions using AMW ®

This procedure was used for fixation of BY-2 suspension cultured cells. 5 mL of the suspension culture were used and the cells were allowed to settle in a centrifuge tube. The medium was removed and replaced by the fixative solution [3% (v/v) glutaraldehyde and 1% (v/v) paraformaldehyde prepared in 0.1M cacodilate pH 6.8], in which the cells were incubated in the dark and with agitation for 16h. Cells were washed three times in 0.1M cacodilate buffer, for 10 minutes each. Cells were then post-fixated in a 1% (v/v) Osmium solution, prepared in 0.1M cacodilate buffer

for 1 hour at room temperature, followed by 3 washes in water, for 10 minutes each and at room temperature. After this washing step the cells were included in a 10% (w/v) gelatine solution (prepared in water), and small blocks of cells/gelatine (1-3 mm^3) were prepared. The dehydration steps in ethanol graded series started at room temperature as follows: 10%, for 10 minutes, 20% for 15 minutes and 30% for 20 minutes. The next dehydration, embedding and polymerisation steps were performed in an AMW device (Leica) and used according the manufacturer instructions. The program used is described in Table 2-6.

Table 2-6: Program used in the AMW device for Dehydration, Embedding and Polymerization of BY-2 suspension cultured cells.

Step	Reagent	Duration (minutes)	Temperature (ºC)
Dehydration	Ethanol	1	RT
	Ethanol	1	RT
	Ethanol	1	RT
	Ethanol	5	RT
	Ethanol	5	RT
	Ethanol	5	RT
	Acetone	3	RT
	Acetone	3	35
	Acetone	3	35
Embedding	Epon:Acetone - 1:2	7	37
	Epon:Acetone - 1:1	7	40
	Epon:Acetone - 2:1	7	45
	Epon	7	50
	Epon	7	50
	Epon	7	50
Polymerisation	Epon	210	60

Cryofixation and Cryosubstution for LR-White Resin Inclusions

For cryofixation BY-2 cells were high pressure frozen using the EMPACT2 system (Leica) as indicated by the manufacturer. The samples were kept in liquid nitrogen until further processing. The samples were subsequently freeze substituted using the AFS2 system (Leica) using the program described in Table 2-7.

Table 2-7: Leica AFS2 program used in cryosubstituion for LR-White resin inclusions.

Step	Temp. Start (ºC)	Temp. End (ºC)	Slope (ºC/h)	Time (h)	Reagent	Content (%)	Transfer	UV
1	-90	-85	7.9	7	Acetone	100	Stay	Off
2	-85	-20	0.9	72	Acetone	100	Stay	Off
3	-20	-20	0	2	Ethanol	100	Exchange/fill	Off
4	-20	-20	0	2	Ethanol	100	Exchange/fill	Off
5	-20	-20	0	2	Ethanol	100	Exchange/fill	Off
6	-20	-20	0	2	Ethanol	100	Exchange/fill	Off
7	-20	-20	0	5	LRW	10	mix	Off
8	-20	-20	0	5	LRW	20	mix	Off
9	-20	-20	0	5	LRW	30	Mix	Off
10	-20	-20	0	5	LRW	40	Mix	Off
11	-20	-20	0	5	LRW	50	Mix	Off
12	-20	-20	0	5	LRW	60	Mix	Off
13	-20	-20	0	5	LRW	70	Mix	Off
14	-20	-20	0	5	LRW	80	Mix	Off
15	-20	-20	0	5	LRW	90	Mix	Off
16	-20	-20	0	5	LRW	100	Exchange/fill	Off
17	-20	-20	0	5	LRW	100	Exchange/fill	Off
18	-20	-20	0	18	LRW	100	Exchange/fill	Off
19	-20	-20	0	6	LRW	100	Exchange/fill	Off
20	-20	-20	0	24	LRW	100	Stay	ON
21	-20	0	20	1	LRW	100	Stay	ON
22	0	0	0	23	LRW	100	Stay	ON

Block Sectioning

The sectioning of LR-White and Epoxi resin blocks was made in an Ultracut UC6 (Leica) ultramicrotome and ultrathin sections of about 70-90 nm were obtained. The LR-White sections were placed in 75 mesh carbon-formvar covered nickel grids and Epoxi resin sections were placed in 300 mesh copper grids.

Immunogold labelling in LR-White sections

Grids were incubated (with the sections facing down) in drops of 1x TBS (10mM Tris and 130 mM NaCl, pH 7.4) with 1% (v/v) tween20 for 10 minutes, followed by an incubation of 10 minutes in 1x TBS with 100 mM glycine. Grids were then transferred to 1x TBS + 100 mM glycine drops with 0.25% (v/v) acetylated BSA for 10 minutes. The

incubation with the primary antibody was performed in drops of 1x TBS + 100 mM glycine + 0.25% acetylated BSA for 1 hour. Following the incubation with the primary antibody 5 washes were made in 1x TBS with 0.25% acetylated BSA, with the duration of 5 minutes each. The incubation with the secondary antibody coupled to 15nm colloidal gold (1:20 dilution) was performed in 1x TBS + 100 mM glycine for 1h. Five washes in 1x TBS of 5 minutes each were performed followed by 5 more washes in distilled water of 5 minutes each. The grids were then allowed to dry on top of a filter paper.

Post-Staining

Ultrathin sections (both from LRWhite or Epoxi) were post-stained with a aqueous 2 % (w/v) uranyl acetate/lead citrate. For the contrasting step a 2 % (w/v) uranyl acetate solution (15 minutes incubation) was used followed by 5 washes in distilled water. The incubation in lead citrate (5 minutes incubation) was performed in a Petri dish with KOH or NaOH pellets, to have a CO_2 free atmosphere, and was followed by 5 washes in distilled water. Grids were allowed to dry on top of a filter paper and stored.

TEM observations

Grids were examined under a JEOL 1400 TEM operating at 120 kV. Images were acquired using a post-column high resolution (11 megapixels) high speed camera (SC1000 Orius, Gatan).

2.3. CARDOSIN A STUDIES IN *ARABIDOPSIS THALIANA* PLANTS

2.3.1. Biological material – maintenance and expression analysis

***Arabidopsis thaliana* system**

Arabidopsis thaliana expressing cardosin A under a dexamethasone inducible system (Samalova et al. 2005) were already available (Duarte et al. 2008) and previously selected by reporter expression till T5 generation. In the course of this

work we selected individuals till T7 and tested them for expression of the reporter and the transgene.

Germination and Maintenance of A. thaliana

A. thaliana seeds were sterilized in 70% (v/v) ethanol for 5 minutes under agitation and left to dry onto a filter paper in the flow hood. Seeds were transferred to MS medium containing 1.5% (w/v) sucrose and 0.7% (w/v) Bacto-agar and stratified for 2 days at 4 ºC. When working with non-homozygous, 20 µg/mL Hygromycin was added to the culture medium to ensure selection of the resistant seedlings. After stratification, seeds were incubated at 21 ºC with 12h light photoperiod for 12-15 days and then transferred to individual pots with fertilized substrate (SiroPlant) and maintained in a growth chamber with the same conditions.

Dexamethasone induction of A. thaliana plants

Induction of transgene expression can be accomplished either in liquid or in solid culture medium, being the conditions the same for both cases. Induction of the transgene expression was performed in MS medium with 20 µM Dexamethasone for periods of 24 hours-7 days at 21 ºC under 12h light photoperiod.

GUS Staining of A. thaliana plants

The screening of transgenic lines can be easily accomplished through GUS staining. This colorimetric assay allows detecting the activity of the protein coded by the GUS reporter gene – β-glucuronidase. *A.thaliana* seedlings were vacuum infiltrated with GUS staining solution [75 mM Phosphate buffer pH 7.0, 10 mM EDTA and 0.5 mg/mL 5-bromo-4-chloro-3-indolyl-β-Dglucopyranoside (X-Gluc, stock solution in DMF, Sigma)] and incubated at 37 ºC for 12 h. After incubation, the staining solution was replaced for 100 µL of 70% (v/v) Ethanol and the samples were incubated at 42 ºC for 30 min. Seedlings were de-stained overnight in 70 % (v/v) Ethanol at room temperature.

Protein extraction and Western blotting

To test for the presence of the transgene, seeds were germinated in solid medium and after reaching the three rosette leave stage were placed in liquid medium with the inducer agent dexamethasone for three days. The seedlings were then collected and frozen in liquid nitrogen before protein extraction as described in section 2.1.3. Protein samples were then subjected to an SDS-PAGE denaturing gel followed by Western blotting using the anti-cardosin A antibody as already described in section 2.1.3.

2.3.2.Phenotypic analysis

To understand if cardosin A expression returns any phenotype to the cells or a delay in the development, cardosin A *A. thaliana* plants were compared to Wild Type plants. Two different assays were made: a growth analysis, focusing key steps of *A. thaliana* development and ultrastructural studies at the cellular level.

A. thaliana Growth Stage–Based Phenotypic

To asses if cardosin A expression retrieved any phenotype a detailed assay based on development processes was carried out (Boyes et al. 2001)comparing Wild Type plants to cardosin A expressing plants induced and non-induced ones. Seeds were germinated in solid medium, as already described, and were passed to soil in the seedling stage, when the root was more than 6 cm long. The induced plants were watered with a solution of dexamethasone. The time of appearance of different developmental points were recorded for further analysis: seed imbibition; radicle emergence, hypocotyl and cotyledon emergence; four stages of leaf development; cotyledons fully opened and two, three rosette leaves and four rosette leaves; first flower buds visible; first flower open and presence of first silliques.

Ultrastructural studies - Cryofixation and Cryosubstution for Epoxi Resin Inclusions

For cryofixation the plant material (*A. thaliana* radicles and cotyledons) was cut in small pieces and high pressure frozen using the EMPACT2 system (Leica) as indicated by the manufacturer. The samples were kept in liquid nitrogen until further processing.

The samples were subsequently freeze substituted using the AFS2 system (Leica) using the program described in Table 2-8.

Table 2-8: Leica AFS2 program used in cryosubstituion for Epoxi resin inclusions.

Step	Temp. Start (ºC)	Temp. End (ºC)	Time (h)	Reagent
1	-90	-90	16	Acetone + 1% osmium tetroxide
2	-90	-60	15	Acetone + 1% osmium tetroxide
3	-60	-60	20	Acetone + 1% osmium tetroxide
4	-60	-30	15	Acetone + 1% osmium tetroxide
5	-30	-30	8	Acetone + 1% osmium tetroxide

The specimens were then removed from the AFS2 system and placed on ice for further processing. The samples were washed three times in ice-cold acetone, for 1 hour each before the embedding. For the embedding steps a series of mixed baths were prepared where the solvent (propylene oxide) was progressively substituted by the Epoxi resin (Agar low viscosity premix kit medium, Agar) as follows: 1/4 resin + 3/4 propylene oxide for 1 hour, 1/3 resin + 2/3 propylene oxide for 3 hours, 1/2 resin + 1/2 propylene oxide for 16 hours, 2/3 resin + 1/3 propylene oxide for 1 hour, 3/4 resin + 1/4 propylene oxide for 3 hours, pure resin for 1 hour, pure resin for 16 hours, pure resin for 8 hours and finally pure resin for 16 hours. The polymerisation was performed at 60 ºC for 18 hours.

Sectioning of the resulting blocks and observation under TEM were performed as described before (sections 2.2.4).

2.3.3. Cell Imaging at the light level

PEG Embedding

A. thaliana seeds were germinated according to the described in section 2.3.1 and two steps of seed germination were selected for PEG embedding: 24h hydrated seed and 3 days of germination. The seedlings were fixated in 3% (v/v) paraformaldehyde diluted in 1x PBS (140 mM Sodium Chloride, Potassium Chloride 2.7 mM, 10 mM Sodium Hydrogen and 1.8 mM potassium hydrogen) at room temperature for 90 minutes in glass vials, with constant shaking. Finished the time of fixation, 5 washes were made in PBS 1x, for 10 minutes each. Then, the process of dehydration was initiated incubating the samples in a graded ethanol series for 30

minutes each mixture - 30% (v/v), 50% (v/v), 70% (v/v), 90% (v/v) and 100% (3 times). The samples were maintained in the last 100% ethanol and placed 42 °C for 10 minutes to reach the embedding medium temperature. An equal volume of the wax solution (90 g of PEG 400 distearate and 10 g of hexadecanol, mixed at 65 °C, but used at 42 ºC) was added to the 100 % ethanol bathing and incubated overnight at 42 °C. The mixture was then replaced by pure wax solution and maintain at 42 ° C for at least 4 hours. The specimens were placed in plastic embedding moulds and left to polymerise at room temperature. Fully polymerised blocks were conserved at 4 ºC.

Poly-L-Lysine coating

The slides used for immunolocalisation studies were coated with poly-L-lysine. New slides were washed with Extran MA 0.1 alkaline (Merck) for 5 minutes and then rinsed in water to remove the excess of detergent. The slides were after incubated for 5 minutes in 70% (v/v) ethanol and then in 0.1% (v/v) poly-L-lysine solution for 10 minutes and left to dry at 55 ºC for 2-3 h.

Immunolocalisation in PEG sections

Thin sections of PEG-embedded blocks were placed in poli-L-lysine coated slides moistened with 1x PBS and were allowed to dry on the slides overnight. The tissues were then rehydrated by a decreasing series of ethanol (100%, 100%, 100%, 90%, 70%, 50%, 30%, prepared in PBS) for 10 minutes each. It is important that once the rehydration is started the preparations are not allowed to dry. The slides were washed twice in 1x PBS for 10 minutes and incubated in blocking solution (10mg/mL BSA in 1x PBS) for 15 minutes. The incubation with the primary antibody (diluted in 1x PBS) was performed in a moisten chamber at 26 °C for 1 hour and the following 5 washing steps were made in 1x PBS with 1 % (v/v) fish gelatin, with the duration of 10 minutes each. After the washing the sections were incubated with the secondary antibody (Alexa 488 ®, Invitrogen), diluted in PBS, at room temperature for 1 hour. Two new washes were made in 1x PBS with fish gelatin for 10 minutes and the excess liquid was removed and the slides coated with a few drops of Citifluor ® and sealed with a coverslip and nail polish. The slides were stored at 4 °C in the dark prior to imaging in a fluorescence microscope or CLSM, as described before.

2.3.4. Transmission Electron Microscopy

Cryofixation and Cryosubstution for LR-White Resin Inclusions

For cryofixation the plant material (*A. thaliana* radicles and cotyledons) was cut in small pieces and high pressure frozen using the EMPACT2 system (Leica) as indicated by the manufacturer. The samples were kept in liquid nitrogen until further processing. The samples were subsequently freeze substituted using the AFS2 system (Leica) using the program described in Table 2-7.

Subsequent analysis involving immunogold labeling, block sectioning, post-staining and observation was performed as described before, in section 2.2.4. The antibodies used in immunogold labeling are described in Table 2-13.

Drug treatment assays

A. thaliana seedlings were germinated in liquid MS medium and, after 3 days germinating, dexamethasone was added to the medium. Twenty four hours later (to allow initial Cardosin A expression) 50 µg/mL BFA was added and samples were collected at 0, 2, 4, 8 and 20 hours of drug treatment. The seedlings were cryofixed for LRWhite inclusion and for Epoxi resin inclusion. As control, non-induced seedlings were used and treated in a similar way.

2.4. MOLECULAR BIOLOGY PROTOCOLS AND TOOLS

Agarose Gel Electrophoresis

The DNA was analysed on an agarose gel [0.8 to 1% (w/v) in 1x TAE buffer (40mM Trizma base, 10% (v/v) glacial acetic acid and 10mM EDTA)] containing 0.5 µg/mL ethidium bromide. The electrophoretic separation was carried out at 200 V in 0.25x TAE buffer and, as molecular weight marker, "DNA Ladder Mix GeneRuler" (Fermentas) was used. The DNA was visualized by ethidium bromide fluorescence UV (302-365 nm), and image was acquired using the Gel Doc XR system (BioRad).

Minipreparation of Plasmid DNA from E. coli

The isolation of plasmid DNA for positive clones screening and to be used in the subcloning processes was performed using the boiling extraction method. A single colony was inoculated in LB medium supplemented with the proper antibiotic and incubated at 37 ºC, for 12-16 h. The culture was transferred into a 1.5 mL sterile tube which was centrifuged for 20 seconds at 16000 xg. The supernatant was removed and the pellet resuspended in 200 µL of STET buffer [8% (w/v) sucrose, 0.1% (w/v) Triton X-100, 50mM EDTA and 50mM Tris-HCl, pH 8], supplemented with 5 mL of 50 µg/mL lysozyme. Cells were incubated at room temperature for 5 minutes and were then boiled for 45 seconds to inactivate the enzymes (DNases and lysozyme). The tubes were centrifuged for five minutes at 16000 xg, the pellet was removed and 200 µL of isopropanol was added to the supernatant to promote the precipitation of nucleic acids. Then, centrifugation was performed at 16000 xg for 10 minutes. Finally, the supernatant was discarded and the pellet washed with 70% ethanol (v/v). The pellet was air dried and resuspended in 20 µL of sterile water.
Extraction of plasmid DNA to be used in DNA sequencing and *A. tumefaciens* transformation was performed using the "GenElute Plasmid Miniprep Kit" (Sigma) according to manufacturer's instructions.

Minipreparation of Plasmid DNA from A. tumefaciens

The isolation of plasmid DNA from *A. tumefaciens* was based on alkaline lysis of the cells. An isolated colony was inoculated in LB medium supplemented with 25µg/mL of kanamycin and 0.4mM IPTG, which was incubated at 28 °C in with orbital shaking at 150 rpm and for approximately 16 h. One mL of the culture was transferred to a 1.5mL tube and cells were centrifuged at 16000 xg for 30 seconds. The pellet obtained was resuspended in 200µL of solution I (50mM glucose, 25mM Tris and 10mM EDTA). After incubation on ice for 10 minutes, 400µL of lysing solution (0.2M NaOH and 1% (v/v) SDS), were added mixing the suspension gently and placing again on ice for 10 minutes. Next, 300µL of neutralization solution (3M KAc and 12% (v/v) acetic acid) were added and the tubes were inverted to mix the sample and incubated on ice for 5 minutes. The tubes were then centrifuged at 16000 xg for 20 minutes and at 6 °C. The supernatant was transferred to a new tube and 0.7 volumes of isopropanol were added. The samples were centrifuged at 16000 xg for 30 minutes at 6 °C. Finally, the supernatant was discarded, the pellet washed

with 70% ethanol (v/v) and air dried. The DNA obtained was resuspended in sterile water and stored at -20 °C.

Digestion of Plasmid DNA

Digestion of plasmid DNA, for colony screening or for subcloning into the expression vector, was always performed according to the instructions of the manufacturer of the restriction enzymes used. The result of this digestion was evaluated by electrophoresis on agarose gel and, if needed, the band corresponding to the DNA of interest was extracted and DNA purified as described above.

Polymerase Chain Reaction

For amplification of the modified cardosin A cDNA a polymerase with proofreading activity - "Pfu DNA polymerase (recombinant)" (Fermentas) – was used to minimize the inclusion of errors in the amplified sequence. The PCR reaction was performed as described in Table 2-9, and cardosin A cDNA (Duarte et al. 2008) was used as template.

Table 2-9: PCR reaction used for amplification of cardosin A constructs.

Reagents	Concentration used
Template DNA	20 - 50 ng
10x Pfu buffer with $MgSO_4$	1x
dNTPs	0.2 mM
Primer Forward	0,3 mM
Primer Reverse	0,3 mM
Pfu DNA polymerase	1U
Sterile distilled water	Up to 25 µL

The reactions were conducted in a termoclycler *Martercycler gradient* (Eppendorf), and in accordance with the conditions on Table 2-10.

Table 2-10: Conditions for PCR reactions

Step		Temperature / Duration
Initial denaturation		94 ºC / 5 min
Cycles x 35	Denaturation	94 ºC / 30 sec
	Annealing	52-56 ºC / 30 sec
	Extension	72 ºC / 2 min per Kb
Final elongation		72 C / 7 min

Site-Directed Mutagenesis

The site-directed mutagenesis technique was used to create point mutations in the nucleotide sequence of cardosin A, to obtain mutants affected in the active site and in the glycosylation sites. The constructions were obtained by PCR using a polymerase with proofreading activity - "Pfu DNA polymerase (recombinant)" (Fermentas). The PCR reaction and conditions are summarized in Table 2-11 and Table 2-12.

Table 2-11. PCR reaction used for site-directed mutagenesis.

Reagents	Concentration used
Template DNA	500 ng – 1 µg
10x Pfu buffer with $MgSO_4$	1x
dNTPs	0.3 mM
Primer Forward	0,4 mM
Primer Reverse	0,4 mM
Pfu DNA polymerase	2.5 U
Sterile distilled water	Up to 25 µL

Table 2-12: Conditions for site-directed mutagenesis reactions.

Step		Temperature / Duration
Initial denaturation		94 ºC / 5 min
Cycles x 12	Denaturation	94 ºC / 30 sec
	Annealing	54 ºC / 30 sec
	Extension	72 ºC / 2 min per Kb
Final elongation		72 ºC / 15 min

After the amplification, the PCR product obtained was digested with DpnI restriction enzyme (Fermentas) for 1 hour at 37 °C, followed by inactivation of the enzyme at 65 °C for 15 minutes. This enzyme requires the presence of Dam methylation type (N6-methyladenine) in the recognition sequence, which is only present in the template DNA molecules obtained from the expression in *E. coli*. Thus, by digesting the PCR product with this enzyme, the synthesized molecules during the PCR reaction (with the mutation) are not damaged. The product of DpnI restriction was used to transform competent *E. coli* cells.

DNA Gel Extraction

The bands containing the DNA of interest were excised from the agarose gel preventing excessive UV exposure in order to minimize DNA damage by UV.. The DNA was recovered from the gel using the "GenElute Gel Extraction Kit" (Sigma) according to the manufacturer's instructions.

Ligation of DNA Fragments

Cloning of the DNA fragments obtained by PCR was performed using a commercial kit for specific cloning of fragments with blunt ends - "Zero Blunt PCR Cloning Kit" (Invitrogen) -, according to the manufacturer's instructions.
Ligation of DNA fragments for sub-cloning into the expression vector, pVKH18-EN6, was performed using "T4 DNA ligase" (Fermentas) and the reaction prepared according to the manufacturer's instructions.

Bacterial Strains

Throughout this work two bacterial strains were used: *Escherichia coli*, strain DH5α (*E. coli*) and *Agrobacterium tumefaciens*, strain GV3101::pMP90 (*A. tumefaciens*). *E. coli* was cultured in Luria Bertani medium (LB) [10 g tryptone, 5 g yeast extract, 10 g NaCl to 1L of medium; to obtain a solid medium 1.5% (w/v) microagar was added – LB-Agar] at 37 °C, under orbital agitation. Cultures of *A. tumefaciens* were also obtained by growing the cells in LB and LB-Agar mediums, but the incubation temperature was 28 °C.

Preparation of DH5α Competent Cells

To obtain chemically DH5α competent cells, a single colony was inoculated in 25 mL of LB medium and the culture placed at 37 °C with orbital shaking at 150 rpm. After 16 h of growth, the pre-culture was added to 225mL of LB medium supplemented with 0.4M $MgCl_2$ and 0.4M $MgSO_4$, and was allowed to grow under the same conditions, until the Optical Density (OD) at 600 nm ranges 0.7. The culture was then placed on ice for 10 minutes, after which was divided by 50mL tubes and centrifuged at 800 xg for 5 minutes. The supernatant was removed and the pellet resuspended in 100mL of RF1 [100mM RbCl, 30mM CaCl2 and 15% glycerol (v/v), pH 5.8, 50mM KAc]; the cell suspension was incubated on ice. After

15 minutes, the cell suspension was centrifuged at 800 xg for 5 minutes and the supernatant was discarded. Finally the cells were resuspended in 16mL of RF2 (1mM RbCl, 223mM CaCl2, 10mM MOPS and 1.5% (v/v) glycerol, pH 8.0) and divided into aliquots of 100µL. The cells were stored at - 80 °C until use.

Transformation of DH5α Competent Cells

Transformation of competent cells was performed using the heating shock method. One hundred µL of competent cells was added to the appropriate volume of plasmid DNA (or ligation product) and the mixture incubated on ice for 30 minutes. Next, a heating shock was induced by transferring the cells rapidly to 42 °C (90 seconds) and then again to ice. To allow recovery of the cells and consequent expression of the genes of interest, 300µL of LB medium was added and tubes were placed at 37 °C for 30 minutes. Finally, the cells were spread on LB-Agar supplemented with the appropriate antibiotic (50µg/mL kanamycin or 100µg/mL ampicillin). The petri dishes were placed at 37 °C for approximately 16 h.

Preparation of Electrocompetent A. tumefaciens Cells

For preparation *A. tumefaciens* electrocompetent cells one single colony was inoculated in 10 mL of LB medium and the culture placed at 28 °C with orbital shaking at 150 rpm. After saturation, the pre-culture was added to 200 mL of LB medium and returned to the same growing conditions until the optical density at 600 nm corresponds to an absorbance between 0.5 and 0.6. The culture was then incubated on ice for 30 minutes and the volume was divided by 50 mL tubes. The tubes were centrifuged for 10 minutes at 1800 xg and the supernatant discarded. The pellet was resuspended in 25 mL of 1 mM HEPES buffer, cooled in ice and the cultures were centrifuged again and the pellet resuspended in 25 mL of 1 mM HEPES buffer. The centrifugation step was repeated and the pellet was resuspended in 20 mL of 1 mM HEPES buffer supplemented with 10% (v/v) glycerol. A last centrifugation was performed the same manner as before, and the pellet was finally resuspended in 0.5 mL of 1 mM HEPES buffer with 10% (v/v) glycerol and aliquoted in 50 µL per tube. The cells were frozen in liquid nitrogen and stored at -80 °C.

Transformation of *A. tumefaciens* by Electroporation

The transformation of *A. tumefaciens* was performed by electroporation, as it is proved to be a more efficient method than the thermal shock. To 50 µL of electrocompetent cells was added 10 µmL of purified DNA and the mixture was transferred to an electroporation cuvette (0.2 cm gap), pre-cooled in ice. Electroporation was performed in the apparatus Bio-Rad Gene Pulser electroporation system (Bio-Rad) at 25 mF, 2.5kV and 200Ω. Immediately after electroporation, 1 mL of LB medium was added to the cells. The recovery of cells was allowed at 28 °C, without agitation, for 4 hours. Finally, the bacterial suspension was spread on LB-agar supplemented with 25 µg/mL of kanamycin and 0.4 mM IPTG and incubated at 28 °C for 48h.

Antibodies

Immunodetection of cardosin A and several endomembrane markers were conducted in the different plant species and tissues under study and even by different techniques. The primary antibodies used and the respective dilutions used in each technique are described in Table 2-13.

Table 2-13: Primary antibodies for immunolocalisation of cardosin A and endomembrane markers.

Antibody	Reference	Dilution		
		Western Blotting	Immunofluorescence	Immunocytochemistry
Anti-cardosin A	(Faro et al. 1999)	1:1000	1:200	1:200
Anti-PSI	(Ramalho-Santos et al. 1998)	Not used	1:250	1:175
Anti-α-TIP	(Jauh et al. 1999)	Not used	Not used	1:75
Anti-γ-TIP	(Jauh et al. 1999)	Not used	Not used	1:50
Anti-δ-TIP	(Jauh et al. 1999)	Not used	Not used	1:25
Anti-mRab	(Bolte et al. 2004)	Not used	1:100	1:100
JIM84	(Satiat-Jeunemaitre & Hawes 1992)	Not used	1:25	Not used
Anti-mCherry	BioVision	1:1500	Not used	Not used

3. RESULTS

CHAPTER I – DEFINITION OF THE TOOLBOX FOR CARDOSIN A BIOGENESIS AND TRAFFICKING STUDIES

Published work:

Spencer C. Brown, Susanne Bolte, Marie Gaudin, Claudia Pereira, Jessica Marion, Marie-Noëlle Soler, Béatrice Satiat-Jeunemaitre (2010) "Exploring Plant Endomembrane Dynamics Using the Photoconvertible Protein Kaede". The Plant journal, 63(4) 696-711.

3.1. BACKGROUND

The use of cardosins as protein models to study plant aspartic proteinases is complicated by the lack of protocols for cardoon transformation, making therefore imperative the search for an heterologous system to study their biogenesis and trafficking. Three approaches were performed, where the right expression and maturation of cardosins had to be checked in order to design the most efficient and convenient heterologous system for cardosins trafficking studies: *Nicotiana tabacum* transient expression system, BY-2 cell suspension cultures and *Arabidopsis thaliana* stable expression.

Each system has its advantages and constraints:

Nicotiana tabacum transient expression in leaf epidermis, *Agrobacterium*-mediated, is a very well characterized model providing a highly efficient transformation of the cells, when comparing to other transformation methods (Sparkes et al. 2006; for review Denecke et al. 2012). Transient expression in *N. tabacum* has a great advantage relative to stable expression as it gives the possibility to test several constructs at the same time and in a short time-lapse (Sparkes et al. 2006). Co-expression of different constructs is also easy, with good expression rates for both, and the use of drugs, affecting cellular endomembranes for example, is also straight forward with this method. For these reasons, this is a popular model of choice for intracellular sorting studies (Boevink et al. 1998; Kotzer et al. 2004; Sparkes et al. 2006; Bubeck et al. 2008; Paris et al. 2010). It also has

the advantages to be highly convenient for live cell imaging by confocal microscopy because of the planarity of the leave. Moreover, epidermal cells are devoided of chloroplasts, facilitating the fluorescence studies. Side-by-side with all the advantages, the model has several constraints as well: transformation is limited in terms of cell types (epidermis and some mesophyll cells) and the system is easily saturated due to overexpression, conducting to mis-sorting of proteins and consequently being difficult to interpret (Sparkes et al. 2006).

***Nicotiana tabacum* cv. Bright Yellow 2 (BY-2)** suspension cultured cells is a well-characterized cell line, growing in darkness and devoided of chloroplasts, highly homogeneous and with a growth rate quite pronounced (increase of 80 to 100 times in one week, due to the short time needed for a whole cell cycle -12h00), being considered the "HeLa" cells of the plant kingdom (Nagata et al. 1992). BY-2 has emerged as a stable expression system with great potential. Originally, BY-2 cells gained attention for its potential as green factories in the large-scale production of secondary metabolites (Geelen & Inze 2001), but their characteristics rapidly turned them into a plant-cell model for several type of studies. Furthermore, BY-2 cells are easily transformable after protoplast formation or directly via electroporation and particle bombardment or by co-cultivation with *Agrobacterium tumefaciens*. Consequently, studies of subcellular localization have become increasingly popular as well as the study of cell dynamics and cell cycle proteins, using fluorescent proteins reporters or by indirect immunofluorescence (Geelen & Inze 2001). The use of BY-2 cells in the study of intracellular sorting is strengthened by the increasing availability of transgenic cell lines expressing markers of different cell compartments.

Arabidopsis thaliana is a plant model with widespread acceptance due to the genetic and genomic methods and resources that are available for study (Somerville & Koornneef 2002). There are several characteristics that make Arabidopsis an attractive model for several studies. Its small size and simple growth without major requirements make it easy to keep in laboratory conditions. Moreover, an unconditional advantage is that their entire life cycle, from seed germination until maturation of the first seed, takes only 6 weeks (Meinke et al. 1998) and it is able to produce many offsprings in a short time, from a single specimen. Furthermore, it is easily transformed by simply spraying the flowers with *Agrobacterium* containing a gene of interest and then select the plants for the presence of the transgene in successive generations. These advantages promoted an increasing interest by the

scientific community resulting in the characterization of various genes. Indeed, it is the first plant whose entire genome has been sequenced (Somerville & Koornneef 2002) and it has been created a database where all Arabidopsis-related information is available.

Two of these three model plants have actually been tested in our laboratory for cardosin A expression (alone, without fluorescent tag) by biochemical analyses: transient expression in *Nicotiana tabacum* leaves, and stable expression of the transgene in *Arabidopsis thaliana* (Duarte et al. 2008). In the present work, we aimed to go further in these analyses of cardosin expression in heterologous systems by visualizing putative effects of a fluorescent tag on protein expression/maturation, and following the dynamics of cardosins trafficking. We have also tempted to establish a BY-2 cell suspension culture model that would allow tracking cardosin A *in vivo*.

3.2. RESULTS

3.2.1. Transient expression in Nicotiana tabacum leaf epidermis

Protocol set-up

Analysis of expression and targeting of the modified cardosin A constructs obtained in this work was performed on *N. tabacum* leaves, through a transient expression system mediated by *A. tumefaciens*. All the constructs produced in this work destined for analysis by this expression method were cloned into pVHK18-EN6 binary vector (Batoko et al. 2000), in which the transgene is under the control of different regulatory sequences, including six repetitions of the 35S promoter of cauliflower mosaic virus (CaMV) (Figure 3.1).

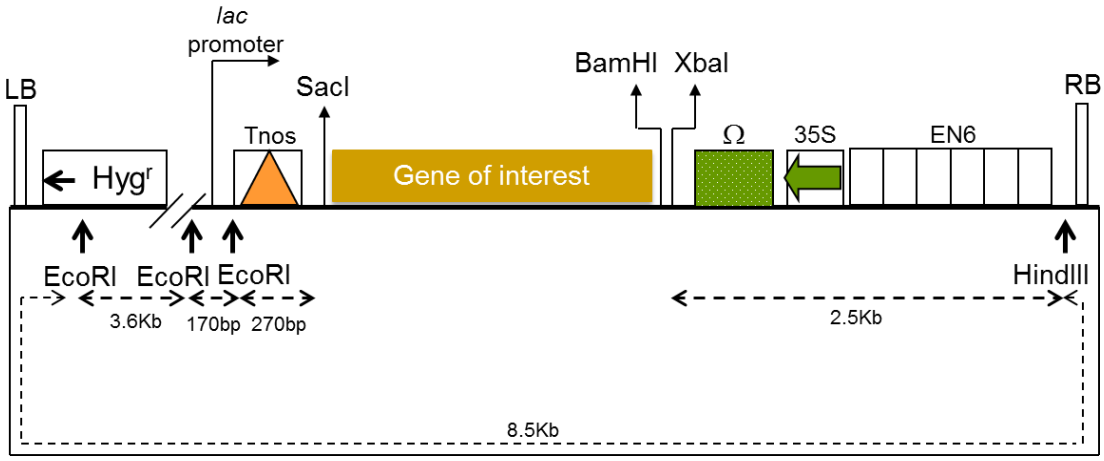

Figure 3.1 Schematic representation of pVKH18-EN6 binary vector, used for transient expression of cardosin A and its mutated versions in tobacco leaves. En6 - 35S CaMV promoter + 6x enhancer; Hygr - hygromycin resistance gene; LB - left border, RB - right border; Tnos - nopaline synthase terminator. Adapted from Batoko et al. (2000).

N. tabacum plants (Figure 3.2 a, b and c) were maintained at constant conditions during growth and after infiltration, since variations in temperature, humidity and photoperiod can be sufficient to initiate changes in expression levels.

Figure 3.2 *Nicotiana tabacum* plants in several developmental stages. (a) 2-3 weeks old plants; (b, c) 5-6 weeks old plants, ready to be transformed; (d) Infiltration procedure; (e) Leaf prepared for infiltration; (f, g) 5 days after infiltration (black arrowheads indicate the infiltrated areas); (h) Infiltrated areas removed for protein extraction and /or imaging.

The transient transformation of the leaves was obtained by infiltration of the lower epidermis (Figure 3.2 d). Fully expanded leaves of plants with approximately 5 to 6 weeks germination (Figure 3.2 e) were used. For time-course and imaging assays, the spaces between the ribs were infiltrated with the same or different constructs (Figure 3.2

f, g and h) and for protoplasts and vacuoles preparations an entire infiltrated leaf was used.

Cardosin A and Cardosin A-mCherry time-course assays revealed proper protein maturation

Cardosin A and cardosin A-mCherry expression and processing were first analyzed by means of a time-course assay. Leaf fragments were sampled at 24 h, 48 h, 3 days, 5 days, and 7 days after *Agrobacterium tumefaciens* infiltration (agro-infiltration). Leaf protein extracts were analysed on western blot using an anti-cardosin A specific antibody (Figure 3.3).

Cardosin A was first detected 24 h after infiltration. The antibody revealed two bands at this time point: a 34 kDa band corresponding to the intermediate form of the heavy chain with the pro-segment and a 31 kDa band corresponding to the mature form. As time went on, the 34 kDa intermediate form reduced in intensity and eventually disappeared, while the intensity of the 31 kDa band increased over time, showing a peak of expression at 5 days after infiltration (Figure 3.3 a). This suggests that cardosins are properly processed with time.

To investigate the intracellular localisation of Cardosin A, vacuoles were purified from leaf protoplasts, and protein samples were obtained at 3 and 5 days after infiltration (Figure 3.3 a). In both the protoplasts and in the vacuolar protein extracts obtained 3 days after infiltration, the same two bands, corresponding to the intermediate and mature forms, were detected, being the 31 kDa band the most intense. At 5 days after leaf infiltration only the mature form was detected in the vacuolar fraction. The Cardosin A precursor form, calculated to measure 61 kDa, was never detected in any of the assays, showing that initial processing steps are very fast in this system.

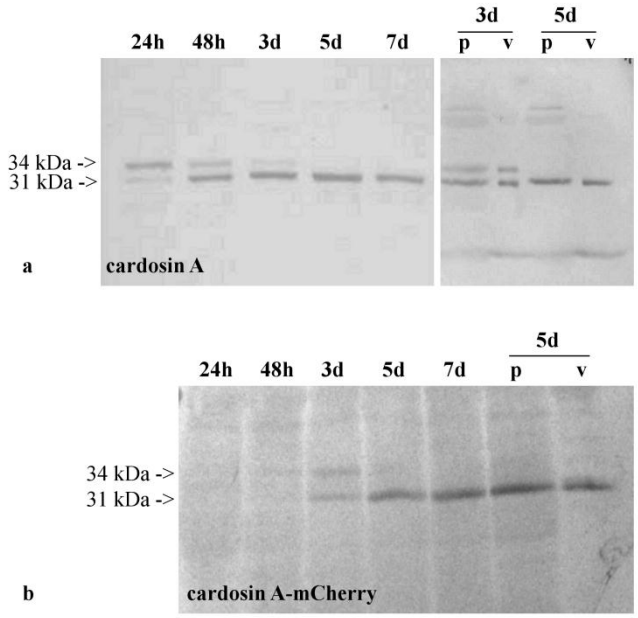

Figure 3.3 Protein gel blot analysis of *Nicotiana tabacum* leaves overexpressing cardosin A and cardosin A-mCherry fusion. 15 µg of total protein extracts from total leaf, or protoplasts and vacuole preparations isolated 3 and 5 days after infiltration, were separated on SDS PAGE and transferred onto nitrocellulose for western analysis. Blots were incubated with a specific antibody recognizing the heavy chain of Cardosin A. (a) cardosin A time course, protoplasts and vacuoles fractions; (b) cardosin A-mCherry expression during a time course, protoplasts and vacuoles fractions. d – days, h – hours, p – protoplasts, v – vacuoles.

Next, the impact of the fluorescent tag mCherry on this maturation process was observed. The choice of the fluorescent tag mCherry instead of GFP, for example, was related to its photostability in the acidic pH of the lytic vacuole (Shaner et al. 2004). It is known that GFP gradually losses brightness when accumulated in the vacuole and, since our protein is most probably accumulating in this organelle, mCherry was chosen to overcome a possible problem right from the beginning of the work. The m-Cherry tagged version of cardosin A was only detected in the blot 48h after leaf infiltration and in its 34 kDa intermediate form. Three days after leaf infiltration the 31 kDa form was visible and in the next time-points - 5 and 7 days – this was the only form detected (Figure 3.3 b). This observed delay in expression and processing of the protein when compared with the non-tagged version is probably due to the fusion with mCherry that being a larger protein is more difficult to process. Nevertheless, the fusion was detected in protoplasts and vacuoles fractions obtained from leaves 5 days post-infiltration and only one band was visible, corresponding to the processed mature form (Figure 3.3 b).

This result designs the cardosin A-mCherry protein as a valuable protein model to study cardosin A trafficking, with a correct protein (but slightly delayed) processing.

Cardosin A-mCherry fusion accumulates in the Vacuole

The expression and localisation of the fusion protein cardosin A-mCherry was therefore analysed by Confocal Laser Scanning Microscopy (CLSM). In a first optimization step two different *A. tumefaciens* titrations (OD600nm = 0.03 or 0.3) were used and images were acquired 3 days after leaf infiltration. With 0.03 *A. tumefaciens* OD, the results obtained confirmed the vacuolar localisation of cardosin A-mCherry fusion (Figure 3.4 a and b). For an OD of 0.3, more cells became labelled, but no significant differences were detected in the cellular localisation (Figure 3.4 c and d).

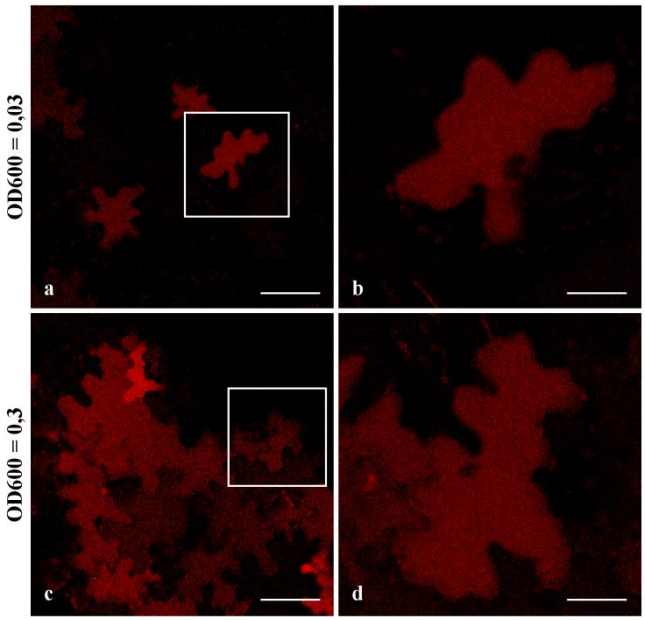

Figure 3.4 Subcellular localisation of mCherry-tagged cardosin A. Cardosin A-mCherry was transiently expressed in tobacco leaves using agro-infiltration. Images were taken 3 days after infiltration. (a, b) Expression of cardosin-mCherry using an *A. tumefaciens* OD of 0,03; (c, d)) Expression of cardosin-mCherry using an *A. tumefaciens* OD of 0,3. Images were acquired using the 561 nm laser for mCherry. Bars: a, c, 75 µm; b, d, 25 µm.

In all cases, cardosin A-mCherry fluorescence was predominantly detected inside the vacuoles confirming the previous biochemical analyses. Using the samples infiltrated with the higher 0.3 OD the assay was extended till 7 days after infiltration and cardosin A-mCherry fusion was always detected in the vacuole of *N. tabacum* cells (FIGURE 3.5 a, b and c).

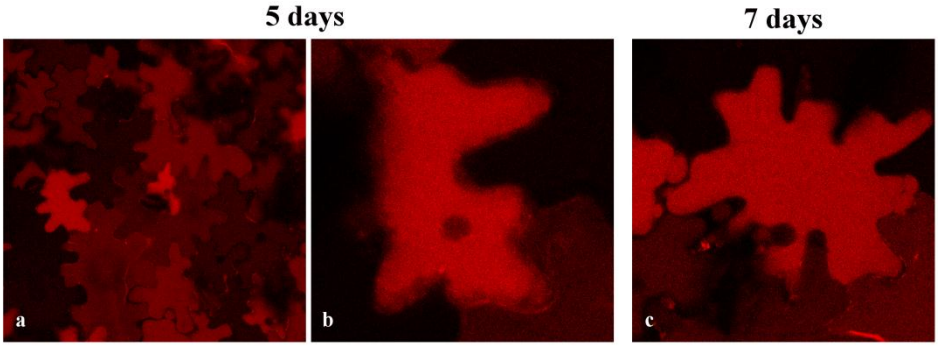

Figure 3.5 Subcellular localisation of cardosin A-mCherry. Cardosin A-mCherry was transiently expressed in tobacco leaves using agro-infiltration. Images were taken 5 (a and b) and 7 days (c) after infiltration. Expression of cardosin-mCherry using an *A. tumefaciens* OD of 0,3. Images were acquired using the 561 nm laser for mCherry. Bars: a, 75 µm; b, c, 25 µm.

Cardosin A-mCherry uses a ER-(X)- PVC pathway to reach the vacuole

Considering these results, the next question was to ascertain if all cardosin A molecules being produced were already in the vacuole or if some amount of cardosin A-mCherry was still trafficking to this compartment. In order to detect any transport through the secretory pathway, co-expression of cardosin A-mCherry with well-known fluorescent markers for Endoplasmic reticulum (GFP-HDEL, Boevink et al. 1998), Golgi apparatus (GA) (ST-GFP, Saint-Jore et al. 2002), Prevacuolar Compartment/Vacuole (Aleurain-GFP, Di Sansebastiano et al. 2001) and to the Cell Wall (Sec-GFP, Zheng 2005) were performed and resulting fluorescent patterns were observed 3 days after infiltration by confocal microscopy .

When cardosin A-mCherry was co-expressed with GFP-HDEL its vacuolar accumulation was not altered, and no co-localisation with the ER marker was observed (Figure 3.6 a). The typical ER pattern may however be affected par the expression of the construct, as GFP fluorescence was sometimes detected in the cell periphery as green fluorescent aggregates. Co-expression of ST-GFP with cardosin A-mCherry did not affect the expression of either construct: red fluorescence was detected in the vacuole, and green in small dots in the cytoplasm at the periphery of the cell, corresponding to the GA (Figure 3.6 b). No co-localisation was observed with this Golgi marker. No co-localisation with the marker Sec-GFP (Figure 3.6 d) was found either, with cardosin A accumulating in the vacuole, and the Secreted GFP being found in the ER and in the cell wall. The picture was different when co-expressing cardosin A-mCherry with the PVC/Vacuolar compartments aleurain GFP (Figure 3.6 c): some yellow dots, corresponding to the superimposing of mCherry with GFP, were visible in the periphery

of the cell (Figure 3.6 c, arrow-heads), corresponding probably to the Prevacuolar Compartment.

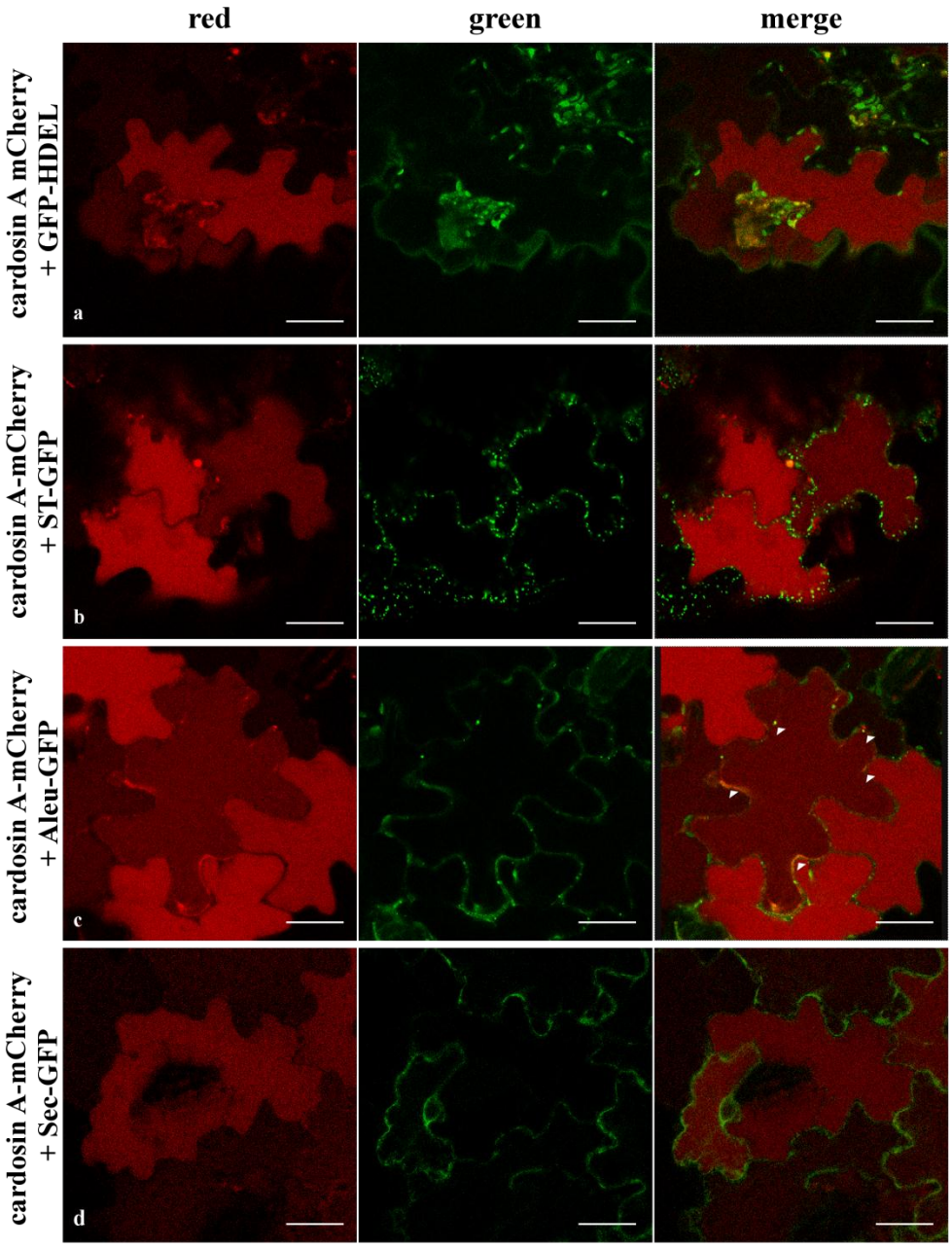

Figure 3.6 Co-localisation of cardosin A-mCherry with GFP-HDEL, ST-GFP, Aleu-GFP or Sec-GFP in *N. tabacum* epidermal cells. Cardosin A and the endomembrane markers were transiently expressed in tobacco leaves using agro-infiltration. For co-expression of two constructs, the respective Agrobacterium strains were mixed prior to infiltration. Images were taken 3 days after leaf infiltration and acquired using a 488 nm laser for GFP and a 561 nm laser for mCherry. (a) Co-expression of cardosin A-mCherry and GFP-HDEL (ER marker); (b) Co-expression of cardosin A-mCherry and ST-GFP (GA marker); (c) Co-expression of cardosin A-mCherry and Aleu-GFP (PCV/vacuole marker). White arrowheads mark co-localization of cardosin A-mCherry with Aleu-GFP; (d) Co-expression of cardosin A-mCherry and Sec-GFP. Bars: 25 µm.

These data suggested that most of the cardosin A-mCherry proteins were accumulated in the vacuole at 3 days post infiltration, with some proteins still in prevacuolar compartments, confirming an ER - (X) – PVC - Vacuolar pathway. (X) being potential stop in intermediate compartments such as Golgi. However no ER-Golgi trafficking could be observed in this experimental system **The impact of overexpression on ER morphology may explain the processing delay observed for this construct in the previous paragraph. The establishment of a stable transformation system may permit to diminish this impact.**

3.2.2. Stable expression in BY-2 cells

In regards to the objectives of live cells imaging of cardosin A trafficking, two fluorescent tags were tested to elaborate a stable BY2 cell line expressing Cardosin A.

Cardosin A-Kaede

The ultimate goal of this work was to perform some pulse chase experiments to follow the dynamics of Cardosin A trafficking in BY-2 cells. Therefore, the fluorescent tag Kaede was used to obtain a photoconvertible protein permitting such experiments (Brown et al. 2010). In a stable expression system with constitutive expression of the protein, photoconversion of a cell population or a subpopulation of proteins would allow a direct visualisation of the turnover and the *de novo* synthesis of the proteins, or its fate within the cell. Protocols were first set-up on a well-known Golgi marker to validate the approach (ST-Kaede), and results revealed the excellent potentiality of such photoconvertible fluorescent populations to decipher biological questions (Brown et al. 2010). Results were also promising for Cardosin A-Kaede constructs.

BY2 cells expressing cardosin A-Kaede showed a punctate pattern of fluorescence (Figure 3.7 a). The fluorescent protein was functional and it was possible to photoconvert the entire protein after a 30 seconds UV pulse (Figure 3.7 b) and the fluorescence pattern remained unaltered. Fluorescence was, however, never observed in the central vacuole. Fluorescent punctate pattern may correspond to a GA labeling or Prevacuolar compartments labeling as suggested by the transient expression experiments in epidermal leaf cells. To identify the localization of cardosin A-KAEDE, these cells were treated with Brefeldin A (BFA), which induces the redistribution of GA membranes within the cells. After 30 minutes treatment, a clear redistribution of cardosin

A-Kaede proteins within an ER-like pattern indicating that the construct was possibly labeling GA compartments (Figure 3.7 c). Moreover, immunolocalisation of JIM84 (GA marker) and mRab (Prevacuolar compartment marker) was undertaken in these cells, and images were acquired after total photoconversion of the fluorescent protein. After immunolocalisation with JIM84, there was a clear co-localisation in GA stacks (Figure 3.7 d and e), confirming the results obtained with the drug BFA. Immunolabelling of these cells with mRab antibodies also clearly demonstrated that none of the cardosin A-Kaede proteins reached the post-GA compartments (Figure 3.7 f).

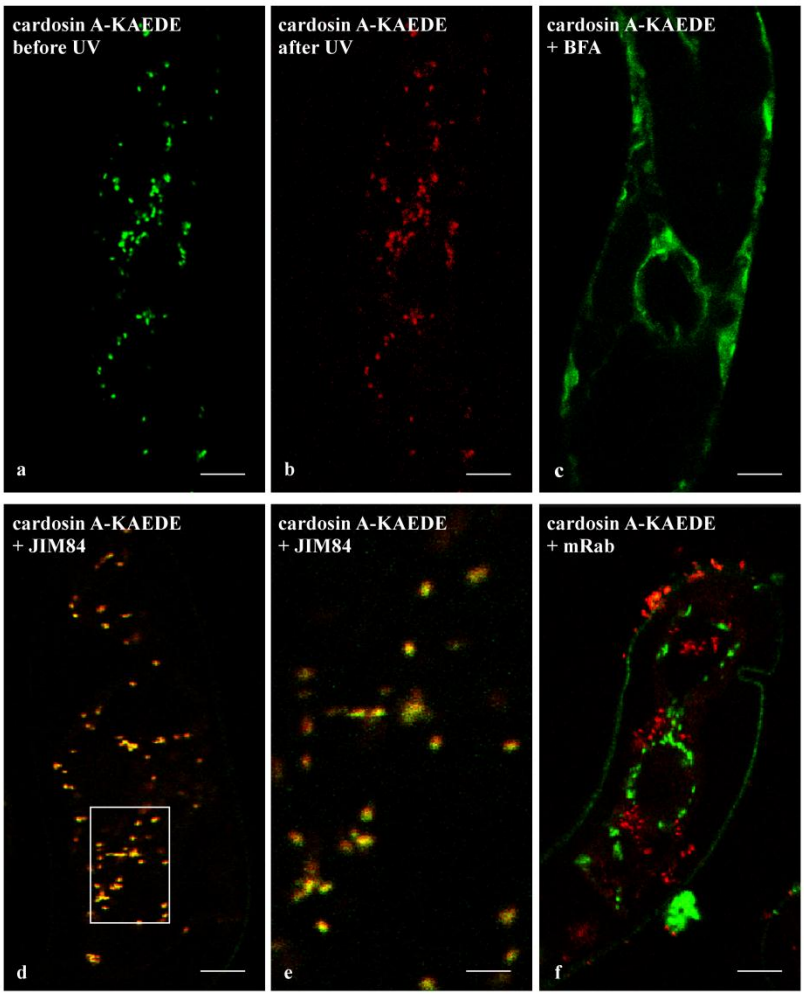

Figure 3.7 Mapping cardosin A-Kaede labelling in BY2 cells. Confocal microscopy of Cardosin A-Kaede before (a) and after (b) photoconversion with the 63x objective in wide-field mode (A4 UV block). Expression pattern after BFA treatment (c). Co-localisation of photoconverted Cardosin A-Kaede (red) with the Golgi marker JIM84 (green, d and e) and with the pre-vacuolar marker mRab (green, f). These data show that cardosin A-Kaede is localised in the Golgi. Bars: a, b, c, d, f, 10 µm; e, 5 µm.

These data suggest that the construct cardosin A-Kaede was actually exported to the GA and blocked within it, and therefore was not a proper model

protein to study cardosin A trafficking to the vacuole. **Kaede is a tetrameric protein, and the size of the construct probably interfered with the cardosins proper processing. It however suggested that cardosins may enter the ER-GA pathway, but this had to be thoroughly investigated through a correct expression system before to be validated.**

Cardosin A-mCherry

A BY-2 cell line expressing cardosin A-mCherry, a monomeric fluorescent protein was thereafter produced. Unfortunately, the transformation rate or the signal intensity in transformed cells was quite low, as most of the cells were not fluorescent. The few fluorescent cells showed however a clear mCherry signal in the vacuole (Figure 3.8 a and b). In an attempt to isolate the fluorescent cells population, it was tried to select fluorescent cells and grow them on solid medium to obtain isolated fluorescent calli, but again the mCherry signal was often too low to be detected easily by confocal microscopy.

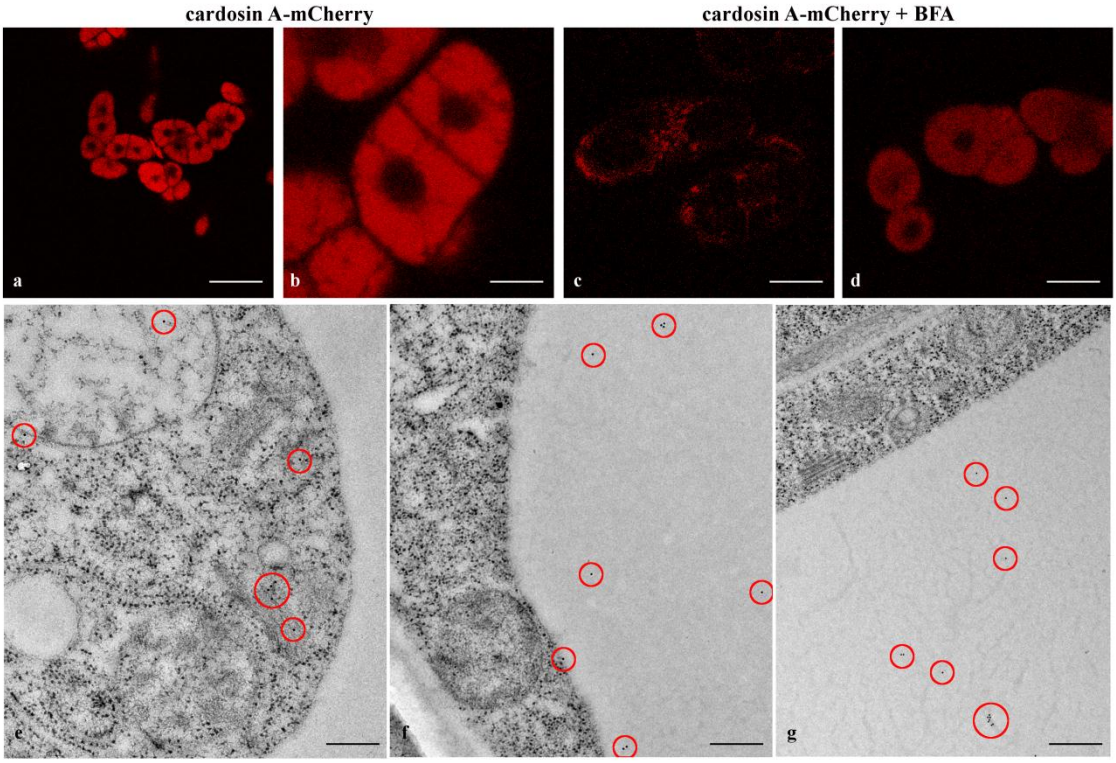

Figure 3.8 BY-2 cell line expressing cardosin A-mCherry. (a, b) CLSM images of cardosin A-mCherry fluorescence in living cells; (c, d) CLSM images of BFA treated cardosin A-mCherry BY-2 cells; (e, f, g) Immunolocalisation of cardosin A in Cryofixed and LR-White embedded BY-2 cells expressing cardosin A-mCherry (red circles marks the gold dots). Bars: a, 40 µm; b, c, 10 µm; d, 20 µm; e, f, 200 nm; g, 400 nm.

We also treated the cells with BFA (50 µM) for 30 minutes, hoping to block some trafficking events and therefore accumulate fluorescent signals in a subcellular compartment. We detected some cells presenting an ER-like pattern of fluorescent (Figure 3.8 c), suggesting an initial GA localization, while others, from the same sample, seemed to be not affected by the drug, with the protein being accumulated in the vacuole (Figure 3.8 d).

These observations were completed by some electron microscopy observations, in order to have a better resolution of the ongoing events. Ultrastructural analyses showed that the transformed cells appeared to have normal ultrastructure, and most organelles, like mitochondria and GA were also presenting a typical shape (Figure 3.9 a, b and c), when compared to the Wild Type cells (Figure 3.9 d, e and f). However, a closer look allowed seeing that ER cisternae were in a higher number and much enlarged compared to the non-transformed cells (Figure 3.9 b and c), confirming a slight impact of the transformation on ER biology.

Furthermore, cardosin A-mCherry proteins were co-localised at the electron microscopy level, using an anti-cardosin A specific antibody. The results showed some labeling mostly in the lytic vacuole (Figure 3.8 f and g, red circles). Some gold particles were also observed associated with the GA (Figure 3.8 e, red circles).

At this time of our study, these data were interpreted as some mislocalisation events of the cardosin constructs due to the BY2 biological model (BY2 cells expressing cardosin A-Kaede), or a rather poorly successful protein expression (in the case of BY-2 cells expressing cardosin A-mCherry), designing these cell lines as poor heterologous systems for cardosin expression. ***The preliminary results obtained from Brefeldin A (BFA) experiments may however point out two ways for cardosin A-mCherry trafficking to the vacuole: a BFA sensitive and a BFA insensitive one.*** At this stage of the study, these results were however far to be conclusive, and it was chosen to concentrate on a third heterologous system.

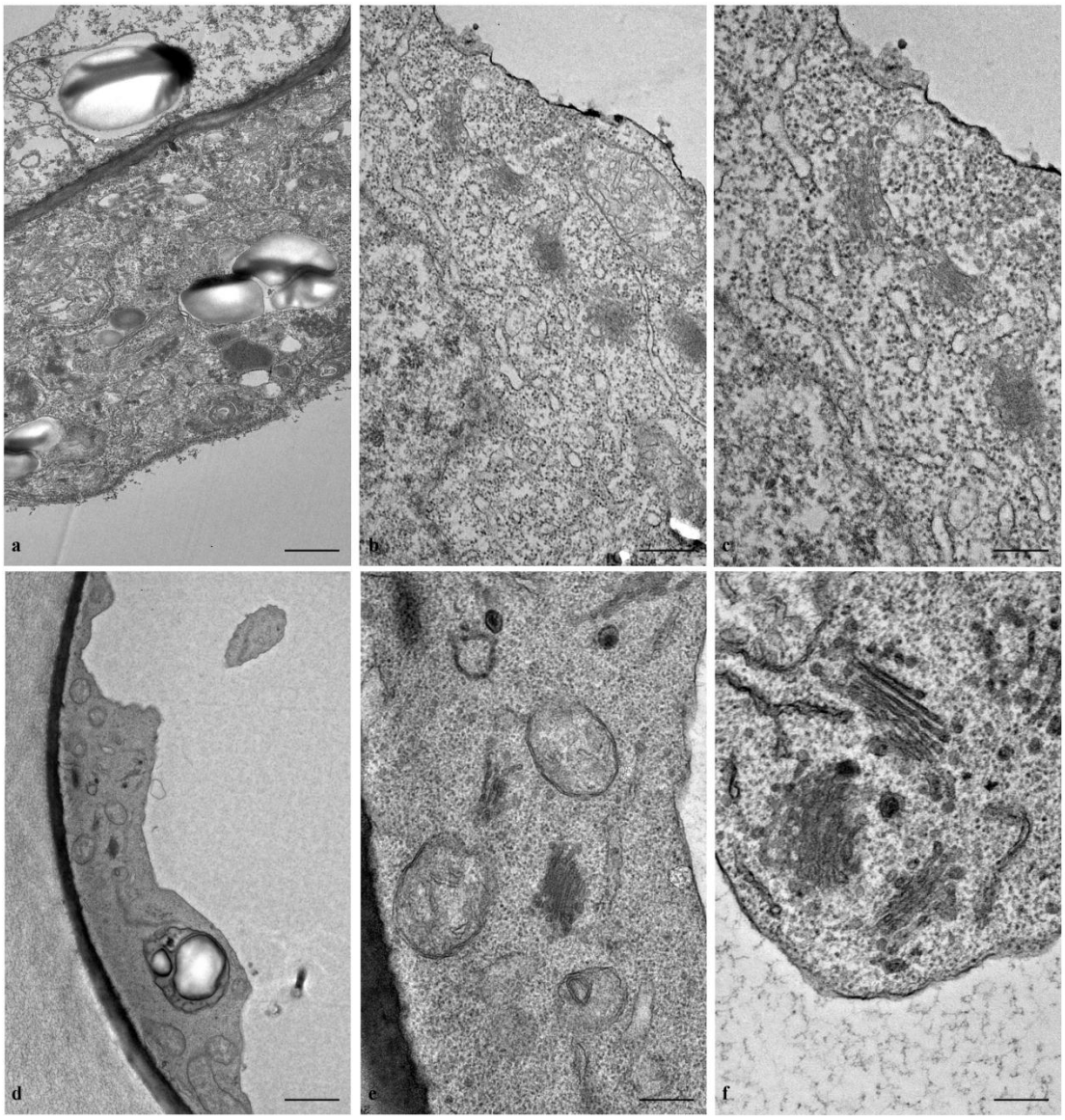

Figure 3.9 Morphological aspects of BY-2 cell line expressing cardosin A-mCherry. Micrographs of cell ultrastructure were obtained from cells embedding in Epoxy resin. (a, b, c) cardosin A-mCherry BY-2 cell line; (d, e, f) Wild type BY-2 cells. Scale bars: a, d, 1 µm; b, 500 nm; c, e, f, 200 nm

3.2.3. *Arabidopsis thaliana heterologous system*

Along with the existing constitutive expression commonly used for stable Arabidopsis transformation, and keeping in mind the necessity to control the induction of cardosin A expression, it was chosen to develop an inducible expression system for our constructs. Craft and coworkers (2005) developed an inducible expression system - LhGR, where the occurrence of a phenotype with the expression of a transgene only occurs upon induction with a chemical agent. The inducible system LhGR was developed from another system, the LhG4, described by

Moore and colleagues (1998). Briefly, the system consists in crossing activating plants (having the chimeric transcription factor activator LhG4) with reporter plants (having the gene of interest cloned downstream of a minimal promoter - pOp - comprised of a TATA-box and binding sites for the LhG4 transcription factor activator). Thus, the transgene would be specifically expressed in the progeny resulting from crossing between the activating lines and reporter lines (Figure 3.10) (Moore et al. 1998).

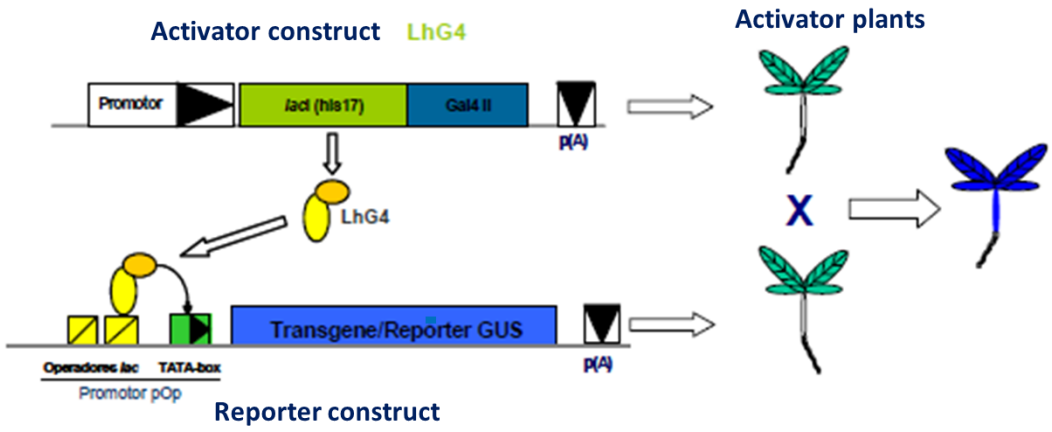

Figure 3.10 Schematic representation of the LhG4 system. The transgene expression occurs in the offspring resulting from crosses between activator plants and reporter plants. Adapted from Macedo (2005).

The LhGR system (Craft et al. 2005) has the great advantage of not requiring crossing between activator and reporter plants for the transcription of the transgene to occur. The activator construct LhGR encodes a chimeric transcription activating factor to which a sequence corresponding to a binding domain for a glucocorticoid was added. In the LhGR system activator plant lines are directly transformed with a reporter construct which includes, in the same T-DNA, the reporter gene and the transgene of interest. The activator plants, both before and after transformation with the reporter construct in the absence of the glucocorticoid inducer dexamethasone (Dex), the activating transcription factor resulting from the expression of the activator construct, form an inactive complex with chaperonin (Hsp90). When dexamethasone is applied exogenously, it will compete with the Hsp90 in the association to the activator transcription factor (Craft et al. 2005).

The complex glucocorticoid:transcription activator thus assumes an active form allowing transcription initiation. The reporter construct allows transcription in two directions: the reporter gene (GUS) to one side and the transgene or cDNA of interest to the other (Figure 3.11).

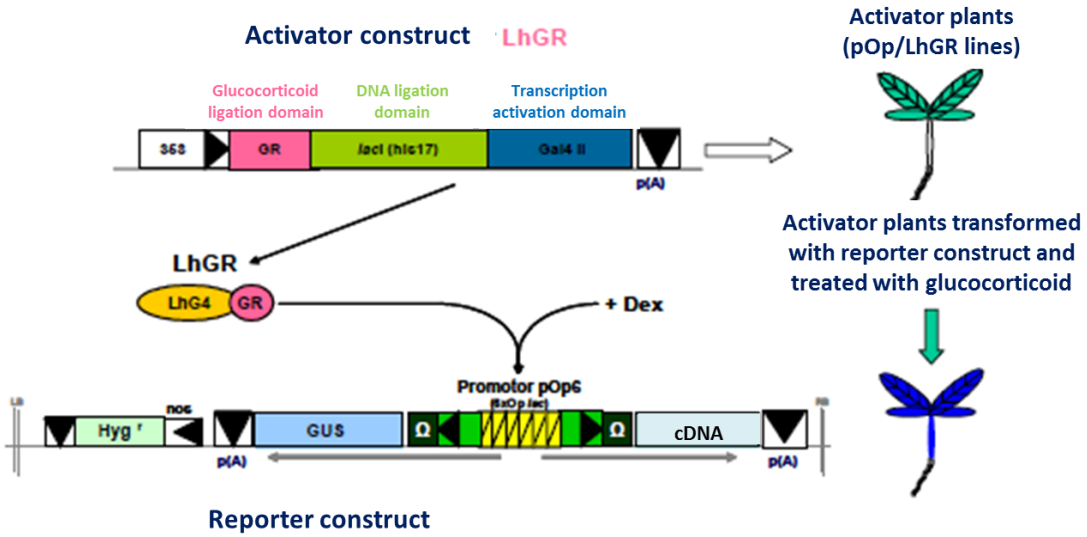

Figure 3.11 Schematic representation of LhGR chemically inducible system. The activator construct is incorporated into the genome of plants belonging to the activating line. The cDNA of interest can be cloned into the reporter construct and then used to generate transgenic plants. In this case the activation of transcription of the transgene is dependent on the exogenous application of glucocorticoid dexamethasone (Dex). Adapted from Macedo (2005).

Arabidopsis thaliana lines expressing cardosin A under the LhGR dexamethasone-inducible promoter were already made available in the laboratory (Duarte et al. 2008). They had been characterized for the expression of cardosin A through GUS staining and Western blotting in seedlings. This line was already in the T4 generation and during this work new individuals were germinated and tested till the T6, confirming that this progeny corresponds to homozygous lines. To fully interpret any data on the dynamics and localisation of the construct in these transformed plants, the stability of the transformation over the generations had to be checked. Also, the correct processing of the cardosins and the integrity of the ultrastructural architecture of the transformed plant cells were evaluated.

SIX different T6 lines were germinated in dexamethasone and hygromycin (Figure 3.12 a) and all the individuals were resistant to the antibiotic confirming that this line was indeed homozygous. When transplanted to soil the plants developed normally (Figure 3.12 b). Furthermore, each plant was tested independently for the reporter gene expression and for the transgene (cardosin A) expression. For the reporter gene a GUS activity assay was carried out in dexamethasone induced plants as well as non-induced plants to serve as a control of leaky expression of the reporter. The six lines tested showed to have a good expression of the reporter (+ Dex plants) and no expression was detected in the non-induced plants (- Dex) (Figure 3.12 c). Finally, the confirmation of cardosin A expression and correct processing was carried out by Western blotting

using protein extracts obtained from leaves of dexamethasone-induced plants and using a specific antibody against cardosin A. The results showed a clear band of approximately 31 kDa corresponding to the heavy chain of the protein (mature form), confirming that the tested lines have the correct expression of the transgene (Figure 3.12 d). Having validated that the lines tested corresponding to T6 had the correct transgene expression and were homozygous lines, these lines were used in the forthcoming work.

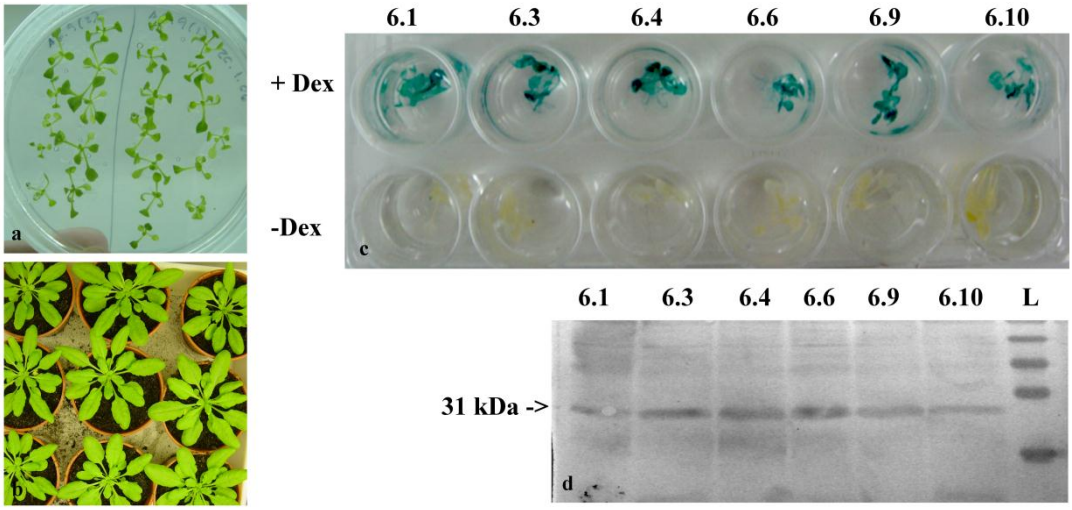

Figure 3.12 *Arabidopsis thaliana* lines from T6 generation expressing cardosin A under an inducible promoter. (a) germination of individuals in MS medium supplemented with dexamethasone and hygromycin; (b) cardosin A-expressing *A. thaliana* plants in soil; (c) GUS activity assay; (d) Western blot of leaf protein extracts from *A. thaliana* lines expressing cardosin A, detected with an anti-cardosin A antibody. Dex: dexamethasone, L: All blue prestained protein ladder (BioRad).

There was no apparent phenotype of the transformed plants when compared to wild type (WT) plants or non-induced ones: the seeds germinated and seedlings developed at approximately the same rate as WT plants and they generated new individuals. To confirm the normality of the main growth stages during Arabidopsis development (Boyes et al. 2001), a more detailed assay was carried out. Ten different developmental stages were chosen (seed imbibition; radicle emergence, hypocotyl and cotyledon emergence; four stages of leaf development: cotyledons fully opened and two, three rosette leaves and four rosette leaves; first flower buds visible; first flower open and presence of first siliques) and the time taken to reach each stage was measured for cardosin A expressing lines with, and without, dexamethasone and for WT, grown in the same conditions (Table 3-1). About 20 plants were analyzed from each line and two different assays were performed, in a different time span, and the time-values indicated correspond to an average between the ones obtained for all the plants.

Table 3-1 Arabidopsis development stages analyzed for the phenotype and the respective time interval between each stage observed for WT and cardosin A induced and non-induced plants.

Developmental stages analyzed / *Arabidopsis thaliana* lines	**Wild type**	**Cardosin A induced**	**Cardosin A non-induced**
	hours	hours	Hours
Seed Germination	0	0	0
Seed imbibition	72	72	72
Radicle emergence	96	135	138
Hypocotyl and cotyledon emergence	120	162	168
Cotyledons fully opened	140	192	201
Two rosette leaves	239	276	291
Three rosette leaves	269	297	309
Four rosette leaves	295	324	332
First flower buds visible	496	489	534
First flower open	652	624	675
Presence of first siliques	704	696	714

With the results obtained from the developmental observations, a scheme of the chronological progression for each line was obtained (Figure 3.13). Analysing the drawing obtained, a slight delay in cardosin A (both inducible and non-inducible) seed germination is visible, when compared to the WT control. This delay was maintained throughout development. When comparing the dexamethasone induced plants with the non-induced, it was observed a growing gap between them, from the first stage of leaf development on. In the end of the assay this difference was more pronounced, with the non-induced plants taking more time to reach the development of siliques (Figure 3.13 third line).

These results confirmed the previous assays on cardosins expression in heterologous systems, suggesting that the overexpression, by delaying some processing events, may actually slightly impact the chronology of plant development.

Figure 3.13 Scheme of the chronological progression of the 10 principal growth stages chosen for phenotypical comparison between cardosin A Arabidopsis lines and wild type plants.

Furthermore, WT and cardosin A *A. thaliana* lines were analysed at the subcellular level, to ascertain if there were phenotypic differences in their ultrastructure. To evaluate if cardosin A retrieves any phenotype to the cells, seeds were germinated and 3 days old radicle and cotyledon segments were high-pressure cryofixed and embedded in Epoxy resin for ultrastructural analysis at the TEM level. In root cells (Figure 3.14 a), the ultrastructure is comparable in induced (Figure 3.14 b and c), non-induced (Figure 3.14 d) and WT (Figure 3.14 e) plants. The morphology, shape and size of several subcellular structures, namely ER, GA and Mitochondria are similar.

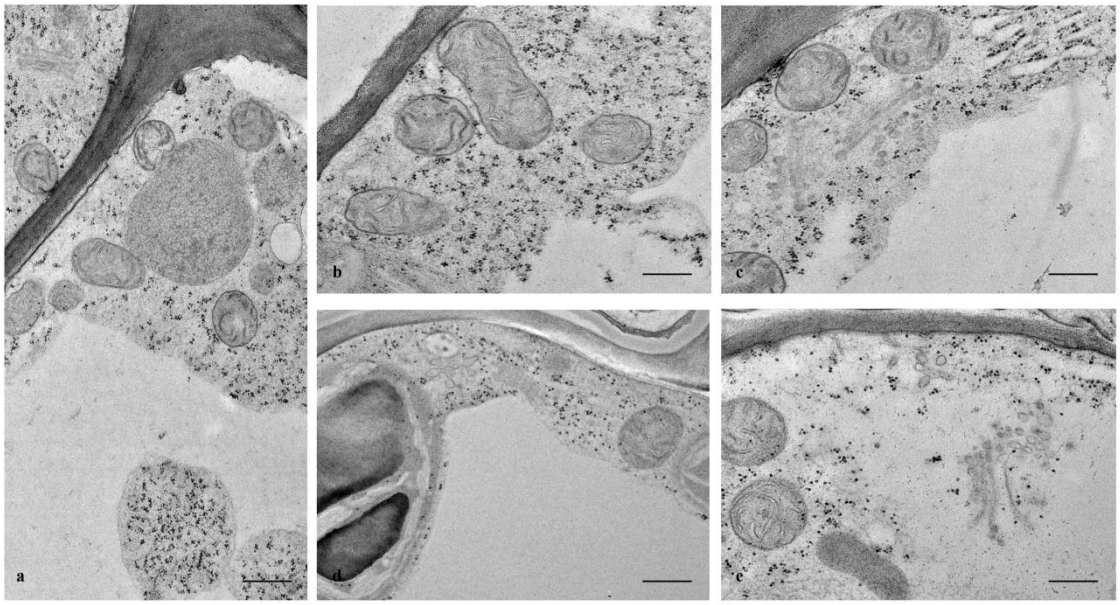

Figure 3.14 Ultrastructural aspects of *A. thaliana* radicle cells expressing cardosin A under a dexamethasone inducible promoter. Micrographs of cell ultrastructure were obtained from 3 days old seedlings. Sections of radicles evidencing the general organization of the cells (a), details of mitochondria (b) and the Golgi apparatus

(c). As a control, non-induced (d) and wild type (e) seedlings were used and treated in the same manner. Scale bars: a, 500 nm; b, c, d, e, 250 nm.

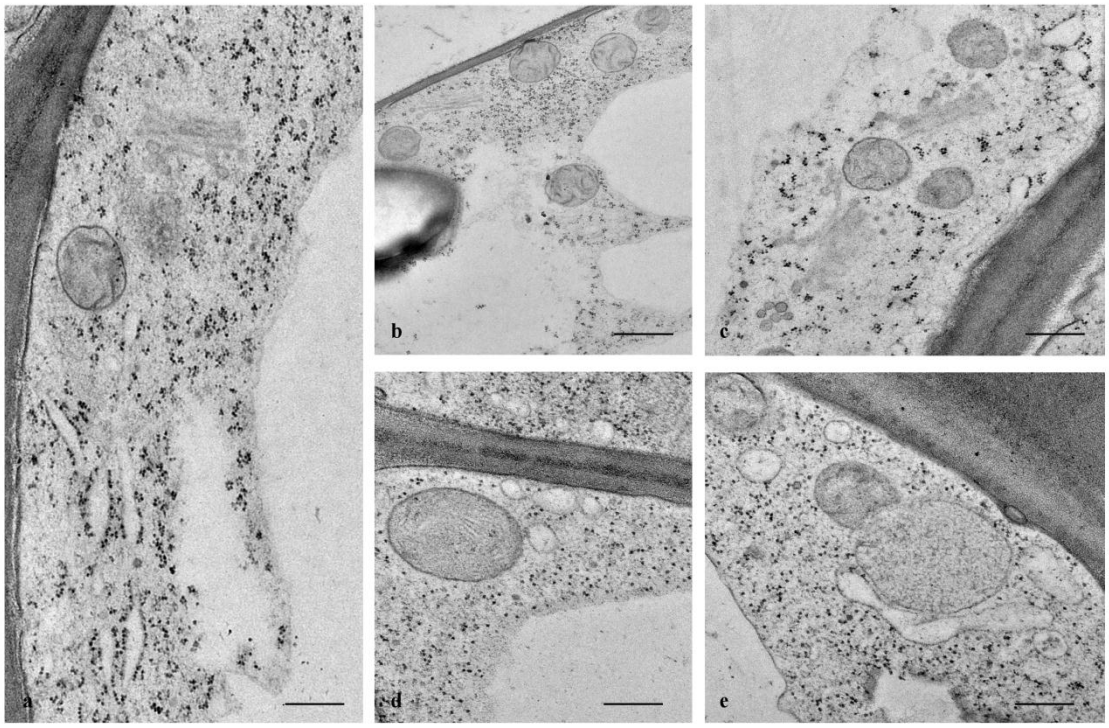

Figure 3.15 Ultrastructural aspects of *A. thaliana* cotyledon cells expressing cardosin A under a dexamethasone inducible promoter. Micrographs of cell ultrastructure were obtained from 3 days old seedlings. Sections of cotyledons evidencing the general organization of the cells (a, b) and details of mitochondria and Golgi apparatus (c). As a control, non-induced (d) and wild type (e) seedlings were used and treated in the same manner. Scale bars: a, c, 400 nm; b, 500nm; d, e, 300 nm.

Similarly, in cotyledon cells (Figure 3.15), the ultrastructure reveals no subcellular effect of cardosin A expression in cells and organelles being observed.

The results indicate that cardosin A expression does not retrieve any phenotype at the ultrastructural level and define this stable transformed cell line as a good heterologous system to work with in analyzing cardosins trafficking mechanisms.

3.3. OUTCOMES

The aim of the study was to define a proper heterologous expression system for cardosin A and cardosin A-fluorescent tags to facilitate functional exploration of aspartic proteinases trafficking. Previous work suggested that cardosin A mature and accumulate in vacuoles, so it was expected, in a right expression system, to have a vacuolar accumulation of the mature form of the protein, without altering the other cell features or plant development.

THE EXPRESSION OF CARDOSIN A-FLUORESCENT TAG IN BY2 CELL LINES IS NOT A GOOD HETEROLOGOUS SYSTEM TO ANALYSE CARDOSINS TRAFFICKING: Cardosin A-Kaede was never observed in the vacuole, but was retained in the GA. A possible explanation resides in the fact that the chimeric protein may prevent some processing steps by possibly masking its signal peptide. Another possibility is that the tetrameric nature of Kaede anchors the fusion protein artefactually in the Golgi body. Being tetrameric makes Kaede a big protein and may compromise the folding of both cardosin A and Kaede causing the construct to be retained due to quality control mechanisms existing in the GA. EOS-FP, a monomeric photoconvertible fluorescent protein (Mathur & Radhamony 2010), may be more suitable for these type of studies and should be tested in the future. BY-2 cells expressing Cardosin A-mCherry were far more promising as mCherry fluorescence was labeling the vacuole, indicating that the sorting of the protein was correct. However the low level of cells accumulating the model protein defines this BY2 expressing system as a weak system for our purpose and questions the validity of the system. Weak labeling may be due to mCherry cleavage from cardosin A (and eventually secretion into the culture medium), or to defects in ER biology as abnormal proliferation/swelling of ER cisternae along the cell were observed. In all cases, it is possible to conclude that BY2 cells will not be the right heterologous system to use for expressing cardosins constructs.

N. TABACUM LEAVES REVEALED TO BE A GOOD HETEROLOGOUS SYSTEM FOR CARDOSINS EXPRESSION: Cardosin A (tagged and non-tagged version) accumulates in the vacuole of N. tabacum epidermal cells and is correctly processed along its route to the vacuole. The presented observations in this heterologous systems may also give some hints on cardosin A trafficking pathways: Cardosin A was never detected in the ER or GA compartments, either because its passage through these compartments is very rapid and the time-points studied did not allow to catch these initial trafficking steps, or

because they do not go through the Golgi. On the other hand, it partially co-localises with Aleurain:GFP, a vacuolar marker, that also labels the Prevacuolar compartment, indicating a route to the vacuole via the prevacuole. This expression system was chosen to carry further the studies on deciphering the trafficking mechanisms of aspartic proteinase in plant cells (chapter 2).

CARDOSIN A EXPRESSION IN ARABIDOPSIS THALIANA IS A GOOD MODEL TO STUDY ITS LOCALISATION AND TRAFFICKING ALONG DEVELOPMENT: **IN** this work were used *Arabidopsis thaliana* lines expressing cardosin A that were already available and tested for its expression (Duarte et al. 2008). The first goal was to validate the model for further studies, involving: (1) to obtain new progenies from the available lines; (2) to select homozygous lines; (3) to test if cardosin A expression retrieves any phenotype to the plants/cells. Results obtained clearly demonstrate that T6 lines are homozygous and that cardosin A is expressed at high levels. Although cardosin A lines show a slight delayed development in relation to WT plants it is not significant as cardosin A expressing plants develop normally and generate viable seeds. At the subcellular level no phenotype is detected, with the cellular organelles presenting its ordinary shape. As a whole, *Arabidopsis thaliana* inducible system has the potential to be a good model to study cardosin A with the advantages of being possible to study its expression in different cell types, along different developmental stages, but also it is possible to control and induce its expression at a given time-point. Therefore, this model was used to explore cardosin A localisation and trafficking routes during seed germination (chapter 3).

CHAPTER II – DECIPHERING CARDOSIN A TRAFFICKING PATHWAYS IN *NICOTIANA TABACUM*

Submitted manuscript:

Cláudia Pereira, Susana Pereira, Béatrice Satiat-Jeunemaitre and José Pissarra (2012) "Characterization of two new vacuolar sorting signals uncovers different vacuolar routes". Submitted to Molecular Plant.

3.1. BACKGROUND

Little is known about the intracellular route Cardosin A follows to reach its final vacuolar destination or about the sorting signal(s) responsible for its vacuolar targeting. This question outlines the poor knowledge we have so far on the trafficking mechanisms of aspartic proteinases such as cardosins or on the partial understanding of vacuolar proteins in plant cells. Deciphering the mechanisms by which cardosins are addressed to subcellular compartments will contribute to a better understanding of Cardosins biology on one hand, but also to gain an insight in the knowledge on aspartic proteinases trafficking. As Cardosin A accumulates in vacuolar compartment both in native systems (Ramalho-Santos et al. 1997; Pissarra et al. 2008; Pereira et al. 2008; Oliveira et al. 2010) and in heterologous systems (Duarte et al. 2008; chapter 1 of this manuscript), it makes a good reporter for the study of vacuolar transport in plant cells. Our preliminary data had shown that cardosin A ended in the vacuole using a ER-(X)- PVC- vacuolar pathway, but further studies were needed to dissect more thoroughly the involved mechanisms and potential intermediate compartments on this pathway.

In this chapter the protein sequence of Cardosin A will be altered and subsequent biochemical and cell biology analyses will be performed to gain insight on the functional domains of the proteins and their potential involvement in the regulation of Cardosin A maturation and vacuolar trafficking. Comparison with other aspartic proteinases characteristics will allow a more general discussion on the variety of mechanisms involved in plant vacuolar targeting pathways. Therefore, the aim in this chapter is to: (1) assess the involvement of the catalytic domains of Cardosin A in protein maturation and targeting; (2) look for functional vacuolar sorting determinant (s) in Cardosin A; (3)

identify the route(s) taken by Cardosin A to reach its final destination and (4) investigate the impact of glycosylation sites on cardosins and AP transports in plant cells.

3.2. RESULTS

3.2.1. Effects of inactivation of cardosin A catalytic sites on cardosin A processing and localisation

It is already documented that the cardosin A processing steps needed to acquire the mature form involved other proteases (most probably cysteine proteinases), but some of these processing steps can be achieved by self-processing (Ramalho-Santos et al. 1998; Simões & Faro 2004). With the aim of asserting the effects of disruption of cardosin A catalytic sites on protein localisation and processing, point mutations were made in the native sequence to block the first [cardosin A D(103)>A], the second [cardosin A D(286)>A] or both sites [cardosin A D(103,286)>A] (Figure 3.16).

The disruption of the catalytic sites does not seemed to affect protein localisation as mCherry fluorescence was still detected in the vacuole of *N. tabacum* leaves in a similar way as the non-mutated version of cardosin A (Figure 3.16 a, b, d, e, g and h). On the other hand, the mutations in the active sites seemed to have influence in protein processing as seen in the Western blot obtained from a time-course assay of non-tagged version of the mutated proteins. Contrary to what has been observed for unmodified cardosin A, the disruption of the catalytic sites caused the appearance of the precursor form of the protein (61kDa band corresponding to procardosin A) along the entire assay (Figure 3.16 c, f and i). The precursor form band was more pronounced for cardosin A D(103)>A (Figure 3.16 c) than for cardosin A D(286)>A and for the double mutant (Figure 3.16 f and i, respectively). This fact is an indication that cardosin A indeed has the ability of self-processing and the inactivation of one or both catalytic sites partially impairs, or at least delays, the processing events. Nevertheless, the processed mature form (31 kDa band) was still detected in the blot, indication that probably other enzymes (other APs or cysteine proteinases), which already participate in the process, assume the functions lost by the mutated cardosin A.

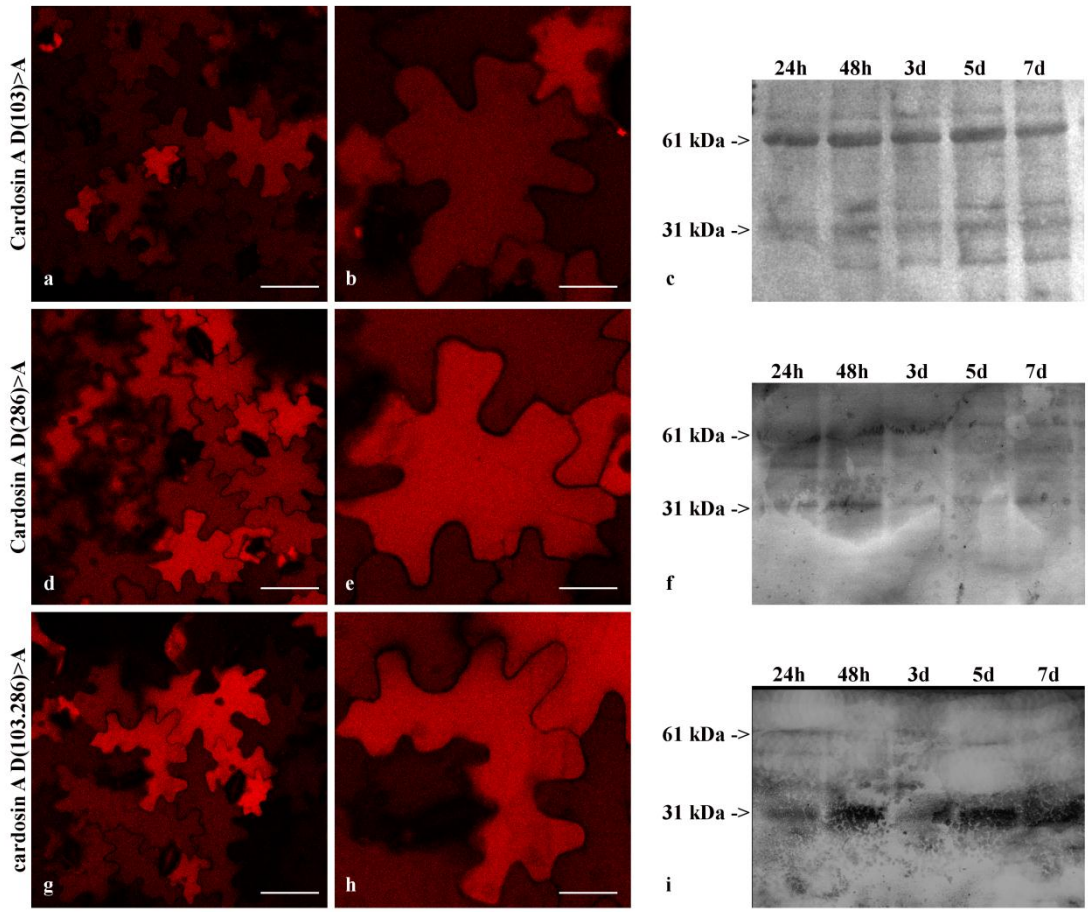

Figure 3.16 Expression of cardosin A inactive mutated forms in *Nicotiana tabacum* leaves. CLSM images were obtained from fusions with mCherry, taken 3 days after leaf infiltration (left and middle columns) and a time course assay of the non-tagged version was analysed by Western blotting using an anti-cardosin A antibody. (a-c) cardosin A D(103)>A expression. (d-f) cardosin A D(286)>A expression. (g-i) Cardosin A D(103, 286)>A expression. d – days, h – hours. Scale bars: a, d, g, 75 µm; b, e, h, 25 µm.

These results ***outline a complex integration of protein interactions occurring during Cardosin A transport to the vacuole***. They also demonstrate ***that blockage of cardosin A catalytic activity does not interfere with the protein trafficking and thus, mechanisms of signal recognition and transport are not affected by the inactivation of cardosin A catalytic sites.*** This is particular relevant for our functional studies (see sections below) because deletion of domains within the protein sequence could interfere with cardosin folding and consequently with its autocatalytic activity and maturation process.

3.2.2. Search for Vacuolar Sorting Determinants (VSDs) in Cardosin A sequence

It is well accepted that, in eukaryotic cells, protein transport from the GA to vacuoles (i.e. the vacuolar pathway) or lysosomes requires information embedded in the protein. In plant cells the targeting signal is part of the protein sequence, and named Vacuolar Sorting Determinant (VSD). Several types of these VSDs have been identified in plant and most proteins possessing VSDs are plant-specific vacuolar storage proteins. Due to the variety in plant models, cell types and experimental approaches used to decipher vacuolar targeting processes, it is not clear whether the three groups of VSDs (sequence specific, c-terminal and physical structure SVDs) exhaust all the vacuolar targeting mechanisms in plants, nor if they reflect certain protein types or families. Furthermore, some storage proteins carry two types of VSDs, questioning the sorting efficiency of a single VSD (Nishizawa et al. 2006). The vacuolar sorting of Aspartic Proteinases (AP) (for review see Simões & Faro, 2004) is expected to follow yet another mechanism, as no VSDs have been identified so far for this protein family. Moreover, the APs are an intriguing group of proteins, not only because different APs accumulate in distinct compartments but also the same protein can be either secreted to cell surface or directed to vacuole, depending on cell type and developmental stage, suggesting a tight mechanism of regulation of trafficking (Oliveira et al. 2010; da Costa et al. 2010). Interestingly, cardosins and other plant APs contain specific sequences known as Plant Specific Inserts (PSIs), protein domains of 100 amino acids between the enzyme's heavy and light chains.

From these data, three main working hypotheses need to be investigated to sort out models for Cardosin A/AP vacuolar trafficking:

(1) Firstly, a role of PSI domains. This PSI domain may be involved in vacuolar targeting. It has been suggested that PSI domains interact with ER or GA membranes (Faro et al. 1999; Kervinen et al. 1999). This was based on sequence analysis and the crystallographic structure of the plant AP phytepsin, suggesting an interaction with a receptor in the Golgi membrane. However, the role of PSI domains in vacuolar targeting is not clearly defined and some published data are even contradictory. Terauchi et al. (2006) suggested that the function as vacuolar determinant, which has been attributed to the PSI, may

actually be dependent on the type of vacuole in which the AP resides. Therefore the exact role of the PSI in vacuolar targeting of APs remains to be elucidated.

(2) The second hypothesis proposes that the C-terminal regions of plant APs contain the VSD. This is based on the fact that the C-terminal peptide of barley lectin (VFAEAIA), which is very similar to the C-terminal sequence of Cardosin A and of several other plant APs, is responsible for the protein targeting to the lytic vacuole (Ramalho-Santos et al. 1998).

(3) A third hypothesis proposes that sorting of APs to the vacuole is dependent on the interaction between two or more motifs present in AP sequence that would arrange together when the proteins reach an active conformation.

In order to establish which of these hypotheses on vacuolar targeting of APs is correct, Cardosin A was expressed in *Nicotiana* epidermal leaves as a model system to study its vacuolar pathway. A systematic analysis of cardosin A and cardosin A truncated forms trafficking was then undertaken. Cardosin A forms were generated, lacking either the PSI domain, or the C-terminal peptide, or both regions, as well as fusions between these truncated cardosin A forms and the fluorescent reporter protein mCherry. These constructs were expressed in leaf cells and their expression and localisation were then monitored by biochemical and bio-imaging approaches.

Biochemical studies on the effects of Cardosin A truncations on protein expression, processing and targeting

Several truncated versions of cardosin A were produced and analyzed by biochemistry and compared to the native protein. For the reader convenience, the scheme of the constructs described in Material and Methods section is recalled below (Figure 2.2). They were then expressed in *N. tabacum* using agro-infiltration as described in chapter 1.

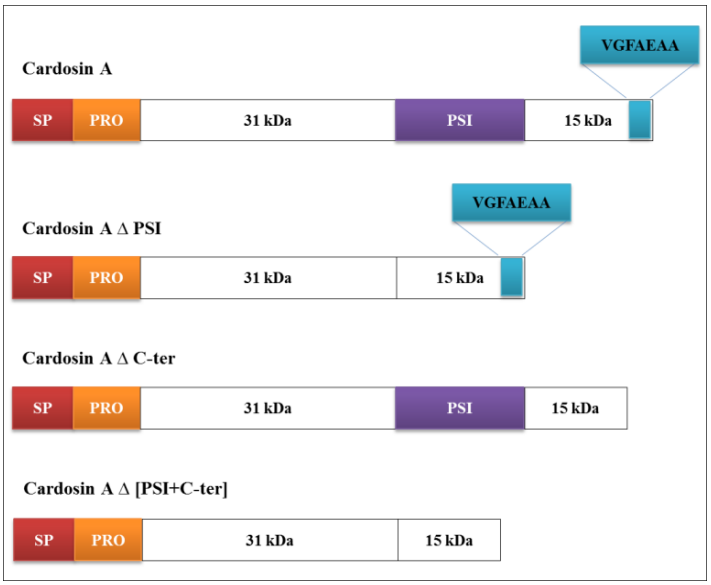

Figure 2.2: Schematic representation of CdA and CdA mutated versions. Three CdA mutated versions were obtained in order to test its putative VSDs - CdAΔPSI: CdA after removal of the PSI domain; CdAΔC-ter: CdA without the C-terminal peptide VGFAEA; CdAΔ[PSI+C-ter]: CdA lacking both regions.

A Cardosin A without PSI domain (Cardosin AΔPSI) was generated to test the significance of the PSI domain for vacuolar targeting. Western blot analysis of protein extracts of leaves that had been infiltrated with Cardosin AΔPSI revealed that the mutant protein was expressed at lower levels (Figure 3.17 a) compared to wild-type Cardosin A. In fact, the 31 kDa band corresponding to the mature Cardosin A was only detected 5 and 7 days after infiltration. The 34 kDa intermediate form and a 45 kDa band, probably corresponding to non-dissociated chains of the enzyme (Ramalho-Santos et al. 1998), were detected (Figure 3.17 a). The 45 kDa band was also detected in protoplasts and vacuoles fractions at the both time-points essayed. The 34 kDa band was not detected in protein extracts from protoplasts and vacuoles obtained at 3 and 5 days after infiltration, but the band corresponding to the mature protein was detected in the extracts obtained 5 days after infiltration (Figure 3.17 b). This implies that the Cardosin A without the PSI region still accumulated in the vacuole, despite the alteration in its processing. ***These results suggested that the PSI is essential for correct processing of cardosin A, but not for its vacuolar targeting.*** The same is true for the mCherry tagged version, which is found to accumulate in the protoplasts and vacuoles fraction 5 days after infiltration (Figure 3.17 c).

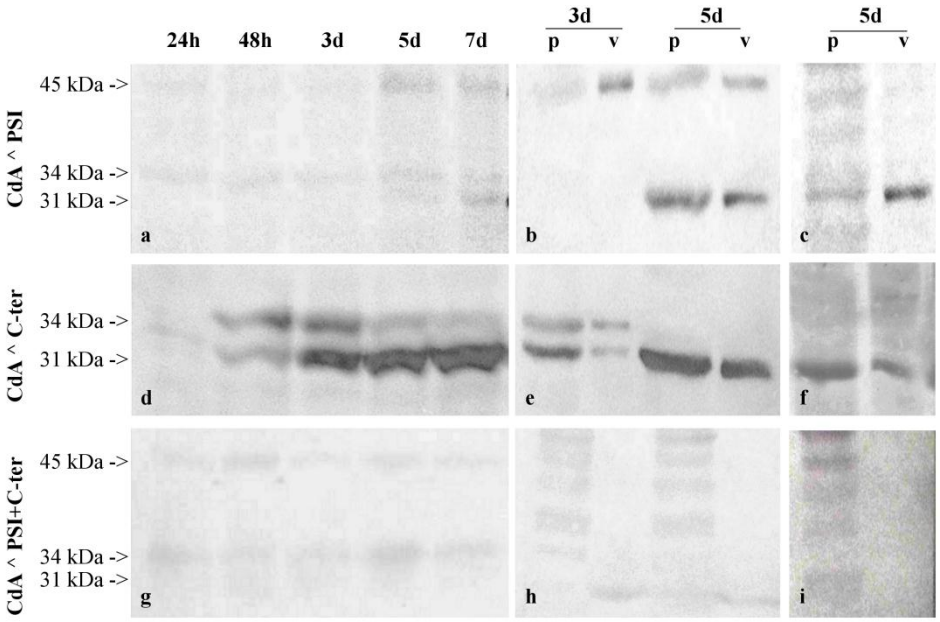

Figure 3.17 Protein gel blot analysis of *Nicotiana tabacum* leaves overexpressing Cardosin A mutated versions. 15 µg of total protein extracts from total leaf (a, d and g), or protoplasts and vacuole preparations isolated 3 and 5 days after infiltration (b, c, e, f, h and i), were separated on SDS PAGE and transferred onto nitrocellulose for western analysis. Blots were incubated with a specific antibody recognizing the heavy chain of cardosin A. (a, b, d, e, g, h) non-tagged versions of the constructions; (c, f, i) mCherry tagged versions of cardosin A constructs. d – days, h – hours, p – protoplasts, v – vacuoles.

A cardosin A without C-terminus (cardosin AΔC-ter) was generated to test the significance of the C-terminus for vacuolar targeting. The protein processing steps observed for cardosin AΔC-ter on western blot was similar to that detected when unmodified cardosin A was expressed, with clear bands corresponding to both the 34 and the 31 kDa form after 48 h (Figure 3.17 d). However, there was a delay in the detection of the processed forms (24h after infiltration for cardosin A and 48h for the mutated protein), and in the peak of expression (5 days after infiltration for unmodified cardosin A comparing to the peak at 7 days in the mutated protein). Cardosin AΔC-ter protein was detected in the vacuolar fraction as early as 3 days after the infiltration (Figure 3.17 e). At this time point, two bands, one of 34 kDa and one of 31 kDa, were detected. At 5 days after infiltration, only the 31 kDa band, corresponding to the mature form, was observed both for the non-tagged construction (Figure 3.17 e) and the mCherry chimaera (Figure 3.17 f). ***These results show that the removal of the C-terminal peptide causes no significant changes in the vacuolar localisation, or in the processing of the protein, suggesting that the C-terminal peptide is neither essential for Cardosin A processing nor for vacuolar targeting.***

When both the PSI and the C-terminal peptide were removed (cardosin AΔ[PSI+C-ter]), marked changes were observed in the expression and targeting of the mutant protein. The time-course experiment, visualized on western blot, showed bands corresponding to the intermediate forms of 34 kDa and 45 kDa although in low amounts, whereas the 31 kDa mature form was barely detected (Figure 3.17 g). In the protoplast and vacuole fractions, on the other hand, neither the bands corresponding to the mature form, nor to the intermediate forms were visible. However, several non-specific bands had appeared (Figure 3.17 h). The picture is similar when cardosin AΔ[PSI+C-ter]-mCherry is expressed, with non-specific bands being detected in the protoplasts fraction (Figure 3.17 i). ***These results demonstrate that deletion of both the PSI and the C-terminal region completely abolishes the vacuolar accumulation of Cardosin A, while its processing is also compromised.***

To summarize, these biochemical data clearly suggest that PSI domain, but not the C-ter domain, is essential for a correct cardosin A processing. They also show that removal of either C-ter or PSI domains still allow a vacuolar accumulation of the proteins, questioning their functions as true vacuolar sorting determinants. As the addition of the mCherry tag did not change these data, we were confident to use m-Cherry as fluorescent reporter for the live imaging studies of the cardosin A and cardosin A mutated forms in plant cells.

Bio-Imaging of the Cardosin A-mCherry and its truncated forms

The effect of deleting either the PSI and/or the C-terminal peptide on cardosin A trafficking to the vacuole was visualised by confocal microscopy using mCherry as reporter protein for all the tested constructs. As above, the scheme of the constructs used described in Material and Methods section is recalled below (Figure 2.3). 3 days after infiltration, leaf samples expressing the fluorescent chimeras, and protoplasts isolated from the same leaves, were visualized under a confocal microscope.

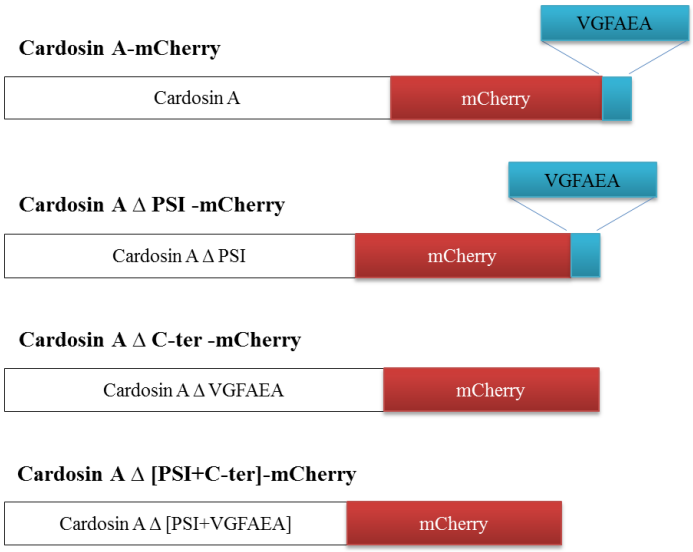

Figure 2.3: Schematic representation of CdA fluorescent chimaeras. CdA and the CdA mutated versions were fused to the N-terminus of mCherry.

Results clearly show that in our experimental conditions cardosin A mCherry-tagged version is accumulated in the vacuole both in leaf samples and in protoplasts (Figure 3.18 a, b and c), as reported before. Cardosin AΔPSI-mCherry fusion protein is also found in the vacuoles of the epidermal cells of infiltrated leaves and also of protoplasts (Figure 3.18 d, e and f). ***These results are in agreement with the immunoblots data, suggesting that the removal of the PSI did not impair the vacuolar localisation of cardosin A, although sorting was delayed. Therefore the C-ter may be the one VSD for this truncated form, confirming the biochemical results.***

The use of a cardosin AΔC-ter-mCherry construction where the C-ter domain was deleted showed, however, that another vacuolar sorting determinant may exist within the protein. The cardosin AΔC-ter-mCherry fusion protein was still accumulated predominantly in the vacuole of epidermal cells and in protoplasts at 3 days after infiltration (Figure 3.18 g, h and i). These results were again in agreement with the western blots, suggesting ***that deletion of the C-terminal peptide did not alter vacuolar trafficking.***

Finally, the double mutant protein cardosin AΔ[PSI+C-ter]-mCherry was mainly observed in the ER and in globular bodies at the cell periphery (Figure 3.18 j and k), and never in the vacuole. In protoplasts the ER pattern was clear, with mCherry labelling the ER network (Figure 3.18 l). ***These results, confirm that both PSI and C-terminal domains are involved in vacuolar targeting and that there is***

not another sequence acting as VSD within the protein. It cannot be excluded that the absence of vacuolar targeting might be caused by profound alterations in the protein structure, thus the role of the PSI or the C-terminal peptide in the vacuolar accumulation was further tested independently.

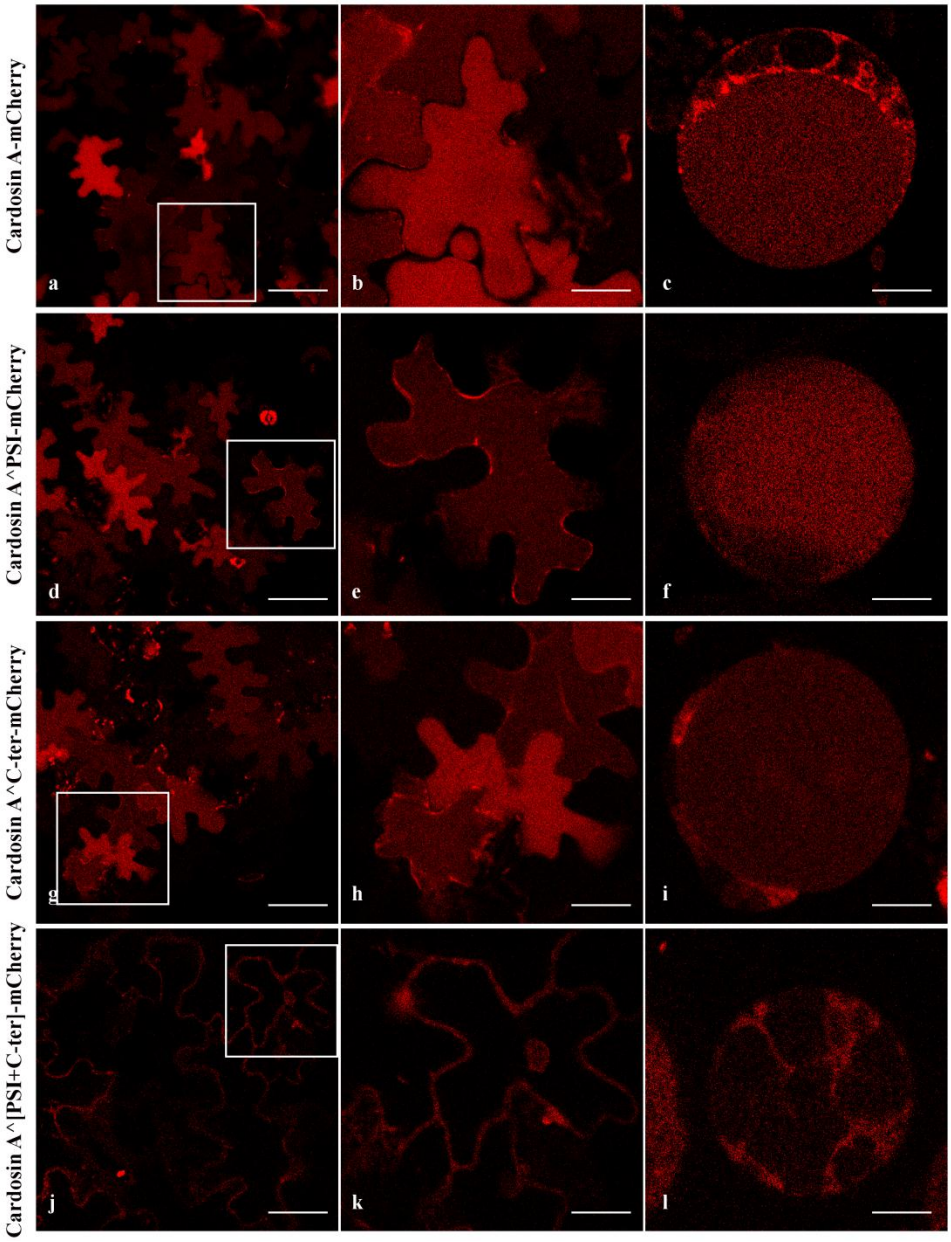

Figure 3.18 Subcellular localisation of mCherry-tagged Cardosin A and its mutated versions. Cardosin A and the constructions tagged to mCherry were transiently expressed in tobacco leaves using agro-infiltration. Images were taken 3 days after infiltration. Protoplasts were isolated from leaves 3 days after infiltration and immediately imaged. (a, b, c) Expression of Cardosin A-mCherry; (d, e, f) Expression of Cardosin AΔPSI-mCherry; (g, h, i) Expression of Cardosin AΔC-ter-mCherry; (j, k, l) Expression of Cardosin AΔ[PSI+C-ter]-mCherry. Images were acquired using the 561 nm laser for mCherry. Bars: a, d, g, j, 75 µm; b, c, e, f, h, i, k, l, 25 µm.

Cardosin A PSI domain or the C-terminal peptide are efficient vacuolar sorting determinants

To validate the previous hypothesis that both the PSI domain and the C-terminal peptide VGFAEAA were able to target cardosin A to the vacuole, the functionality of these putative VSDs on mCherry trafficking was tested independently. Fusions between the PSI or the C-terminal peptide with mCherry were generated and preceded by a signal peptide (SP) to make sure they are translocated to the ER and enter the secretory pathway. The schematic representation of the constructs produced represented in Material and Methods section is copied below (Figure 2.4). mCherry with the signal peptide (SP-mCherry) was used as a negative control, since such construct is secreted to the cell surface (Figure 3.19 a and b). As a positive control of the expression system, the Barley lectin VSD (Dombrowski et al. 1993) was placed at the end of SP-mCherry construct (SP-mCherry-BlVSD). mCherry fluorescence was detected in the vacuole, as expected (Figure 3.19 c and d).

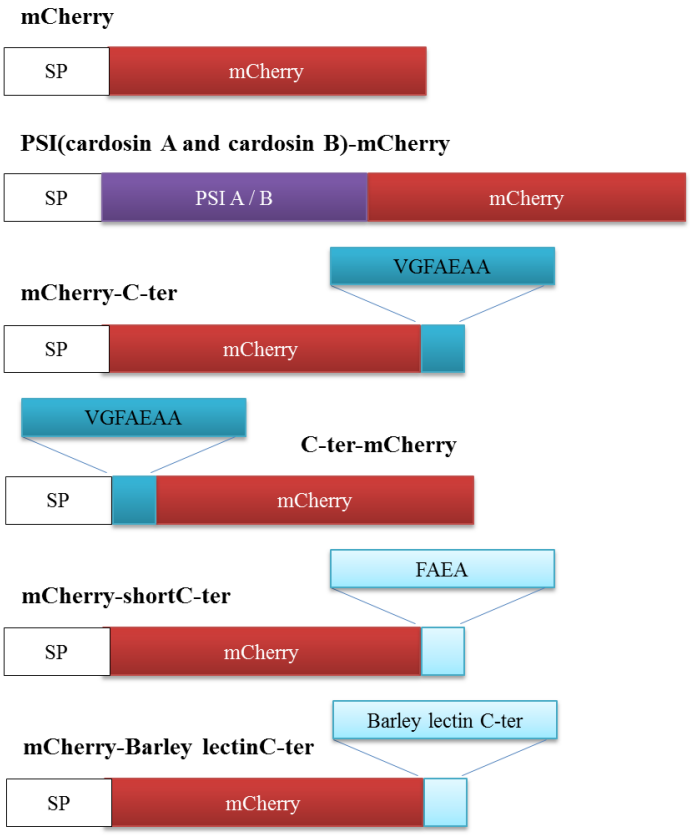

Figure 2.4 Schematic representation of mCherry variants containing the putative sorting motifs. The PSI domain was cloned between the signal peptide and mCherry, while CdA peptide VGFAEA was tested at the C-terminal and N-terminal ends of mCherry. A short C-ter peptide (FAEA) fused to mCherry was also produced. SP-mCherry and Barley lectin C-ter were used as a controls. SP – signal peptide

The PSI region was placed between the signal peptide and mCherry. This seemed to be the most appropriate order, given that the PSI is an internal signal. The SP-PSI-mCherry fusion protein showed a clear signal in the vacuole as early as 3 days after infiltration (Figure 3.19 e and f). At this time point, the fluorescence was exclusively observed in the vacuole.

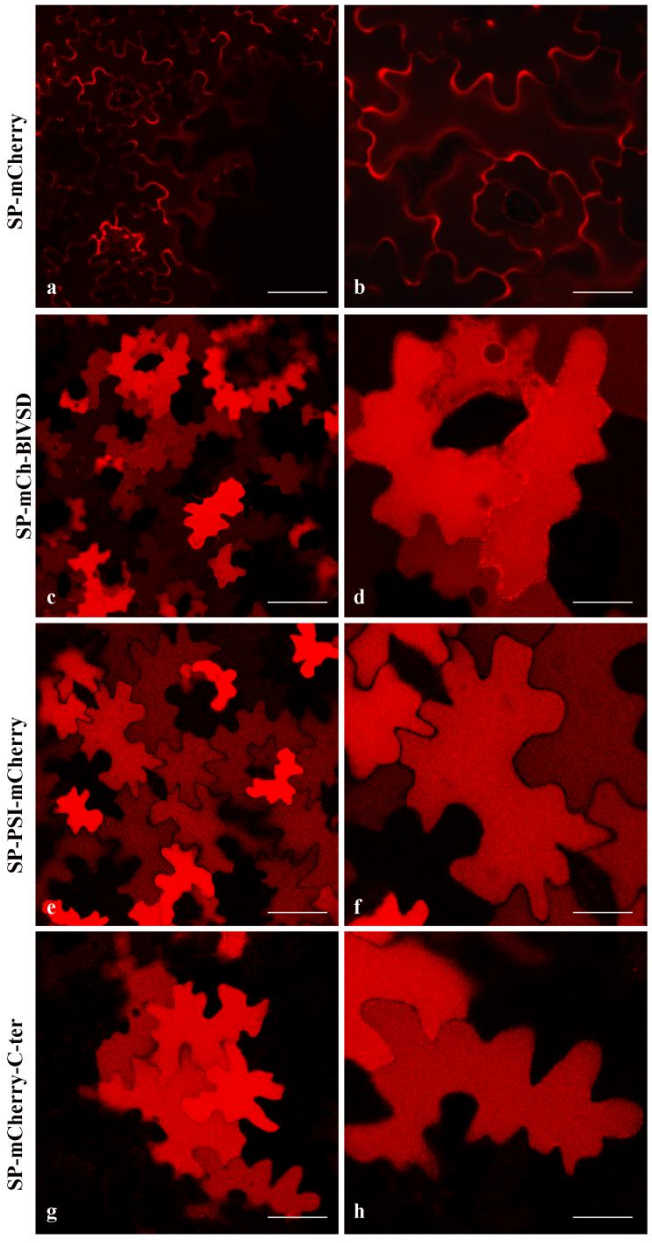

Figure 3.19 Subcellular localisation of mCherry fused to putative sorting determinants from Cardosin A. mCherry was fused to the putative vacuolar determinants from Cardosin A, and transiently expressed in tobacco leaves using agro-infiltration. Tobacco epidermal cells expressing SP-mCherry (a and b), SP-mCherry-BlVSD (c and d); SP-PSI-mCherry (e and f) and SP-mCherry-C-ter (g and h) were imaged 3 days after infiltration. Images were acquired with a 561 nm laser. Bars: a, c, e, g, 75 µm; b, d, f, h, 35 µm.

Similarly, the C-terminal sequence of cardosin A directed mCherry to the vacuole, when placed at its C-terminal end, and the patterns were very similar to those with SP-PSI-mCherry (Figure 3.19 g and h). SP-mCherry-C-ter fluorescence was detected in the vacuole at 3 days after leaf infiltration in almost all the cells.

Concluding, these results confirm that either the PSI or the C-terminal peptide VGFAEAA are indeed capable of sorting mCherry to the vacuole.

C-ter peptide is a ctVSD

The above results showed that cardosin A C-ter peptide is a vacuolar sorting domain that falls in the ctVSDs (C-terminal Vacuolar Sorting Determinants) category. By definition, this type of VSD needs to be exposed at the C-terminal end of the protein to work properly and is independent of the peptide sequence. To get a complete picture of how cardosin A C-ter works in sorting the protein to the vacuole, an extra construct was made, where the C-ter peptide was placed between the SP and mCherry: SP-C-ter-mCherry. Furthermore, when comparing this short peptide with the same sequence from other APs and with Barley lectin VSD (Figure 3.20), it was observed that four aminoacids were conserved among them, except in the case of phytepsin. It was questioned if this conserved short peptide was enough to target the protein to the vacuole, so two novel proteins were constructed, one with the short peptide FAEA at the C-terminus of mCherry and other with the same peptide at the mCherry N-terminus.

```
vignaAP             --VGFAEAA-- 7
cathepsinD          --VGFAEAARL 9
AtAP1               -QVGFAEAA-- 8
tomatoAP            -QVGFAEAA-- 8
cardosinA           -LVGFAEAA-- 8
cardosinB           -RVGFAEAV-- 8
Barley_lectin       DGV-FAEAIA- 9
                       : **:*
```

Figure 3.20. Aligment of aminoacid sequences of the C-terminal peptides from several plant APs, a mammalian AP (cathepsin D) and Barley lectin VSD. The yellow boxes highlight the conserved aminoacids in the C-terminal end.

The results obtained showed that ***the short peptide FAEA was sufficient to target mCherry to the vacuole*** (Figure 3.21 a and b), despite mCherry was still visible in the ER network of some cells (Figure 3.21 b). When placed at the N-terminus of

mCherry, the C-terminal peptide does not function in delivery the protein to the vacuole, being retained earlier in the secretory pathway, probably in the ER (Figure 3.21 c and d). The picture was similar in the case of the shortened C-terminal peptide, with the fluorescence being observed in the early endomembrane system (Figure 3.21 e and f). In the end and taking together the results presented, cardosin A C-terminal peptide is not a sequence specific VSD and it can be placed in the category of ctVSDs. Furthermore, only 4 aminoacids from the C-terminal sequence are sufficient to target mCherry to the vacuole.

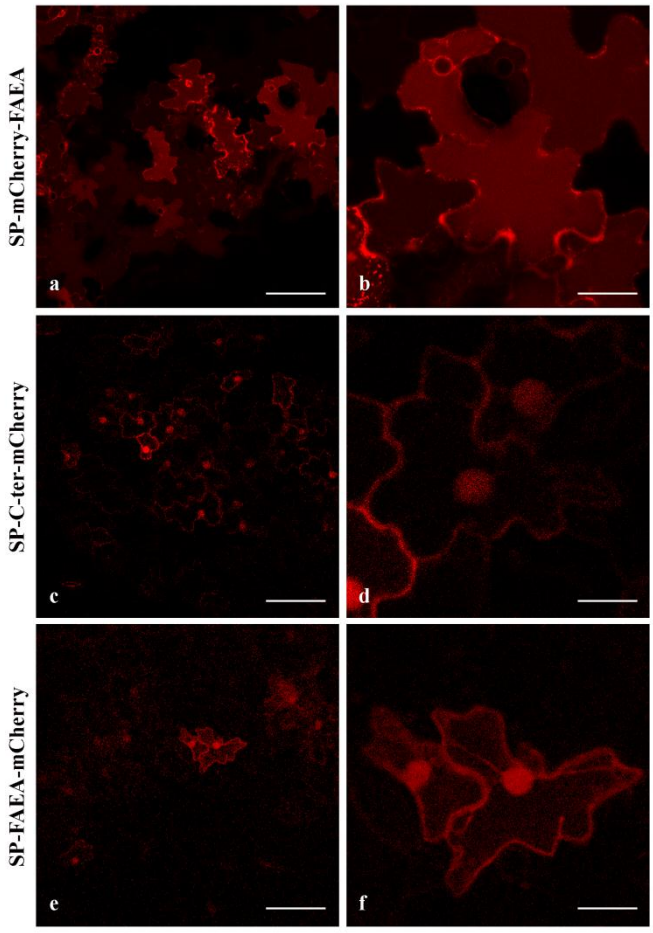

Figure 3.21 Subcellular localisation of mCherry fused to C-terminal peptides from cardosin A. The constructs were transiently expressed in tobacco leaves using agro-infiltration. Tobacco epidermal cells expressing SP-mCherry-FAEA (a and b), SP-C-ter-mCherry (c and d) and SP-FAEA-mCherry (e and f) were imaged 3 days after infiltration. Images were acquired with a 561 nm laser. Arrows indicate the cell wall. Bars: a, c, e, 75 µm; b, d, f, 35 µm.

3.3.1. Deciphering the cardosin A route(s) to the vacuoles

The occurrence of two vacuolar sorting determinants on the same protein may be related either to a functional redundancy in one vacuolar targeting pathway, or to distinct vacuolar pathways. The putative choice may be for instance to go through the GA and then directed to vacuole, to go directly from the ER to vacuoles bypassing the GA. In this section these questions were addressed by using pharmacological or genetics approaches to block some steps of the secretory/vacuolar pathway and analysing the impact of such modifications on protein trafficking.

Blocking ER-to-GA trafficking by Brefeldin A

Two distinct pathways would react differently to an experimental blockage of the ER-Golgi pathway. Therefore, leaf cells expressing cardosin A-mCherry, each of its fluorescent truncated forms (cardosin AΔPSI and cardosin AΔC-ter) and SP-PSI-mCherry and SP-mCherry-C-ter constructs were therefore treated with Brefeldin A (BFA), known to block protein export from the Golgi to the ER (Satiat-Jeunemaitre et al. 1996).

Upon addition of the drug, three time-points were analyzed: 0h, 1h and 2h. As a negative control of the experiment, GNL1-YFP was used, which showed to be not affected by BFA (Richter et al. 2007) (Figure 3.22 a) and a secreted GFP as a positive control, that is retained in the ER under BFA treatment (Figure 3.22 b). Results showed that all constructs [cardosin A-mCherry (Figure 3.22 c), cardosin AΔPSI-mCherry (Figure 3.22 d), cardosin AΔC-ter-mCherry (Figure 3.22 e)] and the cardosin A domains fused to mCherry [SP-PSI-mCherry (Figure 3.22 f) and SP-mCherry-C-ter (Figure 3.22 g)] were blocked in the ER and eventually in ER-Golgi bodies by the drug 1 h after the treatment. ***This suggested, at first sight, that they all go through the ER-Golgi complex on their way to the vacuole.*** As Brefeldin A, however, may target not only molecular machinery associated with ER-Golgi transport but also lipid composition of ER membranes (Mérigout et al. 2002), it was favored the use of dominant negative mutants of the ER to Golgi molecular machinery trafficking pathway to further analyze the process.

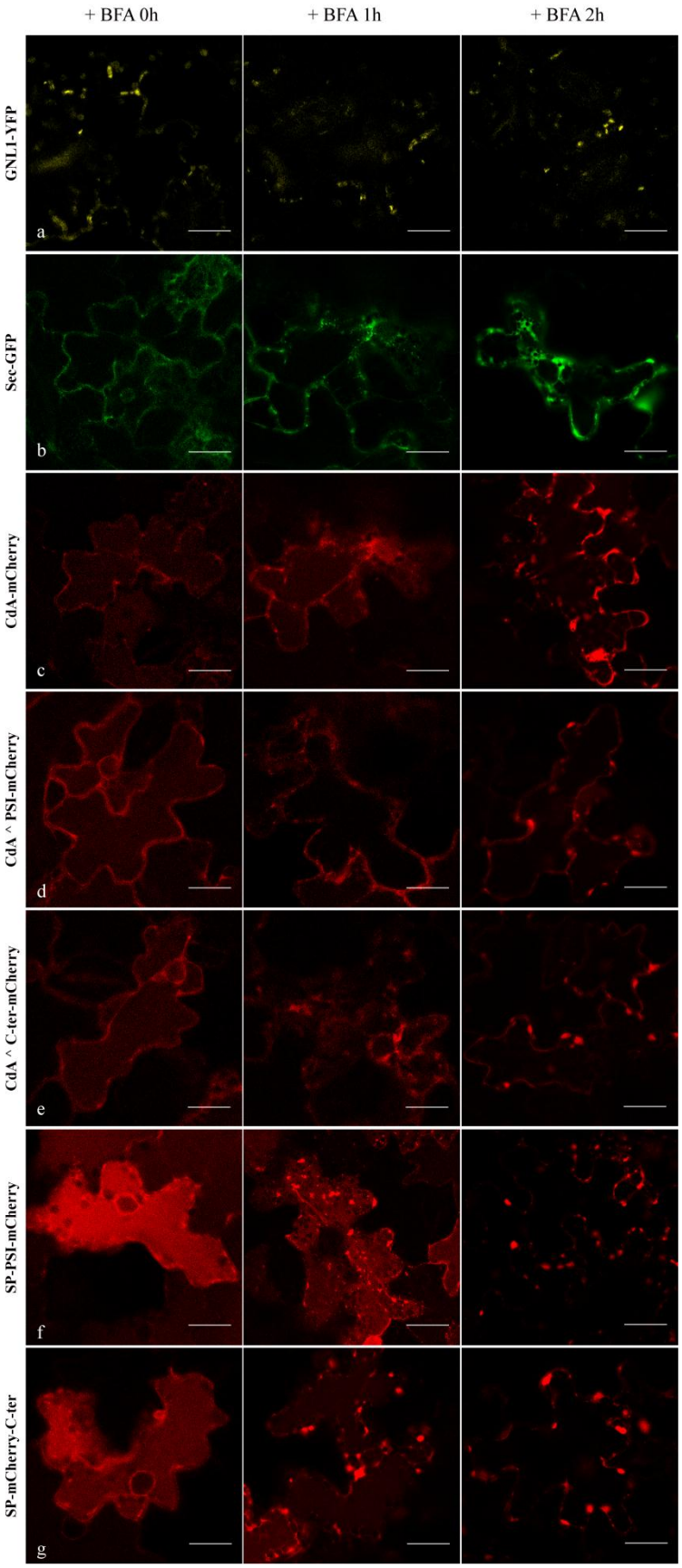

Figure 3.22 Effect of BFA on Cardosin A localisation. Cardosin A-mCherry and the mCherry variants fused to the putative VSD signals were transiently expressed in tobacco leaves using agro-infiltration. Leaves were treated with BFA, at 36–40 h after infiltration. Images were acquired at 0, 1 and 2 hours after BFA treatment. BFA

treatment after infiltration with GNL1-YFP (a) secreted-GFP (b), Cardosin A-mCherry (c), Cardosin AΔPSI-mCherry (d), Cardosin AΔC-ter-mCherry (e) SP-PSI-mCherry (f), and SP-mCherry-C-ter (g). Bars: 25 µm.

Blocking the ER-Golgi pathway by dominant negative mutants

Dominant negative mutants were used to specifically block the molecular machinery involved in the ER to Golgi trafficking pathway. The previous constructs were co-expressed with the dominant negative mutant RabD2a N121I, which specifically blocks transport between ER and the Golgi by inhibiting the activity of a GEF cofactor (Batoko et al. 2000). As a control, Aleurain-GFP (a vacuolar marker that labels the prevacuolar compartment – Figure 3.23 a) was co-infiltrated with RabD2a N121I and was detected in the ER network (Figure 3.23 b), confirming that the blockage of this pathway was effective. The three vacuolar constructs containing the C-ter determinant (i.e. cardosin A-mCherry, cardosin AΔPSI-mCherry and SP-mCherry-C-ter, Figure 3.23 d, g and p), when co-expressed with RabD2a N121I, were also retained in the ER (Figure 3.23 e, h and q, respectively). In contrast, cardosin AΔC-ter and SP-PSI-mCherry were still observed in the vacuole (Figure 3.23 k and n), suggesting that the constructs containing only the PSI escaped the RabD2a machinery.

To confirm these results, similar experiments were performed using a co-expression with Sar1 H74L, which also blocks the ER-to-Golgi trafficking by impairing COPII vesicle formation (Andreeva et al. 2000). The results obtained were similar with the ones described above (Figure 3.23 f, i, l, o and r), showing a clear inhibition of vacuolar accumulation when C-ter sequence is present in the reporter proteins sequence, but no effective blockage when PSI sequence is embedded in the sequence. This set of results strongly suggests that the PSI domain may take an additional ER to vacuole route, independent of the COPII pathway, and probably by-passing the Golgi.

Therefore, the two cardosin A vacuolar sorting determinants may reflect different pathways to the plant vacuole: a PSI-mediated pathway independent of the COPII pathway and the C-terminal peptide-mediated route through the Golgi.

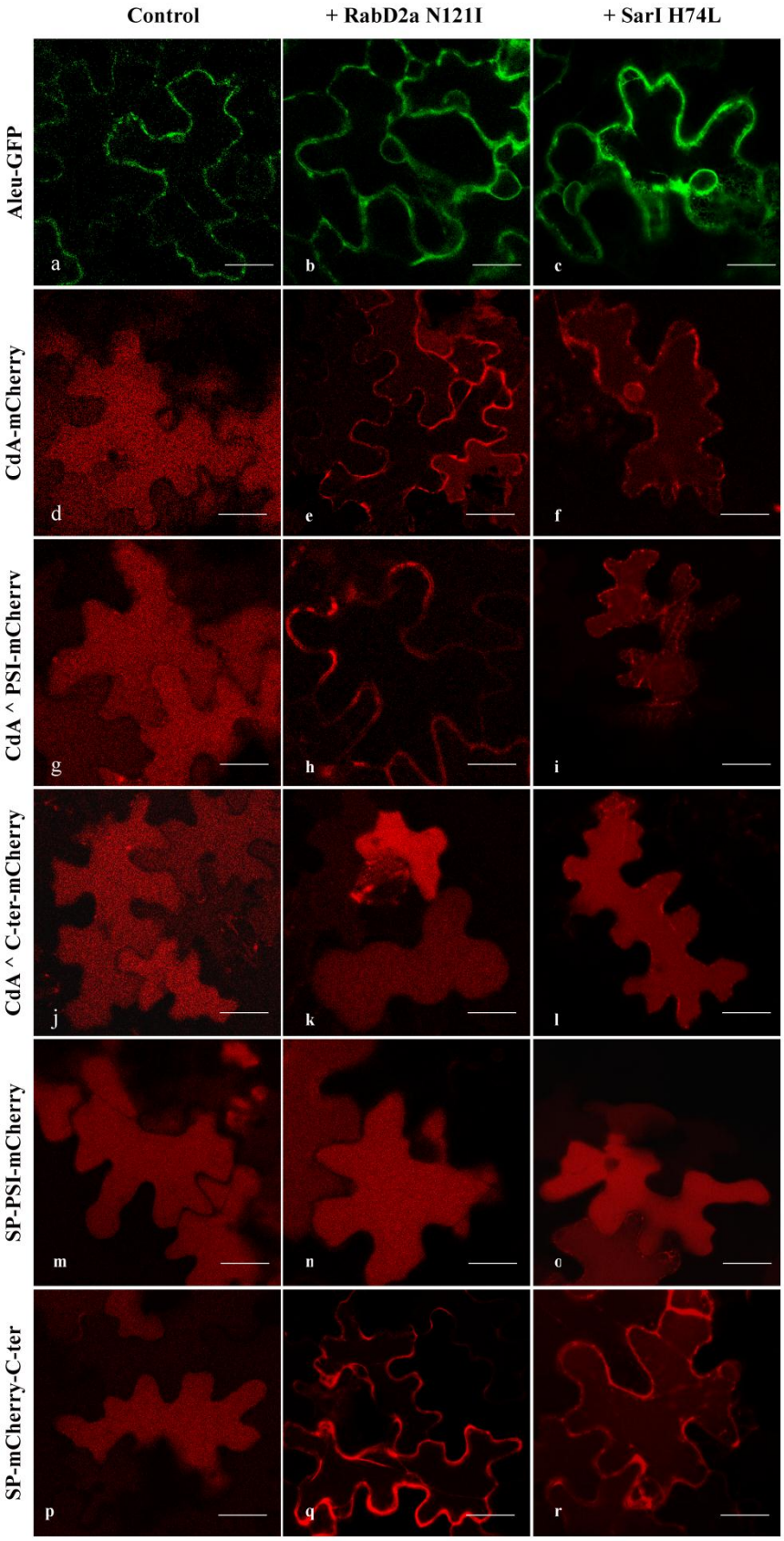

Figure 3.23 Co-expression with the mutants RabD2a N121I and SarI H74L. Controls, cardosin A-mCherry and the mCherry variants fused to the putative VSD signals were infiltrated alone (left column) or co-infiltrated with RabD2a N121I (Column 2) or SarI H74L (column 3). (a-c) Co-infiltration of Aleurain-GFP with RabD2a N121I (b) and

with SarI H74L (c): note the accumulation of fluorescence in cytoplasmic strands and perinuclear labeling, indicative of an ER retention induced by the mutated proteins. (d-f) CdA-mCherry with RabD2a N121I (e) and with SarI H74L (f): Note the lack of vacuolar staining induced by the co-expression with the mutated forms. (g-i) CdAΔPSI-mCherry with RabD2a N121I (h) and with SarI H74L (i): Note the lack of vacuolar staining induced by the co-expression with the mutated forms. (j-l) CdAΔC-ter-mCherry with RabD2a N121I (k) and with SarI H74L (l): Note the vacuolar accumulation of the constructs. (m-o) SP-PSI-mCherry with RabD2a N121I (n) and with SarI H74L (o). (p-r) SP-mCherry-C-ter with RabD2a N121I (q) and with SarI H74L (r). Note the vacuolar accumulation of the constructs. Scale bars: 25 µm.

Blocking post-GA trafficking

To add more evidences to the hypothesis formulated, another blockage of the trafficking pathways was performed, this time affecting post-GA routes. Two different approaches were used to reach this goal: treatment with the drug Wortmannin and co-expression of the constructs with a RabF2b dominant negative mutant.

Wortmannin is a fungal metabolite that was shown to inhibit phosphatidylinositol 3-kinase activity in mammalian cells and to inhibit phosphatidylinositol 4-kinase activity in plant cells (Davidson 1995; Matsuoka et al. 1995). It has been showed that this drug affects vacuolar trafficking of proteins by inhibiting the recycling of BP-80 from the prevacuolar compartment back to the GA, and this blockage is dependent on the dosage of the drug (da Silva et al. 2005). At a concentration of 10 µM, Wortmannin affects BP-80-mediated traffic to the vacuole causing cargo molecules to be directed to the cell surface (da Silva et al. 2005; Pimpl et al. 2003). About 40 hours after infiltration of cardosin A constructs, 10 µM of Wortmannin solution was infiltrated in the leaf and cells were imaged 2 to 4 hours later. Non-treated leaf portions were used as control for Wortmannin action (Figure 3.24 a, d, g, j, m and p). As positive control, Aleurain-GFP was also used and it was observed the redirection of the GFP fluorescence to the cell wall upon treatment with the drug (Figure 3.24 b). The results are in accordance with the ones obtained for the dominant negative mutants affecting the ER-to-GA pathway, with the constructs containing the C-terminal sequence being affected by the drug as their fluorescence is visible in the cell wall and not in the vacuole (Figure 3.24 e, h and q). In contrast, the constructs containing only the PSI as vacuolar sorting determinant are still accumulating in the vacuole, not being affected by the drug (Figure 3.24 k and n).

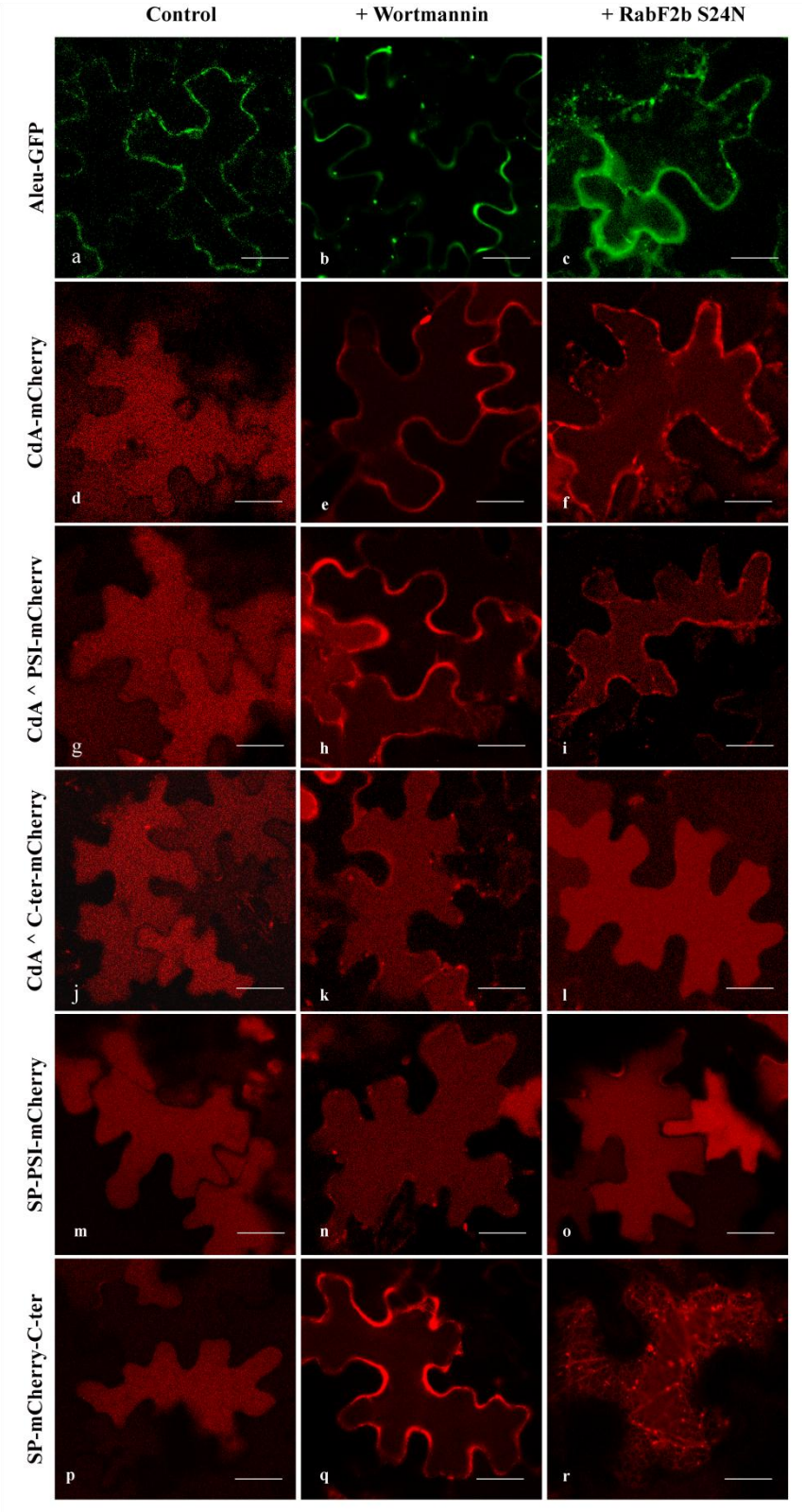

Figure 3.24 Effect of post-Golgi blocking on the constructs localisation. Controls, cardosin A-mCherry and the mCherry variants fused to the putative VSD signals were infiltrated alone (left column) or treated with Wortmannin (Column 2) or co-infiltrated with RabF2b S24N (column 3). (a-c) Aleurain-GFP (a) after Wortmannin treatment (b) and co-infiltration with RabF2b S24N (c): note the accumulation of fluorescence in cytoplasmic strands and in the cell wall, effect of post-Golgi blocking. (d-f) cardosin A-mCherry (d), after Wortmannin treatment (e) Note the lack of vacuolar staining induced by the blockage agents. (g-i) cardosin AΔPSI-mCherry (g)

after Wortmannin treatment (h) and co-infiltration with RabF2b S24N (i): Note the lack of vacuolar staining induced by blockage agents. (j-l) cardosin AΔC-ter-mCherry (j) after Wortmannin treatment (k) and co-infiltration with RabF2b S24N (l): Note the vacuolar accumulation of the constructs. (m-o) SP-PSI-mCherry (m) after Wortmannin treatment (n) and co-infiltration with RabF2b S24N (o): Note the vacuolar accumulation of the constructs. (p-r) SP-mCherry-C-ter (p) after Wortmannin treatment (q) and co-infiltration with RabF2b S24N (r). Scale bars: 25 µm.

The dominant negative mutant RabF2b S24N (Kotzer et al. 2004) impairs vacuolar targeting of proteins by affecting the trafficking between the GA and prevacuolar compartment, causing the vacuolar marker Aleu-GFP to be secreted to the apoplast, as shown in Figure 3.24 c. Repeating the previous co-expression experiments, it was clear that the C-ter containing constructs (cardosin A-mCherry, cardosin AΔPSI-mCherry and SP-mCherry-C-ter) were secreted to the apoplast or retained in dot-shaped compartments (Figure 3.24 f, I and r) and never reached the vacuole. Contrastingly, cardosin AΔC-ter and SP-PSI-mCherry (Figure 3.24 l and o) were still accumulating in the vacuole, meaning that the route to the vacuole was independent from a Golgi-prevacuolar compartment route. These results are consistent with the ones already described and support the idea of a Golgi-bypass pathway.

To summarise, this set of data has shown that cardosin A has two VSDs acting in different vacuolar routes. Cardosin A C-terminal peptide is a ctVSD by definition, guiding the protein to the vacuole trough a classic ER-GA-PVC pathway, as showed by the co-expression with the dominant negative Rab GTPases machinery. Conversely, the PSI domain is an unconventional vacuolar signal involved in the sorting in a GA-independent manner, since its vacuolar localisation is not impaired by the blockage of the ER-GA nor GA-PVC transport.

Besides the identification of Cardosin A VSDs, a next question is to define the influence of glycosylation sites in cardosin A trafficking to the vacuoles, as it may define a specific transport from the ER to the GA in a COPII vesicles-dependent manner.

3.2.3.A role for the Glycosylation site in vacuolar trafficking?

Cardosin A is a N-glycosylated enzyme, with two complex type N-glycosylation sites (one in the heavy and the other in the light chain), suggesting a passage through the GA and therefore a putative role for N-glycosylation processes in direct or indirect transport to the vacuole, as discussed in Rayon et al. (1998).

This assumption was in part supported by the results presented above describing a putative classic ER-GA-PVC-Vacuole route for cardosin A. However, the possible existence of a GA independent route mediated by the PSI raises again the question on the relevance of glycosylation in protein sorting. Using the site-directed mutagenesis technique the glycosylation site in the heavy chain or in the light chain were removed – cardosin Agly1 and cardosin Agly2, respectively – and obtained fusions with mCherry for *in vivo* analysis. Furthermore, an extra glycosylation site was added in the PSI domain of cardosin A – cardosin AglyPSI - to imitate the putative glycosylation site existing in other APs PSIs, including cardosin B and phytepsin.

Results obtained with these glycosylation mutants showed that the protein is still able to travel to the vacuole efficiently in the three cases studied (Figure 3.25), suggesting that cardosin A trafficking is not altered by differences in its glycosylation.

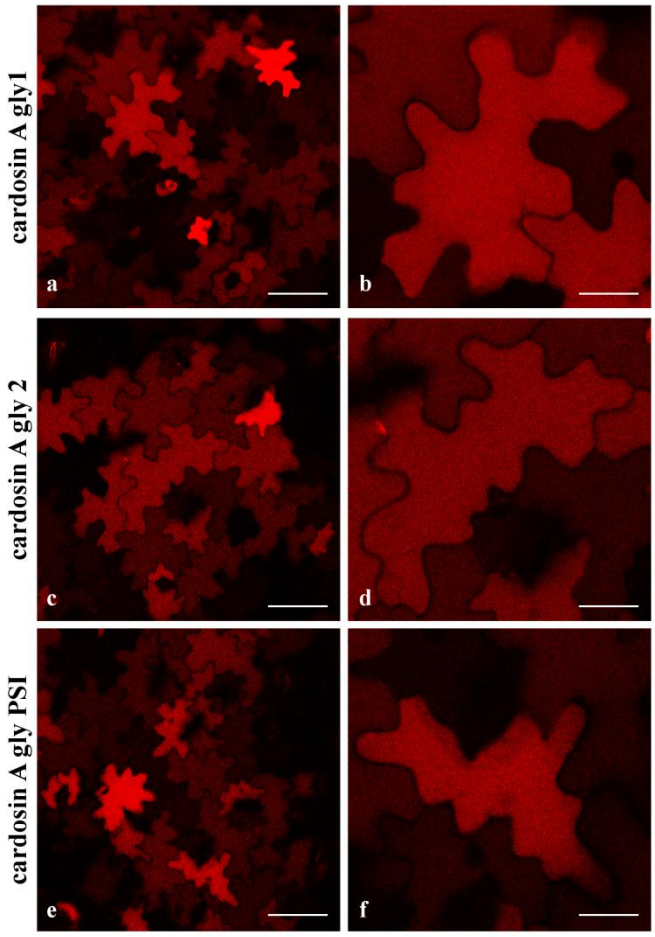

Figure 3.25 Subcellular localisation of cardosin A glycosylation mutants fused to mCherry. The constructs were transiently expressed in tobacco leaves using agro-infiltration and imaged 3 days after infiltration. Tobacco

epidermal cells expressing cardosin A gly1-mCherry (a, b), cardosin A gly 2-mCherry (c, d) and cardosin A gly PSI-mCherry (e, f). Images were acquired with a 561 nm laser. Scale bars: a, c, e, 75 µm; b, d, f, 25 µm.

These data do not however provide information on the route taken by the protein to reach the vacuole, by-passing the Golgi or not. It also questions the effect of glycosylation inhibition on cardosin A trafficking pathways. To answer these questions, we set up a Tunicamycin assay. Tunicamycin is an antibiotic that block glycosylation by inhibiting the formation of dolichyl-pyrophosphoryl-GIcNAc, the first step in the lipid-linked saccharide pathway (Hori & Elbein 1981). It was anticipated that proteins traveling through a Golgi-independent pathway would not be affected by the antibiotic treatment. About 3 days after infiltration with cardosin A and its mutated versions fused to mCherry, Tunicamycin treatment of 2 hours was performed before imaging the cells to evaluate the effect of the drug on cardosin A, and the three glycosylation mutants, vacuolar accumulation. As control experiments, ST-GFP (non-glycosylated protein known as a Golgi marker), cardosin A-mCherry and SP-mCherry-C-ter (travels through the Golgi) and SP-PSI-mCherry (bypassing the Golgi) were used.

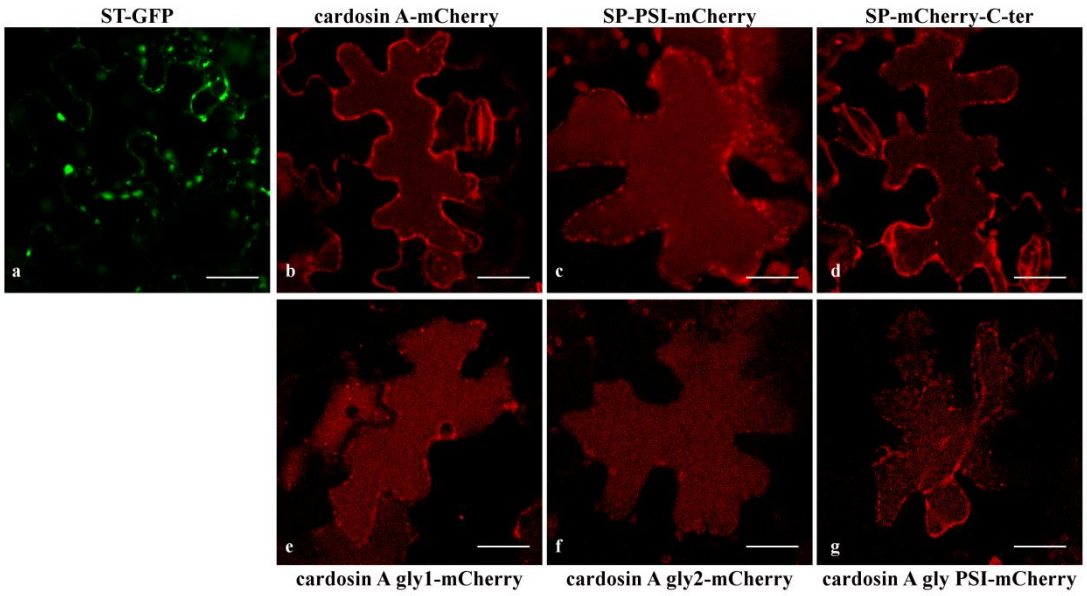

Figure 3.26 Effect of Tunicamycin on the constructs localisation. Control, cardosin A-mCherry SP-PSI-mCherry, SP-mCherry-C-ter and the mCherry variants of cardosin A glycosylation mutants were treated with Tunicamycin. (a) ST_GFP. (b) Cardosin A-mCherry. (c) SP-PSI-mCherry. (d) SP-mCherry-C-ter. (e) cardosin A gly 1-mCherry. (f) cardosin A gly 2-mCherry. (g) cardosin A gly PSI-mCherry. Scale bars: 25 µm.

ST-GFP expression was affected by Tunicamycin and the dot-shaped compartments characteristics of the protein expression in this system were replaced by large fluorescent agglomerates in the cytoplasm (Figure 3.26 a). Cardosin A-mCherry localisation was also altered. Some amount of fluorescent was still visible in the vacuole,

however the majority of the protein was retained in early secretory compartments (Figure 3.26 b). Similar result was obtained for SP-PSI-mCherry, but the amount of protein that reaches the vacuole seemed higher for this construct (Figure 3.26 c). However, SP-mCherry-C-ter construct was completely retained in those earlier secretory pathway compartments and the protein was not accumulating in the vacuole (Figure 3.26 d).

The mutated versions of Cardosin A where the glycosylation site was disrupted were accumulating in the vacuole (Figure 3.26 e and f) in a manner similar to control experiments. Comparing with the results obtained without the treatment (compare with Figure 3.25 b and d) it is clear that the mCherry fluorescence was not as bright in the vacuole and there was still some protein in the ER network, especially in cardosin Agly1-mCherry (Figure 3.26 e). In contrast, the glycosylation site added in the PSI domain caused the protein to be retained upon addition of Tunicamycin (Figure 3.26 g). These results (Table 3-2) open new questions on the role of glycosylation in aspartic proteinases' trafficking. When a glycosylation site is artificially placed in the PSI, the labeling of the construct upon Tunicamycin treatment is similar with the one obtained for ST-GFP, but not with the one obtained for cardosin A-mCherry nor for SP-PSI-mCherry.

In light of these results, the GA-bypass data depending on PSI sorting (presented earlier) seems to be related with the absence of the conserved glycosylation site in this domain.

Table 3-2 Summary of the localisation results obtained for the glycosylation experiment with and without the drug Tunicamycin.

Construct /Localisation	Control	+ Tunicamycin
ST-GFP	ER/GA	ER/GA
Cardosin A-mCherry	Vacuole	Vacuole + ER/GA
SP-PSI-mCherry	Vacuole	Vacuole + ER/GA
SP-mCherry-C-ter	Vacuole	ER/GA
Cardosin A gly1-mCherry	Vacuole	Vacuole
Cardosin A gly2-mCherry	Vacuole	Vacuole
Cardosin A PSI-mCherry	Vacuole	ER/GA

3.2.4. Comparison with cardosin B sorting routes

As already referred along this work cardosin B is another AP from *C. cardunculus* that shares high similarity with cardosin A. In cardoon flowers, while cardosin A has a vacuolar accumulation, cardosin B is secreted to the extracellular matrix (Ramalho-Santos et al. 1997; Vieira et al. 2001). However, it was shown that cardosin B accumulates in the vacuole when heterologously expressed in tobacco leaves (da Costa et al. 2010). In this work the aim was to explore cardosin B domains – PSI and C-terminal – in a similar way as for cardosin A, to evaluate if they share the same sorting characteristics. Therefore cardosin B PSI and C-terminal peptide were isolated and fused with mCherry to obtain the constructs SP-PSIB-mCherry and SP-mCherry-C-terB. Cardosin B and cardosin A PSIs share about 70% similarity in terms of nucleotide sequence, but they have a distinguishable feature: cardosin B PSI has a putative glycosylation site that is absent in cardosin A's PSI. The C-terminal peptide differs in only one aminoacid between the two cardosins.

Both SP-mCherry-C-terB and SP-PSIB-mCherry fluorescence were detected in the vacuole of *N. tabacum* cells (Figure 3.27 a, b and e, f, respectively), indicating that Cardosin B PSI and Cardosin B C-terminal domains are also vacuolar sorting domains for Cardosin B, acting independently and comparable to Cardosin A VSDs.

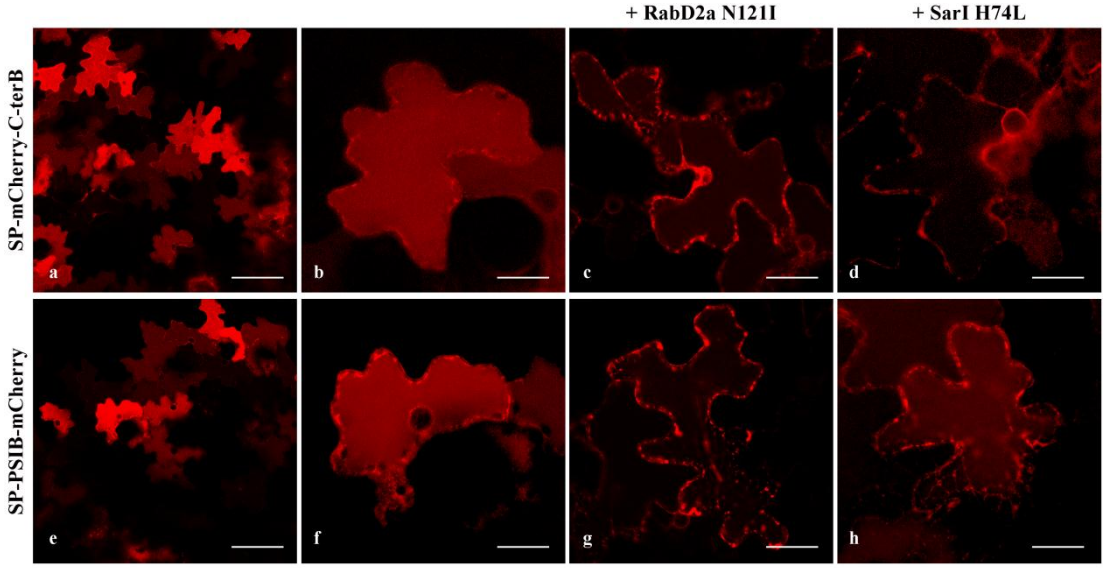

Figure 3.27 Subcellular localisation of m Cherry fusions of cardosin B PSI or C-terminal peptide and co-expression with the mutants RabD2a N121I and SarI H74L. mCherry variants fused to cardosin B domains were infiltrated alone (a, b, e, f) or co-infiltrated with RabD2a N121I (c, g) or SarI H74L (d, h). (a-b) SP-mCherry-C-terB

expression alone: note the vacuolar accumulation. (c) SP-mCherry-C-ter B with RabD2a N121I (d) and with SarI H74L: note the accumulation of fluorescence in cytoplasmic strands and perinuclear labeling, indicative of an ER retention induced by the mutated proteins. (e, f) SP-PSIB-mCherry expression alone: note the perinuclear labeling and fluorescence in peripheric vesicles, indicative of ER localisation. (g) SP-PSIB-mCherry with RabD2a N121I (h) and with SarI H74L: Note the lack of vacuolar staining induced by the co-expression with the mutated forms. Scale bars: a, e, 75 µm; b-d, f-h, 25 µm.

Furthermore, the dominant negative versions of RabD2a and SarI were used to block the trafficking between the ER and GA to compare the behavior of Cardosin B VSDs with Cardosin A VSDs, and especially assess if cardosin B PSI could also reach the vacuole in a GA-independent manner.

As expected mCherry fused to the C-terminal region of cardosin B was retained in the ER (Figure 3.27 c and d) in a way similar to what was observed for cardosin A, suggesting a blockage in the ER-GA transport. The constructs bearing the cardosin B glycosylated PSI remained blocked in the ER when co-expressed with the dominant negative mutant of RabD2a or SarI (Figure 3.27 g and h), suggesting the involvement of a ER-Golgi mediated pathway for this construct. This later result contrasts with the ones observed with cardosin A PSI domain which continued to go the vacuole despite an ER-GA blockage. ***This suggests that not only the PSI domains are Vacuolar Sorting Determinants but are also able to take different vacuolar routes according to their structure. Taking into account the fact that cardosin B PSI domain differs from cardosin A PSI domain by the presence of a glycosylation site, these results highlight a putative role for glycosylation in determining the route to the vacuole.***

3.3. OUTCOMES

The results obtained in this chapter allowed (i) defining cardosin A as a self-processing enzyme, (ii) the identification of two new vacuolar sorting determinants: PSI and C-terminal peptide VGFAEAA, (iii) the disclosure of two different vacuolar routes for the cardosin A-mCherry reporter proteins, (iv) a new insight on PSI domains in APs, and (v) a discussion on the relevance of glycosylation in sorting events. Altogether, these data contribute to discuss and decipher the AP vacuolar trafficking pathways in plant cells.

Cardosin A is a partially self-processing enzyme: The results obtained using mutants without catalytic activity showed an accumulation of cardosin A precursor form. This indicates that processing of cardosin A is an autocatalytic process partially assisted by other proteases as the mature form is still achieved. This delay in processing, however, does not impair cardosin A vacuolar accumulation.

Identification of two new vacuolar sorting determinants: Two domains of cardosin A protein have the ability of sorting the protein to the vacuole – PSI domain and C-terminal peptide VGFAEAA. The results presented demonstrate that the C-terminal peptide fits in the definition of a ctVSD, as it needs to be exposed at the C-terminal of the protein to work. Moreover, only four aminoacids of this peptide are sufficient to correctly target a protein to the vacuole. The PSI domain is also a VSD, but it is a more unconventional sorting domain, that possibly works by interacting with intracellular membranes.

Two different vacuolar routes for cardosin A-mCherry: The two vacuolar sorting determinants identified for cardosin A seem to mediate the protein trafficking to the vacuole through different routes. Blocking the trafficking between endomembrane compartments allowed to define a classic ER-GA-PVC route to the vacuole for cardosin, mediated by the C-terminal signal peptide. In the other hand, the PSI drives the protein to the vacuole using a GA independent pathway. This is not true for cardosin B PSI, as the route taken by this domain is similar to the one described for the C-terminal peptide.

Glycosylation sites are involved in sorting events: Contrary to the majority of plant APs, cardosin A does not have a glycosylation site in the PSI domain. Point mutations to remove the N-glycosylation sites or introducing an extra site in the PSI domain, revealed the importance of glycosylation in cardosin A sorting. The addition of a glycosylation site in the PSI changed its route to the vacuole and caused the protein to be retained in the ER upon treatment with Tunicamycin.

CHAPTER III – CARDOSIN A BIOGENESIS AND TRAFFICKING DURING *ARABIDOPSIS THALIANA* SEED GERMINATION

Manuscript in preparation:

Cláudia Pereira, Ana Oliveira, Susana Abreu, Susana Pereira, José Pissarra and Béatrice Satiat-Jeunemaitre. "Characterization of cardosin A and B sorting routes in Arabidopsis thaliana heterologous system".

3.1. BACKGROUND

Despite being a good system to explore cardosins sorting to the vacuole, expression in *N. tabacum* leaf epidermis does not answer the question on the different sorting of cardosins along developmental stage. In cardoon, cardosins are mostly expressed during flower and seed development (Ramalho-Santos et al. 1997; Vieira et al. 2001; Duarte et al. 2006; Figueiredo et al. 2006; Pereira et al. 2008), being only detected in residual amounts in vegetative tissues such as leaves or callus tissue (Oliveira et al. 2010). Therefore, to fully explore cardosins trafficking and validate its proper expression in stable expression in Arabidopsis systems, studies on cardosin expression and trafficking had been extended to Arabidopsis seed cells.

Seeds are a model of choice for intracellular studies in plants, in particular concerning vacuolar sorting, given the vast changings occurring in a short period of time. After dormancy, storage proteins and minerals need to be mobilized from the protein storage vacuole (PSV) to allow cell expansion, and eventually a central lytic vacuole is formed. Several studies have explained the complex vacuome organization and the remodelling of vacuolar membranes occurring during seed germination (Maeshima et al. 1994; Inoue et al. 1995; Olbrich et al. 2007; Bolte et al. 2011). We choose to study cardosin A accumulation and trafficking in germinating Arabidopsis seedlings, to go further in the understanding of cardosins trafficking in plant cells. Therefore, cardosin A labelling patterns were compared with well-known markers for pre-vacuolar compartments (m-Rab) and protein storage vacuole (TIPs) in non-germinated and germinated seedlings. Furthermore a BFA assay was carried out to assess cardosin A route in these cells.

3.2. RESULTS

Two different stages of seed germination were analysed: 24 hours and 3 days after imbibition. In the first time-point cotyledons were still enclosed in the seed coat but in some seeds the radicle has already emerged (Figure 3.28 a and b), but in the next stage the seed was already fully germinated (Figure 3.28 c).

Figure 3.28 Morphological appearance of the seed germination stages of *Arabidopsis thaliana* inducible expression system used in this study. (a, b) Seeds 24 hours post-imbibition; (c) Germinated seedling, 3 days after imbibition.

Immunofluorescence studies provided a general view of cardosin A distribution in the tissue and cells. Furthermore, its subcellular localisation was evaluated at the intracellular level using immunogold labeling and TEM analysis. Seeds were germinated in MS medium and in the presence of the inducible agent and processed for PEG embedding (light microscopy studies) or/and LR White embedding (TEM studies).

3.2.1. Cardosin A localization in promoter-induced A. thaliana seedlings by immunofluorescence differs with germination

Cardosin A localization was first analysed by immunofluorescence in radicle and cotyledon sections using a polyclonal anti-cardosin A antibody and an anti-rabbit secondary antibody coupled to Alexa fluor 488®. Autofluorescence images were taken at the same time as it highlighted Protein Storage Vacuoles (PSV) due to the autofluorescence of its components.

Cardosin A labeling was detected in radicles and cotyledons in practically all cell types (Figure 3.29 a, c, e and g), which is not surprising, given the usage of a CaMV 35S promoter in the construction of the binary vector. However, when zooming on either radicle cells or cotyledon cells, it appears that intracellular labeling is different between radicles and cotyledons and also changes with the developmental stage.

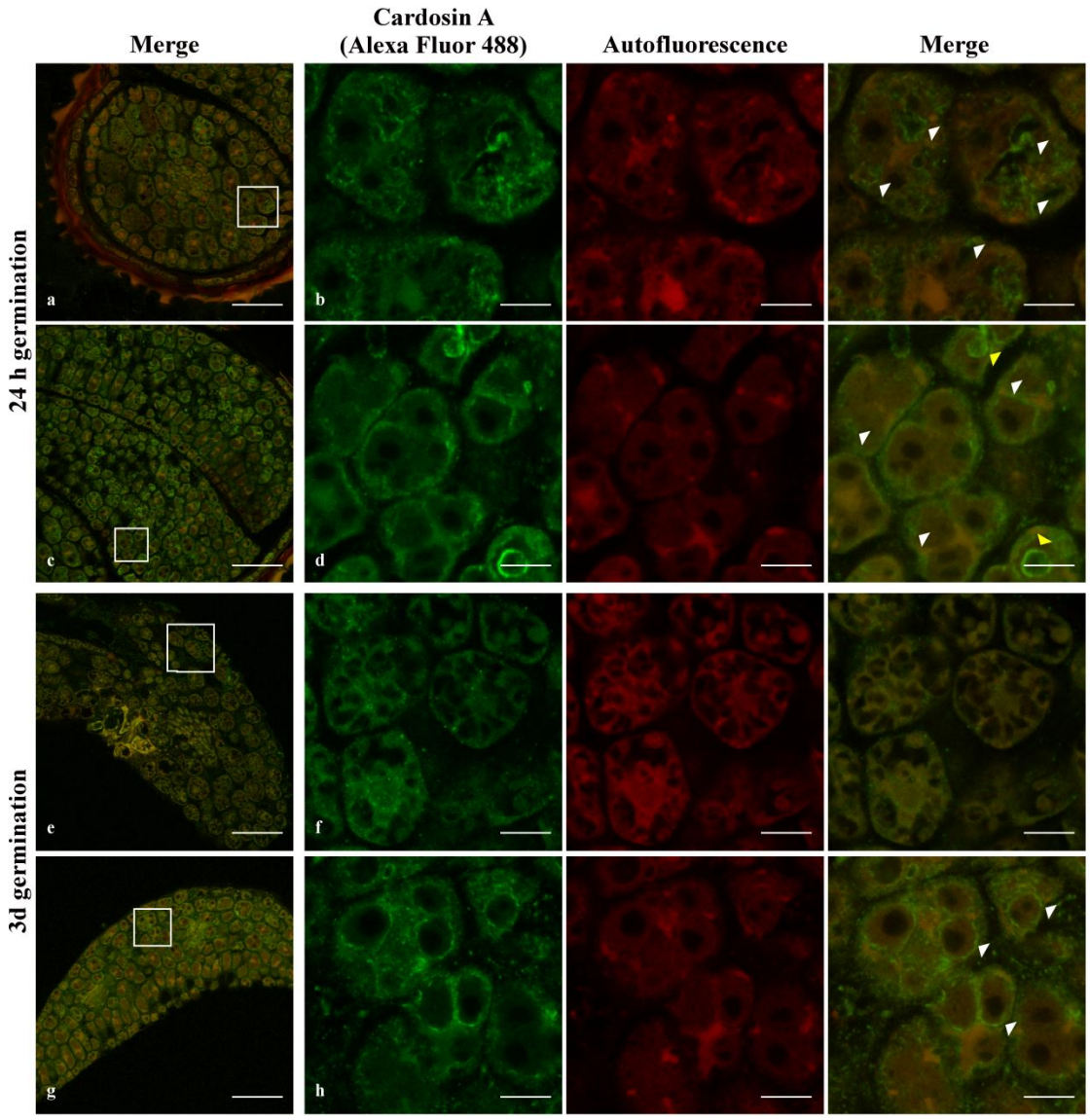

Figure 3.29 Immunofluorescence of cardosin A in radicle (a, b, e, f) and cotyledon (c, d, g and h) sections of *A. thaliana* inducible expression system using polyclonal antibody against cardosin A. 24hours (a, b, c, d) and 3 days old seedlings (e, f, g, h) (germinated with dexamethasone). (a, b) In radicle sections labeling was detected associated with membranes in the cytoplasm (white arrowheads); (c, d) In cotyledon sections, cardosin A was detected in the cytoplasm (white arrowheads) and associated with the a membranous structure inside the PSV (yellow arrowheads); (e, f) cardosin A labeling in the radicle is diffuse; (g, h) labeling in the cotyledon sections is detected surrounding the PSVs (white arrowheads) and also in the cytoplasm. Column 1 corresponds to a low magnification of the seed tissue; Column two corresponds to labeling with anti-cardosin A coupled to AlexaFluor 488 visualised at 488nm; Column 3 corresponds to tissue autofluorecence visualized at 561nm. Column 4 is an

insert of the tissue represented in column 1 (square) and corresponds to merged image of columns 2 and 3. Scale bars: a, c, e, g, 45 µm; b, d, f, h, 9 µm.

In non-germinated seeds (24 hours) cardosin A was found in the radicle sections in the cytoplasm and sometimes associated to membranous structures (Figure 3.29 b, white arrowheads). In cotyledon sections and at the same stage, cardosin A was found in dots in the cytoplasm surrounding autofluorescent PSVs (Figure 3.29 d, white arrowheads) and sometimes is detected in association with a membrane-delimited compartment of the PSV (Figure 3.29 d, yellow arrowheads). This labeling associated with the PSV was not detected in cotyledons from germinated seedlings (Figure 3.29 h).

In germinated seed, Cardosin A labeling became fainter in radicle, being detected as punctate dots in the cytoplasm, which may represent some PSVs (Figure 3.29 f). In cotyledon sections, cardosin A is also detected in the cytoplasm and surrounding PSVs (Figure 3.29 h, white arrowheads).

This first set of data shows a differential localisation of Cardosin A in tissue (i.e. radicle and cotyledons) and in developmental stages (1 day to 3 days post germination). In all cases, labeling of lytic vacuoles was never observed.

3.2.2. Maturation of cardosin A along the secretory pathway is confirmed by the use of anti PSI antibodies

Using another antibody recognizing cardosin A PSI region, it was possible to relate cardosin A processing events with Cardosin A localisation along the vacuolar pathway. This antibody would recognize the precursor form of cardosin A, the PSI region still attached to the light chain and the PSI alone, and would not detect the processed heavy chain as the antibody against cardosin A.

In non-germinated seeds the fluorescence pattern is similar to the one obtained with cardosin A polyclonal antibody, with labeling being detected in the cytoplasm and associated with membranous structures, both in radicles and cotyledons (compare Figure 3.30 a, b, c and d with Figure 3.29 a, b, c and d). Also, in radicle and cotyledons sections, there is a clear labeling of PSV internal membranes in some cells (Figure 3.30 b and d, white arrowheads), as it was observed when using cardosin A polyclonal antibody, in cotyledon sections.

In radicle sections of 3-days germinated seedlings the labeling of anti-PSI antibody is slightly different from the one obtained with the cardosin A antibody, as it appears in small vesicles in the cytoplasm (Figure 3.30 e and f, compare with Figure 3.29 e and f), instead being faintly detected in the cytoplasm. In cotyledons sections of the same developmental stage the picture is also different, as PSI-labeled structures fluorescence appears in dot-shaped compartments in the cytoplasm of the cells instead of in the periphery of PSVs as observed for anti-cardosin A antibody (Figure 3.30 g and h, to be compared with Figure 3.29 g and h).

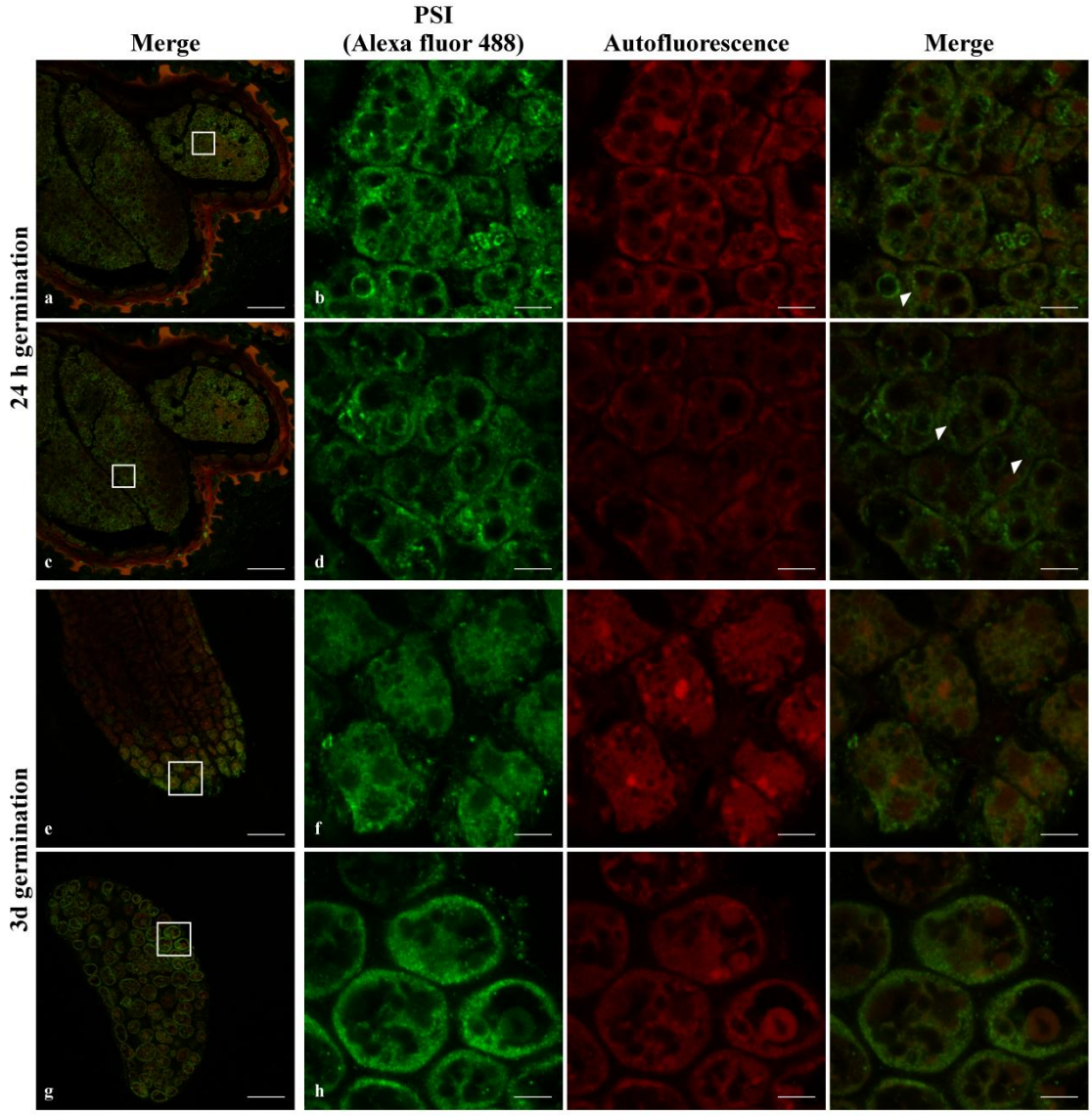

Figure 3.30 Immunofluorescence of cardosin A PSI in radicle and cotyledon sections of *A. thaliana* inducible expression system, using an antibody directed against PSI domains. 24 hours (a, b, c, d) and 3 days old seedlings (e, f, g, h) (germinated with dexamethasone). (a, b) In radicle sections labeling was detected in the cytoplasm and associated to globoids membranes (white arrowheads); (c, d) In cotyledon sections, the PSI was also detected in the cytoplasm and associated with PSV membranes (white arrowheads); (e, f) In radicle sections, PSI labeling in the radicle was associated with small vesicle in the cytoplasm; (g, h) labeling in the cotyledon sections is

detected in dot-shaped compartments in the cytoplasm. Column 1 corresponds to a low magnification of the seed tissue; Column two corresponds to labeling with anti-PSI coupled to AlexaFluor 488 visualised at 488nm; Column 3 corresponds to tissue autofluorescence visualized at 561nm. Column 4 is an insert of the tissue represented in column 1 (square) and corresponds to merged image of columns 2 and 3. Scale bars: a, c, e, g, 45 µm; b, d, f, h, 9 µm.

No cardosin A labeling was detected in sections labeled with anti-cardosin A antibody (both radicle and cotyledons), from non-induced plants (controls - Figure 3.31 a and b) as well as for the anti-PSI (Figure 3.31).

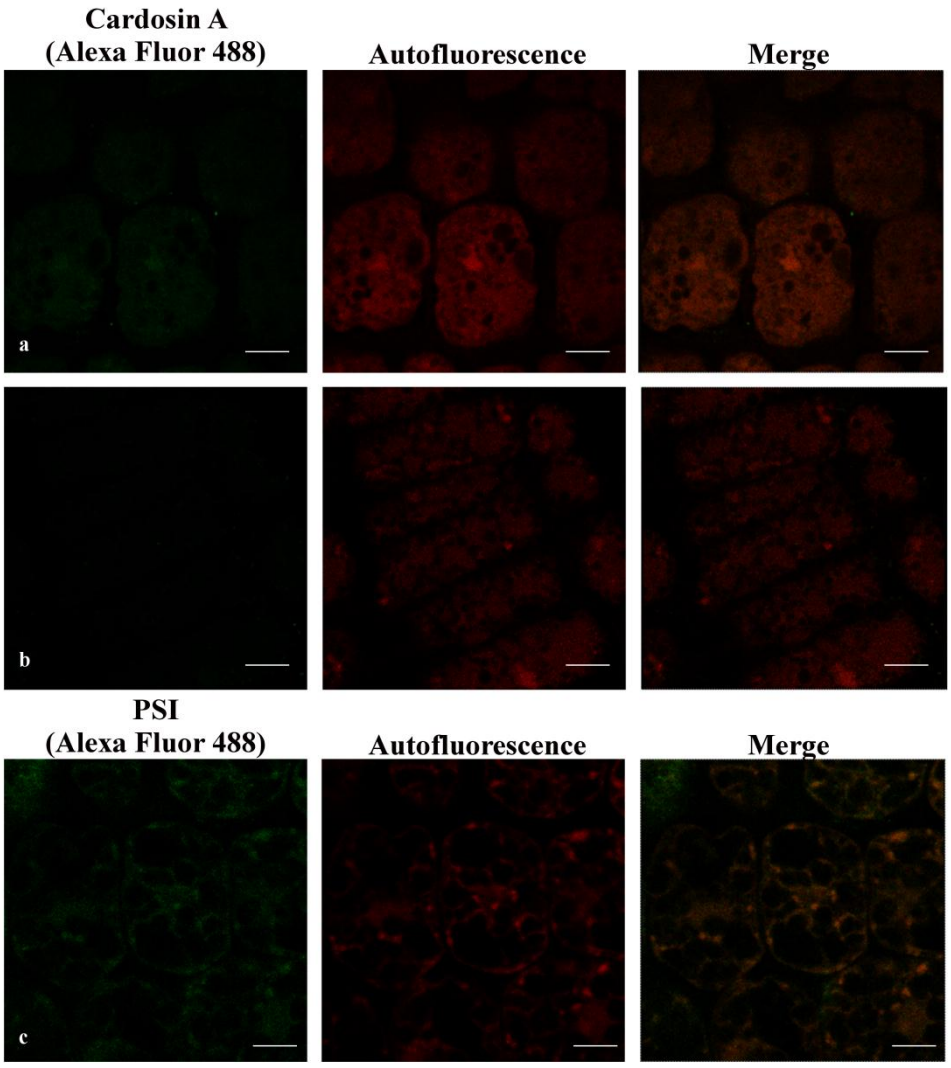

Figure 3.31 Immunofluorescence of cardosin A (a, b) and PSI (c) in radicle and cotyledon sections of non-induced plants of *A. thaliana* inducible expression system. 3 days old seedlings, germinated without dexamethasone (using polyclonal cardosin A antibody. (a) anti-cardosin A in radicle sections; (b) anti-cardosin A in cotyledon sections; (c) anti-PSI in radicle sections. Scale bars: a, b, 9 µm.

Comparing the results obtained with anti-cardosin A and anti-PSI it can be highlighted that in non-germinating seedlings cardosin A must be in its precursor form, since the pattern obtained with both antibodies is similar. On the contrary, in germinating

seedlings the fluorescence pattern obtained differs between the two. This is an indication that cardosin A detected in association with the PSVs (using anti-cardosin A antibody) is already processed and without the PSI domain. ***These results gives an insight about cardosin A processing along the route to the PSV, indicating that the PSI domain must be cleaved off before the protein reaches its destination.***

3.2.3. Immunolocalisation of cardosin A at the ultrastructural level reveals its association with a complex vacuolar system

The information given by immunofluorescence studies in terms of cardosin A localisation was not sufficient to get a clear picture and the resolution allowed by TEM was needed. Immunocytochemistry techniques were performed using the same specific polyclonal antibody raised against cardosin A. Only 3 days germinated seeds were used from this point on, because it was not possible to optimize the protocols to properly embed non-germinated seeds in LR-White. As before, radicles and cotyledons were treated separately.

In radicle sections, the cells are characterized by a complex vacuolar system, characterized by the presence of different types of vesicular compartments. (Figure 3.32 a). The PSVs are recognizable by their size (larger compartments) when compared to other cellular organelles and by its electron-dense appearance under the electron microscope. In the cytoplasm, electron-dense and electron transparent vesicles are found in large number. Large lytic vacuoles were not seen at this stage.

The majority of cardosin A labeling was found in PSVs (Figure 3.32 b and d, red circles). It may also been found in association with the Golgi and with ER (Figure 3.32 c and d, red circles). Some gold dots were also detected in association with some electron transparent vesicles in the cytoplasm (Figure 3.32 e, red circles).

Compared with immnofluorescence data and taking into account the labeling intensities observed at the TEM level, it is tempting to assume that most of the labeling observed at the light level would correspond to the PSV compartments. However, at the light level the fluorescence seems to be localized in the periphery of PSVs rather than inside these structures. TEM labeling may also reveals some ER exit sites, Golgi or even

young lytic vacuoles (transparent vesicles?). No labeling was detected in the control section without primary antibody (Figure 3.32 f, g and h).

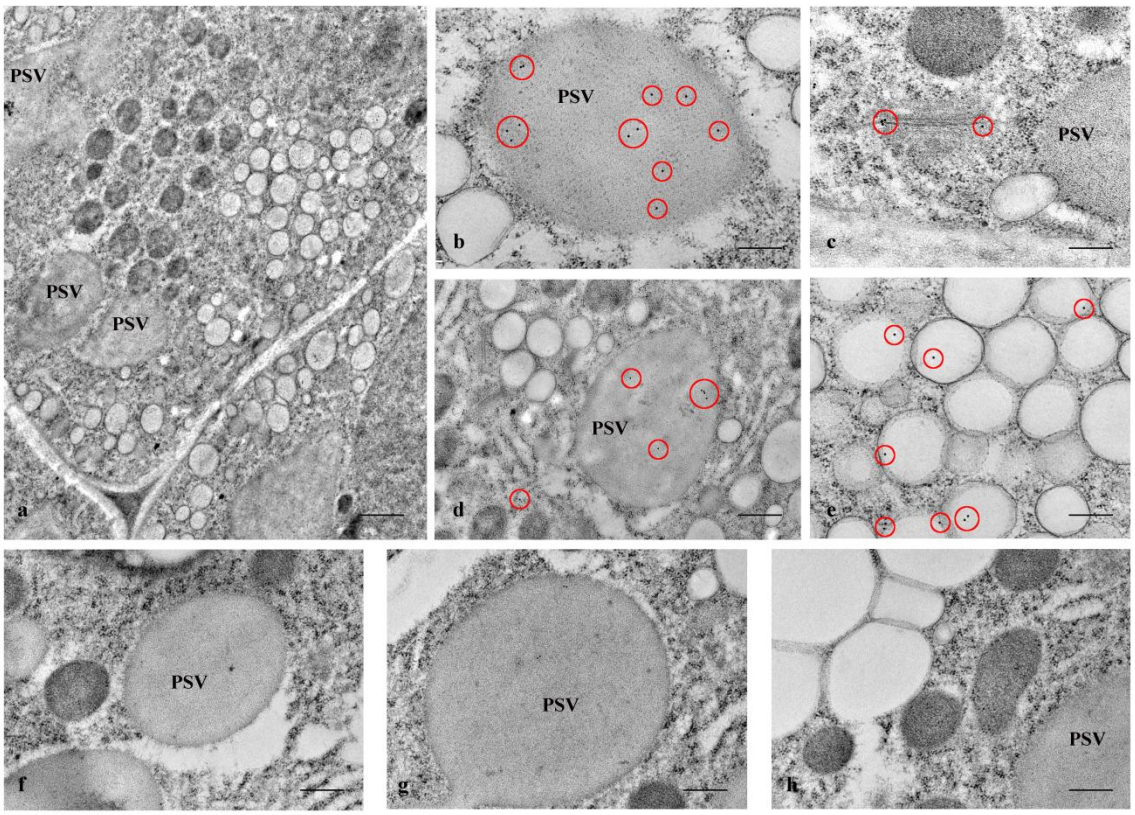

Figure 3.32 Immunogold labeling of cardosin A in radicle sections of *A. thaliana* inducible expression system. 3 days old seedlings, germinated with dexamethasone were used. (a) General view of the cell; (b, d) labeling was detected inside protein storage vacuoles and (c) associated with the Golgi apparatus. Cardosin A was also detected in small electron transparent structures in the cytosol (e). The red circles mark the gold labeling corresponding to cardosin A. As control of the immunolabeling technique, sections without primary antibody (f, g, h) were used. PSV – Protein Storage Vacuole. Scale bars: a, 1 µm; b, c, g, h, 200 nm; d, f, 500 nm; e, 300 nm.

In cotyledon cells, the vacuolar system appears differently structured from radicle cells, with one or more large vacuoles (probably lytic vacuoles?) occupying the cell (Figure 3.33 a). The PSVs are still present in these cells but are smaller than in radicle sections cells. Electron-dense and electron transparent vesicles are still observed in the cytoplasm. Cardosin A localisation is also different between cotyledon and radicle cells, as already observed in the immunofluorescence studies. In cotyledon cells, cardosin A is mostly detected in the central lytic vacuoles (Figure 3.33 c), despite it has also been detected in PSVs (Figure 3.33 b and d). Cardosin A was also found in the cytoplasm (in the periphery of ER and GA) and in association with small dense vesicles (Figure 3.33 b and e, respectively).

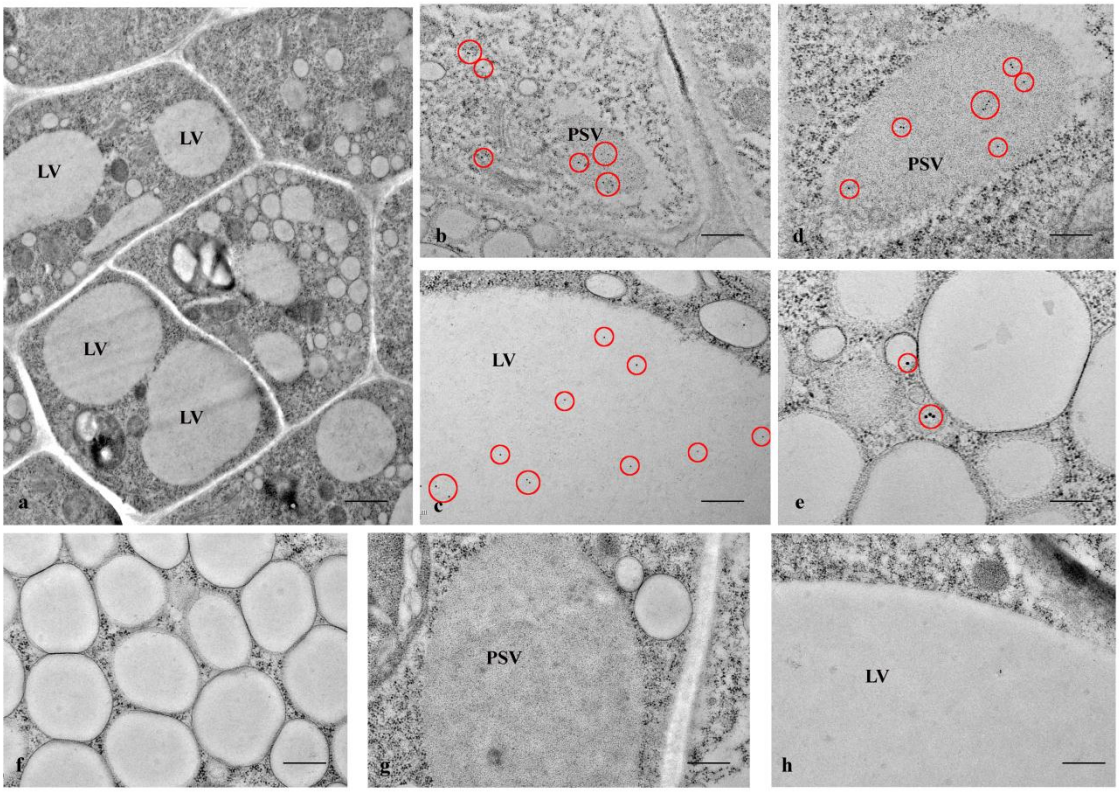

Figure 3.33 Immunogold labeling of cardosin A in cotyledon sections of *A. thaliana* inducible expression system. 3 days old seedlings, germinated with dexamethasone were used. (a) General view of the cell; (b, d) labeling was detected inside protein storage vacuoles and (c) in the large central vacuole. Cardosin A was also detected in small electronodense structures in the cytosol (e). The red circles mark the gold labeling corresponding to cardosin A. As control of the immunolabeling technique, sections without primary antibody (f, g, h) were used. LV – Lytic vacuole; PSV – Protein Storage Vacuole. Scale bars: a, 1 µm; b, 500 nm; c, f, g, h, 400 nm; d, 300 nm; e, 200 nm.

The results obtained in cotyledon cells are, in some aspects, different from the ones obtained with immunofluorescence techniques. In the cotyledon sections observed by immunofluorescence, no labeling of lytic vacuoles was visible, while in TEM section, the existence of at least one large vacuole is clear. It may be due to the maturation level of cotyledon cells that were in an earlier developmental stage than the ones used for TEM studies, or a too low expression of the protein to be detected at the light level.

Taking together the results obtained from LM and TEM approaches, it is clear that cardosin A accumulates in PSVs and is also found in association with the ER and the GA and in some vesicle structures, probably representing post-GA compartments (Table 3-3). As the immunolabelling was performed in a later stage of seed development and the cotyledons are already fully developed cardosin A is also detected in the central lytic vacuoles in this tissue. ***As a whole, it is possible to say that cardosin A is detected along the secretory pathway and that it finally accumulates in the***

vacuole, PSV or LV, depending on the tissue under study. These results are in accordance with previous results obtained in cardoon and confirm that cardosin A localisation and trafficking in *A. thaliana* is also dependent on the developmental stage.

Table 3-3 Summary of cardosin A localisation in cotyledon and radicle sections of *A. thaliana* inducible expression system, by immunofluorescence (IF) and transmission electron microscopy (TEM). ER – endoplasmic reticulum, GA – Golgi apparatus, LV – lytic vacuole, PSV – protein storage vacuole.

	Non-germinated seeds	**Germinated seedlings**	
	IF	**IF**	**TEM**
Radicle cells	Cytoplasm (association to membranes)	Cytoplasm (associated to PSVs) Small vesicles (with anti-PSI)	ER GA PSV Electron transparent vesicles
Cotyledon cells	Cytoplasm (dots surrounding PSVs) Globoid membrane	Cytoplasm PSVs membrane Dots in the cytoplasm (with anti-PSI	Cytoplasm (ER/GA?) PSV LV Electron dense vesicles

3.2.4. Comparison of Cardosin A labelling, prevacuolar and vacuolar labelling in radicles of germinated seeds

To confirm the identity of the cardosin A labeled compartments, we compare Cardosin A labeling pattern with other known markers for prevacuolar compartments, protein storage vacuole, and lytic vacuoles. Immunofluorescence and immunogold labeling was performed in radicle sections of 3 days *A. thaliana* seedlings expressing cardosin A under a dexamethasone-inducible promoter.

mRab is a N-myristoylated plant-specific Rab-GTPase that was found to be located to the prevacuolar compartment and also associated to the GA (Bolte et al. 2004). The pattern of m-Rab labeling in radicle cells appears as fluorescent round structures in the cytoplasm and sometimes associated with membranous structures (Figure 3.34 a and b, white and yellow arrowheads, respectively). This pattern resembles by its fluorescence intensity and pattern to the one obtained for cardosin A using anti-PSI

antibody (compare with Figure 3.30 f and h), where the fluorescence was visible in the cytoplasm and also associated with membranous structures.

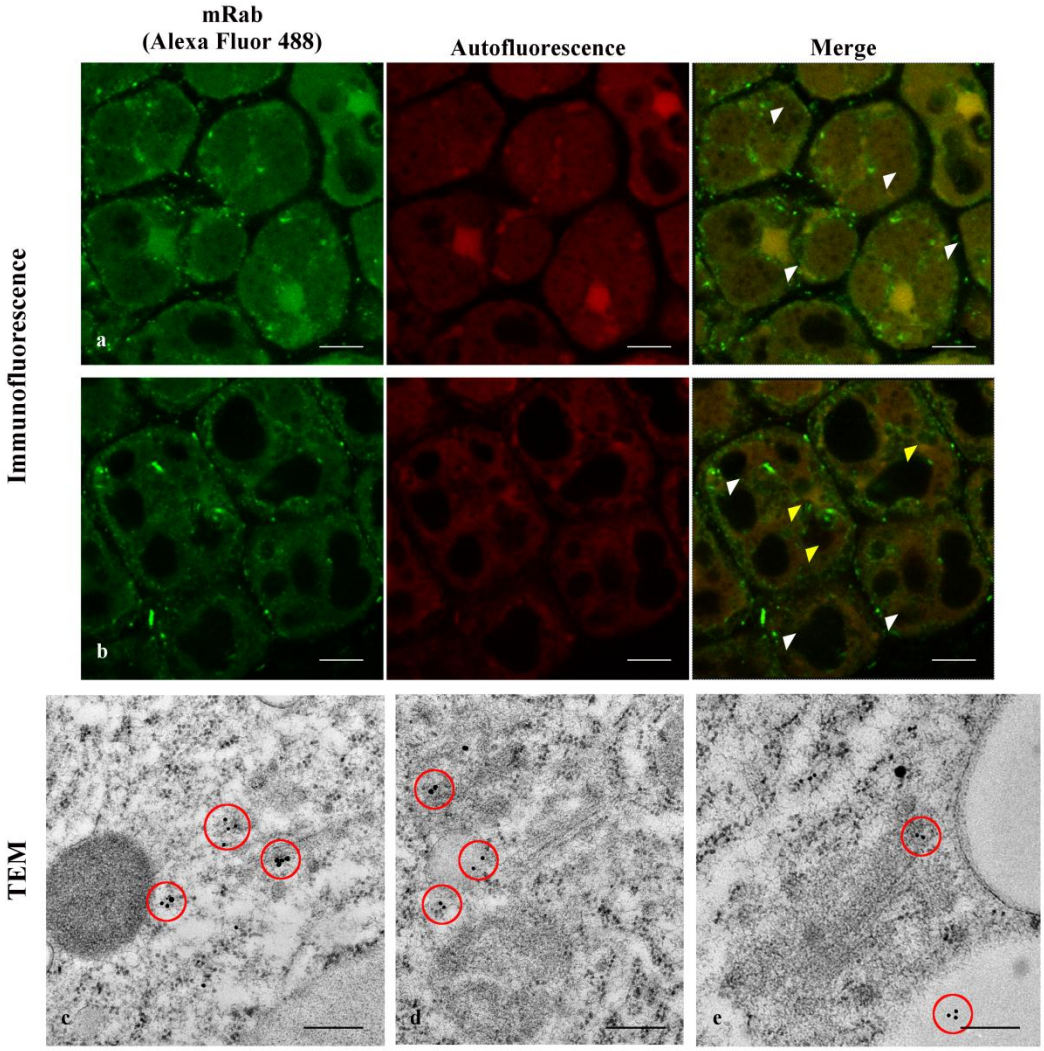

Figure 3.34 Immunolocalisation of mRab in radicle sections of *A. thaliana* expressing cardosin A. (a, b) Immunofluorescence of anti-mRab with Alexa fluor 488 ® secondary antibody. Labeling appears as dots in the cytoplasm (white arrowhead) and in association with membranous structures (yellow arrowheads). (c, d, e) Immunogold labeling of mRab coupled to a 10 nm gold-conjugated secondary antibody. Labeling was detected associated to the Golgi apparatus and with electron dense vesicle (red circles). Scale bars: a, b, 7 µm; c, d, 300 nm; e, 200 nm.

Immunogold labeling at the TEM level show that mRab was always found in association with the Golgi and in electron dense vesicles in its vicinity (Figure 3.34 c, d and e, red circles). mRab was also found in the periphery of some electron transparent vesicles (Figure 3.34 e, red circles), but with a more inconsistent pattern. This labeling is in accordance with immunofluorescence studies previously reported for mRab (Bolte et al. 2011).

m-Rab labeling has finally some characteristics similar to Cardosin A labeling, confirming that Cardosin A labels the PVC, and suggesting a halt in this compartment before final vacuolar targeting. However, double labeling of the two proteins is needed to clarify if they co-localise in these cells.

α-TIP is known as specific marker for vacuoles containing seed storage proteins – PSVs (Paris & Neuhaus 2002). Immunolocalisation of anti- α-TIP was detected associated with membranes and surrounding round-shaped compartments, assumed to be PSVs (Figure 3.35 a and b). At the TEM level the gold dots can be observed in the periphery of protein storage vacuoles (Figure 3.35 c, d and e), thus confirming its identity and confirming that the electron-dense structures where we detected cardosin A accumulation (compare with Figure 3.32) are indeed PSVs.

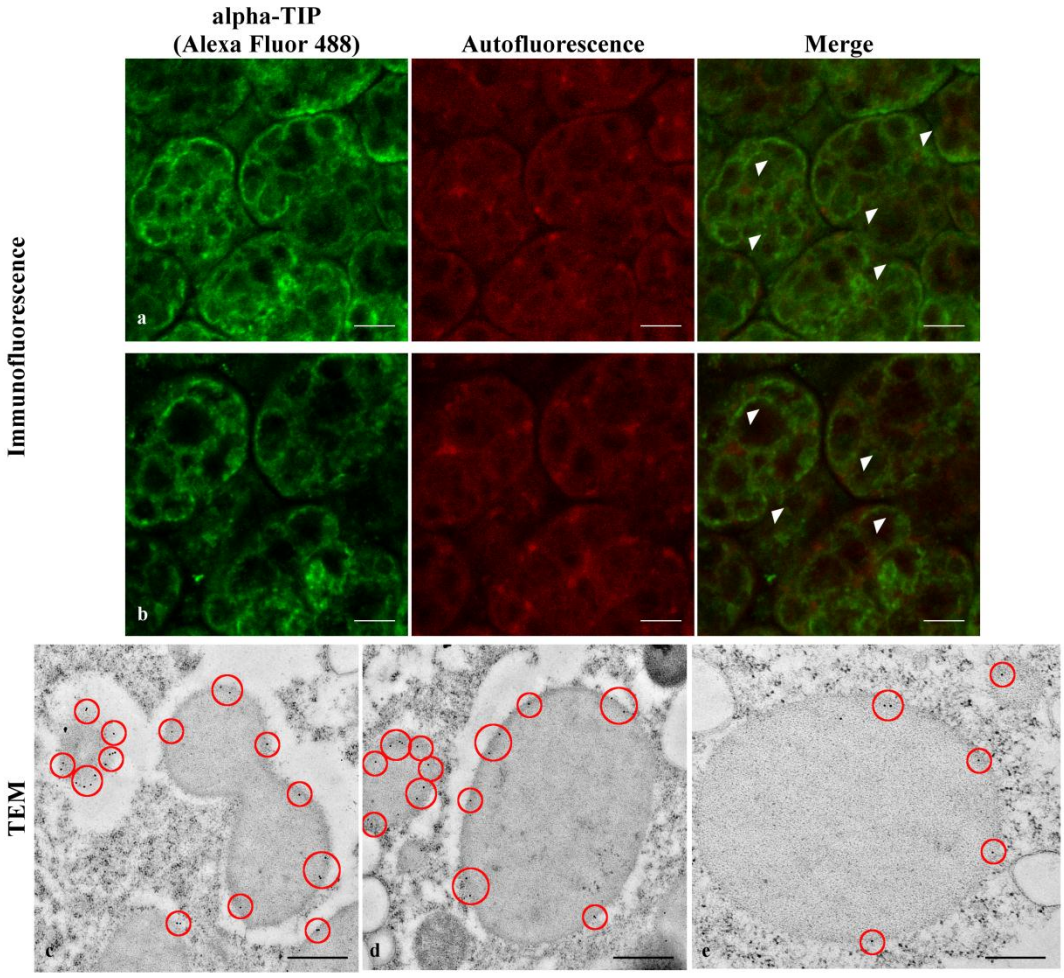

Figure 3.35 Immunolocalisation of α-TIP in radicle sections of *A. thaliana* expressing cardosin A under an inducible expression system. (a, b) Immunofluorescence of anti-α-TIP with Alexa fluor 488 ® secondary antibody. Labeling appears associated with membranes surrounding round-shaped compartments (white arrowheads). (c, d, e) Immunogold labeling of α-TIP was detected in the periphery of protein storage vacuoles (red circles). Scale bars: a, 9 µm; b, 7 µm; c, d, 500 nm; e, 200 nm.

To confirm this observation, a double immunogold labelling of cardosin A and α-TIP was performed to show the intracellular localisation of the two proteins at the same time. This technique allowed a nice picture illustrating cardosin A accumulation in PSVs in radicle cells of *A. thaliana*. Cardosin was detected inside PSVs (15 nm gold dots) while α-TIP (10 nm gold dots, red circles) was found decorating the membrane (Figure 3.36 a and b***). This confirms that Cardosin A labels Protein Storage Vacuoles***

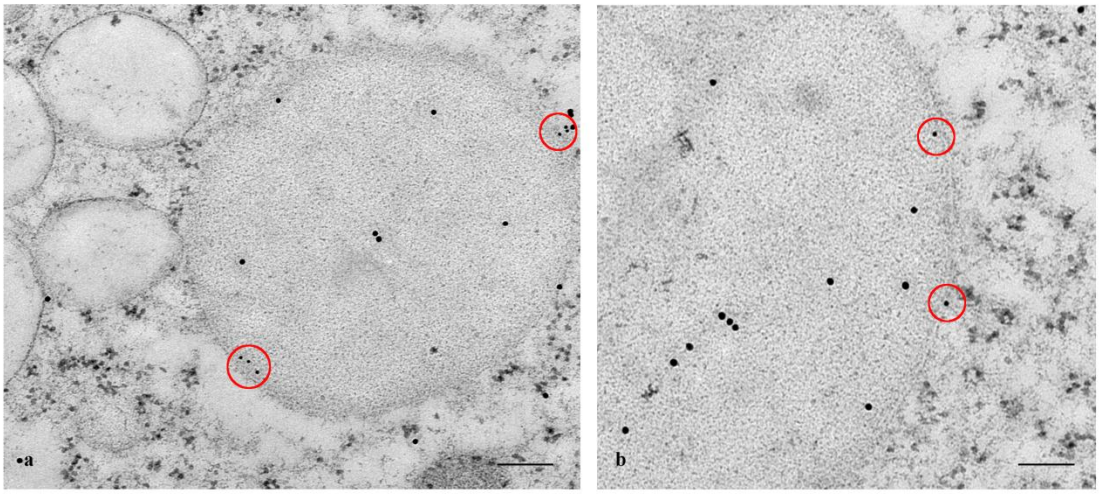

Figure 3.36 Double labeling of cardosin A and α-TIP in radicle sections of *A. thaliana* expressing cardosin A under an inducible expression system. Specific antibodies against cardosin A and α-TIP were used coupled to a 15 nm and 10 nm gold-conjugated secondary antibody, respectively. (a, b) cardosin A labeling was detected inside the protein storage vacuoles while α-TIP decorates the periphery of the same structures (red circles). Scale bars: a, 300 nm; b, 200 nm.

γ-TIP is a marker for the lytic vacuole, but in seed tissues (particularly during seed germination and maturation) it also labels the PSV (Jiang et al. 2001; Hunter et al. 2007). Labeling with anti- γ-TIP was also found decorating the membrane of PSVs in radicle cells (Figure 3.37 a and b, red circles) and also in the membrane of electron transparent vesicles in the cytoplasm (Figure 3.37 c, red circles). Cardosin A labeling was similar with the one obtained for this marker as it was also detected in the electron transparent vesicles (compare with Figure 3.32 e). Given the results obtained it is possible that this small vesicles may correspond to small lytic vacuoles newly formed that will eventually fuse to form a large central vacuole as described recently by Bolte et al. (2011).

δ-TIP is an aquaporine found in the tonoplast of PSVs in seeds and of LV in vegetative tissues (Hunter et al. 2007). Labeling of δ-TIP is more complex to understand

as the antibody seems to label everything in the cell but the interior of PSVs and the γ-TIP labelled vesicles (Figure 3.37 d, e and f). However, there is a clear association with the PSV and with the LV membrane as it was expected.

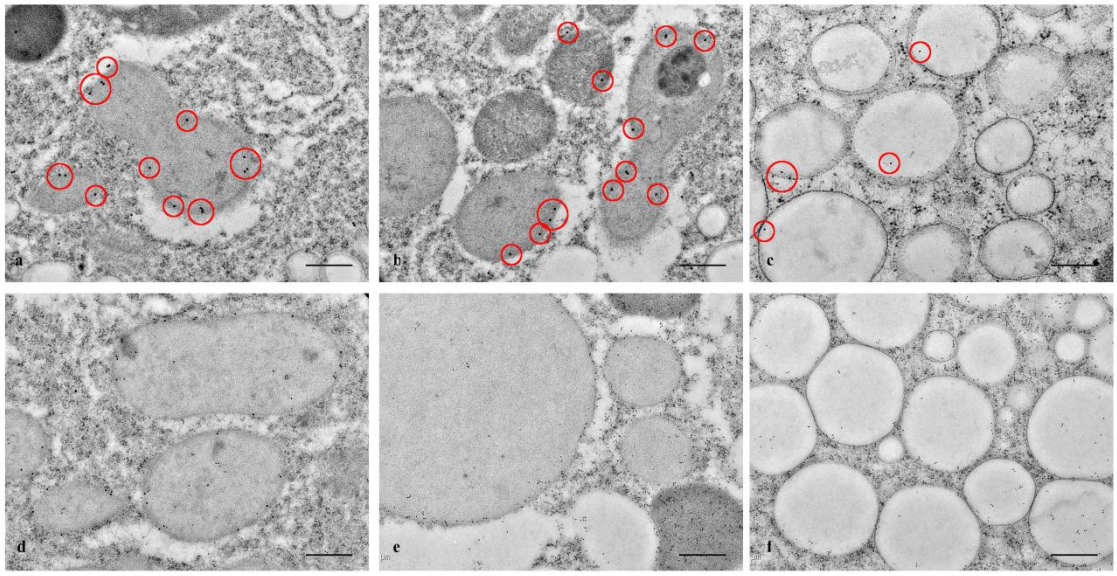

Figure 3.37 Immunolocalisation of γ- and δ-TIP in sections of *A. thaliana* expressing cardosin A under a inducible expression system. (a, b, c) γ-TIP labeling is detected surrounding PSVs and also in the periphery of some vesicles in the cytoplasm (red circles). (d, e and f) δ-TIP is detected in the membrane of PSVs, associated to small vesicles and in the cytoplasm. Scale bars: a, b, 200 nm; c, d, e, f, 400 nm.

As already said for mRab, a double localisation would be necessary to co-localise, or not, cardosin A with these compartments. However, and despite the efforts done to obtain a double labeling, it was not possible to achieve in the frame of this work, but are foreseen in the future. Nevertheless, the compartment identification allowed by these markers were helpful, as the picture obtained is characteristic of these typical markers.

The results obtained with the prevacuolar and vacuolar markers coupled to the results obtained for cardosin A localisation in germinating seeds are synthesized in Figure 3.38. The drawing represents the endomembrane system compartments were cardosin A was found to accumulate. The identity of those compartments was confirmed by the localisation of specific markers. Altogether, the results allowed to propose a working model for cardosin A biogenesis and trafficking, that needs to be further confirmed. It suggests that cardosin A, in this system, enters the secretory pathway in the ER, passes through the Golgi apparatus and goes to the PSV, and eventually to some small lytic vacuoles (Figure 3.38).

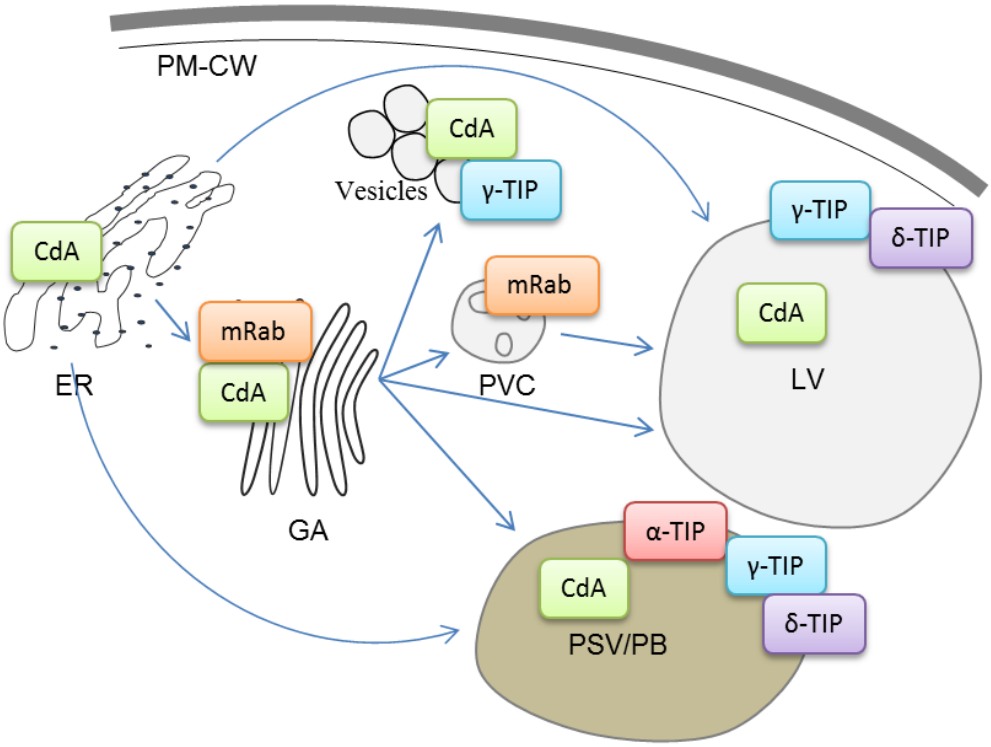

Figure 3.38 Model for cardosin A biogenesis and putative trafficking pathways in *A. thaliana* seedlings. Labeling of the several antibodies used in this study is represented in the scheme. CdA – cardosin A; ER - Endoplasmic reticulum; GA - Golgi apparatus; LV - Lytic vacuole; PB – Protein Body; PM/CW – Plasma membrane/Cell wall; PSV - Protein storage vacuole.

3.2.5. BFA experiments confirm that cardosin A uses the GA in its route to the PSV

The validation of the proposed model started by blocking protein trafficking between cellular compartments with Brefeldin A, to evaluate if cardosin A trafficking and/or localization was altered by this metabolite. The inducible line was used in this experiment because it is easy to control the moment of cardosin A expression with the addition of the chemical inducer. 3-day old seedlings were induced and 24h later, to allow initial expression of the protein, BFA (50 µg/mL) was added. Samples were collected at 0, 2, 4, 8 and 20h upon addition of the drug and were embedded in Epoxy and LR-White resins for TEM analysis.

The first step of BFA treatment was to evaluate the morphology of the cells to check the effect of the drug in this system in Epoxy embedded sections.

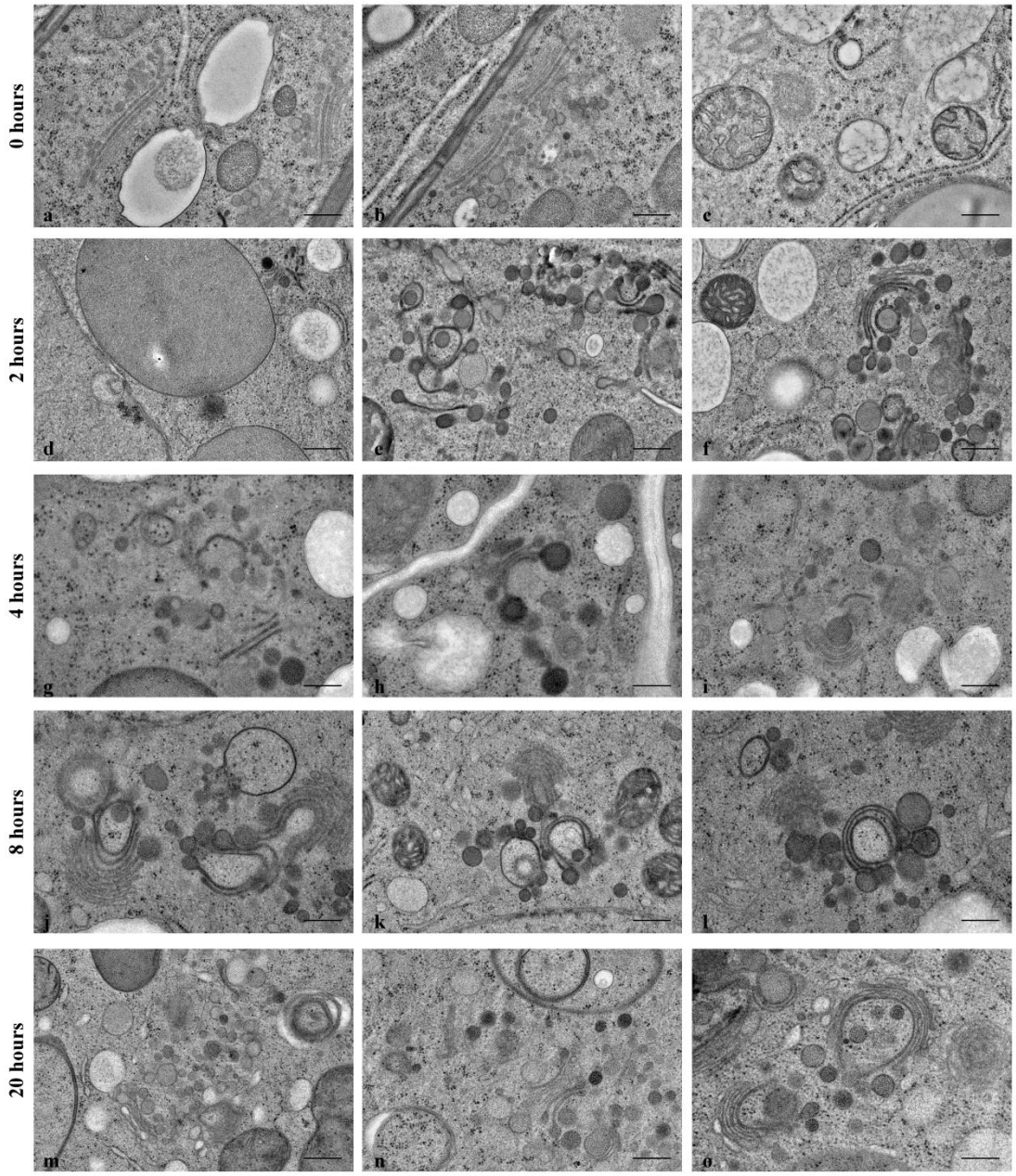

Figure 3.39 Brefeldin A effect on *A. thaliana* radicle cells expressing cardosin A. Micrographs of cell ultrastructure obtained from four days old seedlings after cryofixation. Epoxy resin sections of dexamethasone induced radicles evidencing the general organization of the cell. (a, b, c) 0h treatment; (d, e, f) 2h treatment; (g, h, i) 4h treatment; (j, k, l) 8h treatment; (m, n, o) 20h treatment. Scale bars: 400 nm.

In the control sections - 0h BFA treatment - the GA presents its normal shape as well as the other cellular organelles, such as mitochondria, small vacuoles and ER (Figure 3.39 a, b and c). Sections obtained from samples with two hours of BFA treatment are already different from control ones (Figure 3.39 d, e and f). The GA stacks are disorganized and acquire a semi-circular shape in some cases. The other cellular organelles, however, do not seem to be affected by the drug. In the subsequent time-points the picture is similar with the GA stacks becoming more disorganized (Figure 3.39

g, h and i) and acquiring a round shape figure (Figure 3.39 j, k, l and o). The GA-associated vesicles become larger and denser with time and several membranous structures appear in the cytoplasm (Figure 3.39 j, m and n). As conclusion, the BFA effect is visible two hours after the beginning of the treatment, but its effects become harsh with time. However, at the BFA concentration used, it seems not to affect other organelles in the cell other than the GA.

Immunolocalisation of cardosin A in BFA treated tissues was performed in the same time-points as for the ultrastructural studies to check the BFA effect. In the beginning of the study, corresponding to the control (0h upon BFA addition) cardosin A labeling was found in the cytoplasm associated with the GA (Figure 3.40 a and d, red circles) and with the ER (Figure 3.40 c, red circles), as previously described. Some few gold dots were also detected inside PSVs (Figure 3.40 b, red circles), indicating that in this system cardosin A trafficking to the vacuole is fast, since the production of cardosin A started just 24h before.

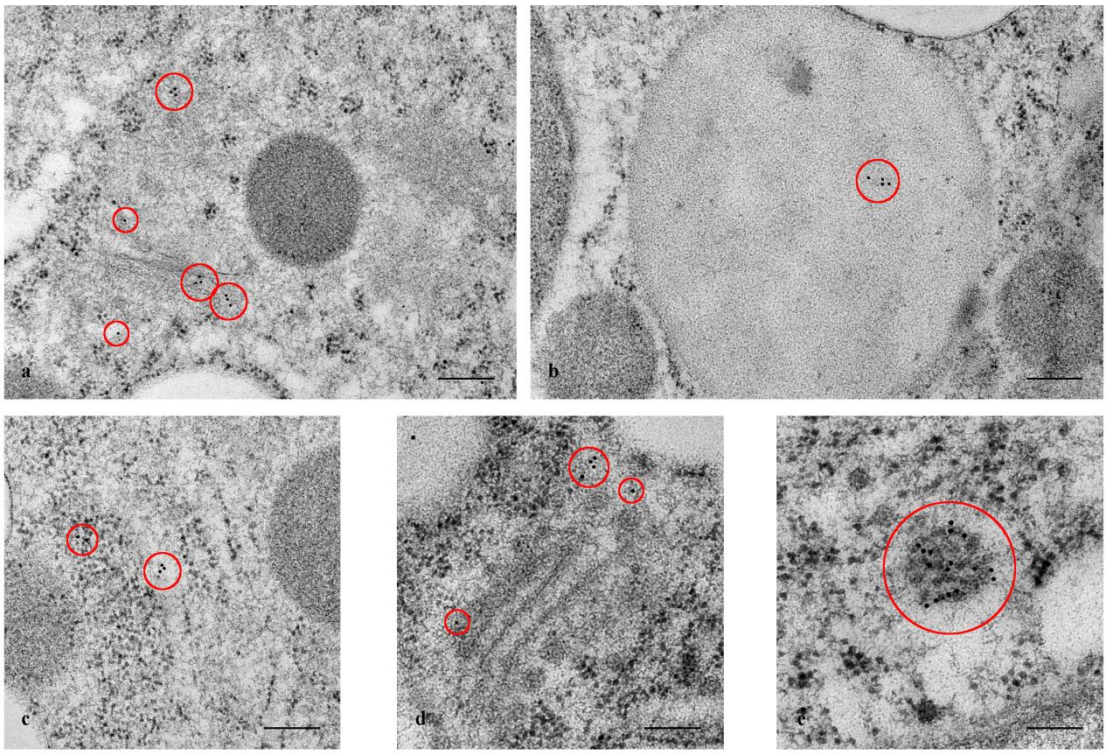

Figure 3.40 Immunogold labeling of cardosin A in radicle sections of *A. thaliana* inducible expression system 0h upon addition of BFA. Labeling was detected in association with the Golgi apparatus (a, d) and also in the protein storage vacuole (b). Some gold dots were observed in the ER (c) and in the prevacuolar compartment (e). Red circles mark the gold labeling of cardosin A. Scale bars: a, b, c, 200 nm; d, e, 100 nm.

Cardosin A was also found in great amounts associated to a membranous structure in the cytoplasm resembling the PVC (Figure 3.40 e, big red circle). These results are coherent with the ones obtained before for cardosin A (compare with Figure 3.32) in radicle sections, without the drug.

The effects of BFA treatment is seen along the treatment by the morphological alterations in the GA stacks, as already documented in the ultrastructural studies. Cardosin A localisation does not change during the time-points studied: 2h (Figure 3.41 a, b and c), 4h (Figure 3.41 d, e and f), 8h (Figure 3.41 g, h and i) and 20h (Figure 3.41 j, k and l). Cardosin A is always found in association with the GA or with the dense vesicles associated to it (Figure 3.41 a, c and f) even when the stacks have lost their regular shape (Figure 3.41 h, i, k and l). Cardosin A accumulation in PSVs is also constant along the study (Figure 3.41 b, d, e, g and j, red circles) and more gold dots in each PSV are visible when comparing with the control. ***This indicates that cardosin A may be still accumulating in the PSV, despite the BFA blockage. Nevertheless, cardosin A accumulation in the GA apparatus indicates a route passing through this compartment in emerging radicles. These two different pathways could be related to the ones described for cardosin A in tobacco leaf epidermis as discussed in chapter two.***

As a whole, the BFA experiment allowed to confirm cardosin A localisation along the secretory pathway. Its localisation in the GA even after several hours of BFA treatment is particularly important; since it was suggested cardosin A route to the vacuole bypassing the Golgi (proposed in chapter 2) could be specific of seed tissues, which is not the case considering the set of data presented. However, the apparent increase of cardosin A labelling in PSVs after the drug treatment is also indicative that at least some protein can escape the BFA blockage mechanism. Further studies involving other blockage mechanisms should be employed to clarify this aspect.

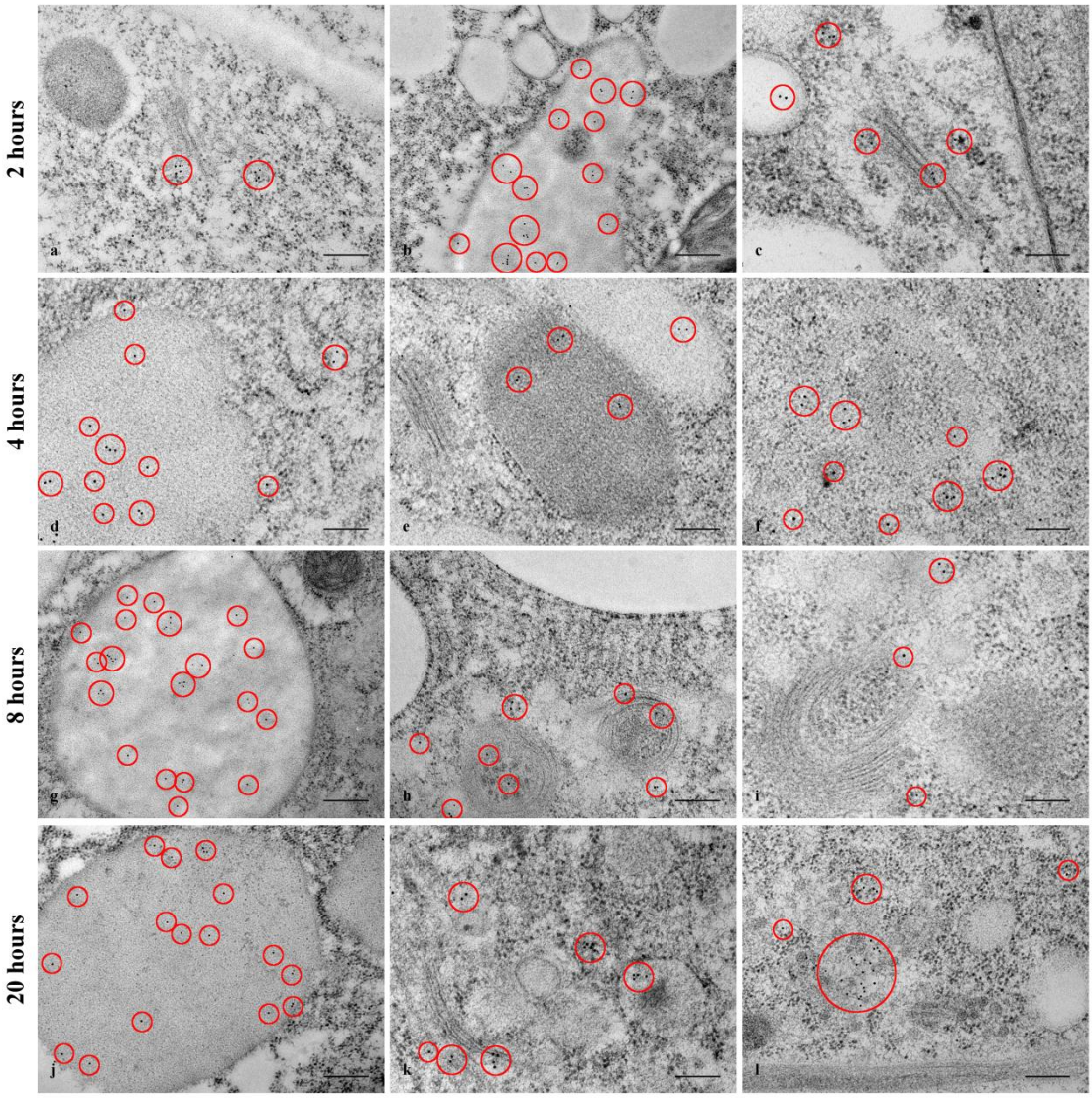

Figure 3.41 Immunogold labeling of cardosin A in radicle sections of *A. thaliana* inducible expression system 2, 4, 8 and 20h upon addition of BFA. Labeling was detected in association with the Golgi apparatus (a, d) in the protein storage vacuole (b) and also in the periphery of electron transparent vesicles in the cytosol (c). Red circles mark the gold labeling of cardosin A. Scale bars: a, b, c, 200 nm; d, 100 nm.

3.3. OUTCOMES

It has been shown that cardosin A accumulates in the PSV of transgenic *A. thaliana* seedlings under an inducible expression system. However, cardosin A was also found in other endomembrane compartments as the ER, GA or electron transparent vesicles found in the cytoplasm. Furthermore, labeling of post-GA compartments allowed to verify the identity of cardosin A accumulating structures and BFA treatment showed an accumulation of cardosin A in GA.

Cardosin A accumulates along the secretory system and in the PSV of A. thaliana transgenic seedlings: In non-germinated seeds cardosin A is found in small vesicles in the cytoplasm that are γ-TIP and VPPase labeled. Since the labeling is identical with anti-PSI antibody it is possible to say that we are detecting the precursor form of the protein, since in the mature protein the PSI is not present. In the seedling stage, cardosin A mature form is detected in the PSV, but using anti-PSI the labeling is still detected in vesicles in the cytoplasm. Probably, more than one form of the protein is present at the same time, but in different compartments within the cell. A longer induction time with dexamethasone may be needed to obtain a full understanding of cardosin A trafficking in this system, since cardosin A processing is a very slow process.

BFA treatment causes cardosin A accumulation in the GA but also in the PSV: The results obtained in this study shows that some protein has already reached the PSV in the beginning of the assay (time = 0 hours), despite the majority was still in intermediate compartments of the secretory system. Along the essay cardosin A was always found in association with the GA, even when the BFA causes the disruption of GA vesicles, indicating that cardosin A passes through the GA in this system. We can consider that part of the protein bypasses this organelle. We did not attempt to quantify cardosin A expression by TEM, but by looking at several micrographs (not only the ones presented in this document) it seems that the amount of gold dots increases with time. Despite no clear conclusion can be made, it is worth to explore if there is any GA-independent pathway for cardosin A in this system.

4. DISCUSSION

The main objectives of this work were:

- to validate the use of an heterologous system to study cardosin A trafficking mechanisms,
- to identify Vacuolar Sorting Determinants in cardosin A,
- to question the mechanisms involved in cardosin A trafficking along plant developmental stages.

The experimental strategy developed has permitted to reach these objectives, as we succeeded to:

- design two heterologous systems adequate for cardosin A expression
- detect a complex mechanism of cardosin A transport to the vacuole, as it may take two independent pathways guided by two vacuolar sorting determinants.
- Show that cardosin accumulates in lytic vacuoles and/or protein storage vacuoles, depending on the type of tissue/cell were it is expressed in.

Discussion around these data sets will show that cardosin A as a suitable model as protein reporter to study vacuolar pathways, and may contribute to the knowledge of transport mechanisms of plant aspartic proteinases, in relation to the state-of-the-art knowledge on membrane trafficking, as discussed below.

4.1. EXPRESSION OF CARDOSIN A IN *ARABIDOPSIS* HIGHLIGHTS CONSERVED EVENTS IN CARDOSIN A VACUOLAR TARGETING AND PROCESSING MECHANISMS IN PLANT TISSUES

4.1.1. Expression and localisation of Cardosin A in heterologous systems

Protein expression in heterologous systems may be delicate to handle and source of pitfalls (Denecke et al. 2012). In this study, transient expression in *Nicotiana tabacum* and stable expression in Arabidopsis plants have been validated as a suitable expression system to express cardosins, based on a proper maturation of cardosin and its final accumulation in the vacuole. Our results were complementary of the biochemical data previously obtained in *Nicotiana tabacum* and *Arabidopsis thaliana* expression systems (Duarte et al. 2008).

Interestingly, the fact that BY2 was not a good system to reveal the vacuolar pathway of Cardosin A may highlight the need for a conserved molecular mechanism in plant tissues which has been lost in the dedifferentiation stage attained in isolated BY2 cells. Such “lost” of specific trafficking pathways had been observed for instance in BY-2 cells lines expressing PIN proteins, where specific endocytic events during mitosis were not observed (Boutté et al. 2006). On the other hand, BY2 cell lines have been successfully used for expression of vacuolar protein such as aleurain (Bolte et al., unpublished data), showing that vacuolar targeted pathway may be mimicked in BY2 cells. Then the failure to target cardosin A to the vacuole in BY2 cells may be due to the loss of information due to the loss of tissue organisation.

Our data do not permit to assume any functionality of these aspartic proteinases in these host cells.

4.1.2. Targeting and Processing of Cardosin A in heterologous systems

To validate our experimental models and study the molecular mechanisms involved in cardosin A vacuolar targeting, three aspects may be considered, which are not necessary related, the targeting of cardosin A, the processing of cardosin A, the right localisation of Cardosin A in the host cell:

a) The targeting process

As in native plants (Ramalho-Santos et al. 1998), Cardosin A was found to accumulate in different types of vacuoles according the tissue type : lytic vacuoles in epidermal leaves, and protein storage vacuoles in *Arabidopsis thaliana* seedlings. In cardoon seeds, from the initial germination steps until later developmental steps, cardosin A is found to accumulate in protein bodies (PBs), and in small lytic vacuoles, as described in this work. Furthermore, in cardoon flowers, cardosin A is also accumulating in PSVs in the stigmatic papillae (Ramalho-Santos et al. 1997; Duarte et al. 2006).

The fact that Cardosin A accumulates in different types of vacuoles confirms that our expression systems are proper experimental set ups where Cardosin A may be used as a protein model to decipher vacuolar trafficking. Furthermore, our work provides a good set of molecular tools available for the scientific community (antibodies, endomembrane markers and mutants).

b) The processing event

Our data confirm that, as in the native system (Ramalho-Santos et al. 1998), cardosin A is processed along a vacuolar pathway: there is an initial accumulation of an intermediate form, which disappears with time and is replaced by the mature form. Tthe last processing step of cardosin A, i.e. the removal of the prosegment, occurs in the vacuole, probably due to its acid environment. Immunocytochemical studies using antibodies against both PSI domains and the whole proteins confirmed the biochemical data showing that the PSI processing must occur after cardosin A passing through ɣ-TIP labeled compartments. Since there is no co-localisation with these two antibodies it is possible to say that we are facing more than one form of the protein and the one accumulating in PSVs is already processed to its mature form.

c) Integration in the host cell machinery

Plant AP need to be cleaved several times in order to go from precursor form to mature form (Simões & Faro 2004). Our results confirmed this initial hypothesis as point-mutations disrupting the catalytic sites causes an accumulation of the precursor form of the enzyme. Maturation of plant APs may be however be achieved by three different mechanisms: totally assisted by other proteases, totally self-processing or self-processing partially assisted. It has been proposed that the processing of cardosin A is a process of self-processing partially assisted by other aspartic or cysteine proteinases (Simões & Faro 2004). In our heterologous systems, Cardosin A processing should then occur partially due to this auto-catalytic mechanism. It could have been expected that the inactivation of the enzyme would reduce the self-processing capacity of cardosin A. However, the mature form was still fully achieved, suggesting that the process of protein maturation was rescued by other proteases present in the host cell, most probably cysteine proteinases.

Nevertheless, the inactivation of cardosin A does not prevent the protein to accumulate in the vacuole. The alteration of a polar and negatively charged aminoacid as is the aspartic acid, by alanine, a non-polar and neutral one, could have severe implications in protein folding and therefore cause its retention by the quality control points along the secretory pathway. That was not observed as the protein was accumulating in the vacuole but the question if the mutated versions travel the same way as the native cardosin A is not answered. Further work should involve the co-expression of these mutants with mutants or drugs impairing the trafficking between cell compartments, in a similar approach to the one developed in this study for cardosin A vacuolar sorting determinants.

Together with the results already available for cardosin A and cardosin B (Duarte et al. 2008; da Costa et al. 2010), and our results, *N. tabacum* and *A. thaliana* are validated as suitable models for cardosins study. The fact that cardosin A accumulates in different type of vacuoles in each system is also interesting as it offers the possibility to study these routes independently. Furthermore, the two systems have very different characteristics allowing different approaches that will allow an integrative view of cardosin A expression and trafficking routes in plant cells.

4.2. TWO VACUOLAR SORTING DETERMINANTS FOR A "POLY-SORTING" MECHANISM?

Our results demonstrate that vacuolar sorting of cardosin A relies on a typical C-terminal VSD or an unconventional PSI signal. This opens several lines of discussion.

4.2.1. FAEA, a new C-ter VSD common to aspartic proteinases

The C-terminal peptide VGFAEAA carried by cardosin A shows similarity to the C-terminal peptide of barley lectin (VFAEAIA), which is responsible for targeting of the lectin to the lytic vacuole (Bednarek and Raikhel, 1991), and was expected to play the role of a VSD. Our results have effectively shown that it acts as a sufficient vacuolar sorting determinant, being more efficient in transporting the protein to the vacuole when placed in the C-terminus of the fusion protein, rather than at the N-terminus. Furthermore, we have also shown that the short peptide FAEA is sufficient to target the protein to the vacuole and is part of a conserved motif present at the C-terminal end common to several APs. From these observations, it can be conclude that cardosin A C-terminal sequence definitely falls into the ctVSD category (Neuhaus et al. 1991; Frigerio et al. 1998; Zouhar & Rojo, 2009).

4.2.2. Questions around PSI domain as VSDs

Beginning this study, the role of PSI domains in AP vacuolar targeting was not clear cut, complicated by the fact that PSI domain is not common among the aspartic proteinases and the functional mechanism involved in its recognition remains unclear.

In our study, as long as the typical C-terminal VSD is carried by the protein, PSI domain is not necessary for the protein to reach the plant vacuole. However, in absence of C-ter VSDs, the PSI domain acts as a VSD, being sufficient for correct vacuolar targeting of aspartic proteinases. Does PSI represent a new class of VSD? Is it always acting as a vacuolar sorting determinant? What are the mechanisms involved in its recognition as VSDs?

a) Cardosin A PSI domain describes a new class of VSD.

The classification of the PSI domain into the main three types of VSDs usually described is indeed quite difficult: it is obviously not a C-ter VSD; even when positioned at the C-terminus of a secretory protein, it caused the protein to be retained in the ER (Törmäkangas et al. 2001). It cannot be considered as a ssVSD in the strict sense of the word as the PSI amino acid sequence is not conserved; the psVSD definition does not apply either, as only a single region of the protein is involved (Jolliffe et al. 2003; Zouhar & Rojo, 2009).

Therefore PSI domain of cardosin A would define a new class of Vacuolar Sorting determinant. Comparison with other PSIs domain would help to define its structural characteristics.

b) PSI domains do not act as VSD in all AP

Some but not all PSI domains of other aspartic proteinases have been shown to play an essential role in vacuolar sorting.

Terauchi and co-workers (2005) have shown that the removal of the PSI region of two soybean vacuolar APs changed the vacuolar accumulation of only one AP. They have therefore proposed that the PSI may be the vacuolar signal for only a small number of APs. They also showed (Terauchi et al. 2006) that removal of the PSI signals altered the APs targeting to the lytic vacuole, but not to the APs trafficking to the protein storage vacuole. PSI may, therefore, act as vacuolar signal only in specific conditions or developmental stages. They also suggested that its action was dependent either on the type of vacuole that they were directed to, or on the type of cells where they were expressed in.

Tormakangas and co-workers (2001) showed that phytepsin's PSI has a role in the vacuolar targeting of this proteinase, since the removal of PSI domain led to the secretion of phytepsin into the culture medium of tobacco protoplasts and to the extracellular space of transgenic tobacco leaves.

Data do not permit so far to determine the features needed for a PSI domain to act or not as VSDs. Searching for the existence of a PSI receptor could be a clue to this question. Comparison of the sequence of AP PSI domains shows that they actually have strong differences in their sequence. The presence or the absence of a glycosylation site is probably a major difference to be taken into account to understand PSI interactions within the cells, as discussed further down. Still, from our results and published data of other laboratories, it is clear that the PSI has a putative role in APs vacuolar targeting that can be dependent on the specific function of each proteinase, on the tissue or cell where it is expressed and can even depend on the developmental stage. The next question is "How may it work?"

4.2.3. *Hypothesis of a cooperative model for two Cardosin A VSD*

The fact that a protein carries two types of VSDs questions the need for a synergy between the two or their ability to act independently (Figure 4.1). Synergy between the two VSDs may cover different mechanisms:

1. A total complementarity is needed as shown for other proteins, two VSDs regions could be part of a larger vacuolar signal, such as a psVSD (Figure 4.1 a), composed of several motifs distributed along the protein sequence, which are only functional in the mature, correctly folded polypeptide (Jolliffe et al. 2003). This type of synergy is probably not true for our Cardosin A protein, as both regions – the PSI and C-terminal region – are able to target cardosin A to the vacuole independently.

2. Alternatively, synergy may also cover an efficient collaboration, reinforcing the efficiency of the targeting compare with the use of only one VSD. That could be the case for Cardosin A. It is known that the PSI interacts with membranes (Egas et al. 2000) and this could be a prerequisite for the C-terminal domain to be

recognized by a specific receptor (Figure 4.1 b). Therefore the PSI and the C-terminus of cardosin A could act cooperatively.

3. A third hypothesis would be a redundancy between the two signals (Figure 4.1 c). Each signal has therefore to be considered as true distinct vacuolar sorting determinant for cardosin A. It is possible that the vacuolar sorting may benefit from a cumulative effects of the sorting signals, as suggested for other proteins (Holkeri & Vitale, 2001; Nishizawa et al. 2006).

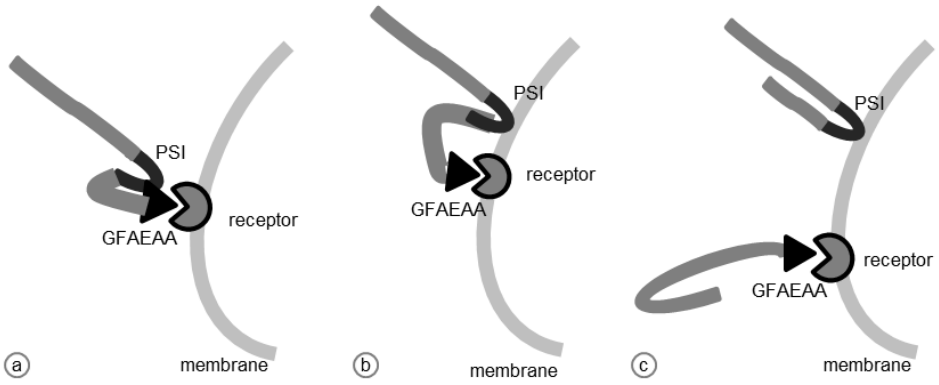

Figure 4.1 Schematic representation of the possible mechanisms for cardosin A transport to the vacuole depending on the PSI and C-terminal domains. (a) synergistic model involving the interaction between the two domains; (b) synergistic model where the recognition of the C-terminal would require the PSI to interact with the membrane; (c) Both domains acting independently in sorting the protein to the vacuole.

In this later case, they would act independently, being involved in two different signalling recognition processes specific for one tissue or for one developmental stage. The presence of such two VSDs on one protein would then ensure a “poly-sorting” ability, give to the AP multifunctions according their final targeting, and will finally permit modulating the vacuolar transport according the cell constraints or need through a specific PSI signalling pathway, which may cohabit with another vacuolar pathway.

Our results favour this later hypothesis as discussed below.

4.3. A SPECIFIC PSI VACUOLAR PATHWAY FOR CARDOSIN A

4.3.1. PSI domain of Cardosin A mediates a COPII independent pathway

Previous work claimed that cardosins use a COPII dependent pathway from the ER to the Golgi (Duarte et al. 2008; da Costa et al. 2010) before reaching post-Golgi compartments and Vacuoles. At first, our assays using Brefeldin A to block the COP II pathway were in accordance with this claim, as both PSI driven or C-ter driven vacuolar trafficking was blocked by the drug. However, the use of dominant negative forms of proteins involved in the COPII dependent pathway was in contradiction with these BFA results, and suggested a more complex regulation for the transport of cardosin A to the vacuoles.

The vacuolar pathway mediated by the C-terminal peptide was effectively blocked by the expression of dominant negative forms of proteins involved in the ER-Golgi-Vacuolar pathway (i.e. RabD2a, Sar1 H74L and RabF2b). An assay using Wortmannin to block the trafficking confirmed that the constructs bearing the C-terminal signal use a route mediated by the GA and PVC to the vacuole.

Contrastingly, the vacuolar pathway driven by PSI domain was not impaired by any of the expression of the dominant negative mutated proteins. This clearly suggests that the C-terminal drives the cardosin A to the lytic vacuole via a COPII mediated ER-Golgi-PVC pathway, while the PSI-mediated targeting may bypass the Golgi.

4.3.2. The glycosylation events may influence the sorting mediated by AP PSI domains.

Our hypothesis of a PSI-mediated COPII independent pathway may appear at first sight contradictory with the ones obtained for cardosin B (da Costa et al. 2010) and phytepsin (Törmäkangas et al. 2001), where the PSI domain was essential to enter a COPII pathway. This apparent discrepancy may be related to differences in the composition of the PSI domains, as cardosin B and phytepsin has a conserved glycosylation site in the PSI domain, which is absent from cardosin A. The presence or the absence of a glycosylation site on the PSI domain can therefore be a key structure in determining the route to be taken by the PSI-driven targeting, an hypothesis which needs further investigation.

It has been long discussed the role of the glycosylation in the vacuolar routes taken by proteins in the secretory pathway, in particular involving GA bypass or not (Rayon et al. 1998; Paris et al. 2010). Cardosin A is a glycosylated enzyme with two putative sites that differs from the majority of plant APs by the inexistence of a glycosylation site in the PSI domain (Frazão et al. 1999). To assess the importance of glycosylation in cardosin A vacuolar accumulation and trafficking we obtained mutated version with disruption of the glycosylation sites and the addition of a glycosylated site in the PSI. Taken together the results obtained for the mutated version alone and after treatment with Tunicamycin, we can conclude that glycosylation does not affect the vacuolar accumulation of cardosin A. However, it does seem to interfere with the route taken by the protein to the vacuole as the mutant with an extra glycosylation site in the PSI gets retained by Tunicamycin while the construct SP-PSI-mCherry (with no glycosylation) still accumulates in the vacuole.

Studies on the AP phytepsin (Törmäkangas et al. 2001) revealed that this AP transport is COPII mediated, and that PSI domain was essential for phytepsin transport through the Golgi. As for the most common APs (including cardosin B), phytepsin has a conserved glycosylation site in the PSI domain. We have shown that replacing the PSI domain of cardosin A (with has no glycosylation site) with the PSI domain of cardosin B (which has a glycosylated site) changes the PSI mechanisms of vacuolar sorting as it shifted from COPII independent transport pathway to COPII dependent transport pathway, as the AP phytepsin. The presence or the absence of a glycosylation site on the PSI domain therefore appears as a key structure in determining the route to be taken by the PSI-driven targeting. Further studies are already undertaken to isolate the cardosin A glycosylated PSI in order to test in more detail the trafficking of the protein. It would also be interesting to produce cardosin B PSI without the glycosylation site to evaluate if the route driven by this sorting domain would be the same.

4.3.3. PSI domain may act for VSD for Cardosin B in N. tabacum

It has already been remarked along this work that cardosin A and cardosin B (the most characterized APs from cardoon) share high homology in terms of nucleotide and aminoacid sequence, yet they have different fates in cardoon flowers: A is vacuolar and B is secreted. From several years the question about cardosins has been “why is cardosin B secreted?” and efforts have been made in order to obtain a clear answer. Expression of cardosins in heterologous systems may provide some hypotheses.

Surprisingly, when expressed in *Nicotiana tabacum* leaves cardosin B was not secreted but accumulated in the large central vacuole similarly to cardosin A (da Costa et al. 2010), provoking more questions : why and how cardosin B becomes vacuolar in this heterologous system? Although more studies are obviously needed to clarify this aspect, it is tempting to propose that the secretion of Cardosin B is bound to specific stages of plant development, which are not fulfilled in Nicotiana leaves, and in that case the Cardosin B PSI domain has a preponderant role in defining the APs' route to the vacuole, through a Golgi-PVC pathway due to its glycosylation site.

When using the Arabidopsis heterologous system, localization of cardosin A and cardosin B are however different: our light and electron microscopy results show that cardosin A accumulates in PSVs in the early germination steps of transgenic *A. thaliana*. In a parallel study on *A. thaliana* expressing cardosin B under the same expression system and in the same developmental stages with the same microscopy approaches, cardosin B was located in the cell wall, not being detected in the PSVs in any time-point (unpublished results). This observation reminds of the results obtained by da Costa et al. (2010) on protoplasts issued from Nicotiana leaves where the cardosin B was finally secreted as well, leading the authors propose a role for the cell wall in regulating intracellular sorting (da Costa et al. 2010).

In all cases, A. *thaliana* seems to be potentially interesting as heterologous system to explore the dual target of cardosin A and cardosin B.

Furthermore, an important organ where cardosins expression and targeting should be explored is the flower, as in cardoon is where the variance in accumulation place is more relevant. Further studies on cardosins characterization in *Arabidopsis thaliana* should involve the use of native promoters which would allow a better understanding on their distribution along the plant and probably would maximize the expression levels in certain organs. It is known that despite the CaMV 35S being a constitutive promoter it is not expressed in certain tissues.

4.3.4. Variability in the structure of PSI domain corresponds to distinct roles for PSI as Vacuolar sorting determinant

These data on PSI domains showing that cardosin A PSI is a vacuolar sorting determinant, that it co-exists with another VSDs but may also act on its own provides exciting possibilities to solve previous contradictions on the role of the PSI as vacuolar sorting determinant (Faro et al. 1999; Kervinen et al. 1999; Brodelius et al. 2005). The structure and function of the PSI domain may indeed be a clue in understanding the complexity of APs targeting in plant cells, and specially cardosin A. The dual localisation of cardosin A in protein bodies in cardoon cotyledon cells, and in protein storage vacuoles in flower cells (Pereira et al. 2008), could be related to the existence of a PSI-specific pathway, dependent on the type of tissue, which yet have to be identified.

4.4. BFA TREATMENT CAUSES CARDOSIN A ACCUMULATION IN THE GA BUT ALSO IN THE PSV IN *A. THALIANA* SEEDLINGS

It has been discussed that cardosin A could bypass the GA in its route to the PSV and that this bypass could be PSI-dependent. However, up to date, there is no clear evidence of such pathway, particularly, because the majority of studies undertaken have been conducted in leaves (either in *A. thaliana* or *N. tabacum*), which only have a large lytic vacuole and no PSVs (Duarte et al. 2008; da Costa et al. 2010). Several APs have been detected and isolated from seeds (for review see Mutlu & Gal 1999; Simões & Faro 2004) and are well characterized in terms of processing and proteolytic activity, but very few data is available on their intracellular sorting and routes. Up to date, phytepsin is the only AP on which has been made an attempt to clarify this aspect. Using pulse-chase, endo-glycosidase H and inhibitors, Glathe et al. (1998) showed that phytepsin processing events occur along the secretory pathway to the PSV, passing through the GA and some post-GA compartments, not identified by the authors at the time. In this study we started to uncover cardosin A trafficking to PSVs in Arabidopsis seedlings using BFA to block the trafficking between the ER and GA. We used an *A. thaliana* line only expressing cardosin A upon the addition of an external agent to induce gene expression so it is possible to control the moment the protein starts to be produced. We gave a 24 h interval between the addition of the chemical inductor and the BFA because BFA is known to block germination (Geldner & Palme 2001) and cardosin A processing

and, consequently, trafficking between compartments is a slow process. Nevertheless the results provide some hints on cardosin A trafficking in germinating seeds. Along the essay cardosin A is always found in association with the GA, even when the BFA causes the disruption of GA vesicles, meaning that cardosin A passes through the GA in this system. This is consistent with the data presented by Duarte et al. (2008) that showed that cardosin A was partially endo-glycosidase H resistant in *A. thaliana* seedlings.

4.5. A WORKING MODEL FOR CARDOSIN A SORTING

Gathering the data proposed for AP trafficking mechanisms to the vacuole with the data presented in this work, a working model may be proposed (Figure 4.2). In cardoon seeds cardosin A is transported to the protein bodies (vacuoles specialized in protein storage) directly from the ER (Figure 4.2, arrow 1), where it accumulates in its precursor form (Pereira et al. 2008). In this work it has been shown that the route cardosin A takes to reach the PSV involves a passage through the GA (Figure 4.2, arrow 2). However, it is not clear if cardosin A uses the PVC compartment in its route or if it is transported in dense vesicles to the vacuole. Moreover, it is not known if cardosin A sorting in this route is mediated by the PSI or the C-terminal domains, despite in the first case (GA bypass in cardoon seeds) evidences point to an involvement of the PSI domain in cardosin A transport (Pereira et al. 2008). Furthermore, we have shown a C-terminal mediated sorting that would correspond to a COPII dependent ER-to-GA pathway to the vacuole, and may be favored according tissues and developmental stages (Figure 4.2 arrow 3). A glycosylated PSI-mediated targeting dependent on COPII vesicles (Figure 4.2 arrow 4) has already been described for phytepsin (Törmäkangas et al. 2001), and may concern other PSIs-containing AP such as cardosin B. However, a second vacuolar route mediated by non-glycosylated PSI-domains, COPII independent (Figure 4.2 arrow 5) has to be considered. A sixth route (Figure 4.2 arrow 6), in which cardosin A goes to the periphery of the cell, before reaching the vacuole has already been proposed (Duarte et al. 2008).

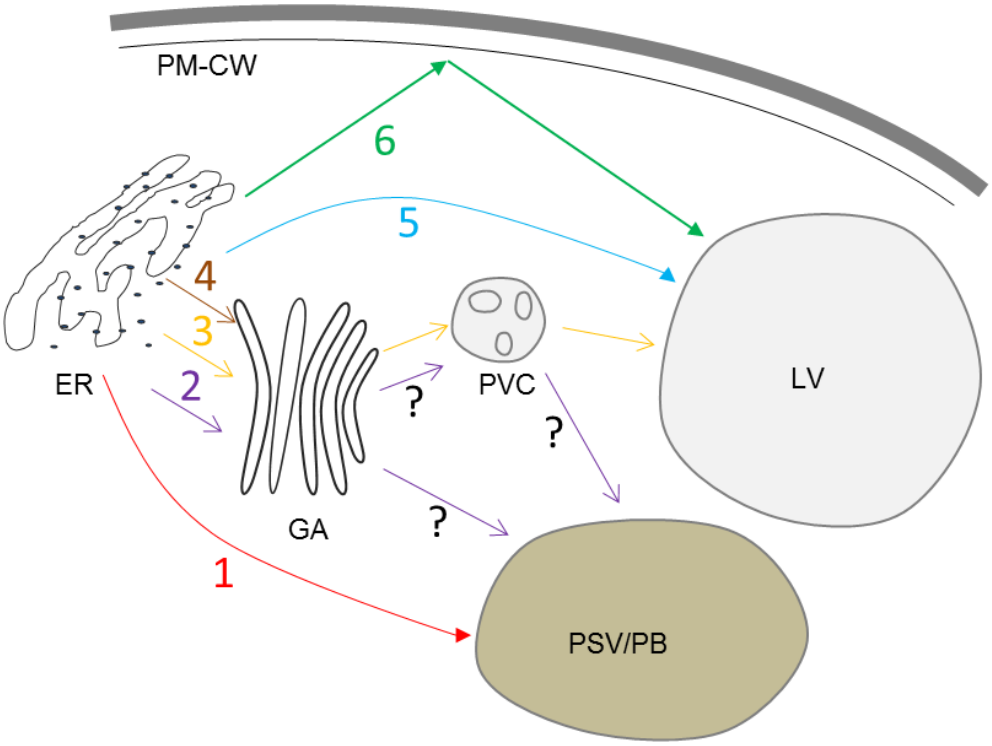

Figure 4.2 Putative models for transport of cardosin A to the plant vacuole. (1) Transport of cardosin A directly from the ER to PB observed in cardoon seeds (red arrow). (2) The route to the PSV in germinating seeds is still a question in terms of post-Golgi compartments (purple arrows). (3) COPII dependent pathway, mainly mediated by C-ter VSD, or glycosylated PSI determinant (orange arrows). (4) COPII independent pathway, sorted by PSI vacuolar sorting determinant without glycosylation site (brown arrow), with a possibility to by-pass the Golgi (5, blue arrow). A sixth route (6) guiding the proteins to the plasma membrane before specific targeting to the vacuole may also be considered (green arrows). ER – Endoplasmic Reticulum; GA – Golgi Apparatus; LV – Lytic Vacuole; PB – Protein Body; PM-CW – Plasma Membrane-Cell Wall complex; PSV – Protein Storage vacuole; PVC – Prevacuolar compartment.

Regarding cardosin A, *in planta*, the dual localisation of cardosin A in protein bodies in cardoon cotyledon cells (Pereira et al. 2008), and in protein storage vacuoles in flower cells (Duarte et al. 2006), could be related to the existence of a PSI-specific pathway, dependent on the type of tissue. In fact, in cardoon, it was shown that cardosin A accumulates in protein bodies in a GA independent manner (Pereira et al. 2008). Our hypothesis is that the PSI-mediated way is more relevant in metabolic active organs (such as flowers and seeds), where protein storage vacuoles are predominant over lytic vacuoles, and cells have different needs. The C-terminal domain would be more important in vegetative tissues with large central lytic vacuoles and has a parallel with the classic vacuolar pathway.

5.CONCLUSIONS AND PERSPECTIVES

Taking together the results obtained along this work, it can be concluded that both *Nicotiana tabacum* and *Arabidopsis thaliana* are good expression systems to study cardosin A biogenesis and trafficking routes. The use of both systems allowed complementary approaches, given their different characteristics, resulting in the validation of cardosin A as a model protein in the study of vacuolar trafficking. Indeed, the fact that cardosin A accumulates in two different types of vacuole coupled to the existence of two different vacuolar sorting signals in its protein sequence, reflecting different sorting routes, covers almost all the possible routes to the plant vacuoles described so far. The knowledge acquired in the course of this thesis already contributes to uncover some aspects of aspartic proteinases trafficking, but more questions have arised.

Cardosin A has two sorting determinants, the PSI and the C-terminal peptide. However, is one stronger than the other and which one works and in which situation? Probably this must be related to the physiological role of the protein and consequently to the tissue/organ where it is being expressed. The transient expression in *Nicotiana tabacum* system allowed to obtain good results on the identification and characterization of the two VSDs. However, to further explore the functionality of each domain, a stable expression system is needed to allow mimicking the protein expression in the native system. It was proven during this work that *Arabidopsis thaliana* is a good model for cardosin A studies, thus it could be used to obtain stable lines expressing the cardosin A constructs tested during this work in *N. tabacum.* It would be very interesting to observe their expression and localisation in during flower and seed development, as in the native system cardosin A accumulates preferentially in these tissues.

Furthermore, and also using *A. thaliana* as expression model, it would also be interesting to obtain lines expressing at the same time cardosin A and cardosin B, tagged with different coloured fluorescent proteins to allow an in vivo tracking of the two aspartic proteinases in the same tissues. This would provide interesting results, not only considering their localisation and trafficking, but also could give more insights towards the comprehension of their physiological roles in the plant.

In this work it was hypothesised that proteins' glycosylation is related to the route that aspartic proteinases follow to the vacuole. The relevance of glycosylation in protein sorting has long been discussed, but no concrete data it still available. This work has contributed to the discussion of this problematic, but still more data is needed. In the particular case of aspartic proteinases it seems to be related to the glycosylation site found in the PSI domain. Further studies should involve the a more thorough investigation of this domain in terms of vacuolar accumulation, the routes it takes to get there, and employ biochemical tools to analyse the glycosylation patterns, as Endo-

glucosidase H assays or PNGase F. It would be interesting to expand the study to other aspartic proteinases' PSIs, such as phytepsin and soybean aspartic proteinases, to understand if this is a conserved mechanism among plant aspartic proteinases or is a particular feature of cardosins.

The putative GA bypass attributed to the PSI that was described in this work as a great potential in recombinant protein production. The available studies in this subject point to a stunning increase in protein production when it is targeted to the vacuole. The problem of targeting foreign proteins to the vacuole is that once entering the secretory pathway, proteins undergo post-translation modifications such as glycosylation. Despite plants produce the same glycosylation patterns as mammals in the ER, when entering the GA the trimming of the glycans is sufficiently different to cause immunogenicity risks. The targeting of therapeutic proteins to the vacuole bypassing the GA would be an exciting approach to overcome the plant-specific glycosylation problem. The use of the PSI as a tool for efficient production of non-immunogenic therapeutically relevant proteins in plants needs to be explored.

As a whole, this work provided good results on cardosin A expression and targeting in two different heterologous systems, allowing to draw several hypothesis on its biogenesis, sorting routes and localisation in different tissues. At the same time it provided the basis for more detailed studies on cardosins biology and to start uncovering the whys and wherefores for the differences observed between the two more relevant cardosins, A and B. In the end, it has also provided good tools for the study of cardosins, in particular, and aspartic proteinases, in general, that can be explored in future studies.

6.BIBLIOGRAPHIC REFERENCES

Alberts, B., Johnson, A., Lewis, J., Raff, M., Roberts, K. & Walter P., 2004. Molecular Biology of the cell. 4th Edition. Garland Science, New York.

Almeida, C.M., Pereira, C., da Costa, D. S., Pereira, S., Pissarra, J., Simões, I. & Faro, C., 2012. Chlapsin, a chloroplastidial aspartic proteinase from the green algae Chlamydomonas reinhardtii. *Planta*. 236(1), pp.283-96.

Andreeva, A.V. Zheng, H., Kutuzov, M. A., Evans, D. E. & Hawes, C. R., 2000. Organization of transport from endoplasmic reticulum to Golgi in higher plants Plant ER and GA visualization with green fluorescent protein (GFP) Plant homologues of the proteins involved in ER-to-GA transport. *Biochemical Society Transactions*, pp.505-512.

Barlowe, C., 2003. Signals for COPII-dependent export from the ER: what's the ticket out? *Trends in Cell Biology*, 13(6), pp.295-300.

Bassham, D.C. & Raikhel, N.V., 2000. Unique features of the plant vacuolar sorting machinery. *Current opinion in cell biology*, 12(4), pp.491-5.

Batoko, H, Zheng, H.Q., Hawes, C & Moore, I, 2000a. A rab1 GTPase is required for transport between the endoplasmic reticulum and golgi apparatus and for normal golgi movement in plants. *The Plant cell*, 12(11), pp.2201-18.

Batoko, H, Zheng, H.Q., Hawes, C & Moore, I, 2000b. A rab1 GTPase is required for transport between the endoplasmic reticulum and golgi apparatus and for normal golgi movement in plants. *The Plant cell*, 12(11), pp.2201-18.

Beck, R. Rawet, M., Ravet, M., Wieland, F. T. & Cassel, D., 2009. The COPI system: molecular mechanisms and function. *FEBS letters*, 583(17), pp.2701-9.

Bethke, P.C., Hillmer, S. & Jones, R.L., 1996. Isolation of Intact Protein Storage Vacuoles from Barley Aleurone (Identification of Aspartic and Cysteine Proteases). *Plant physiology*, 110(2), pp.521-529.

Boevink, P., Oparka, K., Santa Cruz, S., Martin, B., Betteridge, A. & Hawes, C, 1998a. Stacks on tracks: the plant Golgi apparatus traffics on an actin/ER network. *The Plant journal : for cell and molecular biology*, 15(3), pp.441-7.

Bolte, S., Lanquar, V., Soler, M. N., Beebo, A., Satiat-Jeunemaître, B., Bouhidel, K. & Thomine, S., 2011. Distinct lytic vacuolar compartments are embedded inside the protein storage vacuole of dry and germinating Arabidopsis thaliana seeds. *Plant & cell physiology*, 52(7), pp.1142-52.

Bolte, Susanne, Brown, S. & Satiat-Jeunemaitre, Béatrice, 2004. The N-myristoylated Rab-GTPase m-Rabmc is involved in post-Golgi trafficking events to the lytic vacuole in plant cells. *Journal of cell science*, 117(Pt 6), pp.943-54.

Boutté, Y. Crosnier, M. T., Carraro, N., Traas, J. & Satiat-Jeunemaitre, B., 2006. The plasma membrane recycling pathway and cell polarity in plants: studies on PIN proteins. *Journal of cell science*, 119(Pt 7), pp.1255-65.

Boyes, D.C. Zayed, A. M., Ascenzi, R., McCaskill, A. J., Hoffman, N. E., Davis, K. R. & Görlach, J., 2001. Growth stage-based phenotypic analysis of Arabidopsis: a model for high throughput functional genomics in plants. *The Plant cell*, 13(7), pp.1499-510.

Bradford, M.M., 1976. A rapid and sensitive method for the quantitation of microgram quantities of protein utilizing the principle of protein-dye binding. *Analytical biochemistry*, 72, pp.248-54.

Brandizzi, F., Irons, S. L., Johansen, J., Kotzer, A. & Neumann, U., 2004. GFP is the way to glow: bioimaging of the plant endomembrane system. *Journal of microscopy*, 214(Pt 2), pp.138-58.

Brodelius, M., Hiraiwa, M., Marttila, S., Al Karadaghi, S., Picaud, S. & Brodelius, P. E., 2005. Immunolocalization of the saposin-like insert of plant aspartic proteinases exhibiting saposin C activity. Expression in young flower tissues and in barley seeds. *Physiologia Plantarum*, 125(4), pp. 405–418.

Brodsky, F.M. Chen, C. Y., Knuehl, C., Towler, M. C. & Wakeham, D. E., 2001. Biological basket weaving: formation and function of clathrin-coated vesicles. *Annual review of cell and developmental biology*, 17, pp.517-68.

Brown, S.C., Bolte, Susanne, Gaudin, M., Pereira, C., Marion, J., Soler, M.-N. & Satiat-Jeunemaitre, Béatrice, 2010. Exploring plant endomembrane dynamics using the photoconvertible protein Kaede. *The Plant journal : for cell and molecular biology*, 63(4), pp.696-711.

Bryksa, B.C., Bhaumik, P., Magracheva, E., De Moura, D. C., Kurylowicz, M., Zdanov, A., Dutcher, J. R., Wlodawer, A. & Yada, R. 2011. Structure and mechanism of the saposin-like domain of a plant aspartic protease. *The Journal of biological chemistry*, 286(32), pp.28265-75.

Bubeck, J., Scheuring, D., Hummel, E., Langhans, M., Viotti, C., Foresti, O., Denecke, J., Banfield, D. K. & Robinson, D. G., 2008. The syntaxins SYP31 and SYP81 control ER-Golgi trafficking in the plant secretory pathway. *Traffic (Copenhagen, Denmark)*, 9(10), pp.1629-52.

Cordeiro, M.C., Xue, Z.-T., Pietrzak, M., Salomé Pais, M. & Brodelius, P. E., 1994. Isolation and characterization of a cDNA from flowers of Cynara cardunculus encoding cyprosin (an aspartic proteinase) and its use to study the organ-specific expression of cyprosin. *Plant Molecular Biology*, 24(5), pp.733-741.

da Costa, D.S., Pereira, Susana, Moore, Ian & Pissarra, José, 2010a. Dissecting cardosin B trafficking pathways in heterologous systems. *Planta*, 232(6), pp.1517-30.

da Costa, D.S., Pereira, Susana & Pissarra, José, 2011. The heterologous systems in the study of cardosin B trafficking pathways. *Plant Signaling & Behavior*, 6(6), pp.895-897.

Costa, M.E.L., Gulik, W. M. V., Hoopen, H. J. G., Pais, M. S. S. & Cabral, J. M. S., 1996. Protease and phenol production of Cynara cardunculus L. cell suspension in a chemostat. *Cell*, 0229(96), pp.493-500.

Craft, J., Samalova, M., Baroux, C., Townley, H., Martinez, A., Jepson, I., Tsiantis, M. & Moore, I., 2005. New pOp/LhG4 vectors for stringent glucocorticoid-dependent transgene expression in Arabidopsis. *The Plant journal : for cell and molecular biology*, 41(6), pp.899-918.

Davidson, H.W., 1995. Wortmannin causes mistargeting of procathepsin D. evidence for the involvement of a phosphatidylinositol 3-kinase in vesicular transport to lysosomes. *The Journal of Cell Biology*, 130(4), pp.797-805.

Davies, D.R., 1990. The structure and function of the aspartic proteinases. *Annu. Rev. Biophys. Biophys. Chem.* 19, pp.189-215.

Denecke, J., Aniento, F., Frigerio, L., Hawes, C., Hwang, I., Mathur, J., Neuhaus, J.-M. & Robinson, D. G., 2012. Secretory Pathway Research: The More Experimental Systems the Better. *The Plant Cell*, 24(4), pp. 1316-1326.

Dombrowski, J.E., Schroeder, M.R., Bednarek, S.Y. & Raikhel, N.V., 1993. Determination of the functional elements within the vacuolar targeting signal of barley lectin. *The Plant cell*, 5(5), pp.587-96.

Duarte, P., Figueiredo, R., Pereira, Susana & Pissarra, José, 2006. Structural characterization of the stigma-style complex of Cynara cardunculus (Asteraceae) and immunolocalization of cardosins A and B during floral development. *Canadian Journal of Botany*, 84(5), pp.737-749.

Duarte, P., Pissarra, José & Moore, Ian, 2008. Processing and trafficking of a single isoform of the aspartic proteinase cardosin A on the vacuolar pathway. *Planta*, 227(6), pp.1255-68.

Ebine, K. & Ueda, T., 2009. Unique mechanism of plant endocytic/vacuolar transport pathways. *Journal of plant research*, 122(1), pp.21-30.

Egas, C., Lavoura, N., Resende, R., Brito, R. M., Pires, E., de Lima, M. C. & Faro, C, 2000. The saposin-like domain of the plant aspartic proteinase precursor is a potent inducer of vesicle leakage. *The Journal of biological chemistry*, 275(49), pp.38190-6.

Farid, A. Pabst, M., Schoberer, J., Altmann, F., Glössl, J. & Strasser, R., 2011. Arabidopsis thaliana alpha1,2-glucosyltransferase (ALG10) is required for efficient N-glycosylation and leaf growth. *The Plant journal : for cell and molecular biology*, 68(2), pp.314-25.

Faro, C, Ramalho-Santos, M., Vieira, M., Mendes, a, Simões, I, Andrade, R., Veríssimo, P., Lin, X., Tang, J. & Pires, E., 1999. Cloning and characterization of cDNA encoding cardosin A, an RGD-containing plant aspartic proteinase. *The Journal of biological chemistry*, 274(40), pp.28724-9.

Figueiredo, R., Duarte, P., Pereira, Susana & Pissarra, José, 2006. The embryo sac of Cynara cardunculus: ultrastructure of the development and localisation of the aspartic proteinase cardosin B. *Sexual Plant Reproduction*, 19(2), pp.93-101.

Foresti, O & Gershlick, D., 2010. A recycling-defective vacuolar sorting receptor reveals an intermediate compartment situated between prevacuoles and vacuoles in tobacco. *The Plant Cell* ….

Foresti, O. & Denecke, J., 2008. Intermediate organelles of the plant secretory pathway: identity and function. *Traffic (Copenhagen, Denmark)*, 9(10), pp.1599-612.

Frazão, C., Bento, I., Costa, J., Soares, C M., Veríssimo, P., Faro, C., Pires, E., Cooper, J. & Carrondo, M a, 1999. Crystal structure of cardosin A, a glycosylated and Arg-Gly-Asp-containing aspartic proteinase from the flowers of Cynara cardunculus L. *The Journal of biological chemistry*, 274(39), pp.27694-701.

Frigerio, L., de Virgilio, M., Prada, A., Faoro, F. & Vitale, A, 1998. Sorting of phaseolin to the vacuole is saturable and requires a short C-terminal peptide. *The Plant cell*, 10(6), pp.1031-42.

Frigerio, Lorenzo & Hawes, Chris, 2008. The endomembrane system: a green perspective. *Traffic (Copenhagen, Denmark)*, 9(10), p.1563.

Futai, E., Hamamoto, S., Orci, L., Schekman, R., 2004. GTP/GDP exchange by Sec12p enables COPII vesicle bud formation on synthetic liposomes. *The EMBO journal*, 23(21), pp.4146-55.

Geelen, D.N.V. & Inze, D.G., 2001. A Bright Future for the Bright Yellow-2 Cell Culture. *PLANT PHYSIOLOGY*, 127(4), pp.1375-1379.

Geldner, N. & Palme, K., 2001. Auxin transport inhibitors block PIN1 cycling and vesicle trafficking. , 413(SEPTEMBER), pp.425-428.

Glathe, S., Kervinen, J., Nimtz, M., Li, G H., Tobin, G J., Copeland, T D., Ashford, D., Wlodawer, A & Costa, J., 1998. Transport and activation of the vacuolar aspartic proteinase phytepsin in barley (Hordeum vulgare L.). *The Journal of biological chemistry*, 273(47), pp.31230-6.

Gomez, L. & Chrispeels, M.J., 1993. Tonoplast and Soluble Vacuolar Proteins Are Targeted by Different Mechanisms. *The Plant cell*, 5(9), pp.1113-1124.

Hanton, S.L., Bortolotti, L. E., Renna, L., Stefano, G. & Brandizzi, F., 2005. Crossing the divide--transport between the endoplasmic reticulum and Golgi apparatus in plants. *Traffic (Copenhagen, Denmark)*, 6(4), pp.267-77.

Hanton, S.L., Matheson, L. A., Chatre, L. & Brandizzi, F., 2009. Dynamic organization of COPII coat proteins at endoplasmic reticulum export sites in plant cells. *The Plant journal : for cell and molecular biology*, 57(6), pp.963-74.

Hanton, S.L., Matheson, L. A., Chatre, L., Rossi, M. & Brandizzi, F., 2007. Post-Golgi protein traffic in the plant secretory pathway. *Plant cell reports*, 26(9), pp.1431-8.

Hanton, S.L., Matheson, L. a & Brandizzi, Federica, 2006. Seeking a way out: export of proteins from the plant endoplasmic reticulum. *Trends in plant science*, 11(7), pp.335-43.

Hara-Nishimura, I., Shimada, T., Hatano, K., Takeuchi, Y. & Nishimura, M., 1998. Transport of storage proteins to protein storage vacuoles is mediated by large precursor-accumulating vesicles. *The Plant cell*, 10(5), pp.825-36.

Hara-Nishimura, I. & Hatsugai, N., 2011. The role of vacuole in plant cell death. *Cell death and differentiation*, 18(8), pp.1298-304.

Hawes, Chris & Satiat-Jeunemaitre, Béatrice, 2005. The plant Golgi apparatus--going with the flow. *Biochimica et biophysica acta*, 1744(2), pp.93-107.

Held, M. a, Boulaflous, A. & Brandizzi, F., 2008. Advances in fluorescent protein-based imaging for the analysis of plant endomembranes. *Plant physiology*, 147(4), pp.1469-81.

Holkeri, H. & Vitale, A, 2001. Vacuolar sorting determinants within a plant storage protein trimer act cumulatively. *Traffic (Copenhagen, Denmark)*, 2(10), pp.737-41.

Hori, H. & Elbein, a D., 1981. Tunicamycin inhibits protein glycosylation in suspension cultured soybean cells. *Plant physiology*, 67(5), pp.882-6.

Hunter, P.R., Craddock, C.P., Di Benedetto, S., Roberts, L.M. & Frigerio, L., 2007. Fluorescent reporter proteins for the tonoplast and the vacuolar lumen identify a single vacuolar compartment in Arabidopsis cells. *Plant physiology*, 145(4), pp.1371-82.

Inoue, K., Motozaki, a, Takeuchi, Y., Nishimura, M. & Hara-Nishimura, I., 1995. Molecular characterization of proteins in protein-body membrane that disappear most rapidly during transformation of protein bodies into vacuoles. *The Plant journal : for cell and molecular biology*, 7(2), pp.235-43.

Jauh, G., Phillips, T. & Rogers, J., 1999. Tonoplast intrinsic protein isoforms as markers for vacuolar functions. *The Plant cell*, 11(10), pp.1867-82.

Jiang, L., Phillips, T. E., Rogers, S. W. & Rogers, J. C., 2000. Biogenesis of the Protein Storage Vacuole Crystalloid. *The Journal of Cell Biology*, 150(4), pp.755-770.

Jiang, L., Phillips, T E., Hamm, C A., Drozdowicz, Y M., Rea, P A., Maeshima, M., Rogers, S W. & Rogers, J C, 2001. The protein storage vacuole: a unique compound organelle. *The Journal of cell biology*, 155(6), pp.991-1002.

Jolliffe, N a, Craddock, C.P. & Frigerio, L, 2005. Pathways for protein transport to seed storage vacuoles. *Biochemical Society transactions*, 33(Pt 5), pp.1016-8.

Jolliffe, Nicholas a, Ceriotti, A., Frigerio, Lorenzo & Roberts, L.M., 2003. The position of the proricin vacuolar targeting signal is functionally important. *Plant molecular biology*, 51(5), pp.631-41.

Jurgens, G., 2004. Membrane trafficking in plants. *Annual review of cell and developmental biology*, 20, pp.481-504.

Kang, B.-H., Nielsen, E., Preuss, M. L., Mastronarde, D. & Staehelin, L A., 2011. Electron tomography of RabA4b- and PI-4Kβ1-labeled trans Golgi network compartments in Arabidopsis. *Traffic (Copenhagen, Denmark)*, 12(3), pp.313-29.

Kervinen, J., Tobin, G.J., Costa, J., Waugh, D.S., Wlodawer, a & Zdanov, a, 1999. Crystal structure of plant aspartic proteinase prophytepsin: inactivation and vacuolar targeting. *The EMBO journal*, 18(14), pp.3947-55.

Kotzer, A.M., Brandizzi, Federica, Neumann, U., Paris, Nadine, Moore, Ian & Hawes, Chris, 2004. AtRabF2b (Ara7) acts on the vacuolar trafficking pathway in tobacco leaf epidermal cells. *Journal of cell science*, 117(Pt 26), pp.6377-89.

Lerouge, P., Cabanes-Macheteau, M., Rayon, C., Fischette-Lainé, A. C., Gomord, V. & Faye, L, 1998. N-glycoprotein biosynthesis in plants: recent developments and future trends. *Plant molecular biology*, 38(1-2), pp.31-48.

Luis, L.P., Snapp, E. L., Lippincott-schwartz, J., Hawes, C. & Brandizzi, F., 2004. Endoplasmic Reticulum Export Sites and Golgi Bodies Behave as Single Mobile Secretory Units in Plant Cells. *The Plant Cell*, 16(July), pp.1753-1771.

Luis, L.P., Taylor, J. P., Hadlington, J.L., Hanton, S. L., Snowden, C. J. & Fox, S. J., 2005. Receptor Salvage from the Prevacuolar Compartment Is Essential for Efficient Vacuolar Protein Targeting. *The Plant Cell*, 17(January), pp.132-148.

Macedo, P., 2005. Biogenesis of cardosin A: expression and biosynthetic pathways. PhD thesis, Faculty of Sciences, University of Porto, Portugal.

Maeshima, M., Hara-Nishimura, I., Takeuchi, Y. & Nishimura, M., 1994. Accumulation of Vacuolar H+-Pyrophosphatase and H+-ATPase during Reformation of the Central Vacuole in Germinating Pumpkin Seeds. *Plant physiology*, 106(1), pp.61-69.

Martinoia, E., Maeshima, Masayoshi & Neuhaus, H.E., 2007. Vacuolar transporters and their essential role in plant metabolism. *Journal of experimental botany*, 58(1), pp.83-102.

Masclaux, F.G., Galaud, J.-P. & Pont-Lezica, R., 2005. The riddle of the plant vacuolar sorting receptors. *Protoplasma*, 226(3-4), pp.103-8.

Matheson, L. a, Hanton, S.L. & Brandizzi, Federica, 2006. Traffic between the plant endoplasmic reticulum and Golgi apparatus: to the Golgi and beyond. *Current opinion in plant biology*, 9(6), pp.601-9.

Mathur, J & Radhamony, R., 2010. mEosFP-based green-to-red photoconvertible subcellular probes for plants. *Plant Physiology,* 154, pp. 1573–1587.

Mathur, Jaideep, 2007. The illuminated plant cell. *Trends in plant science*, 12(11), pp.506-13.

Matsuoka, K., Bassham, D. C., Raikhel, N. V. & Nakamura, K., 1995. Different sensitivity to wortmannin of two vacuolar sorting signals indicates the presence of distinct sorting machineries in tobacco cells. *The Journal of cell biology*, 130(6), pp.1307-18.

Matsuoka, K. & Nakamura, K., 1991. Propeptide of a precursor to a plant vacuolar protein required for vacuolar targeting. *Proceedings of the National Academy of Sciences of the United States of America*, 88(3), pp.834-8.

Mazorra-Manzano, M.A., Tanaka, T., Dee, D. R. & Yada, R. Y., 2010. Structure-function characterization of the recombinant aspartic proteinase A1 from Arabidopsis thaliana. *Phytochemistry*, 71(5-6), pp.515-23.

Meinke, D.W., 1998. Arabidopsis thaliana: A Model Plant for Genome Analysis. *Science*, 282(5389), pp.662-682.

Moore, I., Gälweiler, L., Grosskopf, D., Schell, J. & Palme, K, 1998. A transcription activation system for regulated gene expression in transgenic plants. *Proceedings of the National Academy of Sciences of the United States of America*, 95(1), pp.376-81.

Moreau, P., Brandizzi, F., Hanton, S., Chatre, L., Melser, S., Hawes, C. & Satiat-Jeunemaitre, B., 2007. The plant ER-Golgi interface: a highly structured and dynamic membrane complex. *Journal of experimental botany*, 58(1), pp.49-64.

Mutlu, A. & Gal, S., 1999. Plant aspartic proteinases: enzymes on the way to a function. *Physiologia Plantarum*, 105(3), pp.569-576.

Mérigout, P., Képès, F., Perret, A.-M., Satiat-Jeunemaitre, B. & Moreau, P., 2002. Effects of brefeldin A and nordihydroguaiaretic acid on endomembrane dynamics and lipid synthesis in plant cells. *FEBS Letters*, 518(1-3), pp.88-92.

Nagata, T., Nemoto, Y. & Hasezawa, S., 1992. Tobacco BY-2 Cell Line as the “HeLa” Cell in the Cell Biology of Higher Plants. *International Review of Cytology*, 132, pp.1-30.

Nebenführ, A., Gallagher, L. A., Dunahay, T G., Frohlick, J A., Mazurkiewicz, A M., Meehl, J B. & Staehelin, L A., 1999. Stop-and-go movements of plant Golgi stacks are mediated by the acto-myosin system. *Plant physiology*, 121(4), pp.1127-42.

Nebenführ, A. & Staehelin, L. A., 2001. Mobile factories: Golgi dynamics in plant cells. *Trends in plant science*, 6(4), pp.160-7.

Nebenführ, A., 2002. Vesicle traffic in the endomembrane system: a tale of COPs, Rabs and SNAREs. *Current Opinion in Plant Biology*, 5(6), pp.507-512.

Neuhaus, J.-M. & Rogers, J.C., 1998. Sorting of proteins to the vacuoles of plant cells. *Plant molecular biology*, 38, pp.127-144.

Neuhaus, J.M., Sticher, L., Meins, F. & Boller, T, 1991. A short C-terminal sequence is necessary and sufficient for the targeting of chitinases to the plant vacuole.

Proceedings of the National Academy of Sciences of the United States of America, 88(22), pp.10362-6.

Neumann, U., Brandizzi, Federica & Hawes, Chris, 2003. Protein transport in plant cells: in and out of the Golgi. *Annals of botany*, 92(2), pp.167-80.

Niemes, S., Labs, M., Scheuring, D., Krueger, F., Langhans, M., Jesenofsky, B., Robinson, D.G. & Pimpl, P., 2010. Sorting of plant vacuolar proteins is initiated in the ER. *The Plant journal : for cell and molecular biology*, 62(4), pp.601-14.

Nishizawa, K., Maruyama, N. & Utsumi, S., 2006. The C-terminal region of alpha' subunit of soybean beta-conglycinin contains two types of vacuolar sorting determinants. *Plant molecular biology*, 62(1-2), pp.111-25.

Olbrich, A., Hillmer, Stefan, Hinz, Giselbert, Oliviusson, P. & Robinson, David G, 2007. Newly formed vacuoles in root meristems of barley and pea seedlings have characteristics of both protein storage and lytic vacuoles. *Plant physiology*, 145(4), pp.1383-94.

Oliveira, A., Pereira, C., Costa, D. S., Teixeira, J., Fidalgo, F., Pereira, S. & Pissarra, J., 2010. Characterization of aspartic proteinases in C. cardunculus L. callus tissue for its prospective transformation. *Plant Science*, 178(2), pp.140-146.

Otegui, M.S. & Spitzer, C., 2008. Endosomal functions in plants. *Traffic (Copenhagen, Denmark)*, 9(10), pp.1589-98.

Paris, N., Stanley, C. M., Jones, R. L. & Rogers, J C, 1996. Plant cells contain two functionally distinct vacuolar compartments. *Cell*, 85(4), pp.563-72.

Paris, N., Saint-Jean, B., Faraco, M., Krzeszowiec, W., Dalessandro, G., Neuhaus, J.-M. & Di Sansebastiano, G. P., 2010. Expression of a glycosylated GFP as a bivalent reporter in exocytosis. *Plant cell reports*, 29(1), pp.79-86.

Paris, Nadine & Neuhaus, J.-M., 2002. BP-80 as a vacuolar sorting receptor. *Plant molecular biology*, 50(6), pp.903-14.

Park, J.H., Oufattole, M. & Rogers, J.C., 2007. Golgi-mediated vacuolar sorting in plant cells: RMR proteins are sorting receptors for the protein aggregation/membrane internalization pathway. *Plant Science*, 172(4), pp.728-745.

Park, M., Lee, D., Lee, G.-J. & Hwang, I., 2005. AtRMR1 functions as a cargo receptor for protein trafficking to the protein storage vacuole. *The Journal of cell biology*, 170(5), pp.757-67.

Park, M. & Jürgens, G., 2011. Membrane traffic and fusion at post-Golgi compartments. *Frontiers in plant science*, 2(January), p.111.

Pattison, R.J. & Amtmann, A., 2009. N-glycan production in the endoplasmic reticulum of plants. *Trends in plant science*, 14(2), pp.92-9.

Pedrazzini, E., Giovinazzo, G., Bielli, A., de Virgilio, M., Frigerio, L., Pesca, M., Faoro, F., Bollini, R., Ceriotti, A. & Vitale, A,1997. Protein quality control along the route to the plant vacuole. *The Plant cell*, 9(10), pp.1869-80.

Pereira, C.S., da Costa, D.S., Pereira, S., de Moura Nogueira, F., Albuquerque, P.M., Teixeira, J., Faro, C. & Pissarra, J., 2008. Cardosins in postembryonic development of cardoon: towards an elucidation of the biological function of plant aspartic proteinases. *Protoplasma*, 232(3-4), pp.203-213.

Pimentel, C., Van Der Straeten, D., Pires, E., Faro, C. & Rodrigues-Pousada, C., 2007. Characterization and expression analysis of the aspartic protease gene family of Cynara cardunculus L. *The FEBS journal*, 274(10), pp.2523-39.

Pimpl, P., Taylor, J. P., Snowden, C., Hillmer, S., Robinson, D. G. & Denecke, J., 2006. Golgi-mediated vacuolar sorting of the endoplasmic reticulum chaperone BiP may play an active role in quality control within the secretory pathway. *The Plant cell*, 18(1), pp.198-211.

Pimpl, P., Hanton, S. L., Taylor, J. P., da Silva, L. L. & Denecke, J., 2003. The GTPase ARF1p Controls the Sequence-Specific Vacuolar Sorting Route to the Lytic Vacuole. , 15(May), pp.1242-1256.

Pissarra, José, Pereira, C., Costa, D.S. da, et al., 2007. From Flower to Seed Germination in Cynara cardunculus: A Role for Aspartic Proteinases. *Internation Journal of Plant Developmental Biology*, pp.274-281.

Pompa, A., De Marchis, F., Vitale, A., Arcioni, S. & Bellucci, M., 2010. An engineered C-terminal disulfide bond can partially replace the phaseolin vacuolar sorting signal. *The Plant journal : for cell and molecular biology*, 61(5), pp.782-91.

Pratelli, R., Sutter, J.-U. & Blatt, M.R., 2004. A new catch in the SNARE. *Trends in plant science*, 9(4), pp.187-95.

Ramalho-Santos, M., Pissarra, J, Veríssimo, P., Pereira, S, Salema, R., Pires, E. & Faro, C.J., 1997. Cardosin A, an abundant aspartic proteinase, accumulates in protein storage vacuoles in the stigmatic papillae of Cynara cardunculus L. *Planta*, 203(2), pp.204-12.

Ramalho-Santos, M., Veríssimo, P., Cortes, L., Samyn, B., Van Beeumen, J., Pires, E. & Faro, C, 1998. Identification and proteolytic processing of procardosin A. *European journal of biochemistry / FEBS*, 255(1), pp.133-8.

Rayon, C., Lerouge, Patrice & Faye, L., 1998. The protein N-glycosylation in plants. *Journal of Experimental Botany*, 49(326), pp.1463-1472.

Richter, S., Geldner, N., Schrader, J., Wolters, H., Stierhof, Y.-D., Rios, G., Koncz, C., Robinson, D. G. & Jürgens, G., 2007. Functional diversification of closely related ARF-GEFs in protein secretion and recycling. *Nature*, 448(7152), pp.488-92.

Richter, S., Voss, U. & Jürgens, G., 2009. Post-Golgi traffic in plants. *Traffic (Copenhagen, Denmark)*, 10(7), pp.819-28.

Robinson, D G, Hinz, G & Holstein, S.E., 1998. The molecular characterization of transport vesicles. *Plant molecular biology*, 38(1-2), pp.49-76.

Robinson, David G, Oliviusson, P. & Hinz, Giselbert, 2005. Protein sorting to the storage vacuoles of plants: a critical appraisal. *Traffic (Copenhagen, Denmark)*, 6(8), pp.615-25.

Rutherford, S. & Moore, I, 2002. The Arabidopsis Rab GTPase family: another enigma variation. *Current Opinion in Plant Biology*, 5(6), pp.518-528.

Saint-Jore, C.M., Evins, J., Batoko, Henri, Brandizzi, Federica, Moore, Ian & Hawes, Chris, 2002. Redistribution of membrane proteins between the Golgi apparatus and endoplasmic reticulum in plants is reversible and not dependent on cytoskeletal networks. *The Plant journal : for cell and molecular biology*, 29(5), pp.661-78.

Samalova, M., Brzobohaty, B. & Moore, Ian, 2005. pOp6/LhGR: a stringently regulated and highly responsive dexamethasone-inducible gene expression system for tobacco. *The Plant journal : for cell and molecular biology*, 41(6), pp.919-35.

Sanderfoot, A.A. & Raikhel, N.V., 1999. The specificity of vesicle trafficking: coat proteins and SNAREs. *The Plant cell*, 11(4), pp.629-42.

Di Sansebastiano, G.P., Paris, N., Marc-Martin, S. & Neuhaus, J. M., 2001. Regeneration of a lytic central vacuole and of neutral peripheral vacuoles can be visualized by green fluorescent proteins targeted to either type of vacuoles. *Plant physiology*, 126(1), pp.78-86.

Sarmento, A.C., Lopes, H., Oliveira, C. S., Vitorino, R., Samyn, B., Sergeant, K., Debyser, G., Van Beeumen, J., Domingues, P., Amado, F., Pires, E., Domingues, M. R. M. & Barros, M. T., 2009. Multiplicity of aspartic proteinases from Cynara cardunculus L. *Planta*, 230(2), pp.429-39.

Satiat-Jeunemaitre, B., Cole, L., Bourett, T., Howard, R. & Hawes, C., 1996. Brefeldin A effects in plant and fungal cells: something new about vesicle trafficking? *Journal of microscopy*, 181(Pt 2), pp.162-77.

Satiat-Jeunemaitre, B, Boevink, P. & Hawes, C, 1999. Membrane trafficking in higher plant cells: GFP and antibodies, partners for probing the secretory pathway. *Biochimie*, 81(6), pp.597-605.

Satiat-Jeunemaitre, B & Hawes, C, 1992. Redistribution of a Golgi glycoprotein in plant cells treated with Brefeldin A. *J. Cell Sci.*, 103(4), pp.1153-1166.

Schoberer, J. & Strasser, R., 2011. Sub-compartmental organization of Golgi-resident N-glycan processing enzymes in plants. *Molecular plant*, 4(2), pp.220-8.

Shaner, N.C., Campbell, R.E., Steinbach, P. a, Giepmans, B.N.G., Palmer, A.E. & Tsien, R.Y., 2004. Improved monomeric red, orange and yellow fluorescent proteins

derived from Discosoma sp. red fluorescent protein. *Nature biotechnology*, 22(12), pp.1567-72.

Shaner, N.C., Patterson, G.H. & Davidson, M.W., 2007. Advances in fluorescent protein technology. *Journal of cell science*, 120(Pt 24), pp.4247-60.

Sheen, J., Hwang, S., Niwa, Y., Kobayashi, H. & Galbraith, D. W., 1995. Green-fluorescent protein as a new vital marker in plant cells. *The Plant Journal*, 8(5), pp.777-784.

Simões, I. & Faro, C., 2004. Structure and function of plant aspartic proteinases. *European journal of biochemistry / FEBS*, 271(11), pp.2067-75.

Somerville, C. & Koornneef, M., 2002. A fortunate choice: the history of Arabidopsis as a model plant. *Nature reviews. Genetics*, 3(11), pp.883-9.

Sparkes, I., Hawes, Chris & Frigerio, Lorenzo, 2011. FrontiERs: movers and shapers of the higher plant cortical endoplasmic reticulum. *Current opinion in plant biology*, 14(6), pp.658-65.

Sparkes, I. a, Runions, J., Kearns, A. & Hawes, Chris, 2006. Rapid, transient expression of fluorescent fusion proteins in tobacco plants and generation of stably transformed plants. *Nature protocols*, 1(4), pp.2019-25.

Terauchi, K., Asakura, T., Ueda, H., Tamura, T., Tamura, K., et al., 2006. Plant-specific insertions in the soybean aspartic proteinases, soyAP1 and soyAP2, perform different functions of vacuolar targeting. *Journal of plant physiology*, 163(8), pp.856-62.

Timotijević, G.S., Milisavljević, M.D., Radović, S. R., Konstantinović, M. M. & Maksimović, V. R., 2010. Ubiquitous aspartic proteinase as an actor in the stress response in buckwheat. *Journal of plant physiology*, 167(1), pp.61-8.

Tohge, T., Ramos, Magali S., Nunes-Nesi, A., Mutwil, M., Giavalisco, P., Steinhauser, D., Schellenberg, M., Willmitzer, L., Persson, S., Martinoia, E & Fernie, A. R, 2011. Toward the storage metabolome: profiling the barley vacuole. *Plant physiology*, 157(3), pp.1469-82.

Törmäkangas, K., Hadlington, J.L., Pimpl, P, Hillmer, S, Brandizzi, F, Teeri, T.H. & Denecke, J, 2001. A vacuolar sorting domain may also influence the way in which proteins leave the endoplasmic reticulum. *The Plant cell*, 13(9), pp.2021-32.

Veríssimo, P., Faro, C., Moir, A. J., Lin, Y., Tang, J. & Pires, E, 1996. Purification, characterization and partial amino acid sequencing of two new aspartic proteinases from fresh flowers of Cynara cardunculus L. *European journal of biochemistry / FEBS*, 235(3), pp.762-8.

Vieira, M., Pissarr, J., Veríssimo, P., Castanheira, P., Costa, Y., Pires, E. & Faro, C, 2001. Molecular cloning and characterization of cDNA encoding cardosin B, an

aspartic proteinase accumulating extracellularly in the transmitting tissue of Cynara cardunculus L. *Plant molecular biology*, 45(5), pp.529-39.

Vitale, A & Denecke, J, 1999. The endoplasmic reticulum-gateway of the secretory pathway. *The Plant cell*, 11(4), pp.615-28.

Vitale, A & Galili, G., 2001. The endomembrane system and the problem of protein sorting. *Plant physiology*, 125(1), pp.115-8.

Vitale, A. & Raikhel, N., 1999. What do proteins need to reach different vacuoles? *Trends in plant science*, 4(4), pp.149-155.

Vitale, A. & Boston, R.S., 2008. Endoplasmic reticulum quality control and the unfolded protein response: insights from plants. *Traffic (Copenhagen, Denmark)*, 9(10), pp.1581-8.

Wang, H., Rogers, J.C. & Jiang, Liwen, 2011. Plant RMR proteins: unique vacuolar sorting receptors that couple ligand sorting with membrane internalization. *The FEBS journal*, 278(1), pp.59-68.

Zheng, H., 2005. A Rab-E GTPase Mutant Acts Downstream of the Rab-D Subclass in Biosynthetic Membrane Traffic to the Plasma Membrane in Tobacco Leaf Epidermis. *Society*, 17(July), pp.2020-2036.

Zouhar, J, 2010. Functional specialization within the vacuolar sorting receptor family: VSR1, VSR3 and VSR4 sort vacuolar storage cargo in seeds and vegetative tissues. *The Plant Journal*.

Zouhar, Jan & Rojo, E., 2009. Plant vacuoles: where did they come from and where are they heading? *Current opinion in plant biology*, 12(6), pp.677-84.